

**I κ B_{NS} differentially affects *in vivo* CD4⁺ and CD8⁺ T cell activation
and plays a detrimental role in innate immunity
to *Listeria monocytogenes* infection in mice**

Dissertation

zur Erlangung des akademischen Grades

**doctor rerum naturalium
(Dr. rer. nat.)**

genehmigt durch die Fakultät für Naturwissenschaften
der Otto-von-Guericke-Universität Magdeburg

von M.Sc. Sarah Frentzel
geb. am 02.04.1989 in Haldensleben

Gutachter: Prof. Dr. Dunja Bruder
Privatdozent Dr. Thomas Jacobs

eingereicht am: 16.04.2018

verteidigt am: 09.10.2018

Contents

Contents	I
Publications	IV
Conference contributions	V
Supervision and contribution of student projects	VI
Abstract.....	VII
List of Abbreviations	VIII
List of Figures	X
List of Tables	XII
1. Introduction	1
1.1 <i>Listeria monocytogenes</i> as a model pathogen for a systemic infection.....	1
1.1.1 Pathophysiology of <i>Listeria monocytogenes</i> infection.....	1
1.1.2 Immune responses against <i>Listeria monocytogenes</i>	2
1.2 Methodological basis of research on antigen-specific T cell responses	6
1.3 Marker for the analysis of antigen-specific T cell activation and effector functions.....	7
1.4 Identification of immune cell subsets by flow cytometry.....	9
1.5 The transcription factor NF- κ B	11
1.6 Regulation of NF- κ B through inhibitory proteins (I κ Bs)	13
1.7 The classical NF- κ B pathway.....	15
1.8 The atypical non-structural κ B protein I κ B _{NS}	16
1.8.1 The structure of I κ B _{NS}	16
1.8.2 Cell-type specific effects of I κ B _{NS}	17
1.9 Aims of the thesis	19
2. Materials	21
2.1 Consumables	21
2.2 Technical devices	22
2.4 Antibodies.....	23
2.5 Buffers and Media	24
2.6 Mouse models.....	24
3. Methods	26
3.1 Genotyping of inbred mouse strains	26

3.2 Organ isolation and single cell preparation	27
3.3 CD4 ⁺ and CD8 ⁺ T cell isolation by magnetic activated cell sorting (MACS)	27
3.4 <i>In vitro</i> stimulation of T cells	28
3.5 CFSE staining of T cells	28
3.6 Adoptive T cell transfers.....	29
3.7 Infection of mice with <i>Listeria monocytogenes</i>	29
3.8 Determination of bacterial burden	29
3.9 <i>In vivo</i> cytotoxicity assay.....	29
3.10 Flow cytometric analysis of adoptively transferred T cells	30
3.11 Histopathology of liver and spleen from WT and conventional I κ B _{NS} ^{-/-} mice.....	30
3.12 Liver dissociation with GentleMACS dissociator	31
3.13 Isolation of CD45 ⁺ and CD45 ⁻ cell populations by MACS	31
3.14 Real-time Polymerase chain reaction (PCR).....	31
3.15 Serum preparation and measurement of ALT level	33
3.16 Flow cytometric analysis of cellular composition in organs during LM infection	33
3.17 Flow cytometric cell sorting	35
3.18 LacZ fluorochrome reporter assay	36
3.19 Microarray.....	36
Statistics.....	37
4. Results.....	38
4.1 Probing of antigen-specific T cell responses <i>in vitro</i>	38
4.1.1 Loss of I κ B _{NS} does not affect the activation of CD4 ⁺ T cells following <i>in vitro</i> stimulation....	39
4.1.2 Loss of I κ B _{NS} does not affect the proliferation of <i>in vitro</i> stimulated CD8 ⁺ T cells, but results in reduced IFN γ secretion.....	41
4.2 Impact of I κ B _{NS} on antigen-specific T cell activation <i>in vivo</i>	44
4.2.1 I κ B _{NS} -deficiency has distinct effects on <i>in vivo</i> activation of OVA-specific CD4 ⁺ T cells during LM infection.....	44
4.2.2 I κ B _{NS} -deficiency has only marginal effects on the activation of CD8 ⁺ T cells following <i>in vivo</i> pathogen encounter	50
4.2.3 Impact of I κ B _{NS} in CD4 ⁺ and CD8 ⁺ T cells on pathogen clearance.....	60
4.2.4 Impact of I κ B _{NS} on <i>in vivo</i> cytotoxicity.....	61
4.3 The role of I κ B _{NS} in immunity against <i>Listeria monocytogenes</i>	64
4.3.1 I κ B _{NS} -deficiency confers robust protection against high-dose LM infection.....	64

4.3.2 Bacterial clearance in high-dose LM infection is not affected by I κ B _{NS} -deficiency	65
4.3.3 Reduced immunopathology in I κ B _{NS} -deficient mice following LM infection	66
4.3.4 Blunted inflammatory immune response in I κ B _{NS} ^{-/-} mice.....	69
4.3.5 Broad alterations in the gene expression profile in the liver of I κ B _{NS} -deficient mice during LM infection	72
4.3.6 I κ B _{NS} expression in hematopoietic and non-hematopoietic liver cells during the course of LM infection	83
4.3.7 Altered immune cell distribution in livers and spleens of I κ B _{NS} -deficient mice during the course of LM infection	85
4.3.8 I κ B _{NS} -dependent activation of an inflammatory program in monocytes as potential underlying mechanism for the detrimental course of high-dose LM infection.....	96
5. Discussion	100
5.1 Impact of I κ B _{NS} on antigen-specific T cell activation.....	100
5.2 The role of I κ B _{NS} in the immune response against <i>Listeria monocytogenes</i>	106
References	112
Appendix	121
Acknowledgements	135
Selbstständigkeitserklärung	136
Curriculum vitae	137

Publications

Pieler MM*, **Frentzel S***, Bruder D, Wolff MW, Reichl U.

A cell culture-derived whole virus influenza A vaccine based on magnetic sulfated cellulose particles confers protection in mice against lethal influenza A virus infection.

Vaccine. 2016 Dec 7;34(50):6367-6374. doi: 10.1016/j.vaccine.2016.10.041.

*contributed equally.

Other publications

Peschel B., **Frentzel S.**, Laske T., Genzel Y, Reichl U.

Comparison of influenza virus yields and apoptosis-induction in an adherent and a suspension MDCK cell line.

Vaccine, 2013. 31(48), 5693-5699. doi:10.1016/j.vaccine.2013.09.051.

Conference contributions

Sarah Frentzel, Andreas Jeron, Ingo Schmitz and Dunja Bruder. I κ B_{NS}-deficient mice are protected against high-dose *Listeria monocytogenes* infection. **Poster presentation.** 4th European Congress of Immunology, Vienna, 2015.

Sarah Frentzel, Michael Pieler, Michael Wolff, Udo Reichl and Dunja Bruder. Immunization with Influenza A virus-loaded magnetic sulphated cellulose particles protects mice against lethal Influenza A virus challenge. **Poster presentation.** 46th Annual Meeting German Society for Immunology (DGfI), Hamburg, 2016.

Sarah Frentzel, Andreas Jeron, Ingo Schmitz and Dunja Bruder. I κ B_{NS} plays a detrimental role in the course of *Listeria monocytogenes* infection. **Poster presentation.** 46th Annual Meeting German Society for Immunology (DGfI), Hamburg, 2016.

Sarah Frentzel, Marat Gajsin, Ingo Schmitz, Andreas Jeron and Dunja Bruder. I κ B_{NS}-dependent activation of an inflammatory profile in monocytes as a potential underlying mechanism for the fatal course of high-dose *Listeria monocytogenes* infection in mice. **Oral presentation.** 22. Symposium "Infektion und Immunabwehr" der FG Infektionsimmunologie (DGfI) und des AK Infektionsimmunologie der DGfI, Burg Rothenfels, 2018.

Supervision and contribution of student projects

Master theses

Isabel Bernal “The role of atypical inhibitory kB protein I κ B_{NS} in influenza-specific T effector cells”, Otto-von-Guericke University Magdeburg, 2016.

Martha Böning “Untersuchungen zum Einfluss des atypischen NF κ B- Inhibitorproteins I κ B_{NS} auf NK-Zell-vermittelte Immunantworten im Rahmen einer *Listeria monocytogenes* Infektion“, Ernst-Moritz-Arndt University Greifswald, 2017.

Alexander Pausder “Analyse der zeitlichen und zellulären Expression des atypischen I κ B-Proteins I κ B_{NS} in einer *Nfkbid/lacZ* Reportermaus im Rahmen einer Listerien-Infektion“, Otto-von-Guericke University Magdeburg, 2017.

Note: Analyses of the *Nfkbid* promotor activity (see chapter 4.3.7) was performed by A. Pausder in the framework of the mentioned master thesis.

Marat Gajsin “Untersuchung der Funktion von I κ B_{NS} in Monozyten und Makrophagen in einem murinen Modell der Listeriose“, Otto-von-Guericke University Magdeburg, 2018

Note: Cell sorting of inflammatory monocytes from LM-infected liver and spleen samples was performed by M. Gajsin. Furthermore, the RT-PCR analysis of the sorted cells (see chapter 4.3.8) was carried out by M. Gajsin in the framework of the mentioned master thesis.

Abstract

The inducible transcription factor NF- κ B is involved in the regulation of a plethora of immunological processes and thus a tight regulation of NF- κ B has to be ensured. This is governed by classical (e.g. I κ B α , I κ B β , I κ B ϵ) and atypical (e.g. Bcl-3, I κ B ζ , I κ B_{NS}) inhibitory κ B proteins. The protein I κ B_{NS} can act as activator as well as suppressor of NF- κ B mediated gene expression in the nucleus. Most scientific work to elucidate the role of I κ B_{NS} in the regulation of immune responses done so far was performed under *in vitro* or *ex vivo* conditions, while the impact of I κ B_{NS} in controlling *in vivo* immune responses during systemic infections still remains elusive.

The first part of this thesis addressed the role of I κ B_{NS} during antigen-specific activation of CD4⁺ and CD8⁺ T effector cells. For this a model system based on the adoptive transfer of ovalbumin (OVA)-specific T cells in combination with OVA-expressing *Listeria monocytogenes* as antigen-specific *in vivo* stimulus was used. This experimental approach revealed that the antigen-specific activation of CD4⁺ T cells following *in vivo* pathogen encounter strongly relies on I κ B_{NS}. The differentiation into Th1 effector cells was affected as indicated by a significantly reduced proliferation, marked changes in expression of activation markers and reduced IFN γ and IL2 production in CD4⁺ T cells lacking I κ B_{NS}. The pathogen-specific *in vivo* activation of CD8⁺ T cells was less affected by I κ B_{NS}-deficiency, and here especially proliferation and secretion of IFN γ does not depend on I κ B_{NS}. Since time-dependent differences were observed with respect to the expression of CD25, PD1 and TNF α between both genotypes, a slightly delayed activation program in CD8⁺ T cells lacking I κ B_{NS} might be reasonable. Despite the aforementioned differences between both genotypes, I κ B_{NS}-deficiency did not affect the capacity of CD8⁺ T cells to establish *in vivo* cytotoxic T cell responses.

The second part of the thesis focused on the impact of I κ B_{NS} on innate immune responses towards LM infection. I κ B_{NS}-proficient (WT) mice succumbed within few days post high-dose LM infection while I κ B_{NS}-deficient (KO) mice were completely protected. Histological examination revealed a mitigated immunopathology 4 days post LM infection in liver and spleen samples of KO compared to WT mice, which was however not the consequence of an improved pathogen clearance but rather due to an overall blunted inflammatory immune response induced in mice lacking I κ B_{NS}. This hypothesis was further supported by comprehensive genome-wide transcriptome analyses of LM infected livers, which confirmed reduced numbers and reduced expression levels of inflammation-associated genes in KO compared to WT mice. In-depth flow cytometric analysis of the immune cell composition in spleen and liver in concert with their cell-specific I κ B_{NS}-promoter activity during the course of LM infection revealed that I κ B_{NS} expression in inflammatory monocytes might represent one of the key factors responsible for inducing hyperinflammation during high-dose LM infection. This was further supported by data obtained from infection experiments done in conditional KO mice lacking I κ B_{NS} specifically in monocytes, macrophages and neutrophils. In summary, I κ B_{NS} was proven to be detrimental during systemic LM infection by promoting a transcriptional program resulting in severe hyperinflammation, which ultimately results in fatal disease course.

List of Abbreviations

% v/v	Volume percent
ACK	Ammonium chloride potassium
ALT	Alanine aminotransferase
ANK	Ankyrin
ARD	Ankyrin repeat domain
APC	Antigen-presenting cell
CD	Cluster of differentiation
CFSE	Carboxy-Fluorescein diacetate succinimidylester
CTL	Cytotoxic T lymphocyte
DC	Dendritic cell
DNA	Desoxyribonucleic acid
dpi	Days post infection
DSS	Dextran sulfate sodium
EAE	Experimental autoimmune encephalomyelitis
EDTA	Ethylenediaminetetraacetic acid
FACS	Fluorescent activated cell sorting
FCS	Fetal calf serum
FDG	Fluorescein Di-D-Galactopyranoside
FITC	Fluorescein isothiocyanate
Flp	Flippase
FRT	Flippase recognition target
Foxp3	Forkhead box protein 3
FSC	Forward scatter
i.v.	Intravenous
IFN	Interferon
IKK	I κ B kinase
I κ B	Inhibitory- κ B-protein
IL	Interleukin
IMDM	Iscove's Modified Dulbecco Medium
IRF	Interferon regulatory factor
ISG	Interferon stimulated genes
LM	Listeria monocytogenes
LM-OVA	Ovalbumin-expressing <i>Listeria monocytogenes</i>
LPS	Lipopolysaccharide
MACS	Magnetic activated cell sorting
MHC	Major histocompatibility complex
mRNA	Messenger ribonucleic acid
mir	Micro RNA
NF- κ B	Nuclear factor kappa light chain enhancer of activated B cells

NLS	Nuclear localization signal
NOS	Nitric oxygen specis
OVA	Ovalbumin
PAMP	Pathogen-associated molecular pattern
PBS	Phosphate buffered saline
PCR	Polymerase chain reaction
PFA	Paraformaldehyde
PMA	Phorbol 12-myristate 13-acetate
PRR	Pathogen-recognition receptor
RHD	REL-homology domain
RNA	Ribonucleic acid
ROS	Reactive oxygen species
Rpm	Rounds per minute
RT	Room temperature
TAD	Transactivation domain
TCR	T cell receptor
TGF	Transforming growth factor
Th1	T helper 1 cell
Th17	T helper 17 cell
TipDC	TNF-and NOS-producing Dendritic cell
TLR	Toll-like receptor
TNF	Tumor-necrosis factor
Treg	Regulatory T cell

List of Figures

Figure 1: Replication cycle of <i>Listeria monocytogenes</i>	2
Figure 2: Schematic overview about innate and adaptive immune cell subsets that contribute to elimination and clearance of <i>Listeria monocytogenes</i> infection	6
Figure 3: Illustration of hematopoiesis	11
Figure 4: The members of NF- κ B/Rel family	12
Figure 5: Overview about inhibitory κ B proteins	14
Figure 6: Overview about the activation cascade of the classical NF- κ B signaling pathway	15
Figure 7: <i>In silico</i> structural prediction of I κ B _{NS}	16
Figure 8: Representative gating scheme.	35
Figure 9: Proliferation of <i>in vitro</i> stimulated WT and I κ B _{NS} ^{-/-} OT-II transgenic CD4 ⁺ T cells.	40
Figure 10: Representative dot plots and summarizing bar charts of the flow cytometric analysis of <i>in vitro</i> stimulated CD4 ⁺ T cells	41
Figure 11: Proliferation of <i>in vitro</i> stimulated WT and I κ B _{NS} ^{-/-} OT-I transgenic CD8 ⁺ T cells	42
Figure 12: Representative dot plots and summarizing bar charts of the flow cytometric analysis of <i>in vitro</i> stimulated CD8 ⁺ T cells	43
Figure 13: Schematic overview about the experimental design of adoptive transfer	45
Figure 14: Representative dot plots showing the activation status of CD4 ⁺ T cells isolated from OT II x WT and OT-II x I κ B _{NS} ^{-/-} mice before adoptive transfer	46
Figure 15: Proliferation of transferred OVA-specific OT-II x WT and OT-II x I κ B _{NS} ^{-/-} CD4 ⁺ T cells at different times post LM-OVA infection	47
Figure 16: Phenotype of adoptively transferred OT-II x WT and OT-II x I κ B _{NS} ^{-/-} CD4 ⁺ T cells 5 days after LM-OVA infection	49
Figure 17: Schematic overview about the experimental design of adoptive transfer of OT-I transgenic CD8 ⁺ T cells followed by LM-OVA infection	51
Figure 18: Representative dot plots showing the activation status of CD8 ⁺ T cells isolated from OT I x WT and OT-I x I κ B _{NS} ^{-/-} mice	52
Figure 19: Proliferation of transferred OVA-specific OT-I x WT and OT-I x I κ B _{NS} ^{-/-} CD8 ⁺ T cells at different times post LM-OVA infection	53
Figure 20: Phenotype of adoptively transferred OT-I x WT and OT-I x I κ B _{NS} ^{-/-} CD8 ⁺ T cells 3 days post LM-OVA infection	55
Figure 21: Phenotype of adoptively transferred OT-I x WT and OT-I x I κ B _{NS} ^{-/-} CD8 ⁺ T cells 5 days after LM-OVA infection	59
Figure 22: Clearance of LM-OVA infection in C57BL/6 mice which received transgenic OVA-specific CD4 ⁺ or CD8 ⁺ T cells from I κ B _{NS} sufficient or deficient donors	61
Figure 23: <i>In vivo</i> analysis of LM-OVA induced CD8 ⁺ T cell cytotoxicity in WT and I κ B _{NS} ^{-/-} mice following LM-OVA infection	62
Figure 24: Weight loss and survival of I κ B _{NS} ^{+/+} , I κ B _{NS} ^{+/-} and I κ B _{NS} ^{-/-} mice following high-dose <i>Listeria</i> infection	65
Figure 25: CFU in different organs in high-dose LM infected WT and I κ B _{NS} ^{-/-} mice	66

Figure 26: Histopathological examinations of uninfected and day 4 LM infected liver and spleen samples	68
Figure 27: Serum ALT levels and expression of inflammatory cytokines in spleen and liver of WT and $\text{I}\kappa\text{B}_{\text{NS}}^{-/-}$ mice during the course of LM infection.....	71
Figure 28: Schematic overview about the evaluation strategy and direct comparison of both genotypes in the uninfected state	73
Figure 29: RA scatter plots of annotated genes assessed by microarray analysis.....	75
Figure 30: Venn diagrams comparing the identified regulated genes from Microarray analysis	76
Figure 31: Transcriptional profile of whole liver tissue from WT and $\text{I}\kappa\text{B}_{\text{NS}}^{-/-}$ mice in the course of LM infection.....	79
Figure 32: $\text{I}\kappa\text{B}_{\text{NS}}$ mRNA expression in CD45^+ and CD45^- liver cells as well as in splenocytes of WT mice during LM infection.....	85
Figure 33: Lymphocyte composition of livers and spleens of WT and $\text{I}\kappa\text{B}_{\text{NS}}^{-/-}$ mice during the course of LM infection	90
Figure 34: Cellular composition of monocytes and macrophages in livers and spleens of WT and $\text{I}\kappa\text{B}_{\text{NS}}^{-/-}$ mice during the course of LM infection.....	93
Figure 35: Cellular composition of myeloid cell subsets in livers and spleens of WT and $\text{I}\kappa\text{B}_{\text{NS}}^{-/-}$ mice during the course of LM infection	95
Figure 36: Expression of inflammatory mediators by inflammatory monocytes.....	97
Figure 37: Survival of conditional knock-out mice	99

Appendix

Figure 1: Lymphocyte composition of livers and spleens of WT and $\text{I}\kappa\text{B}_{\text{NS}}^{-/-}$ mice during the course of LM infection.....	132
Figure 2: Cellular composition of monocytes and macrophages in livers and spleens of WT and $\text{I}\kappa\text{B}_{\text{NS}}^{-/-}$ mice during the course of LM infection	133
Figure 3: Cellular composition of myeloid cell subsets in livers and spleens of WT and $\text{I}\kappa\text{B}_{\text{NS}}^{-/-}$ mice during the course of LM infection	134

List of Tables

Table 1: Chemicals	21
Table 2: Kits	22
Table 3: Technical devices	22
Table 4: Antibodies used for purity check of adoptively transferred OVA-specific T cells	23
Table 5: FACS-panel used in the adoptive transfer experiments	23
Table 6: FACS-panel for characterization of cellular influx during <i>Listeria</i> -infection	23
Table 7: IMDM complete	24
Table 8: FACS buffer	24
Table 9: FACS staining medium for intracellular lacZ activity assay	24
Table 10: Composition of the PCR mix for the amplification reaction	26
Table 11: Used oligonucleotides primers for genotyping of mice	26
Table 12: Thermal cycler program used for genotyping PCR	26
Table 13: Reaction mixture for cDNA synthesis	32
Table 14: Reaction mixture for reverse transcription	32
Table 15: Composition of the real-time RT-PCR reaction mix	32
Table 16: Thermal cycler program used for real-time RT-PCR	32
Table 17: Quantitative real-time RT-PCR primers.	33
Table 18: Gene ontology (GO) enrichment of regulated genes from WT and I κ B _{NS} ^{-/-} mice during LM infection. GO terms from the meta category “Biological process”	81
Table 19: Gene ontology (GO) enrichment of regulated genes from WT and I κ B _{NS} ^{-/-} mice during LM infection. GO terms from the meta category “Molecular Function”	82
Table 20: Gene ontology (GO) enrichment of regulated genes from WT and I κ B _{NS} ^{-/-} mice during LM infection. GO terms from the meta category “Immune system process”	83
Table 21: <i>Nfkbid</i> promoter activity in different immune cell subsets in spleens of uninfected mice	87
Table 22: <i>Nfkbid</i> promoter activity in different immune cell subsets in livers of uninfected mice.	87

Appendix

Table 1: List of regulated genes in course of LM infection identified by microarray analyses of livers from I κ B _{NS} ^{-/-} vs. WT mice.	121
---	-----

1. Introduction

The immune system comprises a variety of mechanisms to protect the host against invading pathogens. It can be subdivided into the relatively unspecific innate immunity, which takes effect immediately upon pathogen encounter and prevents the expansion of the invading pathogen by controlling and limiting the infection by a variety of cellular and chemical reactions. On the other hand, the adaptive immunity is being subdivided into humoral and cellular immune responses that operate in a pathogen-specific manner and most importantly is able to generate an immunological memory to provide protection from re-infection with the same pathogen. Pattern-recognition receptors on innate immune cell subsets lead to the recognition and sensing of invading pathogens resulting in the activation of signaling pathways followed by activation of transcription factors such as the nuclear factor 'kappa-light-chain-enhancer' of activated B cells (NF- κ B). NF- κ B is ubiquitously expressed in nearly all cell types and is involved in gene modulation necessary for different biological processes such as cell proliferation, regulation of inflammation or apoptosis. Thus, a tight regulation of the complex NF- κ B signaling pathway is needed which is primarily ensured by inhibitory κ B proteins, (I κ Bs) which can be further subdivided in classical and atypical proteins such as I κ B_{NS}. Especially in the context of immune responses towards infectious agents an unrestricted functionality of NF- κ B has to be ensured. For example the immunologically well-studied model pathogen *Listeria monocytogenes* triggers NF- κ B mediated signaling pathways resulting in robust innate and adaptive immune responses that are needed to resolve the infection.

1.1 *Listeria monocytogenes* as a model pathogen for a systemic infection

1.1.1 Pathophysiology of *Listeria monocytogenes* infection

The gram-positive bacterium *Listeria monocytogenes* (LM) was first described by Murray, Webb and Swan in 1924 when they isolated this microorganism out of rabbits and guinea pigs suffering from septicemic diseases (Murray et al. 1926). The infectious disease caused by the foodborne pathogen LM is called listeriosis, an opportunistic infection with potentially fatal outcome (Vázquez-Boland et al. 2001). In healthy individuals an infection normally remains unnoticed, whereas it can lead to severe complications in older adults, immune-compromised patients, neonates and pregnant women (Schuchat et al. 1992). LM is a common contaminant of either processed or non-processed foods like cheese, poultry, meat and seafood products (Schlech, 2000). The clinical manifestations of listeriosis include gastroenteritis, meningoencephalitis and abortions in pregnant women (Ooi and Lorber, 2005; Levidiotou et al. 2004; Mateus et al. 2013).

In general, the gastrointestinal tract is thought to be the primary site of entry for the bacterium into the host (Vázquez-Boland et al. 2001). Once arrived in the small intestine it can rapidly spread into lymph and blood stream. Thereby, it disseminates into its main replication sites spleen and liver (Kaufmann, 1993). *Listeria* are intracellular pathogens that benefit from their potential to cross epithelial barriers, their capability to escape from phagosomes and the capability to initialize their own uptake by phagocytes to disseminate and propagate into other cells.

LM possesses dedicated ligands on its surface which can interact with cellular receptors on the surface of host cells. The protein ligand internalin A binds to E-cadherin and internalin B interacts with the hepatocyte growth factor Met on the surface of the host cell to mediate listeria uptake (Bamburg, 2011; Bonazzi et al. 2009). The receptor Met is ubiquitously expressed allowing bacterial internalization in a variety of cell types, whereas E-cadherin is only expressed by a limited number of cells (Bonazzi et al. 2009; Hamon et al., 2006). Upon receptor-mediated internalization *Listeria* is engulfed into the host cell and subsequently is surrounded by a phagocytic vacuole (Figure 1). The membrane of the vacuole is disrupted by the secretion of two phospholipases (PlcA and PlcB) and by the pore-forming toxin listeriolysin O (LLO) (Hamon et al. 2006). Once the bacterium is released into the cytoplasm of the host cell it is highly motile due to the exploitation of polymerization of actin filaments induced by the bacterial surface protein ActA (Welch et al. 1997). Through the actin polymerization the bacterium is able to enter neighboring cells. Once it entered secondary cells, it can pass the resulting double-membrane by the conjugated action of LLO and the phospholipases (Stavru et al. 2011).

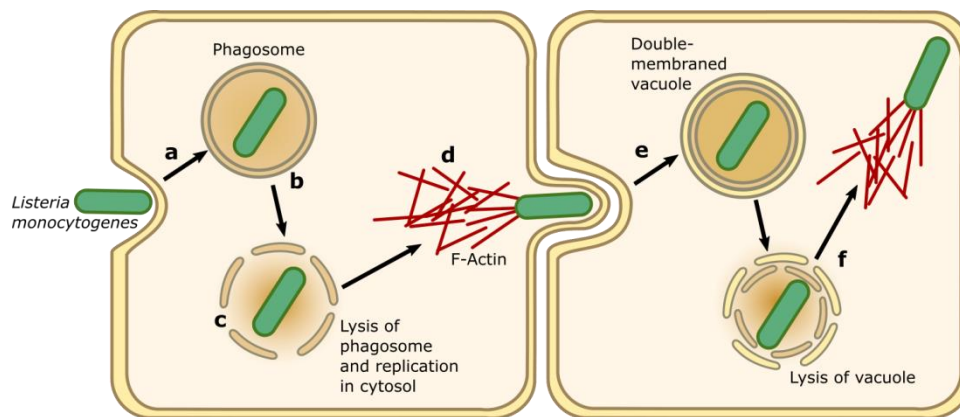


Figure 1: Replication cycle of *Listeria monocytogenes*. The bacterium induces its entry through the interaction of specific cell surface ligands with receptors of the host cell (a) and gets surrounded by a phagosome. (b) The phospholipases PlcA and PlcB together with the toxin listeriolysin O form lytic pores within the membrane of the vacuole (c) allowing the escape from the phagosome. The bacterium can now replicate within the host cell. Actin polymerization induced by the surface protein ActA conciliates intracellular motility to spread to adjacent cells. (d) Once having invaded a neighbor cell (e) it can escape and lyse the resulting double membraned vacuole (f) which completes the replication cycle (adapted from Hamon et al., 2006).

1.1.2 Immune responses against *Listeria monocytogenes*

Innate Immunity

Upon LM infection an innate immune response is rapidly triggered which is essential for controlling the bacterial growth and dissemination as well as confers protection of the host against a systemic lethal infection (Zenewicz and Shen, 2007).

The primary detection mechanism of pathogens is mediated by the recognition of pathogen-associated molecular patterns (PAMPs) by the host's pathogen-recognition receptors (PRRs) such as the membrane-bound toll-like receptors (TLR) that recognize different microbial products. TLR2 for example specifically recognizes peptidoglycan and lipoproteins, TLR4 detects lipopolysaccharides and lipoteichoic acids, TLR5 flagellin and TLR9 recognizes CpG motifs in bacterial DNA (Medzhitov, 2001).

Especially TLR2-signaling contributes to an efficient early control of LM infection as studies revealed that TLR2-deficient mice are more susceptible to systemic LM infection, indicated by higher bacterial burden in the liver and enlarged hepatic micro-abscesses (Torres et al., 2004).

The signaling via TLRs or cytosolic/nuclear oligomerization domain (NOD)-like receptors (NLR) initiates a signaling cascade which in turn activates signaling pathways such as mitogen-activated protein kinase (MAPK), interferon regulating factor 3 (IRF3) or NF- κ B resulting in immune activation and induction of genes which are involved in host defense and cytokine production (Corr and O'Neill, 2009).

As a first line of defense neutrophils are recruited to the site of infection where they directly help to control the bacterial growth by phagocytosis, production of reactive oxygen species (ROS) and indirectly by production of inflammatory cytokines, promoting further anti-microbial immune mechanisms (Witter et al., 2016). The chemokines CXCL1 and CXCL2 have been shown to be involved in neutrophil recruitment to the sites of LM infection following TLR2 signaling (Liu et al., 2012). Moreover, interleukin (IL) 6 and IL8 are involved in the recruitment of neutrophils to infectious foci, where they secrete inflammatory mediators and chemokines (Stavru et al., 2011). IFN γ producing neutrophils are a critical component in the early control of LM infection (Yin and Ferguson, 2009). By secretion of several chemokines such as CXCL8, CXCL1, monocyte chemoattractant protein-1 (MCP1) or macrophage inflammatory protein 1 α (MIP1 α /CCL3) neutrophils contribute to the recruitment of additional neutrophils, monocytes, dendritic cells or NK cells to sites of infection (Tecchio et al., 2014).

Macrophages are the primary targets for replication of LM, but at the same time they contribute to the ingestion and clearance of the pathogen in the early phase of infection. Especially tissue resident macrophages such as Kupffer cells in the liver are important for the initial clearance of bacteria (Zenewicz and Shen, 2007). In response to LM infection they produce large amounts of IL12 and TNF α which evoke the production of IFN γ by natural killer (NK) cells that in turn stimulate infected tissue resident macrophages to eliminate the bacterium (Tripp et al., 1993; Havell, 1987). Furthermore, IL12 produced by macrophages supports the development of LM-specific T helper (Th) 1 CD4⁺ T cells (Hsieh et al., 1993). Moreover, IFN γ serves as a distinct signal for the efficient activation of macrophages to fulfill their effector functions (Stoiber et al., 2001). Activated macrophages produce ROS and nitrogen intermediates, which prevent bacteria from escaping from the vacuole into the cytoplasm of the host cell (Shaughnessy and Swanson, 2010).

Another robust inflammatory innate immune response towards LM infection is orchestrated by lymphocyte antigen 6 complex (Ly6C^{hi}) monocytes. Upon LM infection Ly6C^{hi} monocytes migrate from the bone marrow through the bloodstream to the site of infection, triggered by CCL2- and CCL7-mediated stimulation of the CCR2 chemokine receptor on monocytes (Serbina et al., 2008). Particularly in the liver, the surface protein integrin α -M (CD11b) on monocytes and the cell surface glycoprotein called "intercellular adhesion molecule-1" (ICAM-1) expressed on endothelial cells, help to guide chemotaxis of Ly6C^{hi} monocytes to the infected tissue (Serbina et al., 2012). Moreover, in spleens of LM infected animals Ly6C^{hi} monocytes undergo differentiation into TNF- and inducible nitric oxide synthase (iNOS)-producing dendritic cells (TipDCs) that express MHC class II, co-stimulatory

molecule B7.1 and CD40 on their surface. Absence of these DC subsets was reported to result in an uncontrolled bacterial burden in that organ (Serbina et al., 2003).

Adaptive Immunity

The adaptive immune system is composed of T lymphocytes and B lymphocytes which constitute the effector cells of cellular and humoral immune responses. The adaptive immune response against LM is mainly T cell mediated, generally involving both CD4⁺ and CD8⁺ T cell subsets, but especially cytotoxic CD8⁺ T cells being necessary for effective clearance of intracellular bacteria by eliminating infected host cells (Stavru et al., 2011).

Mature naïve T lymphocytes originate from the thymus and circulate through the blood stream to secondary lymphoid organs such as spleen or peripheral lymph nodes in search of their cognate antigen-MHC complex presented by antigen-presenting cells (APCs). Upon antigen encounter T cells become activated and differentiate into effector T cells with specific functions (Agace, 2006).

The antigen presentation and activation of T cells takes place in draining lymph nodes (Itano and Jenkins, 2003). APCs, such as dendritic cells or macrophages, migrate into the lymph nodes after picking up antigens from the periphery. Sampled antigens are proteolytically processed into small peptides and loaded onto MHC class I and MHC class II proteins. These peptide-MHC complexes are presented to naïve T cells (Guermónprez et al., 2002). Efficient activation of T cells requires three signals. The first signal is provided by the specific recognition of the cognate antigenic peptides presented by MHC molecules. The second signal needed for efficient T cell activation and clonal expansion is provided by interactions with co-stimulatory molecules such as the co-stimulatory receptor CD28 and ligation with members of the B7 molecule family expressed on the surface of activated APCs (Chen and Flies, 2013). TCR stimulation results also in the secretion of IL2, the principal growth factor for T cells, which regulates magnitude and duration of T cell responses (Kim et al., 2001). The receptor for IL2 consists of three subunits - α , β and γ . Resting T cells express only the β and γ chain of the IL2 receptor. Stimulation by antigen encounter leads to the association with the α -chain of the IL2-R which results in the formation of a high affinity receptor for IL2. Autocrine secretion of IL2 results in an increased and prolonged expression of IL2-R α (CD25) which acts as positive feedback regulator for the expression of the high-affinity receptor (Kim et al., 2001; Malek and Castro, 2010).

The third signal for efficient T cell activation is provided by the local cytokine milieu in which a T cell becomes activated. In the absence of an adequate cytokine milieu, antigen encounter and co-stimulatory signals may be insufficient possibly leading to tolerance (anergy) rather than activation of T cells. Essentially, the cytokine milieu promotes and shapes the differentiation into effector T cells with different effector functions (Curtsinger and Mescher, 2010; Zhu et al., 2010).

Antigens from intracellular pathogens such as LM are rapidly proteolytically degraded in the cytosol and the fragments are mainly bound to MHC class I molecules and can be recognized by CD8⁺ T cells (Finelli et al., 1999). Activation of naïve CD8⁺ T cells results in the differentiation into effector CD8⁺ T cells with cytotoxic functions in order to combat the intracellular pathogens. One mechanism used by cytotoxic CD8⁺ T cells to lyse infected host cells is the release of perforin that integrates into the target cell membrane where it forms pores allowing specific enzymes, called granzymes, to enter the cell and

to initiate apoptosis (Wing and Gregory, 2002). A second mechanism to initiate apoptosis is the interaction of Fas ligand (CD95L) with Fas (CD95), which results in the activation of a death-inducing caspase complex (Sharma et al., 2000). Released bacteria from lysed host cells are finally phagocytosed by macrophages.

Moreover, CD8⁺ T cell-derived cytokines such as IFN γ or TNF α are important for resistance to infection (Harty et al., 2000). After proliferation and differentiation into primary effector cells, CD8⁺ T cells undergo a rapid contraction phase in which most of the effector cells are eliminated by apoptosis (Stavru et al., 2011). Typically the CD8⁺ T cell response peaks approximately 7 days post infection followed by the contraction phase. A small fraction of cells remains and becomes long-lived memory T cells which can rapidly expand in case of re-infection (Prlic and Bevan, 2008).

Foreign antigens derived from bacterial proteins processed in lysosomes are presented by APCs to CD4⁺ T cells through MHC class II (Zenewicz and Shen, 2007). LM infection-induced IL12 production by macrophages supports the differentiation into IFN γ secreting T helper (Th) 1 T cells being the main CD4⁺ T cell population involved in protection against LM infection (Campbell and Shastri, 1998; Kursar et al., 2002). Additionally, by providing co-stimulatory interactions with APCs and secretion of distinct cytokines, CD4⁺ T cells are suggested to be involved in helping CD8⁺ T cells to develop an optimal response in terms of augmented production of cytotoxic T cell responses and the development of memory CD8⁺ T cells (Lara-Tejero and Pamer, 2004; Shedlock et al., 2003). Naturally occurring regulatory T cells (Foxp3⁺ CD4⁺ T cells) are not directly involved in combating LM infection, but they are needed to maintain a balance between expansion of pathogen-specific effector T cells that promote pathogen clearance and at the same time limiting collateral host tissue damage by suppressing overwhelming pathogen-specific effector T cell responses (Ertelt et al., 2009).

In summary, efficient elimination and clearance of LM infection relies on the complex interplay between cell subsets from the innate immune compartment and, for final clearance and long-term protection, from cells of the adaptive immune system which is summarized in Figure 2.

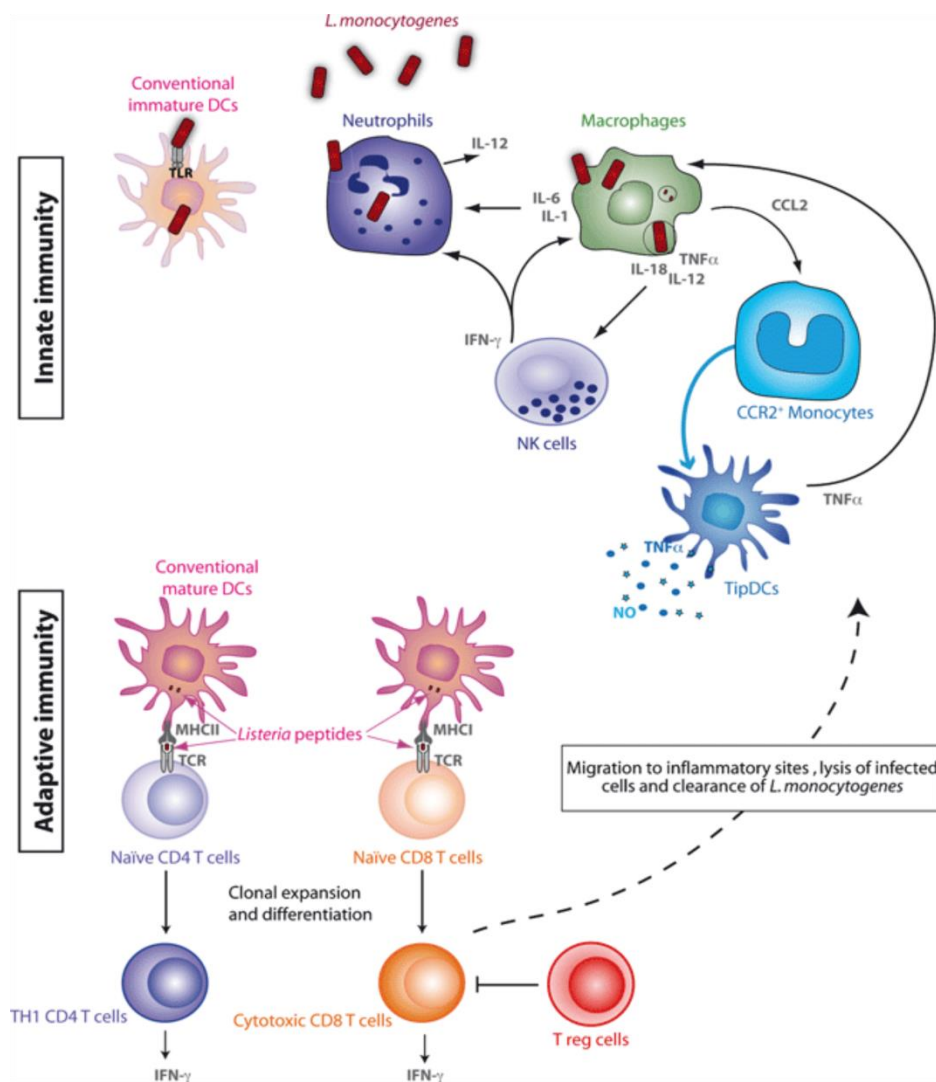


Figure 2: Schematic overview about innate and adaptive immune cell subsets that contribute to elimination and clearance of *Listeria monocytogenes* infection (taken from Stavru et al., 2011).

1.2 Methodological basis of research on antigen-specific T cell responses

The polyclonal CD4⁺ and CD8⁺ T cell pool is comprised of several millions of sub T cell pools, each of which can be defined by means of their specific T cell receptor variant, which has been carefully selected within the thymus to only recognize non self-antigens in context of MHC class I/II antigen presentation (Takaba and Takayanagi, 2017). When studying T cell immune responses, analyses of the entire polyclonal T cell pool alone does not directly allow to deduce the cellular fate and function of certain sub-pools of antigen-specific T cells, as typically specific T cell sub-pools, even during the peak of adaptive immunity, only account for a tiny fraction of all T cells. Thus, ever since immunologists strived to find ways to confine T cell analyses to specific T cell subsets in order to better understand their specific contributions to the adaptive immune response in dependence of their specific antigen. One of the most appreciated tools to do so is the use of model antigens, for which immunogenic peptide sequences are known (Newell and Davis, 2014). Knowledge of immunogenic peptides helped to identify specific T cell subsets e.g. by using synthetically produced pentamer complexes. However,

only the generation of genetically modified peptide-specific animal models allows studying specific T cell responses *in vivo*. All animal models for specific T cell research have in common that by genetic construction they exhibit a constricted pool of T cells with a major fraction being specific for the model peptide. Thus, these animal models represent a source of T cells with defined and known antigen specificity. An immunologically well-studied model antigen is the chicken-derived ovalbumin (OVA) protein, commonly used to study antigen-specific immune responses. OVA is a 42.7 kDa protein (Nisbet et al., 1981), which becomes proteolytically processed by APCs giving rise to the generation of upon others two immunodominant OVA-peptides. Complementary to these immunodominant OVA-peptides, well-established transgenic T cell mouse models exist. TCR transgenic mice are used as donors for antigen-specific T cells that can directly recognize certain sequences of OVA. CD8⁺ T cells from so called OT-I transgenic mice express a MHC class I-restricted TCR specific for the immunodominant OVA peptide OVA₂₅₇₋₂₆₄ (SIINFEKL, Hogquist et al., 1994, Clarke et al., 2000), whereas CD4⁺ T cells derived from OT-II transgenic mice express a MHC class II-restricted TCR specific for the immunodominant OVA-peptide OVA₃₂₃₋₃₃₉ (ISQAVHAAHAEINEAGR, Robertson et al., 2000). An unambiguous detection of both OVA-specific TCR transgenic CD4⁺ and CD8⁺ T cell subsets is feasible by staining them with monoclonal antibodies specific for the TCR α (V α 2) and β (V β 5) chains. Of note, one known drawback of the OT-I transgenic model is that OT-I transgenic CD8⁺ T cells tend to display higher homeostatic proliferation within the OT-I mouse itself, leading to a higher than normal frequency of CD44^{high} T cells (Goldrath and Bevan, 1999), a fact that has to be taken into account when analyzing effector and memory T cell development. For the purpose of cell re-identification following adoptive OT-I/OT-II T cell transfer *in vivo* into recipient mice, the congenic marker Thy1.1 can be used, when previously a congenic Thy1.1 mouse line was crossed into the OT-I and OT-II mouse lines. In the murine system two variants of Thy1, a Glycosyl-phosphatidylinositol (GPI)-anchored cell surface protein exist, which differ in amino acid position 89: arginine in case of Thy1.1 and glutamine in case of the Thy1.2 (Haeryfar and Hoskin, 2004).

OT-I and OT-II transgenic mice used in this study bear the allelic variant Thy1.1, whereas C57BL/6 recipient mice express the Thy1.2 variant. Therefore, it is possible to distinguish between recipient and donor T cell populations by means of monoclonal antibodies against Thy1.1.

1.3 Marker for the analysis of antigen-specific T cell activation and effector functions

Upon cognate antigen encounter *in vivo*, the cellular behavior of T cells changes in multiple ways. This includes cell adhesion, cell-to-cell interaction, cell division, cell migration and cytokine production. All of these behavioral changes involve substantial alterations in cell surface protein expression enabling T cell functions upon TCR engagement. Thus, proteins that show TCR signaling-induced expressional changes are generally useful as activation markers to dissect a polyclonal T cell response and to get insights into the current state of T cell responses in a given moment following infection.

One of the earliest activation markers on the surface of T cells after TCR ligation is CD69. It is an inducible cell surface glycoprotein, which is transiently expressed on activated lymphocytes. Sancho and colleagues suggested that CD69 is involved in the enhancement of the activation and/or

differentiation of T cells, because of its rapid but transient expression (Sancho et al., 2005). CD25, the α -chain of the high-affinity IL2 receptor (IL2R α), is the most prominent T cell activation marker, which is rapidly up-regulated following CD4⁺ and CD8⁺ T cell activation (Bajnok et al., 2017) both with mitogens and specific peptides. In addition, it plays a key role in the responsiveness to IL2 resulting in further IL2 production in a feedback-loop (Fazekas De St. Groth et al., 2004). Moreover, the extent and duration of IL2 production during a primary T cell response affects the differentiation of CD8⁺ T cells influencing them to become short-lived effector T cells or long-lived memory T cells. Otherwise sustained CD25 expression results in strong IL2 signals that amplify the proliferation of CD8⁺ T cells and these cells become apoptosis-prone short lived effector CD8⁺ T cells (summarized by Boyman and Sprent, 2012).

In addition, CD62L mediates the extravasation of naïve T cells and allows T cell migration to infected areas (Bradley et al., 1994). Naïve T cells are typically CD62L^{high} and following activation by TCR engagement the protein is shed from their cell surface. CD62L together with the expression level of the cell-adhesion molecule CD44 is used to further subclassify T cells into naïve, effector and memory T cell phenotypes. Naïve T cells are CD62L^{high}CD44^{low}, and effector/ effector-memory T cells are CD62L^{low}CD44^{high} (Gerberick et al., 1997).

By flow cytometry, T cells are divided into a CD44^{high} population and a CD44^{int} (intermediate) population (Wang et al., 2008) and also in a cell population that does not express CD44 (CD44⁻) at all. In the steady state the majority of CD4⁺ T cells are CD44^{int} and together with the CD44⁻ cells, they can be considered to be antigen-unexperienced naïve T cells (Zhao and Davis, 2010). CD44^{high}CD4⁺ T cells present an activated and also memory-like phenotype (Swain, 1994; Zhao and Davis, 2010) and therefore can be thought of as antigen-experienced T cells.

Additionally, CD44 is highly up-regulated on T cells after activation through TCR signaling (Baaten et al., 2010), rendering CD44 a common T cell activation marker.

IFN γ is an effector cytokine which contributes to CD4⁺ and CD8⁺ T cell mediated immune responses. On the one hand it is secreted by activated and Th1-differentiated CD4⁺ effector T cells and on the other hand by cytotoxic CD8⁺ T cells (Schoenborn and Wilson, 2007).

Terminally differentiated effector CD8⁺ T cells are furthermore characterized not only by expressing high levels of IFN γ , but also by expression of perforin, granzymes and TNF α following activation (Pipkin et al., 2010; Reiser and Banerjee, 2016). TNF α for instance is rapidly produced after TCR engagement and is a potent inflammatory cytokine, which is involved in differentiation processes, cell proliferation and induction of cell death (Brehm et al., 2005).

Programmed death 1(PD1) is another important marker, which is upregulated on CD8⁺ T cells upon activation, and together with its ligands PD-L1 and PD-L2 it delivers inhibitory signals that are needed to regulate the balance between T cell activation, tolerance and immunopathology (Keir et al., 2008). PD1 is expressed on activated T cells and through engagement of PD1 with its ligand during TCR signaling T cell proliferation and cytokine signaling can be blocked. In addition PD1 expression protects against self-reactivity by augmenting induced Treg (iTreg) functions and by suppressing the expansion as well as functions of activated effector T cells (Francisco et al., 2010).

1.4 Identification of immune cell subsets by flow cytometry

Flow cytometry is a reliable tool to examine immune cells in lymphoid and non-lymphoid tissues. Usage of fluorescently conjugated antibodies against specific cell surface markers allows distinguishing different cellular immune cell subsets. Though typically the combination of a set of antibodies to be used in a flow cytometric analysis is heavily dependent on the scientific question to be answered, still there is some general common sense in the way immune cell subsets can be distinguished. By now flow cytometers allow to assess enough fluorescence markers to dissect all major immune subsets in one multi-color staining. However, flow cytometric analyses of especially innate immune cells is challenging due to phenotypic alterations and broad overlap of common surface marker expression. Many studies tried to improve flow cytometric identification of immune cell subsets in lymphoid and non-lymphoid tissues. Most studies were done in lung tissue, where phenotypic plasticity of macrophages and dendritic cells is challenging to dissect (Misharin et al., 2013; Becher et al., 2014; Yu et al., 2016). They all used at least a 10-color panel to distinguish and identify 9 distinct myeloid cell populations. Despite differences in the gating strategy, they commonly use the same markers for immune cell subset identification.

Since all immune cells originate from hematopoietic precursors, distinction of hematopoietic and non-hematopoietic cell subsets can be easily achieved by staining against the general hematopoietic protein CD45. It is a unique and ubiquitous membrane glycoprotein expressed on nearly all cellular subsets of the hematopoietic lineage (Nakano et al., 1990). Hematopoietic immune cells can be further subdivided into lymphoid and myeloid cells, since all immune cells originate from either dedicated lymphoid or myeloid stem cell progenitor cells in the bone marrow (see Figure 3, Janeway et al., 2008).

T cell precursors migrate to the thymus, where they mature and undergo thymic selection (Actor, 2014) whereas B lymphocytes develop in the bone marrow from their hematopoietic precursor cells (Pieper et al., 2013). Murine B cells can be identified by their expression of the pan-B cell marker B220 (Bleesing and Fleisher, 2003), and by the expression of CD19 that is expressed by essentially all B-lineage cells (LeBien and Tedder, 2008).

The different T cell subsets such as T helper CD4⁺ or cytotoxic CD8⁺ T cells can be defined by expression of their respective TCR co-receptor (CD4/CD8) and the invariant TCR chain CD3 ϵ and additionally phenotyped by cell surface markers, activation markers and cytokines they secrete (refer to section 1.1.2 and 1.3).

NK cells differentiate from the same lymphoid precursor cell but in contrast to B and T-lymphocytes they function in an antigen-unspecific manner (Janeway et al., 2008). They can be recognized in flow cytometry by staining against the pan NK-cell marker CD49b and against the alloantigen NK1.1 (Arase et al., 2001). Furthermore, antibodies against the natural cytotoxic receptor NKp46 allows identification of NK cells (Romero et al., 2006).

In general, myeloid cell subsets can be further distinguished into granulocytes (mast cells, eosinophils, basophils and neutrophils) and in mononuclear phagocytes (monocytes, macrophages and dendritic cells).

Granulocytes are relatively short-lived cells, circulating in the blood stream and with expanding cell numbers during immune responses. They then leave the blood stream to migrate to sites of infection or inflammation (Janeway et al., 2008).

Neutrophils are one of the first cell subsets that migrate towards the site of infection and provide phagocytic functions (Witko-Sarsat et al., 2000). They can be easily identified based on their high expression of the neutrophil-specific marker Ly6G (lymphocyte antigen 6 complex locus G6D) and their cellular property of high side scatter light intensity in a flow cytometer (Rose et al., 2012).

Staining against the integrin CD11b allows the identification of monocytes, granulocytes, macrophages and natural killer cells (Solojov et al., 2005). Since CD11b is a subunit of the complement receptor 3 required to phagocytose complement-coated structures, it is present on basically all phagocytes. Fluorescence intensity (CD11b^{high}, CD11b^{int} and CD11b^{low}) is used for further sub-classification. For instance high expression of CD11b permits the separation of monocytes, interstitial macrophages and CD11b⁺ DCs from natural killer cells, which express CD11b only to an intermediate extent (Misharin et al., 2013).

Together with the integrin CD11c that functions as cell surface receptor and mediates leukocyte interactions, myeloid immune cell subsets can be further sub-classified. It is primarily found on myeloid cells, where its expression is for example regulated during monocyte maturation into tissue macrophages (Córbi and Lopéz-Rodríguez, 1997).

Especially tissue macrophages are an extremely heterogeneous cell population based on their specific tissue origin. Basically they are characterized by high expression of the murine macrophage-specific antigen F4/80 (Austyn and Gordon, 1981). Some tissue-specific macrophages are for instance Langerhans cells (skin), Kupffer cells (liver), microglia (brain) or alveolar macrophages (lung). Since they commonly develop from dedicated tissue-specific stem cells, their renewal does not rely on blood monocytes (Davies et al., 2013).

Monocytes are circulating white blood cells derived from bone marrow precursors, which can further differentiate into a range of tissue macrophages and DCs (Auffray et al., 2009). Monocytes can be further subdivided based on their expression of lymphocyte antigen 6C2 (Ly6C) and CD11b; Ly6C^{high} CD11c⁻ cells are referred to as inflammatory or Ly6C⁺ monocytes. They are rapidly recruited to sites of infection or inflammation and contribute to local and systemic inflammation (Shi and Pamer, 2011). In the steady state Ly6C⁺ monocytes differentiate into Ly6C⁻ monocytes which patrol through the periphery monitoring PAMPs, potentially becoming monocyte-derived tissue-resident macrophages (Yang et al., 2014; Misharin et al., 2013). Monocyte-derived macrophages and DCs can be further distinguished by the expression of the Fcγ-receptor CD64. It is highly expressed on macrophages, whereas DCs express only low to no levels of CD64 (Tamoutounour et al., 2012). Yu and colleagues described for instance for lung tissue a good way of discrimination between CD64⁺CD24⁻ macrophages, CD11b⁻CD11c⁺ alveolar macrophages and CD11b⁺CD11c⁻ interstitial macrophages (Yu et al., 2016). Alveolar macrophages function mostly as phagocytic cells to remove microorganisms in the alveoli, whereas interstitial macrophages serve as regulators in inflammation and as antigen-presenting cells (Cai et al., 2014). The above mentioned discrimination strategy was also described to work in other tissues than lung (Yu et al., 2016).

DCs can be divided into plasmacytoid and classical DCs. Plasmacytoid DCs accumulate mainly in the blood and express low levels of MHC class II and CD11c in the steady state. Classical DCs are a subset of hematopoietic cells found in tissues and residing in most lymphoid and non-lymphoid tissue. They can roughly be sub-classified into MHC class II⁺ CD11b⁻ and CD11b⁺ DCs (Merad et al., 2013). Taken together, monocyte-derived immune cells share phenotypic and functional properties, but with the combination of the aforementioned markers it is possible to identify and distinguish most macrophages and DC populations by flow cytometry.

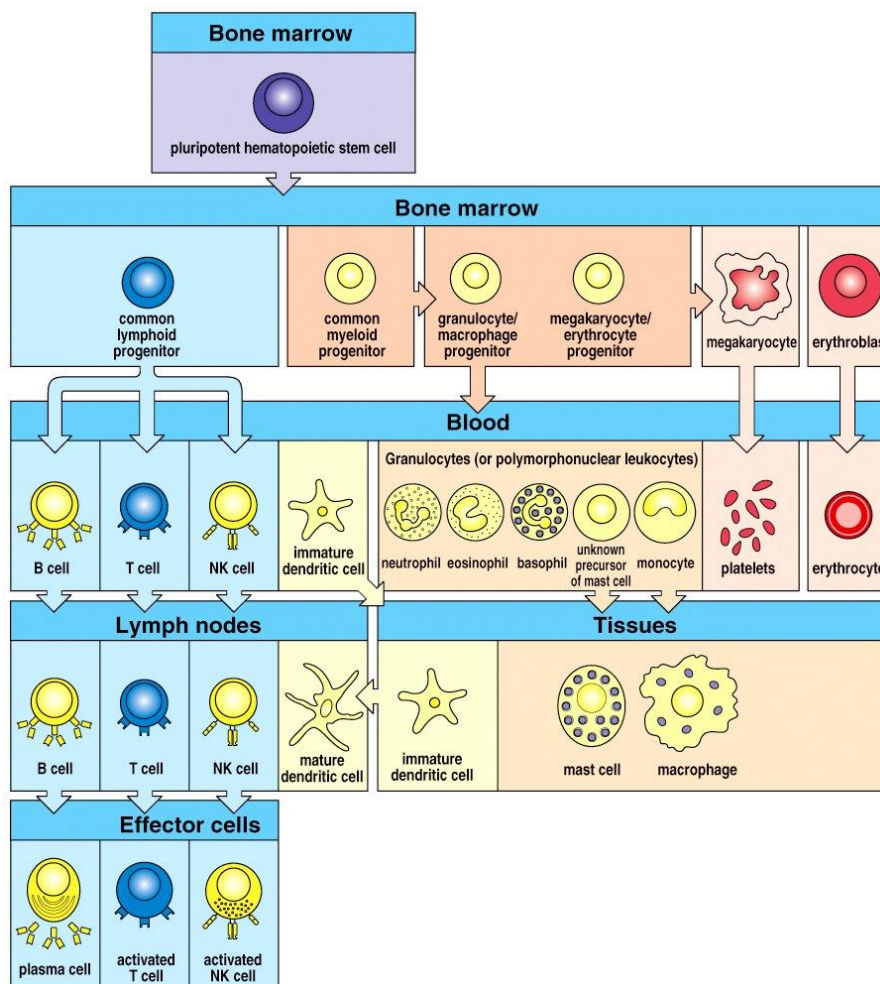


Figure 3: Illustration of hematopoiesis. Pluripotent stem cells can either divide into common lymphoid progenitor cells, which are the precursors for T-, B lymphocytes and NK cells or into common myeloid progenitor cells, which are precursors for granulocytes (basophils, eosinophils and neutrophils), mononuclear phagocytes (monocytes, macrophages, dendritic cells), erythrocytes and megakaryocytes (taken from Janeway et al., 2008).

1.5 The transcription factor NF- κ B

NF- κ B is an inducible transcription factor, which was first described in 1986 by Sen and Baltimore. They found NF- κ B as an inducible protein in LPS-stimulated pre-B cells interacting with a defined site in the κ immunoglobulin enhancer (Sen and Baltimore, 1986). Since its discovery a huge body of knowledge with several thousand publications has been gathered, describing upon others the functions of NF- κ B in the regulation of gene expression of growth factors and effector cytokines upon ligation of receptors involved in immunity (e.g TCR, B cell receptor, tumor necrose factor (TNF)-receptor, Toll/IL-1R family; Ghosh et al., 1998; Hayden and Ghosh, 2004).

NF- κ B is ubiquitously expressed in nearly all cell types and since its discovery responsive κ B sites have been described in promoters and enhancers of various genes mainly involved in immune and inflammatory responses (Ghosh et al., 1998).

NF- κ B is a dimer composed of members of the Rel family that consists of proteins sharing a sequence homology over a 300 amino acid long N-terminal Rel-homology domain (RHD) containing sequences needed for dimerization and DNA binding (Rushlow and Warrior, 1992). Until now, five members of the Rel-family are known: p50, p52, p65, RelB and c-Rel. These members are able to form homo- or heterodimers regulating distinct cellular functions (Mueller and Harrison, 1995).

Based on the amino acid sequence of the C-terminus, which either contains a transactivation domain (TAD) like in p65, RelB and c-Rel, or an ankyrin-repeat domain (ARD) as in p52 and p50, NF- κ B proteins can be divided into two groups (see Figure 4, Hayden and Ghosh, 2008). RelB is unique in as much as it is the only member containing a leucine zipper, which is needed together with TAD to gain full transactivation potential (Dobrzanski et al., 1993). TAD containing Rel-proteins are able to directly activate transcription (Sacconi et al., 2003). The proteins p100 and p105 are distinguished from other Rel family members by their ankyrin repeats that prevent nuclear import, but can be processed into the mature forms p52 and p50, respectively (Wan and Lenardo, 2009; Gilmore 2006). Since p50 and p52 lack a TAD, they have to form heterodimers with TAD-containing REL proteins to activate transcription of target genes. Otherwise, they can also form p50 and p52 homodimers to regulate gene transcription in a negative way by binding and occupying κ B sites of target genes (Yu et al., 2009).

The activation of NF- κ B depends on phosphorylation-induced degradation of inhibitory- κ B proteins, which sequesters NF- κ B in the cytoplasm in resting cells. Release of NF- κ B dimers enables their translocation into the nucleus where they bind to κ B sites on the DNA of target genes (Oeckinghaus and Ghosh, 2009).

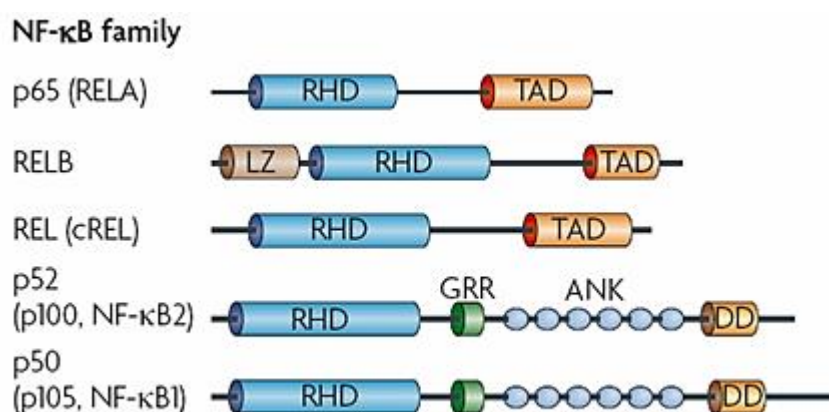


Figure 4: The members of NF- κ B/Rel family. NF- κ B is formed by two members of the REL protein family, whereby homo- or heterodimers are possible. RHD=Rel homology domain; LZ=leucine zipper; TAD=transactivation domain; ANK=Ankyrin repeat; DD=death domain; GRR=glycine-rich region (taken from Hayden and Ghosh, 2008).

1.6 Regulation of NF- κ B through inhibitory proteins (I κ Bs)

The activity of NF- κ B is regulated by inhibitory κ B proteins (I κ Bs). In unstimulated cells, NF- κ B is sequestered in the cytoplasm by binding to I κ Bs which mask the nuclear localization sequence of NF- κ B, preventing translocation of the protein into the nucleus. Thereby NF- κ B complexes cannot mediate their transcription factor activity by binding to κ B-sites in the DNA (Wan and Lenardo, 2010). I κ Bs can be divided into two groups – classical and atypical I κ Bs. Classical I κ Bs such as I κ B α , I κ B β and I κ B ϵ are localized in the cytoplasm and are proteolytically degraded upon stimulation, thereby demasking the NLS of the bound NF- κ B complex. Subsequently, NF- κ B dimers are translocated into the nucleus (Hayden and Ghosh, 2004). Atypical I κ Bs such as Bcl-3, I κ B ζ and I κ B $_{NS}$ act mainly in the nucleus and while they exhibit low expression in resting cells, they can be strongly induced following cell stimulation and specifically NF- κ B activation itself. They bind to NF- κ B dimers, which have previously been translocated into the nucleus and thus are thought to be able to modify and influence the transcriptional action of nuclear NF- κ B complexes (Ghosh and Hayden, 2008). Thus atypical I κ Bs add to the cell's spatial capability to regulate NF- κ B function even in the nucleus.

Common for all I κ Bs is the presence of a highly conserved ankyrin repeat domain (ARD) that mediates the interaction with NF- κ B proteins (Hinz et al., 2012). The ARD is one of the most frequent protein-protein interaction motifs and consists of 33 amino acids which are folded into a typical helix-loop-helix conformation (Mosavi et al., 2004; Hinz et al., 2012).

The classical human I κ Bs display N-terminal to the ARD an unfolded protein structure containing a signal response domain (degron) with conserved serine residues that are required for a stimulus-dependent phosphorylation by I κ B kinases (IKK, Hinz et al., 2012). Located at the C-terminal site of I κ B α and I κ B β are short acidic regions, that are referred to PEST sequences (rich in proline (P), glutamic acid (E), serine (S) and threonine (T)) needed for protein degradation (Rogers et al., 1986). The precursors p105 and p100 contain C-terminal NF- κ B inhibiting ANKs, thus they can act as I κ Bs as well (Siebenlist et al., 2005).

Regarding its function, it has been described that atypical I κ Bs can act as both activator and suppressor of NF- κ B-dependent target gene transcription (Ghosh and Hayden, 2008). Bcl-3 was first identified as a proto-oncogene overexpressed in B-cell chronic lymphocytic leukemia (Ohno et al., 1990). Bcl-3 was described for example to be induced upon stimulation with IL9 and IL4 in T cells and mast cells (Richard et al., 1999). Furthermore, IL10 induces Bcl-3 expression in macrophages and promotes anti-inflammatory responses (Dagvadorj et al., 2009). In this line, Bcl-3 can act as anti-inflammatory regulator in macrophages by attenuating LPS-induced pro-inflammatory cytokines (Wessells et al., 2004). It contains a well-conserved TAD and binds preferentially to p50 and p52 dimers in the nucleus (Nolan et al., 1993; Bours et al., 1993).

The second atypical I κ B containing a TAD is I κ B ζ (also called MAIL) which was identified to be rapidly induced in several murine organs and specifically in macrophages and B cells upon LPS stimulation (Kitamura et al., 2000). Moreover, I κ B ζ mRNA expression is also induced upon stimulation of several TLRs for instance by peptidoglycan (TLR2), flagellin (TLR5) or CpG DNA (TLR9, Yamamoto et al.,

2004). Like Bcl-3, it preferentially interacts with p50 and additionally with p65 and negatively regulates NF- κ B activity in order to prevent excessive inflammation (Yamazaki et al., 2001).

I κ B η was shown to be highly expressed in brain, lung, testis and ovary. I κ B η mRNA is constitutively expressed at basal levels and is slightly up-regulated by TLR signaling in macrophages (Yamauchi et al., 2010). Moreover, it is suggested that I κ B η preferentially binds to p50 and might function as a co-activator of NF- κ B (Hinz et al., 2012).

The atypical protein I κ B_{NS}, which is in the main focus of the present study is described in more detail in chapter 1.8.

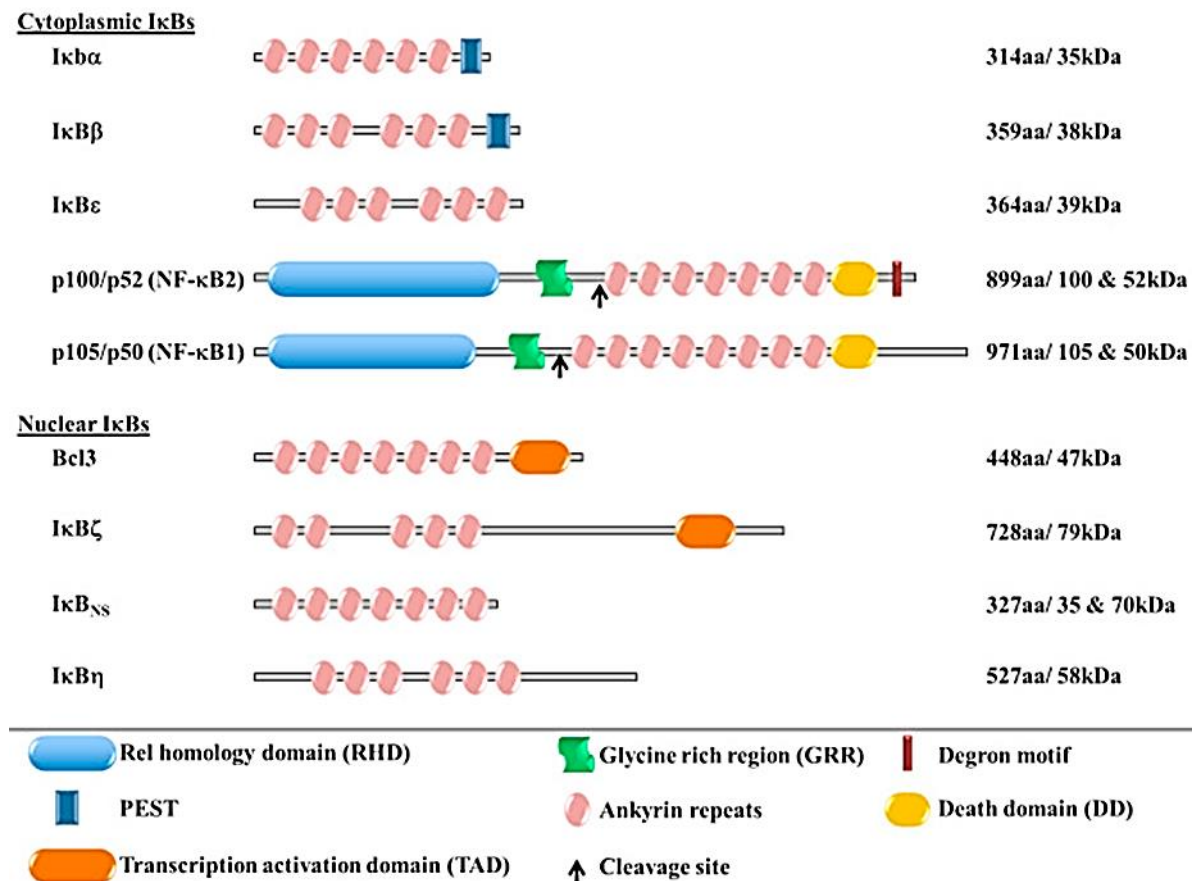


Figure 5: Overview about inhibitory κ B proteins based on their cellular localization in the cytoplasm and nucleus. Common feature of all I κ Bs is the presence of ankyrin repeat domains (taken from Annemann et al. 2016).

Taken together, atypical I κ Bs are stimulation-dependent inducible proteins and act mainly in the nucleus by binding to NF- κ B complexes, thereby they modulate NF- κ B-mediated gene transcription in a pleiotropic manner.

1.7 The classical NF- κ B pathway

The classical or canonical pathway of NF- κ B activation is inducible upon recognition of viral or microbial products by TLRs, inflammatory cytokines or antigen receptor engagement in T cells usually leading to the activation of p65 or cRel containing NF- κ B complexes (Oeckinghaus and Ghosh, 2009; Karin and Ben-Neriah, 2000). In resting cells, the NF- κ B dimers are sequestered in the cytoplasm by classical I κ Bs such as the best-studied I κ B α , which masks the NLS of the Rel proteins (Ghosh and Hayden, 2008). Upon activation with one of the above mentioned stimuli, the serine residues 32 and 36 of I κ B α become phosphorylated by an I κ B kinase (IKK) complex that consists of IKK α and IKK β and a non-catalytic regulatory subunit (NEMO/IKK γ) essential for the stimulus-response coupling of the kinase complex (Chen and Greene, 2004). Upon phosphorylation by the IKK, I κ B α becomes rapidly polyubiquitinated resulting in its proteasomal degradation (Kanarek and Ben-Neriah, 2012; Chen and Greene, 2004). The released NF- κ B translocates into the nucleus and binds promoter and enhancer regions that contain κ B consensus sequences and initiates transcription of dedicated target genes (Hayden and Ghosh, 2008; Bhatt and Ghosh, 2014). I κ B α itself is a negative feedback regulator that controls the duration of NF- κ B signaling and enables reactivation of NF- κ B resulting in oscillatory dynamics (Hoffmann et al., 2002; Fagerlund et al., 2015). In addition *de novo* synthesis of I κ B α is also induced by NF- κ B (Chen and Greene, 2004). Through I κ B α -mediated oscillatory nucleocytoplasmic shuttling NF- κ B complexes are retrieved from the nucleus by bidirectional transport across the nuclear membrane (Korwek et al., 2016). Termination of NF- κ B signaling and displacement from the DNA are achieved by ubiquitination, subsequent proteasomal degradation and by small ubiquitin-like modifiers (SUMO) E3 ligases, which decrease the transcriptional activity (summarized in Figure 6, Ghosh and Hayden, 2008).

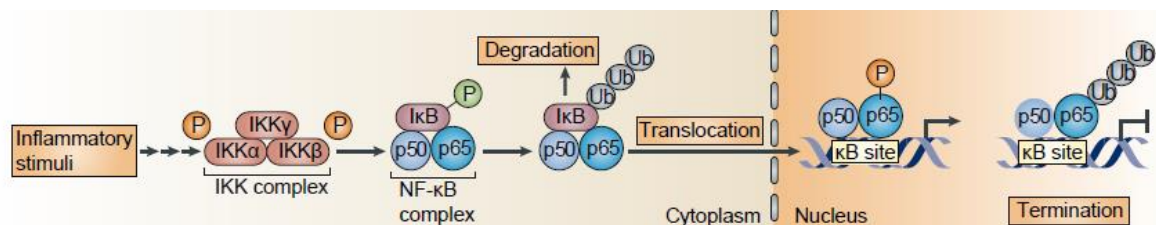


Figure 6: Overview about the activation cascade of the classical NF- κ B signaling pathway (taken from Ghosh and Hayden, 2008).

Next to the classical pathway, a second so-called non-canonical NF- κ B activation pathway is known, which activates RelB/p52 NF- κ B complexes using a mechanism relying on the inducible processing of p100 instead of the degradation of I κ B α (Sun, 2011). In contrast to the classical NF- κ B pathway, the non-canonical pathway is independent from IKK γ /NEMO in the IKK complex, but depends on IKK α (Gilmore, 2006). A NF- κ B-inducing kinase (NIK) is responsible for the phosphorylation of IKK α , which in turn mediates the processing of p100 to p52, leading to the proteolysis and release of the p52/RelB complex and its translocation into the nucleus, where it binds to κ B sites (Gilmore, 2006). In contrast to the classical pathway, which is activated by a variety of stimuli, the non-canonical NF- κ B pathway is activated exclusively by specific receptors and here mainly by TNFR superfamily receptors (Sun, 2011).

1.8 The atypical non-structural κ B protein $I\kappa B_{NS}$

1.8.1 The structure of $I\kappa B_{NS}$

The $I\kappa B_{NS}$ protein is encoded by the *Nfkbid* gene (nuclear factor of kappa light gene enhancer in B cells inhibitor delta) located on the murine chromosome 7 and is comprised of 12 exons (NCBI, <https://ncbi.nlm.nih.gov/gene/243910>). $I\kappa B_{NS}$ was first described in 2002 by Fiorini and colleagues, who identified transcription of $I\kappa B_{NS}$ upon peptide stimulation of immature T cells triggering negative selection of thymocytes (Fiorini et al., 2002). The protein consists of 7 ankyrin repeat domains and with 327 amino acids it is the smallest member of the BCL-3 family (Fiorini et al., 2002). Due to its nuclear localization, it has been proposed that $I\kappa B_{NS}$ contains a nuclear localization signal in its N-terminal region (Yamamoto and Takeda, 2008). On the other hand, Park and colleagues found also a single putative NLS located in the C-terminal region with a sequence well-conserved between mouse and human $I\kappa B_{NS}$ (Park et al., 2014). Furthermore, they reported that $I\kappa B_{NS}$ is an unstable protein, which is degraded by the proteasome similar to the degradation mechanisms known from the classical $I\kappa B\alpha$ involving a PEST sequence in the N-terminal region (Park et al., 2014). The complete 3D protein structure of $I\kappa B_{NS}$ remains elusive until now. However, Manavalan and colleagues performed *in silico* analyses to define structural relationships between cytoplasmic and nuclear $I\kappa B$ proteins. Moreover, to preconceive a potential protein structure of $I\kappa B_{NS}$ a superimposition analysis with a known structural template for the atypical protein Bcl-3 was performed indicating that both proteins have a similar shape, but also variations which are located mainly within the loops of the ANK repeats (see Figure 7, Manavalan et al., 2010).

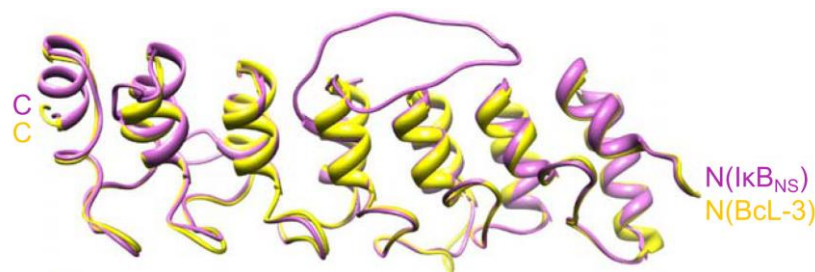


Figure 7: *In silico* structural prediction of $I\kappa B_{NS}$. Superimposition model of Ankyrin repeat domains with a known common structural template of the atypical inhibitory protein Bcl-3. $I\kappa B_{NS}$ is colored in purple and Bcl-3 in yellow (adapted from Manavalan et al., 2010).

Interestingly, Schuster and colleagues could show that T cells stimulated with phorbol 12-myristate 13-acetate (PMA) and ionomycin for 4 h express two $I\kappa B_{NS}$ proteins with different sizes. A 35 kDa $I\kappa B_{NS}$ protein was present in the cytoplasm and a 70 kDa isoform in the nucleus of the T cells (Schuster et al., 2012). This potentially homodimeric twice as large 70 kDa isoform cannot be deduced from the primary amino acid sequence of the translated *Nfkbid* mRNA itself. Since both the 35 kDa and the 70 kDa isoforms are completely missing in $I\kappa B_{NS}$ -deficient T cells, it is indicative that the 70 kDa protein is indeed likely to be an *Nfkbid* gene product, which interacts with NF- κ B complexes in the nucleus (Schuster et al., 2012). The underlying protein-biochemical reasons of this phenomenon are likely to remain elusive until the actual 3D protein structure has been solved experimentally.

1.8.2 Cell-type specific effects of I κ B_{NS}

I κ B_{NS} was first discovered in 2002 in context of peptide-triggered negative but not positive selection of thymocytes, where it was rapidly expressed upon TCR triggering (Fiorini et al., 2002), rendering T cells the first cell type in which I κ B_{NS} was found to have a functional impact on. However, when analyzing I κ B_{NS}-deficient mice regarding cell number or distribution of T cell subpopulations in thymus, spleen or lymph nodes no significant differences were reported between WT and I κ B_{NS}-deficient mice (Touma et al., 2007). Interestingly, the *in vitro* stimulation of I κ B_{NS}-deficient thymocytes and lymphatic T cells with plate-bound anti-CD3 ϵ plus soluble anti-CD28 resulted in a reduced proliferation and diminished expression of IL2 and IFN γ compared to I κ B_{NS}-sufficient T cells (Touma et al., 2007). Schuster and colleagues reported that I κ B_{NS} is necessary for the development of thymic derived and induced Foxp3⁺ Tregs, in which binding of I κ B_{NS} together with p50 and c-Rel and with the conserved non-coding sequence-3 to the Foxp3 promoter leads to a full transcriptional activation of the *Foxp3* locus. *Nfkbid*-deficient mice exhibit a reduction of mature Tregs and an increase of precursor cells due to the impaired transition into Foxp3⁺ Treg cells. Despite the reduction of mature Treg cells, I κ B_{NS} seems dispensable for their functionality, because *Nfkbid*-deficient mice do not develop T cell-mediated autoimmunity (Schuster et al., 2012).

On the other hand, it has been reported that I κ B_{NS} is crucial for the differentiation of CD4⁺ T cells into Th17 cells. Annemann and colleagues showed a high expression of I κ B_{NS} in Th17 cells and in its absence reduced frequencies of IL17A-producing T cells were observed under Th17 polarizing conditions in *in vitro* studies and in *in vivo* *Citrobacter rodentium* infection in mice. Mice lacking I κ B_{NS} showed an increased bacterial burden, but however a diminished tissue damage due to impaired Th17 and IL17A⁺IFN γ ⁺ T cell formation (Annemann et al., 2015).

In line with this, Kobayashi and colleagues showed that I κ B_{NS}^{-/-} T cells were less capable of generating Th17 cells in response to transforming growth factor (TGF)- β and IL6 stimulation *in vitro*. Additionally, they described a resistance of I κ B_{NS}-deficient mice to develop Th17-dependent experimental autoimmune encephalomyelitis (EAE) due to secondary effects of the impaired Th17 cell generation resulting in reduced immunopathology (Kobayashi et al., 2014).

Next to T cells, some studies investigated the impact of I κ B_{NS} on macrophage function. Hirotani and colleagues found that I κ B_{NS} is constitutively expressed in colonic lamina propria macrophages where it is thought to have suppressive functions on inflammatory responses in the intestine. Moreover, they showed that I κ B_{NS} suppresses LPS-induced IL6 production in macrophages through constitutive binding to the *IL6*-promoter together with p50 (Hirotani et al., 2005).

In line with that, Kuwata and colleagues observed that I κ B_{NS}^{-/-} selectively inhibits the expression of IL6, IL12p40 and IL18 in macrophages upon LPS stimulation. I κ B_{NS}-deficient mice succumbed after LPS injection due to an endotoxin shock possibly induced by the sustained production of IL6 and IL12p40. Moreover, oral administration of dextran sulfate sodium (DSS) that induces colitis in mice resulted in a severe intestinal inflammation caused by disruption of the epithelial barrier possibly due to the continuous production of pro-inflammatory mediators (Kuwata et al., 2006).

Touma and colleagues described an impact of I κ B_{NS} on the B cell lineage leading to reduced proliferation in response to stimulation with LPS or anti-CD40 and reduced levels of serum IgM and

IgG3 immunoglobulins in absence of I κ B_{NS}. Moreover, I κ B_{NS}-deficient mice exhibit defects in the development of B1 and marginal zone B cells and the differentiation to plasma B cells (Touma et al., 2011).

A recently published study described that I κ B_{NS} can either negatively or positively regulate the pathologic outcome of asthma dependent on its expression in hematopoietic or non-hematopoietic cells. Yokota and colleagues observed that I κ B_{NS} is important in the suppression of house-dust-mite induced allergic airway inflammation shown by exacerbated eosinophilic airway inflammation in mice lacking I κ B_{NS}. In contrast, absence of I κ B_{NS} in non-hematopoietic cells resulted in attenuation of airway hyper-responsiveness due to impaired production of Muc5a, a hallmark mucin in asthmatic airways (Yokota et al., 2017).

In summary, I κ B_{NS} can act as activator as well as suppressor of NF- κ B mediated gene transcription. Its dedicated effects are cell type specific and dependent on various factors such as stimulatory conditions and the *in vitro* or *in vivo* experimental set-up in which I κ B_{NS} effects are studied. Although several studies already revealed relevance of I κ B_{NS} for a few immune cell types under certain experimental conditions, a thorough integrated description of I κ B_{NS} expression and function in context of an *in vivo* orchestrated immune response is still missing, especially in the context of systemic infections.

1.9 Aims of the thesis

The development and function of immune cells is tightly regulated by transcription factors such as NF- κ B, that induces a specific gene expression profile involved in processes like inflammation, proliferation and immune responses towards pathogens. The activation of NF- κ B is governed by inhibitory κ B proteins. The classical ones such as κ B α , which act in the cytoplasm, are well-characterized whereas the function and regulatory properties of the non-classical κ B proteins, such as κ B_{NS}, in immune cells are still incompletely understood. Most scientific work published so far described an impact of κ B_{NS} on dedicated T cell subsets such as regulatory T cells. Moreover, it was also shown that κ B_{NS}-deficient T cells are hyporesponsive under certain experimental conditions, however, most of these studies were performed *in vitro*. Published data led to the assumption that κ B_{NS} might contribute to the development and function of CD4⁺ and CD8⁺ T effector cells. To extend existing knowledge on κ B_{NS}-mediated effects on the *in vivo* expansion and pathogen-specific T effector cell differentiation during systemic bacterial infection, an *in vivo* approach based on the adoptive transfer of T cells carrying a transgenic TCR specific for the model antigen ovalbumin (OVA) in combination with recombinant *Listeria monocytogenes* expressing the cognate antigen (LM-OVA) will be used.

In a first approach, proliferation and activation of OVA-specific κ B_{NS}-proficient and κ B_{NS}-deficient CD4⁺ and CD8⁺ T cells will be analyzed *in vitro* by stimulation with the cognate OVA peptides. Proliferation will be assessed by CFSE dilution and activation status by flow cytometric analyzes of CD44, CD25 and IFN γ expression. In order to study the *in vivo* impact of κ B_{NS} on T cell activation and development of pathogen-specific effector function, OVA-specific κ B_{NS}-proficient and κ B_{NS}-deficient CD4⁺ and CD8⁺ T cells will be isolated from TCR transgenic donor mice and adoptively transferred into wildtype recipients. After adoptive transfer, recipient mice will be infected with recombinant LM-OVA to provide antigen-specific and at the same time pathogen-specific stimulation of the T cells. At different times post infection liver and spleen, the main replication sites of LM, will be sampled and the proliferation and activation status of the adoptively transferred OVA-specific CD4⁺ and CD8⁺ T cells in response to *in vivo* LM-OVA encounter will be assessed. For this purpose, proliferation will be analyzed by CFSE dilution and by flow cytometric acquisition of the expression of effector molecules such as CD44, CD25, PD1, IL2, IFN γ and TNF α . Moreover, the bacterial burden will be determined in spleens of recipient mice that receive either CD4⁺ or CD8⁺ T cells proficient or deficient for κ B_{NS} in order to analyze if κ B_{NS} in T cells has any impact on pathogen clearance. To overall conclude the effector status of CD8⁺ T cells, the formation of cytotoxic T cell function in response to LM-OVA infection will be analyzed.

In summary, the first part of the thesis will give a detailed overview about the impact of κ B_{NS} on antigen-specific proliferation and activation of CD4⁺ and CD8⁺ effector T cells during systemic *Listeria monocytogenes* infection.

In addition to adaptive immune cells, previous studies described as well an impact of I κ B_{NS} on the function of dedicated subsets of the innate immune response. Nevertheless, so far no comprehensive knowledge has been gathered with respect to the role of I κ B_{NS} in innate immune responses during systemic bacterial infection.

To this end, WT and I κ B_{NS}-deficient mice will be infected with *Listeria monocytogenes*. First the overall health status and survival will be monitored to elucidate if I κ B_{NS} has a general impact on the outcome of a systemic bacterial infection. Moreover, detailed analyses of several relevant parameters will be addressed including pathogen control, immunopathology, cytokine profile and the cellular composition of liver and spleen during the course of LM infection. To overall complete this picture, detailed transcriptome analyzes will be performed from liver samples to identify potential I κ B_{NS}-related differences in the immune response based on differential gene regulation in response to LM infection. Moreover, the expression of I κ B_{NS} itself will be determined in hematopoietic and non-hematopoietic cell fractions of the liver. To complete these data, promoter activity of I κ B_{NS} will be measured in a broad set of leukocyte subsets both in the steady state as well as during the course of LM infection making use of a newly developed reporter mouse. Taken together, the second part of the thesis will provide detailed knowledge regarding the impact of I κ B_{NS} on immune responses induced during systemic *in vivo* LM infection.

In summary, this thesis will address two major objectives:

- Aim 1:** Deciphering the role of I κ B_{NS} on antigen-specific activation, proliferation and effector function of CD4⁺ and CD8⁺ T cells in the context of infection
- Aim 2:** Elucidating the impact of I κ B_{NS} on pathogen-specific innate immune responses during the course of *Listeria monocytogenes* infection.

2. Materials

2.1 Consumables

Table 1: Chemicals

Product	Catalog number	Manufacturer
β-Mercaptoethanol	1001090202	Sigma-Aldrich
Bacto™ agar	214010	BD Biosciences
Bacto™ Brain Heart Infusion	237200	BD Biosciences
BD FACS™ Clean	340345	BD Biosciences
BD FACS™ Flow	342003	BD Biosciences
BD FACS™ Rinse	340346	BD Biosciences
BD FACS™ Shutdown	334224	BD Biosciences
Brefeldin A	420601	BioLegend
CFSE	V12883	Invitrogen
Collagenase A	1108886601	Roche
DNAse I	D5025-15kU	Sigma Aldrich
DMSO	A9941	Carl Roth
Easycoll	L6145	Biochrom
Ethanol, absolut (p.a.)	2246.1000	CHEMSOLUTE®
EDTA	E6758-500G	Sigma-Aldrich
FCS	P4047500	PAN Biotech
Fixable Viability Dye eFlour® 780	65-0865-14	eBioscience
Gentamicin	P11-004	PAA
Igepal® CA-630	18896	Sigma-Aldrich
Glutamax IMDM	31980-022	Gibco
Ionomycin	I0634	Sigma-Aldrich
Lane Marker Reducing Sample Buffer	39000	Thermo Scientific
OT-I peptide	-	synthesized at HZI
OT-II peptide	-	synthesized at HZI
Paraformaldehyde	252549-1L	Sigma-Aldrich
PBS tablets	18912-014	Gibco
Penicillin-Streptomycin	15070-063	Gibco/ Invitrogen
Percoll	17-0891-01	GE Healthcare
PMSF	8553	Cell Signaling
RLT buffer (RNeasy Lysis buffer)	79214	Qiagen
RNAlater	76106	Qiagen
Triton X-100	3051.2	Carl Roth
TWEEN 20	A1379-100mL	Sigma-Aldrich
Trypan blue	15250-061	Gibco

Table 2: Kits

Product	Catalog number	Manufacturer
CD4 ⁺ T cell Isolation kit	130-104-454	Miltenyi Biotec
CD8a ⁺ T cell Isolation kit	130-104-075	Miltenyi Biotec
CD45 Microbeads	130-052-301	Miltenyi Biotec
cDNA synthesis kit	04379012001	Roche
FluoReporter® lacZ Flow Cytometry kits	F-1930	Molecular Probes™
FastStart Essential DNA Green Master	06402712001	Roche
Liver dissociation kit	130-105-807	Miltenyi Biotec
RNeasy Mini kit	74104	Qiagen

2.2 Technical devices

Table 3: Technical devices

Device	Model	Manufacturer
autoMACS	Pro separator	Miltenyi Biotec
Blotting chamber	REL-SD20	Carl Roth
Centrifuge	Allegra® X-15R	Beckman Coulter
Centrifuge	Multifuge® 1 S-R	Heraeus
Clean bench	HERAsafe® KS	Heraeus
CO ₂ incubator	NU-8500E	Integra Biosciences
Counting chamber	Neubauer	Marienfeld Superior
Dispenser	POLYTRON® PT 3100 D	KINEMATICA AG
Flow cytometer	BD FACS Canto™ II	BD Biosciences
Flow cytometer	BD LSRFortessa™	BD Biosciences
gentleMACS	octo dissociator with heaters	Miltenyi Biotec
Incubation shaker	Ecotron	INFORS HT
Laboratory balance	Pioneer®	Ohaus
Magnetic stirrer	C-MAG HS7	IKA
Microscope	CX21	Olympus
Micro centrifuge	5417R	Eppendorf
pH measuring instrument	EL20	Mettler Toledo
Plate reader	Synergy HT	BioTek Instruments
Roller mixer	SRT9	Stuart
Shaker	DOS-10L	neolab
Spectrophotometer	GeneQuant™ pro	Amershan Biosciences
Spectrophotometer	ND-1000	NanoDrop Technologies
Suction pump	Vacusafe	Integra Biosciences
Thermocycler	LightCycler® 480 II	Roche
Thermomixer	Thermomixer comfort	Eppendorf

Transfer membrane	Immobilon®,PVDF, 0.45 µm	Merck Millipore
Vortex	Vortex Genie 2	Scientific Industries
Water bath	WNE 7	Memmert

2.4 Antibodies

In the following section all used antibodies are listed. Every antibody was titrated prior to usage to find the optimal antibody staining concentration.

Table 4: Antibodies used for purity check of adoptively transferred OVA-specific T cells

Antibody	Conjugation	Clone	Manufacturer
CD8a/ CD4	PerCP-cy5.5	53-6.7/ RM4-5	BioLegend
TCR Vα2	PE-Cy7	B20.1	eBioscience
TCR β5.1/5.2	APC	MR9-4	BioLegend
CD44	FITC	IM7	BioLegend
CD25	PE	PC61	BioLegend
CD62L	Biotin	MEL-14	BioLegend
Streptavidin	BV510	-	BioLegend

Table 5: FACS-panel used in the adoptive transfer experiments

Antibody	Conjugation	Clone	Manufacturer
CD16/CD32	-	93	BioLegend
CD8a	BV421	53-6.7	BioLegend
CD4	BV421	GK1.5	BioLegend
CD90.1/Thy1.1	PE-Cy7	OX-7	BioLegend
CD44	Biotin	IM7	BioLegend
CD25	PerCP-Cy5.5	PC61	BioLegend
Streptavidin	BV510	-	BioLegend
IFNγ	APC	XMG1.2	BioLegend
IL2	PE	JES6-5H4	BioLegend
PD-1	Biotin	29F.1A12	BioLegend
TNFα	APC	MP6-XT22	BioLegend

Table 6: FACS-panel for characterization of cellular influx during *Listeria*-infection

Antibody	Conjugation	Clone	Manufacturer
NKp46	Biotin	29A1.4	BioLegend
Ly6C	PerCP-Cy5.5	HK1.4	BioLegend
CD24	PE	M1/69	BioLegend
CD8	PE-Cy5	53-6.7	BioLegend
CD11c	APC	HL3 / N418	BioLegend

Ly6G	AF700	1A8	BioLegend
CD11b	APC-Cy7	M1/70	BioLegend
CD64	BV421	X54-5/7.1	BioLegend
CD4	BV510	RM4-5	BioLegend
CD45	BV605	30-F11	BioLegend
IA/IE	BV650	M5/114.15.2	BioLegend

2.5 Buffers and Media

Table 7: IMDM complete

Component	Final concentration
IMDM + GlutaMAX	500 mL
FCS	10% (v/v)
Penicillin/ Streptomycin	1% (v/v)
Gentamicin	0.1% (v/v)
β - Mercaptoethanol	0.1% (v/v)

Table 8: FACS buffer

Component	Final concentration
PBS	
FCS	2.0% (v/v)
EDTA	2 mM

Table 9: FACS staining medium for intracellular lacZ activity assay

Component	Final concentration
PBS	
FCS	4.0% (v/v)
HEPES	10 nM

2.6 Mouse models

All experiments were performed in strict accordance with the institutional guidelines and approved by the "Landesamt für Verbraucherschutz, Sachsen-Anhalt" under the license "42502-2-1242" or the guidelines of the "Landesamt für Verbraucherschutz und Lebensmittelsicherheit, Niedersachsen" under the license "33.19-42502-04-14/1545".

Constitutive $I\kappa B_{NS}$ knockout mice

Wildtype and constitutive $I\kappa B_{NS}$ knockout mice on C57BL/6 genetic background were bred at the animal facility of the Helmholtz Centre for infection research (HZI) Braunschweig, Germany. For experiments, 8-20 weeks old female animals were transferred to the animal facility (Zentrales

Tierlabor) of the University Hospital Magdeburg and maintained under specific pathogen-free conditions in environmentally-controlled clean rooms.

Mice for adoptive transfer experiments

For the adoptive T cell transfer experiments TCR-transgenic OT-I and OT-II mice, as well as OT-I and OT-II mice crossed on $\text{IkB}_{\text{NS}}^{-/-}$ background were used as T cell donors. Breeding and housing of transgenic mice were carried out in the animal facility of the HZI. Mice of the OT-II strain harbor CD4^+ T cells that express a transgenic T cell receptor specifically recognizing the amino acid sequence ISQAVHAAHAEINEAGR of the chicken ovalbumin protein (OVA₃₂₃₋₃₃₉) on MHC II molecules. In case of the OT-I strain the transgenic T cell receptor is restricted to MHC I and recognizes a specific CD8/MHC I epitope of ovalbumin (OVA₂₅₇₋₂₆₄) with the amino acid sequence SIINFEKL.

As recipient mice for adoptive T cell transfers 8-12 weeks old female wildtype C57BL/6OlaHsd from Harlan Laboratories (since 2015 Envigo) and C57BL/6 mice from Janvier Labs were used. Mice were maintained under specific pathogen-free conditions in the animal facility of the University Hospital Magdeburg.

$\text{Nfkbid}^{\text{LacZ}}$ reporter mice

An IkB_{NS} reporter mouse line from the EUCOMM consortium, called $\text{Nfkbid}^{\text{tm}1\text{a(EUCOMM)Wtsi}}$, kindly provided by Prof. Ingo Schmitz (Helmholtz Centre for Infection Research, Braunschweig), here referred as $\text{Nfkbid}^{\text{LacZ}}$ was used to directly analyze the promoter activity of the *Nfkbid* gene encoding for the IkB_{NS} protein. $\text{Nfkbid}^{\text{LacZ}}$ mice have a promoter-less cassette containing a LacZ coding sequence, which encodes a β -galactosidase, which is knocked into one allele of the *Nfkbid* locus allowing the indirect detection of *Nfkbid* promoter activity through assessment of enzymatic β -galactosidase activity. This can be achieved by using surrogate galactose substrate analogs with fluorescent features like Fluorescein Di-D-Galactopyranoside (FDG), which releases fluorescein dye upon lacZ cleavage. Though $\text{Nfkbid}^{\text{LacZ}}$ mice only have one functional allele for the *Nfkbid* gene they show no specific phenotype and a normal development at least under steady state conditions. Breeding and housing were carried out at the animal facility of the HZI. For infection experiments female mice at the age of 10-20 weeks were used.

Conditional $\text{IkB}_{\text{NS}}^{-/-}$ mice- NSflLysmC

NSflLysmC mice were kindly provided by Prof. Ingo Schmitz (Helmholtz Centre for Infection Research, Braunschweig). The conditional $\text{IkB}_{\text{NS}}^{-/-}$ mouse strain NSflLysmC ($\text{Nfkbid}^{\text{fl/fl}} \times \text{LysMCre}^{\text{tg/wt}}$) created by the EUCOMM consortium was used with a specific deletion of IkB_{NS} in *Lyz2* expressing cells, i.e. macrophages and granulocytes. Mice developed normal and show no specific phenotype in steady state conditions. Breeding and housing were carried out at the animal facility of the HZI. For preliminary infection studies, female and male mice at the age of 10-17 weeks were transferred to the animal facility of the University Hospital Magdeburg.

3. Methods

3.1 Genotyping of inbred mouse strains

Genotyping of the inbred mouse strains was performed by using the KAPA Mouse Genotyping Hot Start kit. A small ear biopsy was digested by adding 2 μL Express Extract enzyme (1 U/ μL) and 10 μL 10x KAPA Express extract buffer. The solution was filled to 100 μL with water and heated for 10 min at 75°C in a thermomixer. This step was followed by another heating step (95°C for 5 min). The solution was mixed and centrifuged for 1 min at full speed. The DNA containing supernatant was transferred to a new tube and 1 μL was used directly as template for the amplification of the respective genotyping locus via PCR.

Table 10: Composition of the PCR mix for the amplification reaction

Component	Volume [μL]
Genotyping Mix	12,5
MgCl ₂ (25 mM)	0,5
Primer sense	1,25
Primer anti-sense	1,25
DMSO	1,5
water	8,5
template	1,0

Table 11: Used oligonucleotides primers for genotyping of mice

oligonucleotide	Sequence 5' → 3'
IkBNS_Neo	AAG CGC ATG CTC CAG ACT GCC TT
IkBNS_rev	CAT TTA GTG CCC CTG GAC AT
IkBNS_fwd	CTC CTC CCA GGC TGT GTT TA
NFKBID_LZ_fwd	TCC ATG AGG TAG GGA TGG AGA GTA
NFKBID_LZ_rev	CTC CCA GTG CTG ATA TTA CAG GCA
NFKBID_LZ_rev1	CCT TCC TCC TAC ATA GTT GGC AGT

Table 12: Thermal cycler program used for genotyping PCR

Cycle step	Temperature	Time	# of cycles
Initial denaturation	95°C	3 min	 35
Denaturation	95°C	15 sec	
Annealing	60°C	15 sec	
Elongation	72°C	15°sec	
Terminal elongation	72°C	10 min	

3.2 Organ isolation and single cell preparation

Mice were euthanatized by inhalation of CO₂. Prior to collection of the organs a transcardial perfusion with 10 mL ice-cold PBS was performed. Afterwards, the respective organs were carefully removed and stored until further usage in PBS on ice.

Spleens were weighed and subsequently meshed through a 100 µm cell strainer. The cell strainer was flushed with 10 mL PBS and the cell suspension was transferred into a falcon tube. The cells were centrifuged (300 xg, 4°C, 10 min) and supernatant was discarded. An erythrocytes lysis was performed by resuspending the cell pellet in 1 mL ACK buffer. The falcon tube was rinsed with an additional 1 mL ACK buffer and after 2 min the lysis was stopped by adding at least 10 mL PBS. Cells were centrifuged (300 xg, 4°C, 10 min), supernatant was discarded and cell pellet was resuspended in PBS. The liver was meshed through a 70 µm cell strainer into a 50 mL falcon tube and the strainer was flushed with 30 mL PBS. The liver samples were centrifuged (300 xg, RT, 10 min) and the supernatant was discarded. The pellet was resuspended in 10 mL 0.2% NaCl for erythrocytes lysis. After 10 sec lysis was stopped by adding 10 mL 1.6% NaCl and 10 mL PBS.

The cell suspension was centrifuged (300 xg, RT, 10 min) and the supernatant discarded. Leukocytes from liver samples were obtained by a density gradient centrifugation using Easycoll (density: 1.124 g/mL). To this end, the cell pellet was resuspended in 10 mL 35% (v/v) Easycoll/PBS solution (density: 1.041 g/mL). Then the cell suspension was centrifuged (360 xg, RT, 20 min, without brake). The supernatant was discarded and the cell pellet containing the leukocytes was washed with 10 mL PBS and centrifuged (300 xg, RT, 10 min). Finally, the cells were resuspended in PBS and stored on ice until further analysis.

3.3 CD4⁺ and CD8⁺ T cell isolation by magnetic activated cell sorting (MACS)

In order to isolate naïve OVA-specific CD4⁺ or OVA-specific CD8⁺ T cells the magnetic activated cell sorting technology (MACS) was used. For this purpose, the CD4⁺ and CD8⁺ T cell isolation kits from Miltenyi were used according to manufacturer recommendations. Initially, spleens, inguinal and cervical lymph nodes from OT-I x WT, OT-I x IκB_{NS}^{-/-}, OT-II x WT or OT-II x IκB_{NS}^{-/-} donor mice were collected. Lymphocytes from spleen samples were isolated as described above (section 3.2). Lymph nodes were meshed through a 70 µm cell strainer, washed with 10 mL PBS and collected by centrifugation (300 xg, 4°C, 10 min). The lymph node cells derived from a certain mouse genotype were pooled together with the respective splenocytes fraction. Then, the pooled cell suspension was adjusted to 1x10⁷ cells in 400 µL FACS buffer containing 1:500 diluted biotinylated CD25 antibody for depletion of natural occurring regulatory T cells and 100 µL biotinylated antibody cocktail against epitopes present on the surface of dendritic cells, macrophages, NK cells or B cells. The cell suspension containing the antibodies was incubated at 4°C for 5 min. Then, 300 µL FACS buffer and 200 µL streptavidin-labeled microbeads were added to the cells followed by 10 min incubation at 4°C. For the separation process the autoMACS device was used applying the isolation program “*depletes*”. This strategy allows the isolation of untouched T cells not being bound to any antibodies. Aliquots of cells before and after MACS were transferred to a 96-well round-bottom plate followed by centrifugation (300 xg, 4°C, 5 min). Afterwards the cells were stained with 100 µL of the antibody

cocktail according to table 4 and incubated in the dark for 10 min. To visualize the non-fluorescent biotin-conjugated anti-CD62L antibody later on in FACS, the cells were stained with 100 μ L fluorescently labeled streptavidin for 10 min in the dark. After a final washing step, the cells were resuspended in 200 μ L FACS buffer and assessed by BD FACS Canto™ II flow cytometer. This staining allows to analyze the isolation efficiency and purity of the MACS-enriched cell populations and to characterize the phenotype of cells prior injection to the recipient mice.

3.4 *In vitro* stimulation of T cells

Spleens of OT-I x WT, OT-I x $I\kappa B_{NS}^{-/-}$, OT-II x WT and OT-II x $I\kappa B_{NS}^{-/-}$ mice were sampled. Splenocytes were isolated and enriched for T cells using the CD4⁺ T cell isolation kit or the CD8⁺ T cell isolation kit from Miltenyi according to manufacturer recommendations (refer to 3.3). After the isolation, OT-II CD4⁺ T cells and OT-I CD8⁺ T cells were stained with Carboxyfluorescein succinimidyl ester (CFSE, refer to 3.5) with a final concentration of 2.5 μ M. 2×10^5 CFSE-stained cells were co-cultured with 3×10^5 30 Gy irradiated syngeneic splenocytes from wildtype C57BL/6 mice in 96 well round-bottom plates. One day prior to stimulation, the 96 well plates were coated with 0.25 μ g/mL anti-CD3 ϵ antibody. On the day of stimulation 1 μ g/mL anti-CD28 antibody was added to the culture. For antigen-specific stimulation conditions specific OVA-peptides were used. CD4⁺ T cells were stimulated with OVA₃₂₃₋₃₃₉ peptide with the amino acid sequence ISQAVHAAHAEINEAGR (10 μ g/mL, 1 μ g/mL, 0.1 μ g/mL) and CD8⁺ T cells were stimulated with different concentrations of the peptide OVA₂₅₇₋₂₆₄ with the amino acid sequence SIINFEKL (100 ng/mL, 1 ng/mL, 0.1 ng/mL).

The cells were incubated for at least 24 h and maximally for 72 h at 37°C for proliferation analysis and to ensure viability of cells. Approximately 4 h before FACS analysis of the cells, the supernatant was discarded from culture plates and 100 μ L fresh IMDM medium containing Brefeldin A (1 μ g/mL) was added to the cells and incubation at 37°C was continued. The addition of Brefeldin A blocks the cytokine transport and ensures that the produced cytokines accumulates in the Golgi apparatus.

3.5 CFSE staining of T cells

T cell proliferation was measured by staining the OVA-specific CD4⁺ or CD8⁺ T cells with the fluorescent cell staining dye carboxyfluorescein succinimidyl ester (CFSE). CFSE is able to pass the cell membrane and binds through covalent esterification to intracellular proteins. Upon cell division the initial amount of CFSE dye is equally distributed between the mother and the daughter cell resulting in two cells with half of the initial dye concentration. Thus, cell division can be followed by means of CFSE dye fluorescence by FACS analysis. For the CFSE staining procedure the cells were resuspended in 4 mL IMDM without fetal calf serum (FCS) to prevent an unspecific interaction of serum proteins with the CFSE dye. CFSE was added to a final concentration of 2.5 μ M. Then, the cells were gently mixed and incubated for 8 min at 37°C protected from light. The CFSE staining was stopped by adding at least twice the volume of FCS followed by 5 min incubation at 37°C. Afterwards the cells were washed twice with PBS. Finally, the cells were resuspended in PBS and stored on ice protected from light until further usage.

3.6 Adoptive T cell transfers

For adoptive T cell transfers OT-II x WT, OT-II x $\text{I}\kappa\text{B}_{\text{NS}}^{-/-}$, OT-I x WT and OT-I x $\text{I}\kappa\text{B}_{\text{NS}}^{-/-}$ mice were used as donors. Spleens, inguinal and cervical lymph nodes were isolated and OVA-specific CD4^+ and OVA-specific CD8^+ T cells were isolated by MACS using the CD4^+ and CD8^+ T cell isolation kits from Miltenyi according to manufacturer instructions (refer to 3.3). The T cells were then stained with 2.5 μM CFSE. After this, cells were washed twice with 10 mL PBS and 3.0×10^6 cells were resuspended in 200 μL sterile PBS and injected via the lateral tail vein into C57BL/6 recipient mice.

3.7 Infection of mice with *Listeria monocytogenes*

In this study a recombinant *Listeria monocytogenes* strain (10403S, Shen et al. 1995) constitutively expressing the model-antigen ovalbumin was used (LM-OVA). For infection experiments fresh cultures were prepared from frozen glycerol stocks in an overnight culture (incubation at 37°C, 180 rpm) in 5 mL BHI broth. Next day a 1:5 dilution was prepared with fresh BHI broth and after 3 h of incubation bacteria were washed twice with PBS and resuspended in PBS and finally the bacterial counts (CFU/mL) was determined by OD_{600} measurement and the desired infection dose for each experiment was diluted in sterile PBS. This suspension was injected via the lateral tail vein into the respective mice. The infection dose was controlled by plating serial dilutions of the inoculum on BHI agar plates and counting the colonies after incubation at 37°C for 24h.

In case of the adoptive T cell transfers a low infection dose (5000 CFU/ 100 μL) was used to ensure that the mice survive the infection and to provide a stimulus for the transferred T cells without orchestrating the hosts immune system in an exceeding inflammatory manner.

3.8 Determination of bacterial burden

For the determination of the colony forming units, the organs of interest were collected from LM-OVA infected mice at different times post infection, weight and homogenized in a mild 0.2% (v/v) IGEPAL CA-630/PBS eukaryotic cell lysis buffer using a homogenizer. The cell lysis buffer is necessary to ensure that the intracellular listeria are released from their host cell and can be detected as colonies on the BHI agar plates later on. 10 μL of ten-fold serial dilutions were plated in fluid stripes on BHI agar plates and colonies were counted after incubation at 37°C for 24 h.

3.9 *In vivo* cytotoxicity assay

For the *in vivo* determination of the cytotoxicity of CD8^+ T cells, WT and conventional $\text{I}\kappa\text{B}_{\text{NS}}^{-/-}$ mice were infected with a sublethal dose (10^4 CFU/ 100 μL PBS) of LM-OVA by intravenous injection. Nine days post infection splenocytes from uninfected C57BL/6 donor mice were isolated and split into two cellular fractions. One fraction was pulsed with 1.0 $\mu\text{g}/\text{mL}$ OVA₂₅₇₋₂₆₄ or 0.1 $\mu\text{g}/\text{mL}$ OVA₂₅₇₋₂₆₄ peptides, respectively, at RT. After 30 min incubation the peptide-loaded cells were stained with 2.5 μM CFSE (CFSE^{high}) and the unloaded control cell fraction was stained with 0.25 μM CFSE (CFSE^{low}). CFSE staining was performed as described in section 3.5. After staining and washing, the peptide-loaded and the unloaded cell fractions were mixed in a 1:1 ratio and finally 1.0×10^7 cells in 200 μL sterile PBS were injected in the tail vein of the previously infected WT and $\text{I}\kappa\text{B}_{\text{NS}}^{-/-}$ animals. Twelve hours after injection, spleens from the LM-OVA infected mice were harvested, splenocytes were isolated and the relative amounts of CFSE^{high} (peptide-loaded) and CFSE^{low} (unloaded control) cells were determined

by flow cytometry. To this end, the transferred cell fractions (CFSE^{low} and CFSE^{high}) were initially re-identified by means of their general CFSE staining. Within this pool of transferred splenocytes the ratio of the frequencies of CFSE^{high} and CFSE^{low} was calculated according to the following equation 1.

$$r = \frac{\text{CFSE}^{\text{low}}}{\text{CFSE}^{\text{high}}} \quad (1)$$

The relative specific lysis R (%) within individual infected animals (r_{infected}) was calculated in relation to uninfected control mice (r_{control}) according to equation 2.

$$R = \left(1 - \frac{r_{\text{control}}}{r_{\text{infected}}}\right) \times 100 \quad (2)$$

3.10 Flow cytometric analysis of adoptively transferred T cells

The isolated cells were transferred into a 96-well round-bottom plate and centrifuged for 5 min at 300 g at 4°C to pellet the cells, the supernatant was discarded. Next, the cells were incubated with anti-CD16/CD32, an antibody that binds specifically to Fcγ III/II receptors to prevent unspecific binding of subsequently used fluorescently labeled FACS antibodies. To exclude dead cells from later analyses LIVE/DEAD Fixable Viability Dye eFluor 780 (eBioscience) was added as well. Cells were incubated for 10 min at 4°C protected from light. After a subsequent washing step cells were stained with 100 μL surface marker antibody mix according to Table 5 for 10 min at 4°C in the dark. Since biotinylated CD44 antibody was used, staining with fluorescently labeled streptavidin (BV510) that specifically binds to the biotinylated antibodies was performed. Streptavidin staining was carried out for 10 min at 4°C protected from light. After washing, the cells were fixed in 100 μL 2% paraformaldehyde (PFA) for 20 min at RT protected from light. Prior to intracellular staining of cytokines, the cells needed to be permeabilized, to enable antibodies to reach their intracellular antigen. Therefore, the cells were permeabilized in 100 μL 0.1% (v/v) IPEGAL® CA-630/PBS detergent and incubated for 4 min at 4°C. After washing, the cells were incubated with the intracellular staining mix according to table 5 for 30 min at 4°C protected from light. Afterwards, the washed cells were resuspended in 200 μL FACS and assessed with BD FACS Canto II flow cytometer (BD Biosciences).

3.11 Histopathology of liver and spleen from WT and conventional $\text{IkB}_{\text{NS}}^{-/-}$ mice

Uninfected and LM infected WT and $\text{IkB}_{\text{NS}}^{-/-}$ mice were euthanatized by inhalation of CO₂. Spleens and livers were carefully removed and shortly washed in PBS. Afterwards, the organs were fixed in 4% paraformaldehyde (PFA).

The histopathology was performed by Dr. Olivia Kershaw from Freie Universität Berlin. The samples were sliced and stained with hematoxylin and eosin and were microscopically scored in a blinded manner to assess the dissemination and quality of pathological alterations by measuring necrotic areas.

3.12 Liver dissociation with GentleMACS dissociator

Mice were euthanized by inhalation of CO₂. Prior to collection of the liver a transcardial perfusion with 10 mL PBS was performed to rinse blood out of the organs. Liver was then isolated and the gallbladder was carefully removed. Cellular contents of the livers were obtained by using the liver dissociation kit from Miltenyi Biotec according to manufacturer recommendations. The whole liver was transferred in a C-tube containing 4.7 mL DMEM with 200 μ L Enzyme D solution, 100 μ L enzyme R solution and 20 μ L enzyme A solution provided by the kit. The C-tube was attached upside down onto the sleeve of the GentleMACS dissociator and the dissociation program 37C_m_LIDK_1 was applied. This procedure combines enzymatic as well as mechanic dissociation of the liver tissue. After termination of the program the C-tube was detached from the device and cells were resuspended and the cell suspension was filtered first through a 100 μ m, then through a 70 μ m and finally through a 30 μ m cell strainer. Cells were filled up with DMEM medium and centrifuged (300 xg, 10 min, 4°C). The supernatant was carefully discarded and the cells were resuspended in an appropriate volume PBS and stored on ice until further use.

3.13 Isolation of CD45⁺ and CD45⁻ cell populations by MACS

To distinguish between hematopoietic and non-hematopoietic cells, the dissociated liver cell suspension was centrifuged (300 xg, 10 min, 4°C). The supernatant was carefully discarded and 1×10^8 cells were resuspended in 900 μ L FACS buffer with 100 μ L CD45 MicroBeads provided by Miltenyi Biotec. The cell suspension was mixed well and incubated for 15 min at 4°C. After the incubation the cells were washed with 10 mL PBS and centrifuged (300 xg, 10 min, 4°C). Subsequently the cell pellet was resuspended in 500 μ L FACS buffer and applied to the autoMACS device applying program “*possel*”. This program involves a positive selection strategy to isolate CD45⁺ cells bound to the MicroBeads provided by the kit. Cell numbers of both fractions (CD45⁺ and CD45⁻) were counted, cells were centrifuged (300 xg, 10 min, 4°C), resuspended in 100 μ L RLT buffer and stored at -20°C until further analysis. Furthermore, the purity of the CD45⁺ enriched cell fraction was confirmed by flow cytometry and generally contained $\geq 90\%$ CD45⁺ cells.

3.14 Real-time Polymerase chain reaction (PCR)

Thawed liver and spleen samples were mechanically homogenized in RLT buffer containing 1% (v/v) β -Mercaptoethanol. The homogenate was centrifuged (10 min, 3000 xg, RT) and 500 μ L of the supernatant was used for the RNA isolation. The RNA was isolated with the RNeasy Mini kit according to manufacturer instructions, DNA was removed by using the RNase-Free DNase set and the RNA was finally eluted in 50 μ L nuclease-free ultrapure water. The RNA concentration was measured with the NanoDrop ND-1000 spectrophotometer. Equal amounts of RNA were used for cDNA synthesis in a reverse transcription reaction.

For the cDNA synthesis the following mixture was pipette according to Table 13.

Table 13: Reaction mixture for cDNA synthesis

component	Volume [μL]
Total RNA	1.0
Oligo-dT-Primer (0.5 $\mu\text{g}/\mu\text{L}$)	0.5
Random Primer (3.0 $\mu\text{g}/\mu\text{L}$)	0.5
DEPC-water	10.0

This mix was heated for 10 min at 70°C in a thermocycler and then placed on ice for additional 10 min. Afterwards the reverse transcription reaction mix was pipetted as described in Table 14.

Table 14: Reaction mixture for reverse transcription

component	Volume [μL]
5x first strand buffer	4.0
Dithiothreitol (0.1 M)	2.0
dNTP-Mix (10 mM)	1.0
SuperScript II Reverse Transcriptase	1.0

For the cDNA synthesis RNA samples were incubated for 60 min at 42°C in a thermocycler. Finally, 8 μL TE 10/1 was added per 1 μg reverse transcribed RNA. Next, real-time PCR was performed in duplicate reactions using a LightCycler 480 system and the Fast-Start Essential DNA Green Master Mix. 1 μL cDNA was used per reaction. The primers were used in a final concentration of 500 nmol/L diluted in nuclease-free water. To test the PCR efficiency of the respective primers a standard curve was generated with 4 serial dilutions of a template mix, which contained a mixture of all cDNA samples from a given experiment. By use of the delta/delta cp (crossing point) method the relative gene expression normalized to a house keeping gene was determined (Rao et al., 2013). Calculations were performed by Roche Light Cycler 480 II software.

Table 15: Composition of the real-time RT-PCR reaction mix

Component	Volume [μL]
Primer mix (forward and reverse, 500 nmol/L each)	5.0
cDNA (1 μL cDNA sample + 4 μL water)	5.0
Fast-Start Essential DNA Green Master Mix	10.0

Table 16: Thermal cycler program used for real-time RT-PCR

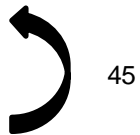
Cycle step	Temperature	Time	# of cycles
Incubation	95°C	5 min	
Amplification	95°C	10 sec	
	60°C	10 sec	
	72°C	10 sec	
Cooling	40°C	hold	

Table 17: Quantitative real-time RT-PCR primers. T_m was 60°C for all primers.

Primer name	Sequence 5' → 3'
RPS9 fwd	CTGGACGAGGGCAAGATGAAGC
RPS9 rev	TGACGTTGGCGGATGAGCACA
β -Actin fwd	CTTCTTTGCAGCTCC
β -Actin rev	TCCTTCTGACCCA TTCCCAC
IL6 fwd	ACCACGGCCTTCCCTACTTC
IL6 rev	GCCATTGCACA ACTCTTTTCTC
IL1 α fwd	TTGGTTAAATGACCTGCAACA
IL1 α rev	GAGCGCTCACGAACAGTTG
IL1 β fwd	TGAAATGAAAGACGGCACACC
IL1 β rev	TCTTCTTTGGGTATTGCTTGG
TNF α fwd	CTGTCTACTGAACTTCGGGG
TNF α rev	CTTGGTGTTTGCTACGACG
Nos2 fwd	TGGAGGTTCTGGATGAGAGC
Nos2 rev	AATGTCCAGGAAGTAGGTGAGG
IFN γ fwd	ATCTGGAGGAACTGGCAAAA
IFN γ rev	TTCAAGACTTCAAAGAGTCTGAGGTA

3.15 Serum preparation and measurement of ALT level

Mice were sacrificed by CO₂-euthanasia and blood was obtained by puncture of the heart with a 25 gauge needle on a 1 mL syringe. Blood samples were incubated first for 20 min at RT and then for another 20 min at 4°C. Afterwards, samples were spun down at full speed at 4°C for 5 min and serum-containing supernatant was collected and stored at -20°C until further analysis. For analysis of the serum alanine transaminase (ALT) level, 32 μ L serum was pipetted on a Refloton® test stripe and measured on the spectrophotometer Reflovet Plus (Roche).

3.16 Flow cytometric analysis of cellular composition in organs during LM infection

To characterize the cellular composition of spleen and liver from WT and conventional I k BNS^{-/-} mice during the course of LM infection, isolated splenocytes and liver-leukocytes were transferred into a 96-well plate and centrifuged (300 xg, 5 min, 4°C). To prevent unspecific binding of FACS antibodies, the cells were incubated with anti-CD16/CD32 antibody for 10 min at 4°C protected from light. To exclude dead cells from the analysis, staining with Fixable Blue dye was carried out for 10 min at 4°C in the dark. After a washing step, the cells were incubated with the staining mix stated in Table 6 for 10 min at 4°C protected from light. After a final washing step, cell pellets were resuspended in 200 μ L FACS buffer and assessed with a BD Fortessa (BD Biosciences). FACS data were analyzed using FlowJo software (Version 9.6.4, Tristar).

For the identification of different cell subsets in lymphoid and non-lymphoid tissues the approach of a previously published study was adapted to develop an appropriate gating strategy (Yu et al., 2016).

In the first gating step, leukocytes were defined based on their cell size and granularity with the forward scatter FSC-A and sideward scatter SSC-A, excluding cell debris. Cell doublets and clumps were excluded next by FSC-A vs. FSC-H gating. Finally to exclude dead cells from the analysis all cells that were negative for the used Live/Dead marker were gated for further analysis.

Based on the expression of the surface protein CD45 discrimination between non-hematopoietic cells, erythrocytes and leukocytes was performed, because CD45 is exclusively expressed on hematopoietic cells (Fornas et al., 2002; van Lochem et al., 2004). In the next step neutrophils were gated by the expression of the neutrophil-specific marker Ly6G and their cellular property of high SSC intensity (Rose et al., 2012).

The remaining cells that were not neutrophils were further gated on CD11b and CD11c to distinguish between myeloid and CD11b⁻CD11c⁻ lymphoid cells. CD11b⁻CD11c⁻ lymphoid cells were further subdivided via MHC class II (IA/IE) and CD24 staining. IA/IE⁺CD24⁺ cells were defined as B cells and the remaining cells that were not positive for either IA/IE or CD24 as T cells. T cells were further sub-classified as CD4⁺ T cells, CD8⁺ T cells and CD4⁻CD8⁻ (DN) lymphocytes. The latter cell population mainly constitutes innate lymphoid cells and other miscellaneous lymphoid cell subsets of unknown origin. Myeloid leukocytes were further sub-classified by their SSC pattern vs. IA/IE intensity. The IA/IE⁻ SSC^{low} fraction can be further distinguished based on the expression of CD64 and CD11b. CD11b^{int}CD64⁻ cells were defined as NK cells and CD11b⁺ CD64⁺ as monocytes. Monocytes were further subdivided into Ly6C⁺CD11c⁻ inflammatory monocytes and into Ly6c^{int}CD11c⁺ resident monocytes. The remaining cells that are not IA/IE⁻SSC^{low} represent macrophages, DCs and eosinophils. Macrophages were classified as CD64⁺CD24^{low} cells which were further subdivided based on their expression of CD11c and CD11b into CD11b⁺CD11c⁻ interstitial macrophages and into CD11c⁺CD11b^{int} resident macrophages. The remaining CD24⁺ cells were classified into DCs and eosinophils, which are IA/IE⁻CD11b⁺. Based on the expression intensity of CD11b together with IA/IE CD11b⁻ DCs and CD11b⁺ DCs were defined.

In summary this gating strategy according to the publication of Yu and colleagues allows to determine different immune cell subsets in one flow cytometric panel. However, in particular with progressive infection, surface marker expression is subject to fluctuations and moreover, tissue damage caused by the LM infection results in increased auto-fluorescence especially in apoptotic cells. Thus, unambiguous subset identification was not always guaranteed especially in the late stage of LM infection. For these reasons and most importantly, to prevent misinterpretations of data, the FACS analysis performed day 4 post LM infection was excluded from the results part.

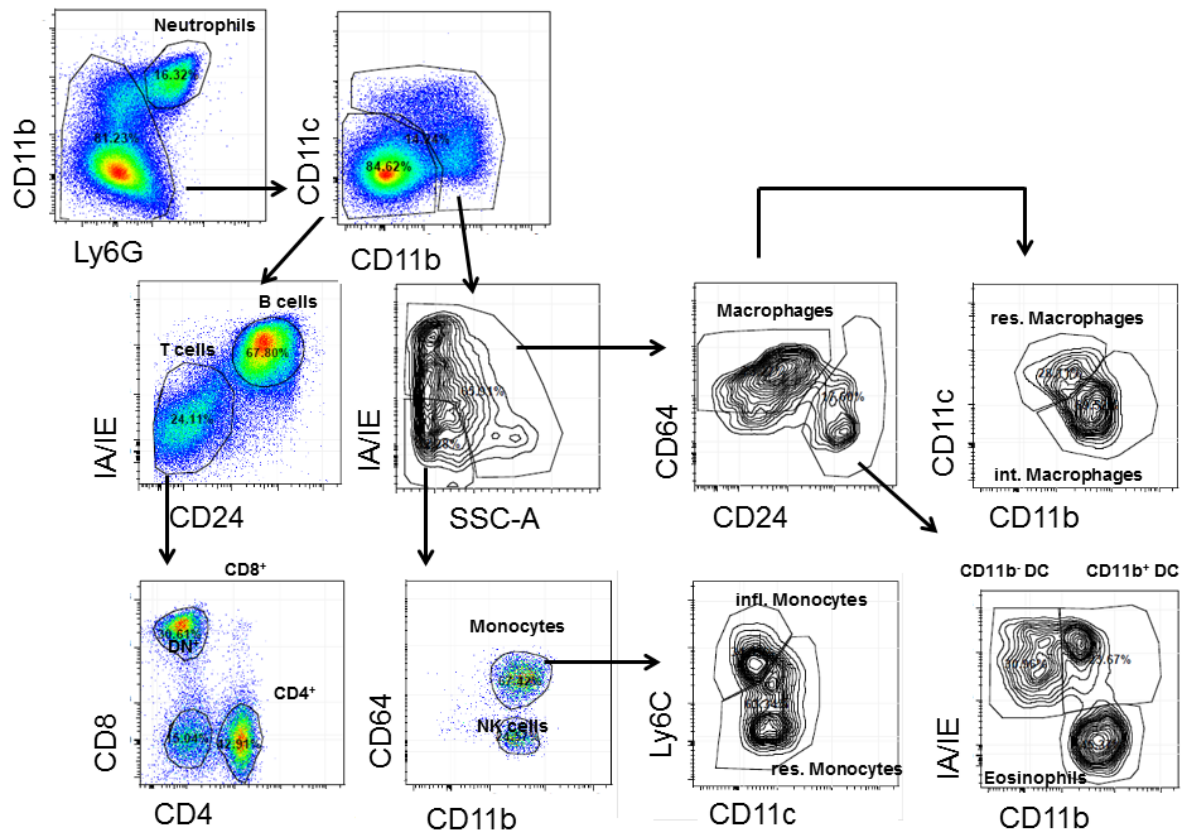


Figure 8: Representative gating scheme to define different cell subsets from LM infected spleen and liver tissue. Cells were pre-gated on leukocytes by FSC vs. SSC and doublets were excluded by FSC-A vs. FSC-H gating. Dead cells were eliminated by staining with live/dead marker and only CD45⁺ cells were further characterized (pre-gating not shown). Based on the expression intensity of indicated surface markers, the 13 major lymphoid and myeloid cell fractions were defined.

3.17 Flow cytometric cell sorting

Spleens and livers were sampled from WT and $I\kappa B_{NS}^{-/-}$ mice on day 3 post LM infection. Spleen samples were treated as described in chapter 3.2 and liver samples were treated with the Liver dissociation kit as described in chapter 3.12. After dissociation density centrifugation was performed with 35% Percoll/PBS (density: 1.041 g/mL, 360 xg, RT, 20 min, without brake). Supernatant was discarded and cell pellet washed with 10 mL PBS (300 xg, RT, 10 min). The cell pellet was resuspended in PBS. Splenocytes were pre-sorted by autoMACS to eliminate B cells and T cells by incubating 1×10^7 cells with 20 μ L biotinylated anti-B220 (1:200 diluted in PBS) and 20 μ L anti-CD3 ϵ (1:200 diluted in PBS) and subsequent use of anti-Biotin Microbeads (Miltenyi Biotec) according to manufacturer recommendations. MACS program “*deplete*” was applied to remove B and T cells from the samples. The resulting negative fraction was washed with 10 mL PBS and the cell number was determined. Cells from 5 individual infected $I\kappa B_{NS}^{-/-}$ and 5 individual infected WT mice were pooled per genotype to ensure sufficient cell numbers after FACS-based cell sorting.

For sorting of inflammatory monocytes the cell suspensions were stained according to the panel shown in table 6 with exclusion of CD4 and CD8, but in addition with F4/80 and CD115. Gating was performed comparable to the scheme in Figure 8. The stained cells were sorted on a BD FACS Aria III (BD Biosciences). The sorted cell fractions were resuspended in 350 μ L RLT buffer and stored at -20°C until further use.

3.18 LacZ fluorochrome reporter assay

To quantify the β -galactosidase activity of the *lacZ* reporter within cells of the *Nfkbid*^{lacZ} mice the FluoReporter™ *lacZ* Flow Cytometry kit from Thermo Fisher was used. The prepared single cell suspension from the respective organs was adjusted to 10^7 cells/mL and 55 μ L of the cell suspension was transferred into a 5 mL flow cytometer tube. The FDG reagent provided by the kit was thawed on ice and a 2 mM working solution was prepared by diluting the thawed FDG reagent 10-fold with deionized water. The working solution was briefly warmed at 37°C and vortexed to obtain a homogenous solution. Afterwards the prepared cell suspension was loaded with FDG by adding 55 μ L of the prewarmed 2 mM working solution to the cell suspension. Through the hypotonic shock the FDG can enter the cells and can be potentially hydrolyzed by the cytoplasmic reporter β -galactosidase enzyme (*lacZ*). After incubation for exactly 1 min at 37°C, the FDG loading was stopped by adding 1 mL ice-cold staining medium. The suspension was centrifuged (5 min, 300 \times g, 4°C) and cell surface staining was performed as described in chapter 3.16. For all staining steps, the cells were kept on ice and protected from light. Flow cytometric acquisition was performed on the same day.

3.19 Microarray

RNA from whole liver homogenates was isolated and purified using the RNeasy Mini Kit and the RNase free DNase kit according to manufacturer recommendations. Per analyzed point in time following infection the RNA concentration of samples from 3-5 WT and *IkB_{NS}*^{-/-} mice was measured with a photospectrometer (NanoDrop) and equal amounts of RNA from each sample were pooled to obtain a representative sample mix integrating biological variances.

Further sample preparation, amplification, fragmentation, microarray hybridization, staining and scanning were performed by the Genome Analytics Group at Helmholtz Centre for Infection Research in Braunschweig (Germany). Samples were analyzed with the GeneChip® Mouse Gene 2.0 ST microarray from Affymetrix Company according to manufacturer instructions. In total 8 microarrays reflecting the following conditions were performed: WT: d0, d2, d3, d4; *IkB_{NS}*^{-/-}: d0, d2, d3, d4.

Microarray raw data were processed by GeneSpring GX11 Software (Agilent Technologies). Data were summarized, \log_2 -transformed and quantile-normalized with RMA algorithm including background subtraction. A percentile filter was applied to the microarray data in a way, that only transcripts with signal intensity above the 20th percentile of all signal intensities in a given microarray were retained and only if this is the case in at least one out of in total 8 microarrays. Differentially regulated genes were identified as follows. Per genotype the comparisons: d2 vs. d0, d3 vs. d0, d4 vs. d0 were considered, resulting in together 6 different conditions. Next, a list of genes was compiled only containing entries with a fold change of differential gene expression of $> \pm 3$ in at least one out of the 6 previous conditions. Scatter dot plots were generated using GraphPad Prism Software v5. K-means cluster analysis of z-score transformed microarray data of differentially regulated genes was carried out by Genesis Software (version 1.8.1, Sturn et al., 2002). Gene Ontology enrichment analysis was performed using Cytoscape software and ClueGO plugin (Bindea et al., 2009).

Statistics

All statistical analyses were performed with the GraphPad Prism Software v5 (GraphPad Software, Inc, La Jolla, USA) by using two-tailed unpaired student's *t*-test or two-way ANOVA with Bonferroni post-test. A p-value of < 0.05 was considered significant.

4. Results

The NF- κ B inhibitory protein I κ B_{NS} was first described in the context of antigen-induced negative selection of thymocytes (Fiorini et al. 2002). Consequently, most of the scientific work performed thereafter dealt with I κ B_{NS} characterization in T cells. Schuster et al. then identified I κ B_{NS} as a regulator of Foxp3⁺ in naturally occurring Treg cell differentiation. This became evident since I κ B_{NS}-deficient mice showed a strong reduction of Tregs in the thymus, spleen and peripheral lymph nodes, without I κ B_{NS} being required for the maintenance and function of mature Tregs (Schuster et al. 2012). Despite reduced number of Tregs, I κ B_{NS}-deficient mice showed no signs of autoimmunity in the steady state, which typically evolve under Treg-compromised conditions due to diminished Treg-control of self-reactive conventional effector T cells. Therefore, it has been speculated what function I κ B_{NS} in general may have in effector T cells. In this line, Touma et al. described on the basis of *in vitro* T cell mitogen stimulation experiments that I κ B_{NS}-deficient polyclonal conventional CD4⁺ and CD8⁺ lymph-node derived T cells exhibit an impaired proliferation and a decreased secretion of IL2 and IFN γ (Touma et al., 2007). However, detailed knowledge on I κ B_{NS} function in conventional T cells following antigen-specific T cell receptor stimulation still remains elusive.

Thus, the first part of this thesis describes the impact of I κ B_{NS} on activation and proliferation of antigen-specific effector CD4⁺ and CD8⁺ T cells utilizing an experimental approach combining *in vitro* T cell stimulation assays and an *in vivo* adoptive T cell transfer model with *Listeria monocytogenes* as antigen-specific stimulus.

4.1 Probing of antigen-specific T cell responses *in vitro*

To address the impact of I κ B_{NS} on parameters such as T cell activation, proliferation and differentiation into effector cells, an experimental system to specifically stimulate the TCR with antigenic peptides was selected. By using irradiated syngeneic splenocytes as antigen-presenting cells, a MHC dependent antigen presentation in the presence of co-stimulus for T cell activation is ensured, thus mimicking a “natural” TCR stimulation.

OVA-specific CD4⁺ T cells from OT-II x I κ B_{NS}^{-/-} and OT-II x WT and OVA-specific CD8⁺ T cells from OT-I x I κ B_{NS}^{-/-} and OT-I x WT mice were isolated by negative selection using autoMACS (refer to chapter 3.3). The isolated cells were stained with CFSE and co-cultured together with lethally irradiated syngeneic splenocytes as antigen presenting cells in the presence of various amounts of the cognate OVA-peptides for 24 h to 72 h. As positive control, cells were stimulated with plate-bound agonistic anti-CD3 ϵ (0.25 μ g/mL) and soluble anti-CD28 (1 μ g/mL) (α CD3/ α CD28) to trigger antigen-unspecific TCR stimulation. As negative control, cells were left unstimulated in the presence of culture media and irradiated splenocytes.

After stimulation the cells were harvested and analyzed by flow cytometry. For testing the functionality of the transgenic OVA-specific CD4⁺ and CD8⁺ T cells in dependence of I κ B_{NS} classical T cell activation markers such as CD25 and CD44 as well as the effector cytokine IFN γ were selected.

4.1.1 Loss of I κ B_{NS} does not affect the activation of CD4⁺ T cells following *in vitro* stimulation

In the first instance the impact of I κ B_{NS} on the activation capacity of CD4⁺ T cells was investigated in the above mentioned *in vitro* stimulation set-up.

First of all, different antigen doses were chosen in order to identify a suitable peptide dose to activate OVA-specific CD4⁺ T cells from OT-II x WT and OT-II x I κ B_{NS}^{-/-} mice.

Since it is known that T cell responses are sensitive to the efficiency and strength of antigen-presentation of their respective antigenic epitope (Lazarski et al., 2006) and quality of co-stimulation by antigen-presenting cells and due to the unknown antigen presenting capacity of the chosen number of antigen presenting cells per T cell, three different doses of OVA₃₂₃₋₃₃₉ peptide were tested. By this, even slightly different T cell responses in dependency of the I κ B_{NS} genotype are expected to become detectable.

As depicted in Figure 9A and as expected, there is an antigen dose-dependent effect on the proliferation of OVA-specific CD4⁺ T cells. With lower amounts of OVA₃₂₃₋₃₃₉, less proliferation (% CFSE^{low}) of CD4⁺ T cells was detected. The stimulation with 0.1 μ g/mL OVA₃₂₃₋₃₃₉ resulted in approximately 30% of responding CD4⁺ T cells irrespective of the genotype. The stimulation in presence of 10 μ g/mL peptide led to about 85% CFSE^{low} OVA-specific CD4⁺ T cells which was comparable to the proliferation induced by stimulation with agonistic antibodies against CD3 ϵ and CD28. In both conditions no significant differences were observed between the genotypes. The intermediate dose of 1 μ g/mL OVA peptide resulted in proliferative response of nearly 60% of the antigen-specific CD4⁺ T cells. Since this peptide dose triggers an intermediate proliferative response with potential for observing increasing or decreasing proliferative responses in both genotypes it was used for all subsequent OT-II peptide-based *in vitro* CD4⁺ T cell stimulations. Figure 9B shows representative histograms, documenting the CFSE loss using 1 μ g/mL OVA₃₂₃₋₃₃₉ peptide or α CD3/ α CD28 stimulation in comparison to unstimulated controls with no significant differences between OVA-specific CD4⁺ T cells from OT-II x WT and OT-II x I κ B_{NS}^{-/-} mice. Thus, OT-II-peptide specific CD4⁺ T cell proliferation does not rely on I κ B_{NS} in this *in vitro* setting.

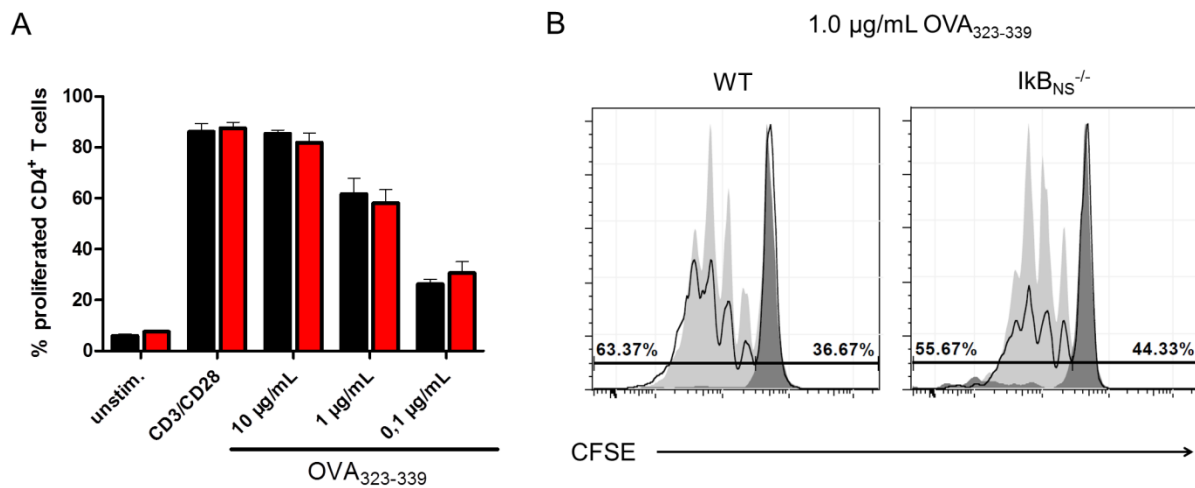


Figure 9: Proliferation of *in vitro* stimulated WT and IκB_{NS}^{-/-} OT-II transgenic CD4⁺ T cells. WT (■) and IκB_{NS}^{-/-} (■) CD4⁺ OT-II transgenic T cells were isolated from spleens of respective mice by autoMACS, CFSE-stained and co-cultured in a 96-well plate with lethally irradiated splenocytes from WT donors. T cells were stimulated with indicated amounts of OVA₃₂₃₋₃₃₉ peptide or as positive control with plate-bound anti-CD3ε plus soluble anti-CD28 or left unstimulated as negative control. Cell number per well was 2 x 10⁵ CD4⁺ T cells plus 3 x 10⁵ feeder cells. Cells were incubated for 72 h with addition of brefeldin A for the last 4 h of incubation. CFSE-loss indicating cell proliferation was analyzed by flow cytometry and the percentage of CFSE^{low} cells was determined. Apoptotic and dead cells were excluded from the analysis. (A) Summary of data from n= 4 OT-II x WT and n= 4-6 OT-II x IκB_{NS}^{-/-} mice. Data represent mean ± SEM. Statistical analyses were performed using two-way ANOVA with Bonferroni's post-test. (B) Representative histograms for CFSE dilution in OT-II x WT and OT-II x IκB_{NS}^{-/-} CD4⁺ T cells following stimulation with 1.0 μg/mL OVA₃₂₃₋₃₃₉ peptide (solid line), anti-CD3ε plus anti-CD28 (light grey) and unstimulated (dark grey).

Next to the proliferation, surface expression of the activation markers CD25 and CD44 as well as the expression of the effector cytokine IFNγ were assessed by flow cytometry.

As depicted in Figure 10, the stimulation with 1.0 μg/mL OVA₃₂₃₋₃₃₉ peptide led to an efficient activation of CD4⁺ T cells with regard to expression of CD25 and CD44 with more than 40% CD25⁺ and CD44⁺ CD4⁺ T cells in both genotypes. Furthermore, T cells which underwent proliferation, in comparison to unproliferated (CFSE^{high}) cells, do express both activation markers, though CFSE^{high} T cells show some CD25 and CD44 expression as well.

CD4⁺ T cells from both genotypes did not secrete IFNγ in response to antigenic stimulation and stimulation with αCD3/αCD28 induced IFNγ production in only 10% of the CD4⁺ T cells, independent of the genotype. This might be due to the fact that in this *in vitro* setting no Th1-differentiating conditions were achieved.

In summary, the obtained results revealed, that in the chosen *in vitro* setting IκB_{NS} has no impact on the antigen-specific proliferation and activation of OT-II CD4⁺ T cells.

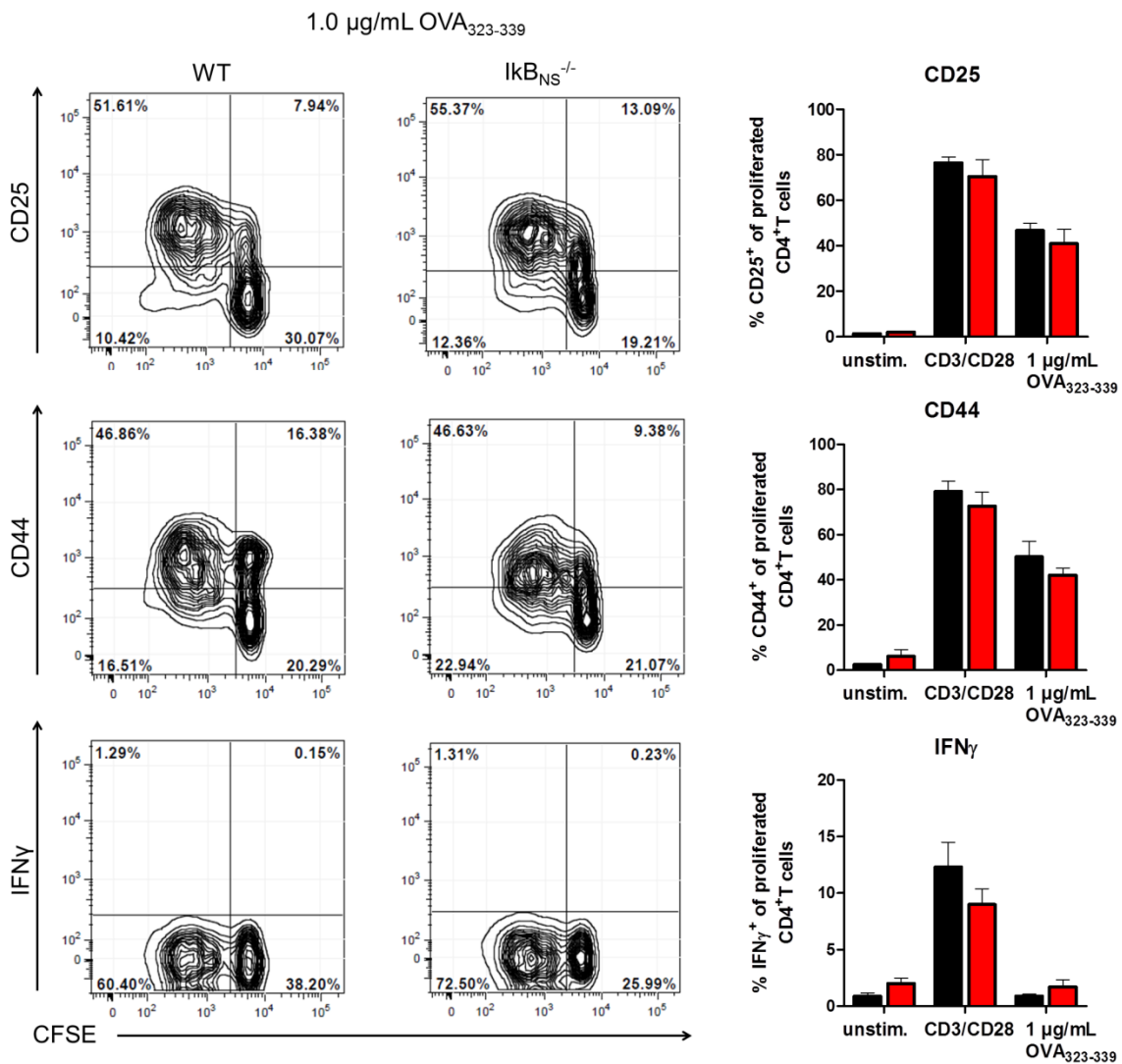


Figure 10: Representative dot plots and summarizing bar charts of the flow cytometric analysis of *in vitro* stimulated CD4⁺ T cells from OT-II x WT and OT-II x lkb_{NS}^{-/-} mice. WT (■) and lkb_{NS}^{-/-} (■) CD4⁺ OT-II transgenic T cells were isolated from spleens of respective mice by autoMACS, CFSE-stained and co-cultured in a 96-well plate with lethally irradiated splenocytes from WT donors. T cells were stimulated with 1 µg/mL OVA₃₂₃₋₃₃₉ peptide or as positive control with plate-bound anti-CD3 ϵ plus soluble anti-CD28 or were left unstimulated as negative control. Cell number per well was 2×10^5 CD4⁺ T cells plus 3×10^5 irradiated splenocytes. Cells were incubated for 72 h with addition of brefeldin A for the last 4 h of incubation. Cells were analyzed by flow cytometry. Apoptotic and dead cells were excluded from the analysis. **Left:** Representative dot plots for CD25, CD44 and IFN γ expression vs. CFSE dilution in OVA-specific WT and lkb_{NS}^{-/-} CD4⁺ T cells. Numbers indicate the percentage of cells in the respective quadrant. **Right:** Summary of data from n= 4 WT and n= 4-6 lkb_{NS}^{-/-} OT-II transgenic mice. Data represent mean \pm SEM. Statistical analyses were performed using two-way ANOVA with Bonferroni's post-test.

4.1.2 Loss of lkb_{NS} does not affect the proliferation of *in vitro* stimulated CD8⁺ T cells, but results in reduced IFN γ secretion

In order to analyze the role of lkb_{NS} in CD8⁺ T cells, the same experimental set-up that was mentioned in the previous chapter 4.1.1 was used to analyze the proliferative capacity and the activation status of *in vitro* stimulated CD8⁺ T cells derived from OT-I x WT and OT-I x lkb_{NS}^{-/-} mice. Since it is known that OT-I derived CD8⁺ T cells compared to OT-II-derived CD4⁺ T cells exhibit a lower antigen threshold for the induction of fulminant *in vitro* proliferation (Clarke et al., 2000), lower OT-I antigen amounts were used for the stimulation. The highest antigen concentration used was 100 ng/mL, followed by 1 ng/mL and 0.1 ng/mL. As positive control plate-bound anti-CD3 ϵ plus soluble anti-CD28 was used for the

stimulation. Homeostatic background proliferation was assessed by means of an unstimulated media-only negative control. After 48 h post stimulation the cells were analyzed by flow cytometry with respect to the CFSE dilution and the expression of CD25, CD44 and IFN γ . This early time point to measure proliferation was selected since the OT-I transgenic CD8⁺ T cells are known to respond faster than OT-II transgenic CD4⁺ T cells (Au-Yeung et al., 2017).

Figure 11 summarizes the results for the CD8⁺ T cell proliferation. Unexpectedly, all tested peptide concentrations were sufficient to trigger equally fulminant T cell proliferation irrespective of the I κ B_{NS} genotype. In addition, even lower peptide concentrations were tested, still inducing proliferation in OT-I transgenic CD8⁺ T cells. However, since under these conditions a decrease in cell viability was observed (data not shown), 0.1 ng/mL was selected as minimal concentration for further analyses. Of note, in contrast to antigen-specific stimulation a significant decrease in proliferation of CD8⁺ T cells derived from OT-I x I κ B_{NS}^{-/-} mice was detectable following stimulation with α CD3/ α CD28 (OT-I x WT: 86% \pm 5%, OT-I x I κ B_{NS}^{-/-}: 58% \pm 10%).

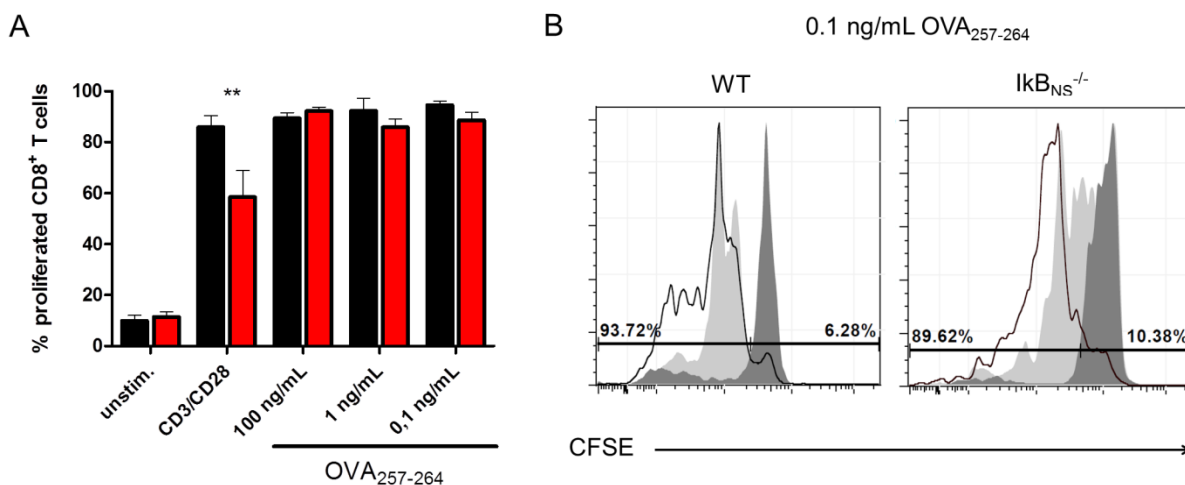


Figure 11: Proliferation of *in vitro* stimulated WT and I κ B_{NS}^{-/-} OT-I transgenic CD8⁺ T cells. WT (■) and I κ B_{NS}^{-/-} (■) CD8⁺ OT-I transgenic T cells were isolated from spleens of respective mice by autoMACS, CFSE-stained and co-cultured in a 96-well plate with lethally irradiated splenocytes from WT donors. T cells were stimulated with indicated amounts of OVA₂₅₇₋₂₆₄ peptide or as positive control with plate-bound anti-CD3 ϵ plus soluble anti-CD28 or left unstimulated as negative control. Cell number per well was 2×10^5 CD8⁺ T cells plus 3×10^5 irradiated splenocytes. Cells were incubated for 48 h with addition of brefeldin A for the last 4 h of incubation. CFSE-loss indicating cell proliferation was analyzed by flow cytometry and the percentage of CFSE^{low} cells was determined. Apoptotic and dead cells were excluded from the analysis. (A) Summary of data from $n = 3-4$ OT-I x WT and $n = 4$ OT-I x I κ B_{NS}^{-/-} mice. Data represent mean \pm SEM. Statistical analyses were performed using two-way ANOVA with Bonferroni's post-test. (B) Representative histograms for CFSE dilution in OT-I x WT and OT-I x I κ B_{NS}^{-/-} CD8⁺ T cells following stimulation with 0.1 ng/mL OVA₂₅₇₋₂₆₄ peptide (solid line), anti-CD3 ϵ plus anti-CD28 (light grey) and unstimulated (dark grey).

With respect to the activation markers CD25 and CD44, no significant differences between CD8⁺ T cells from OT-I x WT and OT-I x I κ B_{NS}^{-/-} mice were observed when stimulated with OVA₂₅₇₋₂₆₄ in an antigen-specific manner (Figure 12). More than 40% of the proliferated CD8⁺ T cells derived from OT-I x WT and OT-I x I κ B_{NS}^{-/-} donors were CD25⁺ and approximately 60% were positive for CD44, irrespective of I κ B_{NS}. In comparison to that, the stimulation with α CD3/ α CD28 led to significantly reduced expression levels of CD25⁺ and CD44⁺ on OT-I x I κ B_{NS}^{-/-} CD8⁺ T cells compared to OT-I x WT CD8⁺ T cells which matches with the reduced proliferation in response to this antigen-unspecific TCR trigger. Regarding the IFN γ expression no differences were detected between CD8⁺ T cells from both genotypes when stimulated with α CD3/ α CD28. Strikingly, a significantly reduced frequency of

IFN γ ⁺ OT-I x I κ B_{NS}^{-/-} CD8⁺ T cells compared to OT-I x WT derived CD8⁺ T cells was observed in response to stimulation with the cognate OVA peptide, suggesting that I κ B_{NS} might have a direct impact on the IFN γ secretion upon antigen-specific TCR engagement. In general, the marker and cytokine expression with the two higher peptide concentrations tested were comparable to these results.

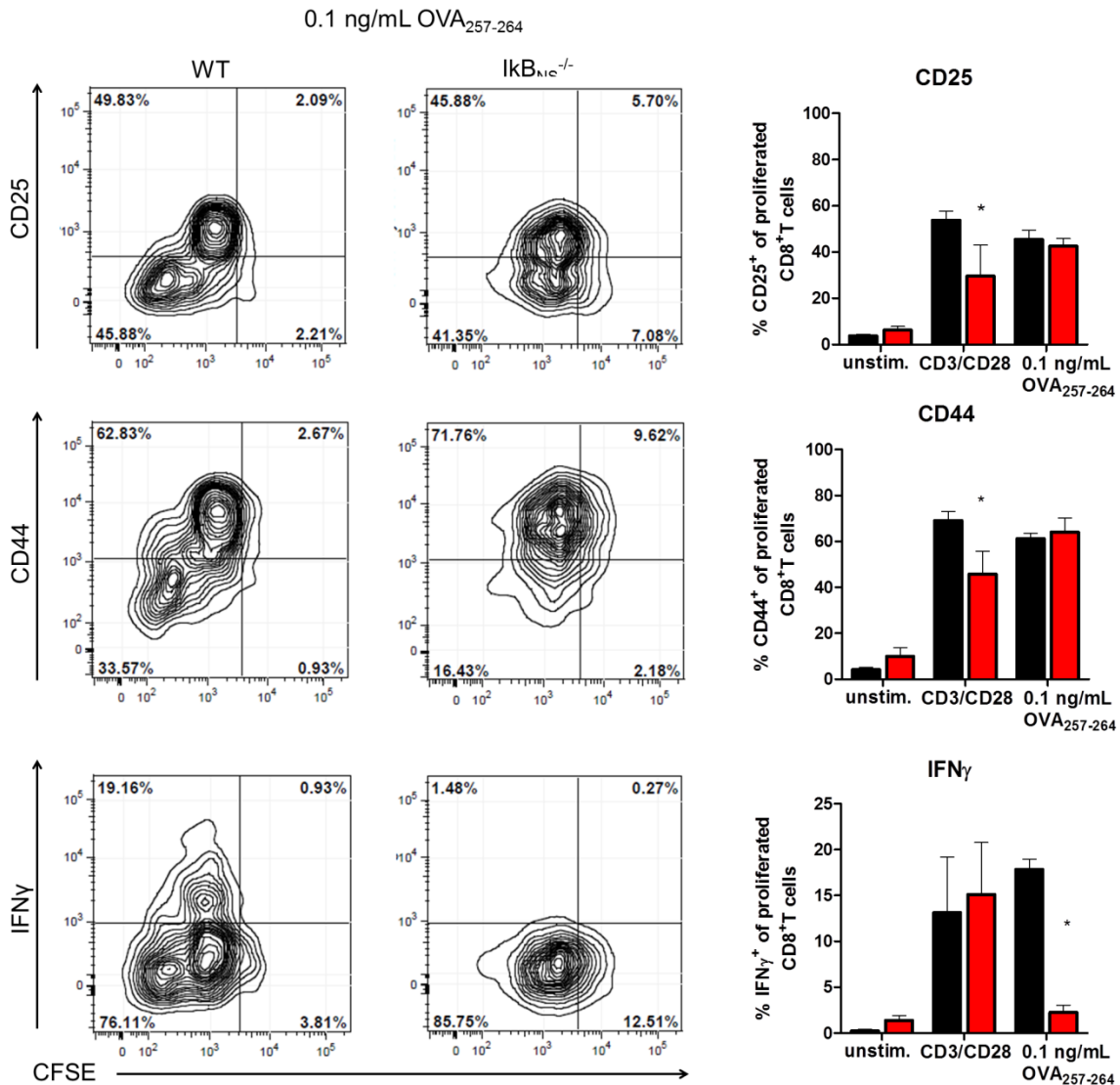


Figure 12: Representative dot plots and summarizing bar charts of the flow cytometric analysis of *in vitro* stimulated CD8⁺ T cells from OT-I x WT and OT-I x I κ B_{NS}^{-/-} mice. WT (■) and I κ B_{NS}^{-/-} (■) CD8⁺ OT-I transgenic T cells were isolated from spleens of respective mice by autoMACS, CFSE-stained and co-cultured in a 96-well plate with lethally irradiated splenocytes from WT donors. T cells were stimulated with 0.1 ng/mL OVA₂₅₇₋₂₆₄ peptide or as positive control with plate-bound anti-CD3 ϵ plus soluble anti-CD28 or left unstimulated as negative control. Cell number per well was 2×10^5 CD8⁺ T cells plus 3×10^5 irradiated splenocytes. Cells were incubated for 48 h with addition of brefeldin A for the last 4 h of incubation. Cells were analyzed by flow cytometry. Apoptotic and dead cells were excluded from the analysis. **Left:** Representative dot plots for CD25, CD44 and IFN γ expression vs. CFSE dilution in OVA-specific WT and I κ B_{NS}^{-/-} CD8⁺ T cells. Numbers indicate the percentage of cells in the respective quadrant. **Right:** Summary of data from $n = 4$ WT and $n = 4$ I κ B_{NS}^{-/-} OT-I transgenic mice. Data represent mean \pm SEM. Statistical analyses were performed using two-way ANOVA with Bonferroni's post-test.

Data obtained using the above described experimental *in vitro* setting moreover confirmed that both CD4⁺ and CD8⁺ OVA-TCR transgenic T cells very well respond to stimulation with their cognate antigens. As such, OT-I and OT-II mice with a WT and I κ B_{NS}^{-/-} genetic background, respectively, also represent an ideal tool to next study the role of I κ B_{NS} on CD4⁺ and CD8⁺ T cell activation, proliferation and effector function during *in vivo* *Listeria monocytogenes* infection utilizing the mice as donors for OVA-specific WT and I κ B_{NS}^{-/-} CD4⁺ and CD8⁺ T cells in adoptive transfer experiments.

4.2 Impact of I κ B_{NS} on antigen-specific T cell activation *in vivo*

Previous reports revealed the role of I κ B_{NS} on proliferation and cytokine expression of differentiated CD4⁺ effector T cells and that for instance T helper 17 (Th17) cells are affected by a loss of I κ B_{NS} as indicated by diminished expression of IL17 and IFN γ (Annemann et al., 2015). In a colitis model and as well in a *Citrobacter rodentium* infection model, I κ B_{NS}-deficiency resulted in impaired Th17 mediated immune response which is known to be necessary to solve the infection. The reduced secretion of the pro-inflammatory cytokine IL17 in I κ B_{NS}^{-/-} mice resulted in reduced tissue damage, but at the same time increased pathogen burden and thereby an overall increased susceptibility to *C. rodentium* infection (Annemann et al., 2015).

Another study reported that I κ B_{NS}-deficiency confers resistance to experimental autoimmune encephalomyelitis (EAE) due to the reduced secretion of the proinflammatory cytokine IL17 by T cells (Kobayashi et al., 2014). While those results were obtained in auto-immune and gut-associated infectious diseases it remains elusive which impact I κ B_{NS} has in the context of T cell-mediated immune responses during systemic infections.

As introduced in chapter 1.1.2, *Listeria monocytogenes* infection in mice is a well-established model to investigate CD4⁺ and CD8⁺ T cell mediated immune responses, because both cellular subsets are stimulated by the pathogen and are involved in the clearance of the infection. Thus, this infection model is highly suitable to elucidate the role of I κ B_{NS} in pathogen-specific T cell activation and effector function *in vivo*.

For this purpose OT-II and OT-I transgenic mice either proficient or deficient for I κ B_{NS} were used as donors for OVA-specific CD4⁺ and CD8⁺ T cells (refer to chapter 4.1). For antigen-specific *in vivo* priming of these transgenic T cells following their adoptive transfer in WT recipient mice a recombinant *Listeria monocytogenes* strain (14030S) expressing both, the OVA₃₂₃₋₃₃₉ (OT-II) and the OVA₂₅₇₋₂₆₄ (OT-I) peptides, was used.

4.2.1 I κ B_{NS}-deficiency has distinct effects on *in vivo* activation of OVA-specific CD4⁺ T cells during LM infection

As described in chapter 4.1.1 the deficiency of I κ B_{NS} had no impact on antigen-specific activation of CD4⁺ T cells *in vitro*. In order to assess the impact of I κ B_{NS} on antigen-specific stimulation *in vivo* the experimental setup depicted in Figure 13 was used. First, lymphocytes from either OT-II x WT or OT-II x I κ B_{NS}^{-/-} mice were isolated from spleens and inguinal as well as cervical lymph nodes. Afterwards, naïve OVA-specific CD4⁺ T cells were isolated by autoMACS by negative selection. Furthermore, a CD25-depletion was performed during the autoMACS separation to deplete natural occurring regulatory T cells and to obtain a naïve T cell pool. Purified cells were CFSE stained and

3.0×10^6 OVA-specific $CD4^+$ T cells were injected into C57BL/6 recipient mice. The relatively high cell number was chosen to ensure sufficient recovery of the transferred cells after several days and to obtain adequate cell numbers for the reanalysis.

One day post transfer the recipient mice were infected with 5000 CFU LM-OVA, which is a rather low dose to ensure that the recipient mice definitely would survive the infection while at the same time being high enough to induce a strong T cell activation. At indicated times post infection (d3, d5) the adoptively transferred cells were re-isolated from spleen and liver (refer to chapter 3.2) representing the main replication sites of LM, and analyzed by flow cytometry with respect to their proliferation, activation status (CD25, CD44) and cytokine secretion (IFN γ and IL2).

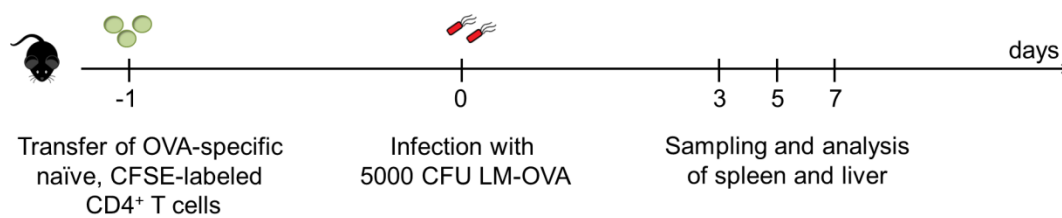


Figure 13: Schematic overview about the experimental design of adoptive transfer of OT-II transgenic $CD4^+$ T cells followed by LM-OVA infection. Naïve OVA-specific $CD4^+$ T cells were isolated from either OT-II x WT or OT-II x $IkB_{NS}^{-/-}$ mice by autoMACS. Afterwards, $CD4^+$ T cells were stained with CFSE and 3×10^6 cells were injected i.v. into C57BL/6 recipients. One day post adoptive transfer, mice were infected with a sublethal dose of LM-OVA. At indicated times post infection, mice were sacrificed, spleens and livers were sampled and the proliferation and activation status of transferred $CD4^+$ T cells were analyzed by flow cytometry.

Prior to adoptive transfer of the isolated OVA-specific $CD4^+$ T cells a purity and phenotype analysis was performed to confirm that recipient mice indeed received a monoclonal pool of naïve OVA-specific $CD4^+$ T cells. Furthermore, the phenotyping prior to transfer is necessary for the later interpretation of the results from re-analyses and to better understand the cellular fate after *in vivo* LM-OVA encounter. Clonality of the transferred T cell pool was confirmed by using antibodies against the TCR V β 5.1/5.2 and V α 2 chains, which are indicative for the transgenic TCRs. Generally, MACS-purified $CD4^+$ T cells from OT-II mice comprised more than 80% T cells with OVA-specificity (data not shown).

Figure 14 shows a representative example of the activation status of MACS-isolated $CD4^+$ T cells from OT-II x WT (left) and OT-II x $IkB_{NS}^{-/-}$ mice (right) in regard to expression of CD25, CD44 and CD62L. Due to the CD25 depletion during the MACS isolation (see chapter 3.3), the $CD25^+$ T cells within the OT-II x WT derived $CD4^+$ T cells (0.33%) and OT-II x $IkB_{NS}^{-/-}$ derived $CD4^+$ T cells (0.20%) were almost absent, indicating that the transferred T cell pool contained only negligible numbers of $CD25^+$ Treg cells with immunosuppressive capacity.

Figure 14 shows that the isolated $CD4^+$ T cells, irrespective of the genotype of the donor mice, showed highest frequencies of the $CD44^{int}$ population (>60%) and about 20% of the $CD4^+$ T cells were $CD44^{neg}$. Interestingly, after MACS enrichment a $CD44^{high}$ fraction was detected, which accounted for about 8% of the OT-II x WT $CD4^+$ T cells and approximately 3% of the OT-II x $IkB_{NS}^{-/-}$ $CD4^+$ T cells. Since it is very unlikely that those T cells could have encountered their specific OVA-peptide within the untreated naïve donor mice, the exact reason for the presence of this population remains unclear.

In addition to CD44, the expression of the adhesion molecule L-selectin (CD62L) was analyzed. Approximately 75% of OVA-specific $CD4^+$ T cells from OT-II x WT and OT-II x $IkB_{NS}^{-/-}$ were $CD62L^{high}$.

Taken together, the majority of transferred $CD4^+$ T cells derived from OT-II x WT and OT-II x $I\kappa B_{NS}^{-/-}$ exhibited a naïve $CD44^{int}$ and $CD25^-CD44^{neg}CD62L^+$ phenotype. No obvious differences were observed between the genotypes, thus providing a well-defined basis for *in vivo* studying antigen-specific T cell activation and effector T cell responses in dependency of $I\kappa B_{NS}$.

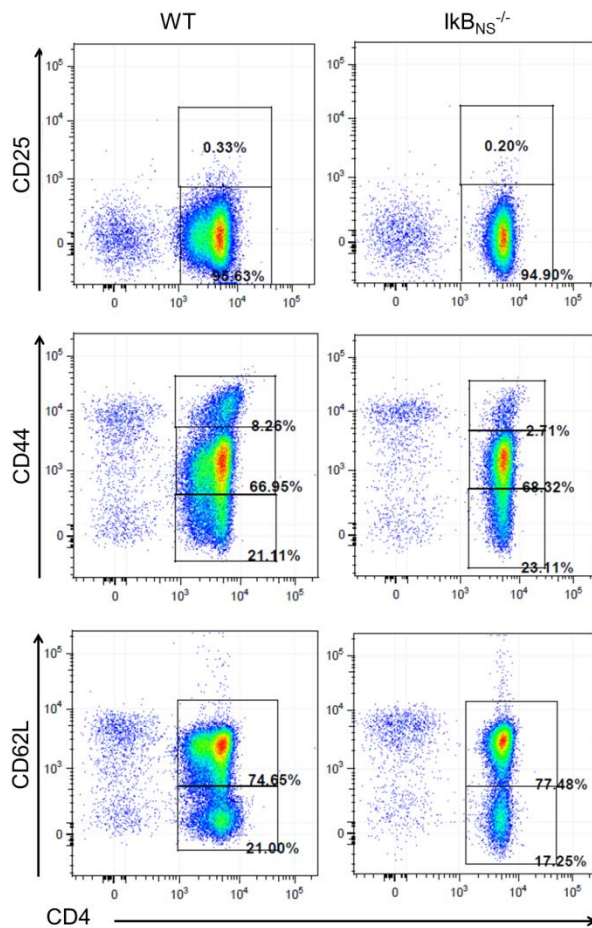


Figure 14: Representative dot plots showing the activation status of $CD4^+$ T cells isolated from OT-II x WT and OT-II x $I\kappa B_{NS}^{-/-}$ mice before adoptive transfer. Lymphocytes from OT-II x WT and OT-II x $I\kappa B_{NS}^{-/-}$ mice were collected from spleen and lymph nodes and $CD4^+$ T cells were isolated by autoMACS. After MACS isolation, cells were stained for the expression of TCR $V\beta 5.1/5.2$, TCR $V\alpha 2$ and $CD4$ as well as the activation markers $CD25$, $CD44$ and $CD62L$ and analyzed by flow cytometry. Cell debris were excluded from the analysis and cells were pre-gated on singlets and TCR $V\beta 5.1/5.2$ vs. TCR $V\alpha 2$ transgenic cells. Numbers represent the percentage of the respective marker positive and also negative cells.

In order to analyze the *in vivo* activation of adoptively transferred OVA-specific OT-II x WT and OT-II x $I\kappa B_{NS}^{-/-}$ $CD4^+$ T cells in response to LM-OVA as antigen-specific stimulus, the cells in spleen and liver were analyzed at different times (d3, d5) post infection. To restrict the re-analysis to the transferred T cells only, the congenic Thy1.1 ($CD90.1$) marker was used for pre-gating.

Figure 15 summarizes individual CFSE distribution patterns of transferred Thy1.1 T cells in LM-OVA infected recipient mice. As depicted in Figure 15A, on day 3 post infection the majority of the transferred OT-II x WT and OT-II x $I\kappa B_{NS}^{-/-}$ $CD4^+$ T cells are still CFSE^{high}, indicating that they did not yet start proliferating. The same was true for re-isolated cells from livers of LM-OVA infected recipients, which basically showed no proliferation. Interestingly, only small numbers of transferred OVA-specific Thy1.1⁺ $CD4^+$ T cells were found in livers 3 days post infection independent of the

genotype. This indicates that even 4 days after T cell transfer the cells did not evenly distribute throughout the organs, but prefer to reside in the spleen.

In contrast, when analyzing the transferred T cells 5 days post infection (Figure 15B) it becomes obvious that a part of the OVA-specific $CD4^+$ T cells indeed underwent several cycles of division both in spleens and livers. Strikingly, the OVA-specific $CD4^+$ T cells sufficient for $I\kappa B_{NS}$ underwent significantly stronger proliferation indicated by a higher CFSE loss compared to $CD4^+$ T cells lacking $I\kappa B_{NS}$. The same result was observed for $CD4^+$ T cells in the livers 5 days post infection. Moreover, at this time more cells were detected in the liver compared to day 3 post infection. This might be due to infection-related migration of the transferred cells.

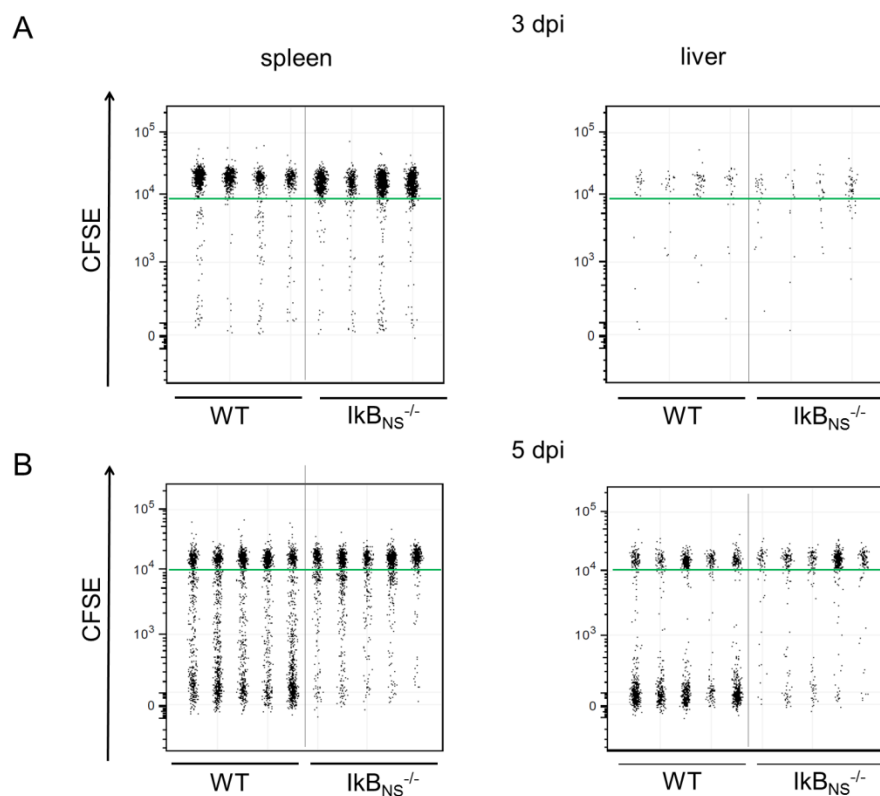


Figure 15: Proliferation of transferred OVA-specific OT-II x WT and OT-II x $I\kappa B_{NS}^{-/-}$ $CD4^+$ T cells at different times post LM-OVA infection. $CD4^+$ T cells from OT-II x WT and OT-II x $I\kappa B_{NS}^{-/-}$ with Thy1.1 congenic background were MACS purified, CFSE labeled and 3×10^6 T cells were adoptively transferred into naïve C57BL/6 recipient mice. One day post transfer recipient mice were i.v. infected with 5000 CFU LM-OVA. 3 days (A) and 5 days (B) post infection recipient mice were sacrificed and CFSE loss on lymphocytes from spleen and liver was analyzed by FACS. FACS data from $n=4-5$ individual mice/group were constrained to alive singlet Thy1.1 $^+$ $CD4^+$ T cells and are shown in columns side-by-side in a concatenated qualitative dot plot in which each column represents data of an individual mouse. The genotype of the analyzed T cells is indicated. Green lines mark the fluorescence intensity below which cells are considered as $CFSE^{low}$.

Since the most obvious LM-OVA induced proliferation and first striking differences between the WT and $I\kappa B_{NS}^{-/-}$ $CD4^+$ T cell genotypes were observed on day 5 post infection, the proliferation and activation status of OVA-specific $CD4^+$ T cells in dependence of $I\kappa B_{NS}$ was analyzed in more detail at this particular time post LM-OVA infection. As described above, OVA-specific $CD4^+$ T cells derived from OT-II x $I\kappa B_{NS}^{-/-}$ mice showed less proliferative capacity following *in vivo* pathogen encounter in comparison to $CD4^+$ T cells from OT-II x WT mice (Figure 16A). This effect was observed in spleens as well as in liver samples. Quantification of the exact frequencies (Figure 16A, upper panel) of $CFSE^{low}$ OVA-specific $CD4^+$ T cells from OT-II x WT mice in spleens revealed that they are in average

2.9 times higher than the frequencies of OT-II x $\text{IkB}_{\text{NS}}^{-/-}$ mice (OT-II x WT: $49\% \pm 6\%$, OT-II x $\text{IkB}_{\text{NS}}^{-/-}$: $17\% \pm 3\%$). The same observation holds true for the cells re-analyzed from livers (Figure 16A, lower panel). Here, 3.4-times higher frequencies of proliferated OVA-specific IkB_{NS} -sufficient CD4^+ T cells ($62\% \pm 7\%$) compared to OVA-specific IkB_{NS} -deficient CD4^+ T cells ($18\% \pm 5\%$) were detected. Analyzing CFSE dilution in conjunction with the expression of CD25, CD44, IFN γ and IL2 allows deeper insights into the fate of transferred T cells in spleen and liver (Figure 16B and C) after LM infection. Concerning CD25 and CD44, lower frequencies of proliferated (CFSE^{low}) CD25⁺ and CD44^{high} OVA-specific CD4^+ T cells from OT-II x $\text{IkB}_{\text{NS}}^{-/-}$ mice were detected compared to cells from OT-II x WT mice. In general, not too many T cells with strong CD25 expression could be detected in both organ compartments and both genotypes (in average about 1-3%). Still, the percentage of CFSE^{low} CD25⁺ CD4^+ T cells from OT-II x WT mice was significantly higher compared to OT-II x $\text{IkB}_{\text{NS}}^{-/-}$ mice (WT spleen: $3.4\% \pm 0.5\%$, $\text{IkB}_{\text{NS}}^{-/-}$ spleen: $1.3\% \pm 0.3\%$; WT liver: $2.6\% \pm 0.7\%$, $\text{IkB}_{\text{NS}}^{-/-}$ liver: $0.7\% \pm 0.4\%$). Given the canonical CD25/IL2 autocrine feedback loop, typically required for exponential T cell expansion, the lack in proliferating CD25⁺ OT-II x $\text{IkB}_{\text{NS}}^{-/-}$ CD4^+ T cells corresponds to the lack in IL2 production by the same cells as well as with their diminished proliferation (compare to Figure 16A). This overall observation holds true for spleen and liver.

In case of the CD44^{high} expression which marks activated or memory T cells, significant differences were observed between OT-II x WT and OT-II x $\text{IkB}_{\text{NS}}^{-/-}$ CD4^+ T cells in both spleen and liver. Here, significantly more CD44^{high} CFSE^{low} OT-II x WT CD4^+ T cells were detected compared to OT-II x $\text{IkB}_{\text{NS}}^{-/-}$ (WT spleen: $27.7\% \pm 8.4\%$, $\text{IkB}_{\text{NS}}^{-/-}$ spleen: $7.0\% \pm 3.9\%$; WT liver: $27.7\% \pm 8.4\%$, $\text{IkB}_{\text{NS}}^{-/-}$ liver: $7.8\% \pm 6.3\%$), indicating a decreased activation of OT-II x $\text{IkB}_{\text{NS}}^{-/-}$ CD4^+ T cells in response to LM-OVA.

Regarding the secretion of IFN γ (Figure 16C) higher frequencies of IFN γ ⁺ CFSE^{low} OVA-specific WT CD4^+ T cells were re-covered from the livers than from spleens (WT spleen: $21.0\% \pm 3.0\%$, $\text{IkB}_{\text{NS}}^{-/-}$ spleen: $4.7\% \pm 0.8\%$; WT liver: $37.7\% \pm 6.5\%$, $\text{IkB}_{\text{NS}}^{-/-}$ liver: $4.6\% \pm 1.0\%$). This organ-dependent effect was not observed for proliferated OVA-specific $\text{IkB}_{\text{NS}}^{-/-}$ CD4^+ T cells. Here, in both organs less than 10% IFN γ ⁺ cells were detected. Of note, when looking on the representative dot plots for OT-II x WT CD4^+ T cells in liver and spleen (Figure 16C), secretion of IL2 and IFN γ clearly corresponds with the degree of CFSE loss, as only T cells that are completely CFSE-negative and thus underwent several consecutive cell divisions, are producers of cytokines. Those cells can be considered differentiated effector T cells, since especially the production of the Th1 effector cytokine IFN γ is a property typically acquired only after several cell divisions under Th1-differentiating conditions. Apparently, $\text{IkB}_{\text{NS}}^{-/-}$ CD4^+ T cells are impaired in this respect, as they show little to no IL2 and especially no IFN γ secretion.

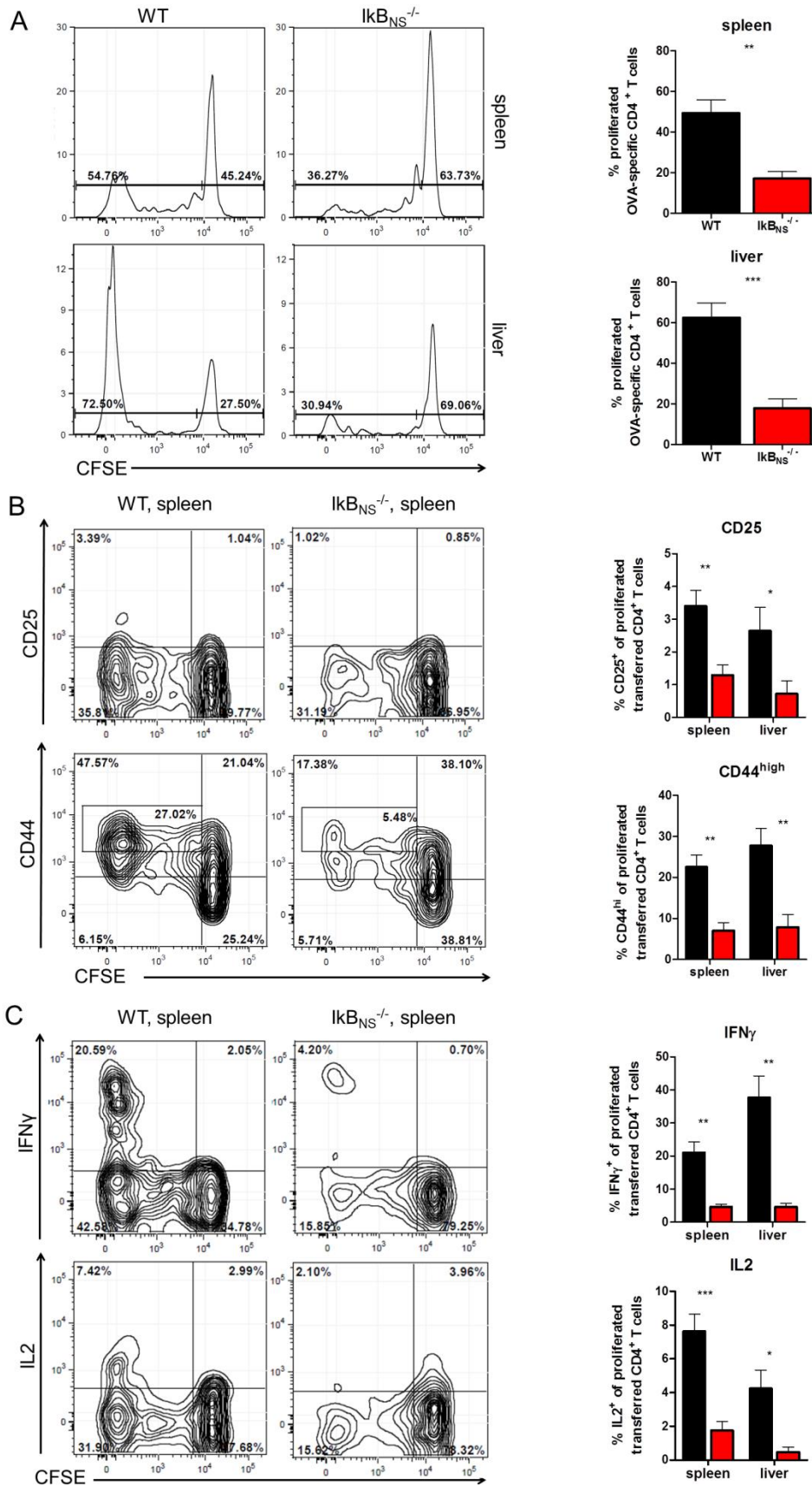


Figure 16: Phenotype of adoptively transferred OT-II x WT and OT-II x IκB_{NS}^{-/-} CD4⁺ T cells 5 days after LM-OVA infection. (Figure legend continues on the next page)

CD4⁺ OT-II x WT (■) and OT-II x IκB_{NS}^{-/-} (■) T cells with Thy1.1 congenic background were MACS-purified, CFSE-labeled and 3 x 10⁶ T cells were adoptively transferred into naïve C57BL/6 recipient mice. One day post transfer recipient mice were i.v. infected with 5000 CFU LM-OVA. 5 days post infection recipient mice were sacrificed and lymphocytes from spleen and liver were stained with antibodies against CD25, CD44, IFNγ or IL2 and re-analyzed by FACS. Prior to intracellular staining of IFNγ and IL2, cells were re-stimulated with 1 μg/mL OVA₃₂₃₋₃₃₉ peptide for 5 h, with brefeldin A added for the last 4 h of incubation. FACS data (n=5 mice/group) were constrained to alive singlet Thy1.1⁺ CD4⁺ T cells. Data are depicted as mean ± SEM. (A) Representative CFSE histograms and summary plots indicating proliferation as percentage of CFSE^{low} T cells. (B) Representative contour plots with 5% probability without outliers for CD25 and CD44 vs. CFSE from OT-II x WT and OT-II x IκB_{NS}^{-/-} CD4⁺ T cells. Summary plots indicate percentage of CD25⁺ and percentage of CD44^{hi} T cells within the CFSE^{low} fraction. (C) Representative contour plots with 5% probability without outliers for IFNγ and IL2 vs. CFSE from OT-II x WT and OT-II x IκB_{NS}^{-/-} CD4⁺ T cells. Summary plots indicate percentage of IFNγ⁺ and percentage of IL2⁺ T cells within the CFSE^{low} fraction. Statistics were performed using two-tailed unpaired student's *t*-test comparing WT and IκB_{NS}^{-/-} CD4⁺ T cells. * *p* < 0.05; ** *p* < 0.01, *** *p* < 0.001.

In summary, IκB_{NS} has a clear influence on the activation and proliferation of CD4⁺ T cells following antigen-specific activation in the context of an *in vivo* LM infection. Data obtained in the chosen experimental setup suggest that especially the differentiation into Th1 CD4⁺ effector T cells is affected when IκB_{NS} is missing. This is in particular interesting with respect to the fact, that OT-II x IκB_{NS}^{-/-} CD4⁺ T cell responses following *in vitro* peptide stimulation was comparable to their WT counterparts (see chapter 4.1.1), highlighting the overall importance of the experimental setting (*in vitro* vs. *in vivo*, T cell stimulation in the presence or absence of infection-related inflammation) in which T cell functions are analyzed.

4.2.2 IκB_{NS}-deficiency has only marginal effects on the activation of CD8⁺ T cells following *in vivo* pathogen encounter

In order to contain and eliminate intracellular infections, CD8⁺ T cell-mediated immune responses play an essential role. Infection with *Listeria monocytogenes* induces strong CD8⁺ T cell expansion and the development of pronounced cytotoxic effector functions (Seaman et al., 2000). An essential effector function is the secretion of inflammatory mediators such as IFNγ and IL2, which in turn further promote the expansion of effector CD8⁺ T cells.

The previous chapter (4.2.1) showed a clear impact of IκB_{NS} on proliferation and priming of CD4⁺ T cells in the context of antigen-specific stimulation during *in vivo* LM infection. Thus, it was next studied whether the *in vivo* CD8⁺ T cell response would also be dependent on IκB_{NS}. This was suggested by the results from the *in vitro* stimulation experiments indicating that CD8⁺ T cells from OT-I x IκB_{NS}^{-/-} mice are impaired in IFNγ secretion when stimulated with the cognate OVA peptide (refer to chapter 4.1.2)

For that purpose, the experimental set-up described in chapter 4.2.1 was used. For the re-analysis of adoptively transferred CD8⁺ T cells additional markers which are described in the context of effector CD8⁺ T cells such as PD1 and TNFα were included. The experimental scheme is represented in Figure 17. Naïve OVA-specific CD8⁺ T cells from OT-I x WT and OT-I x IκB_{NS}^{-/-} mice were isolated by MACS, stained with CFSE and transferred via lateral tail vein injection into C57BL/6 recipients. One day post transfer, recipient mice were infected with LM-OVA and at different times (d1, d3 and d5) post infection, transferred cells were re-analyzed by flow cytometry.

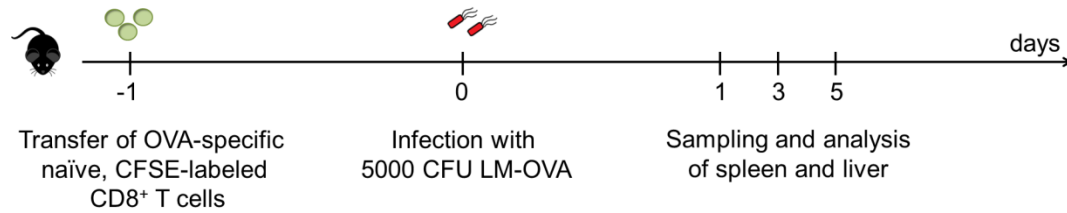


Figure 17: Schematic overview about the experimental design of adoptive transfer of OT-I transgenic CD8⁺ T cells followed by LM-OVA infection. Naive OVA-specific CD8⁺ T cells were isolated from either OT-I x WT or OT-I x I κ B_{NS}^{-/-} mice by autoMACS. Afterwards, CD8⁺ T cells were stained with 2.5 μ M CFSE and 3×10^6 cells were injected into C57BL/6 recipients. One day post transfer, mice were infected with a sublethal dose (5000 CFU/mouse) of LM-OVA. At different times post infection, mice were sacrificed, spleens and livers were sampled and the proliferation and activation status of transferred CD8⁺ T cells were analyzed by flow cytometry.

Prior to adoptive transfer of OVA-specific CD8⁺ T cells the expression of CD25, CD44 and CD62L was analyzed (Figure 18) to ensure that the transferred cells exhibit a naïve phenotype (refer to chapter 4.2.1).

Less than 0.1% CD25⁺ was detected on the surface of OVA-specific CD8⁺ T cells irrespective of the genotype indicating that in both mouse groups the depletion of CD25 was efficient. Interestingly, when analyzing the expression of CD44, it is noticeable that in case of OT-I CD8⁺ T cells from WT donors approximately 27% are CD44^{high} whereas in case of OT-I CD8⁺ T cells from I κ B_{NS}^{-/-} mice only about 11% are highly positive for CD44. Of note, the CD8⁺ T cells were not exposed to the OVA antigen before their isolation, thereby a prior antigen-specific activation can be excluded and the increased CD44^{high} frequency is considered as an artifact of the OT-I mouse model. Regarding the activation marker CD62L, more than 80% of OT-I CD8⁺ T cells from WT as well as I κ B_{NS}^{-/-} donor mice were CD62L^{high}. In summary, the transferred OVA-specific CD8⁺ T cells exhibited a naïve phenotype with exception of the CD44^{high} population (summarized in Figure 18), which was taken into account in subsequent cell-fate analysis.

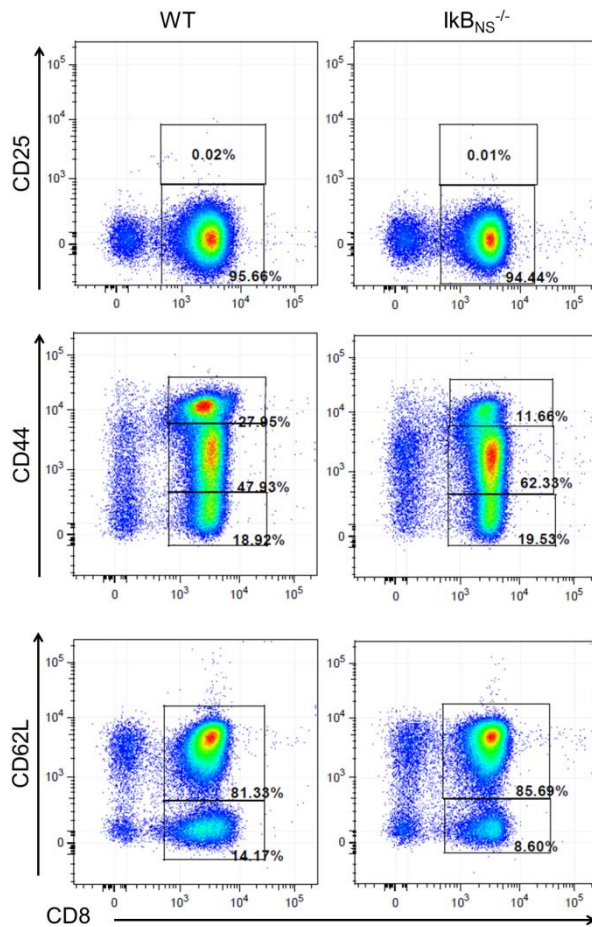


Figure 18: Representative dot plots showing the activation status of CD8⁺ T cells isolated from OT-I x WT and OT-I x Ikb_{NS}^{-/-} mice. Lymphocytes from OT-I x WT and OT-I x Ikb_{NS}^{-/-} mice were collected from spleen and lymph nodes and CD8⁺ T cells were isolated by autoMACS. After MACS isolation, cells were stained for the expression of TCR V β 5.1/5.2, TCR V α 2 and CD8 as well as for the activation markers CD25, CD44 and CD62L, respectively, and analyzed by flow cytometry. Cell debris were excluded from the analysis and cells were pregated on singlets and TCR V β 5.1/5.2 vs. TCR V α 2 transgenic cells. Numbers represent the percentage of the respective marker positive and also negative cells.

To investigate the impact of Ikb_{NS} on CD8⁺ T cell activation in response to *in vivo* LM-OVA infection, different points in time post infection were selected for re-analysis of the transferred cells. Figure 19 represents mouse-individual CFSE dilution patterns. As depicted in Figure 19A, one day post infection the OVA-specific CD8⁺ T cells basically show no CFSE loss in spleens and livers, indicating that they did not proliferate. In the next step, cells were re-analyzed 3 days post infection. As depicted in Figure 19B, at this time all OT-I x WT or OT-I x Ikb_{NS}^{-/-} CD8⁺ T cells recovered from spleens underwent proliferation as indicated by a homogenous loss of CFSE. However, OVA-specific CD8⁺ T cells were hardly detectable in liver samples 3 days post infection. The few CD8⁺ T cells recovered from the livers were CFSE^{low}, whereas at this time still all CFSE-intermediates ranging from high to low can be found in spleens. No genotype-dependent differences in T cell proliferation and tissue distribution became evident on day 3 post LM infection. Finally, the transferred cells were re-analyzed 5 days post infection (Figure 19C). Here, a nearly complete loss of the CFSE dye was detected in spleen and liver samples indicating that the cells underwent intensive proliferation. In addition, generally more cells were detected in both organs compared to day 3 post infection. Next to extensive CD8⁺ T cell expansion

due to proliferation following *in vivo* pathogen encounter this might also be due to an infection-related T cell migration into the primary LM replication sites, e.g. spleen and liver.

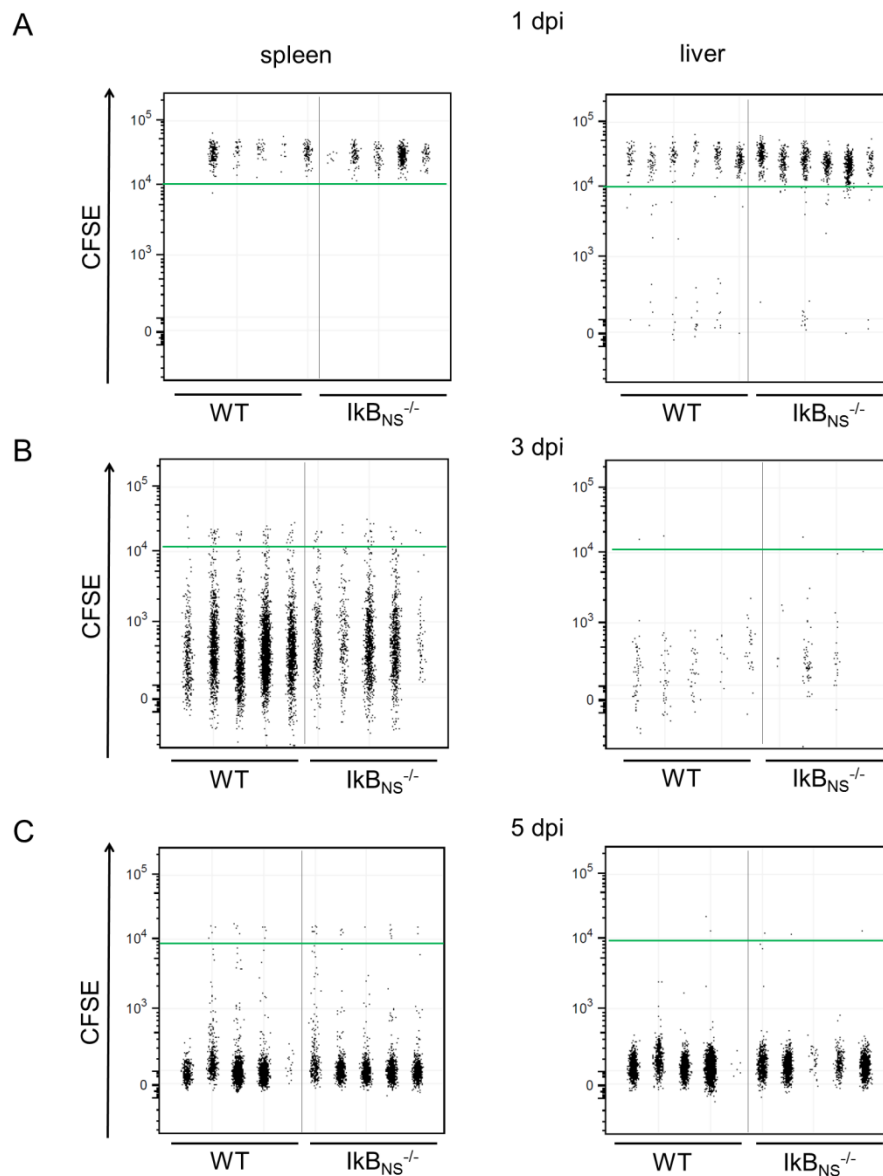


Figure 19: Proliferation of transferred OVA-specific OT-I x WT and OT-I x $I\kappa B_{NS}^{-/-}$ $CD8^{+}$ T cells at different times post LM-OVA infection. $CD8^{+}$ T cells from OT-I x WT and OT-I x $I\kappa B_{NS}^{-/-}$ with Thy1.1 congenic background were autoMACS purified, CFSE labeled and 3×10^6 T cells were adoptively transferred into naïve C57BL/6 recipient mice. One day post transfer recipient mice were i.v. infected with 5000 CFU LM-OVA. 1 day (A), 3 days (B) and 5 days (C) post infection recipient mice were sacrificed and the CFSE intensity of lymphocytes from spleen and liver was analyzed by FACS. FACS data from $n = 5-6$ individual mice/group were constrained to alive singlet Thy1.1 $^{+}$ $CD8^{+}$ T cells and are shown in columns side-by-side in a concatenated qualitative dot plot in which each column represents data of an individual mouse. The genotype of the analyzed T cells is indicated. Green lines mark the fluorescence intensity below which cells are considered as $CFSE^{low}$.

Based on the obtained data, day 3 post infection was selected as earliest time point to elucidate potential differences between OT-I x WT and OT-I x $I\kappa B_{NS}^{-/-}$ $CD8^{+}$ T cells regarding their *in vivo* activation profile.

Similar to the qualitative CFSE distribution patterns (Figure 19) also the quantitative data depicting percentages of $CFSE^{low}$ OVA-specific $CD8^{+}$ T cells clearly indicate a strong proliferation in response to LM-OVA infection irrespective of the presence or absence of $I\kappa B_{NS}$ (Figure 20A). Interestingly, the

frequency of recovered CD25⁺ OVA-specific CD8⁺ T cells derived from OT-I x I κ B_{NS}^{-/-} mice was more than twice as high as the frequency of CD25⁺ CD8⁺ T cells from WT counterparts (OT-I x WT: 14.1% \pm 1.6%, OT-I x I κ B_{NS}^{-/-}: 38.3% \pm 6.0%, Figure 20B). In contrast, the same percentage of transferred OVA-specific CD8⁺ T cells was CD44^{high} independent of the genotype, indicating that the progression to effector and memory phenotype was not affected by loss of I κ B_{NS}. This was confirmed by equally high frequencies of CFSE^{low} IFN γ ⁺ OVA-specific CD8⁺ T cells of both genotypes (Figure 20C). However, OVA-specific CD8⁺ T cells of both genotypes showed only marginal expression of IL2 on day 3 post infection. This was somehow unexpected, since at the same time approximately 40% of OT-I x I κ B_{NS}^{-/-} CD8⁺ T cells were positive for CD25, the α -chain of the high-affinity IL2-receptor (Figure 20C). Furthermore, the expression of the programmed cell death protein 1 (PD1) was examined. Here, 30% of OT-I x WT CD8⁺ T cells expresses PD1 which is significantly more compared to OT-I x I κ B_{NS}^{-/-} CD8⁺ T cells with 14%.

Conversely, significant higher frequency of TNF α producing OT-I x I κ B_{NS}^{-/-} CD8⁺ T cells was detected compared to the WT counterparts. One possible explanation might be that I κ B_{NS} acts as a suppressor for this pro-inflammatory cytokine at a certain stage to prevent an exaggerated effector T cell response.

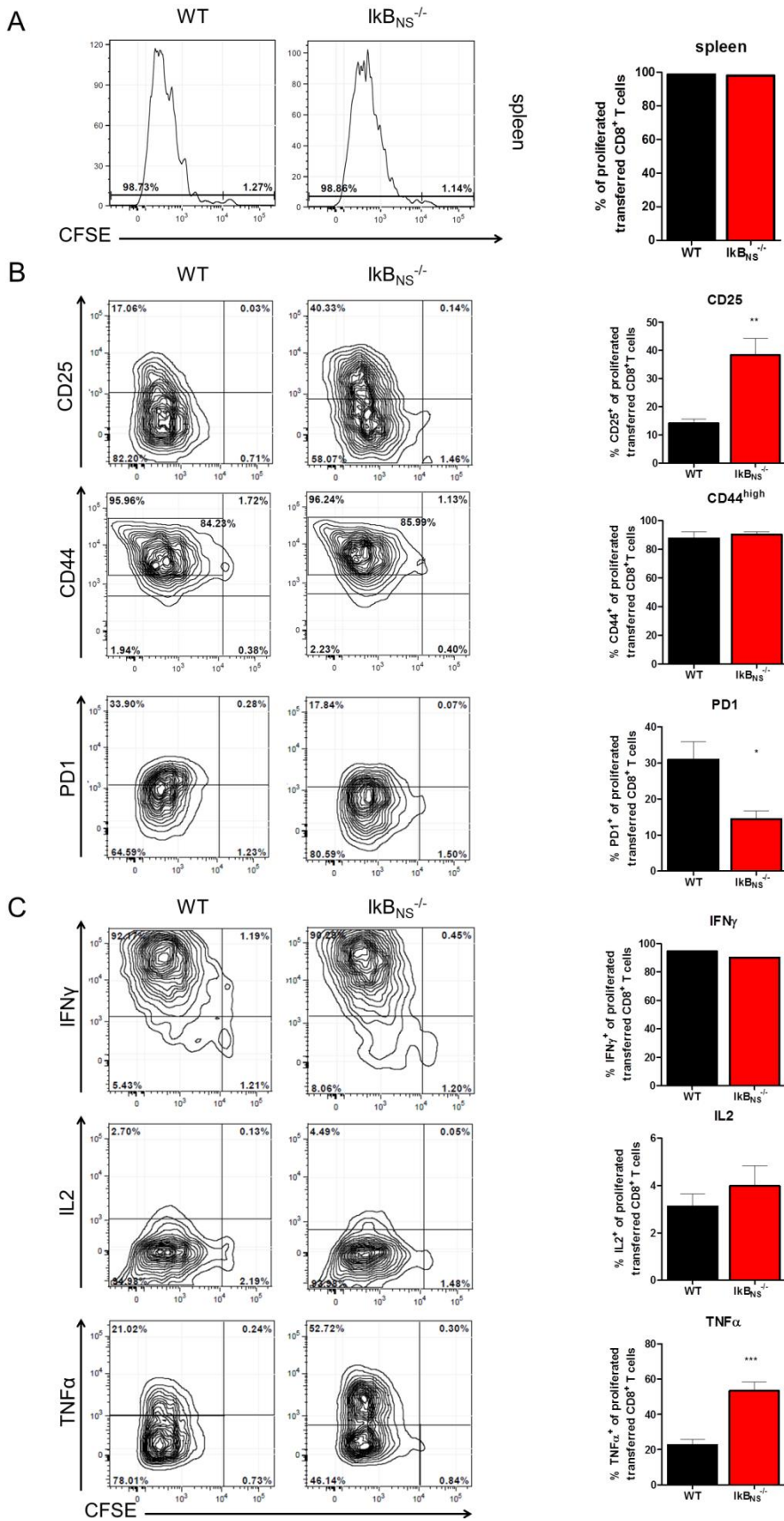


Figure 20: Phenotype of adoptively transferred OT-I x WT and OT-I x $IkB_{NS}^{-/-}$ CD8 $^{+}$ T cells 3 days post LM-OVA infection. (Figure legend continues on the next page)

CD8⁺ OT-I x WT (■) and OT-I x IκB_{NS}^{-/-} (■) T cells with Thy1.1 congenic background were autoMACS-purified, CFSE-labeled and 3 x 10⁶ T cells were adoptively transferred into naïve C57BL/6 recipient mice, respectively. One day post transfer recipient mice were i.v. infected with 5000 CFU LM-OVA. 3 days post infection recipient mice were sacrificed and lymphocytes from spleen and liver were stained with antibodies against CD25, CD44, PD1 or IFN γ , IL2 and TNF α and re-analyzed by FACS. Prior to intracellular staining of IFN γ , IL2 and TNF α cells were re-stimulated with 1 μ g/mL OVA₂₅₇₋₂₆₄ peptide for 5 h, with brefeldin A added for the last 4 h of incubation. FACS data (n= 5 mice/group) were constrained to alive singlet Thy1.1⁺ CD8⁺ T cells. Data are depicted as mean \pm SEM. (A) Representative CFSE histograms and summary plots indicating proliferation as %CFSE^{low} T cells. (B) Representative contour plots with 5% probability without outliers for CD25, CD44 and PD1 vs. CFSE from OT-I x WT and OT-I x IκB_{NS}^{-/-} CD8⁺ T cells. Summary plots indicate percentage of CD25⁺, CD44^{hi} and PD1⁺ T cells, respectively, within the CFSE^{low} fraction. (C) Representative contour plots with 5% probability without outliers for IFN γ , IL2 and TNF α vs. CFSE from OT-I x WT and OT-I x IκB_{NS}^{-/-} CD8⁺ T cells. Summary plots indicate percentage of IFN γ ⁺, IL2⁺ and TNF α ⁺ T cells, respectively, within the CFSE^{low} fraction. Statistics were performed using two-tailed unpaired student's t-test comparing WT and IκB_{NS}^{-/-} CD8⁺ T cells. * p < 0.05; ** p < 0.01, *** p < 0.001.

Taken together, these results indicate that antigen-specific CD8⁺ T cell responses during *in vivo* LM-OVA infection are partially dependent on IκB_{NS}. Whereas proliferation as well as CD44 and IFN γ expression were not affected by a loss of IκB_{NS}, the expression of CD25, PD1 and also TNF α in CD8⁺ T cells is dependent on IκB_{NS}.

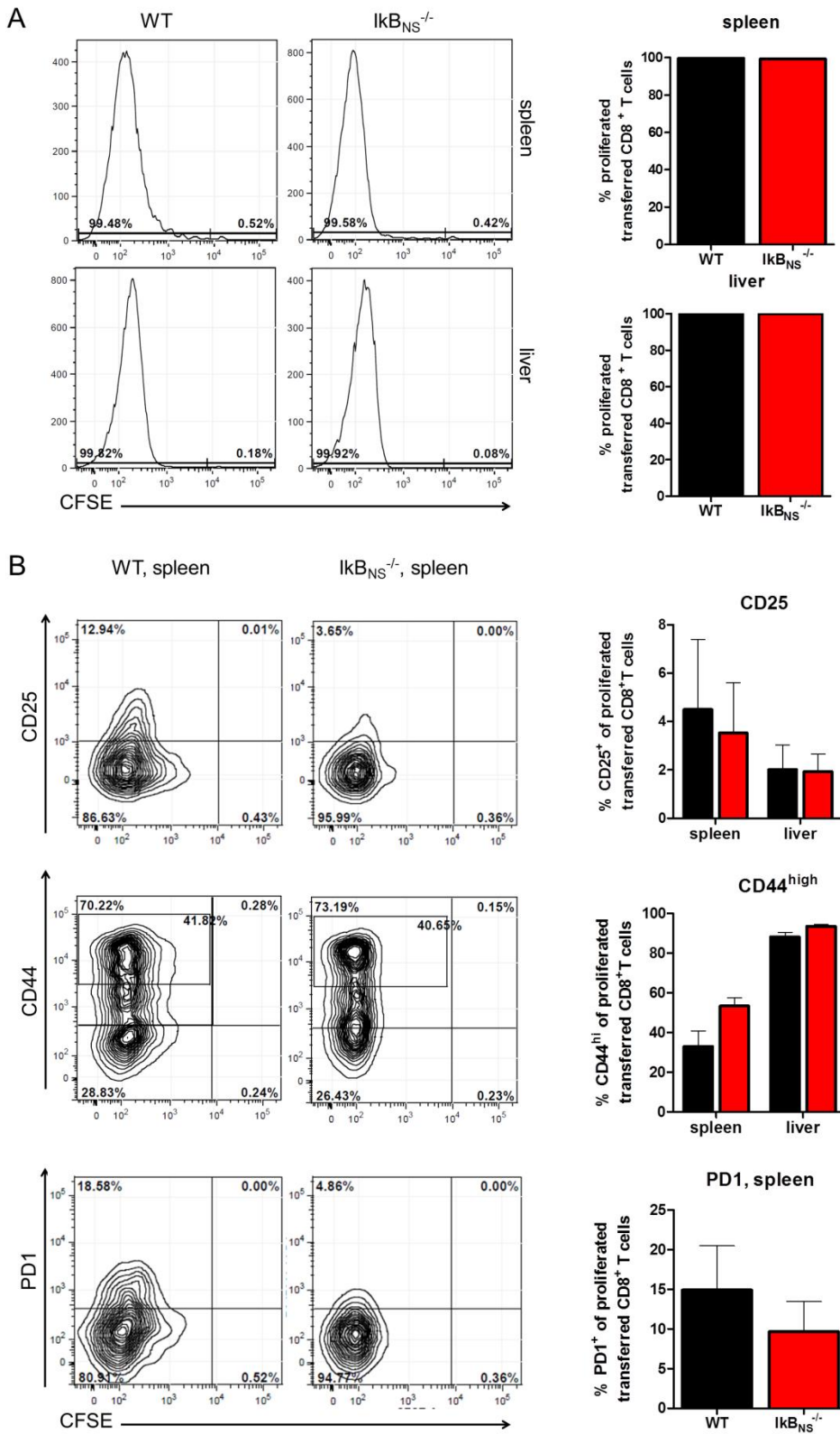
OVA-specific CD8⁺ T cells were next analyzed in more detail 5 days post LM infection. As summarized in the qualitative mouse-individual CFSE distribution plots (Figure 19), almost all OT-I CD8⁺ T cells from both genotypes underwent intensive proliferation in spleen and liver. Quantification of the frequencies of CFSE^{low} OVA-specific CD8⁺ T cells revealed as well no differences between both IκB_{NS} genotypes (Figure 21A). Figure 21B and C summarize the analyses of the activation markers CD25, CD44 and PD1 as well as the cytokines IFN γ , IL2 and TNF α , respectively. In contrast to the day 3 analysis of the spleen (refer to Figure 20B) where significantly more CD25⁺ OVA-specific OT-I x IκB_{NS}^{-/-} CD8⁺ T cells were detected compared to OT-I x WT, no difference regarding CD25 expression was observed 5 days post infection. Though the same frequency of CD25⁺ CD8⁺ T cells were detected, irrespective of the IκB_{NS} genotype, it is important to note that on day 5 post infection only 4% of the CD8⁺ T cells were CD25⁺ as opposed to 10% (OT-I x WT) and 40% (OT-I x IκB_{NS}^{-/-}) on day 3 post infection. This indicates a clear drop in CD25 expression within 2 days occurring in both genotypes. In line with this, 5 days post infection only marginal frequencies of CD8⁺CD25⁺ T cells were detected in the liver as well (approximately 2% in both genotypes). This drop in CD25 expression on day 5 compared to day 3 might be due to the fact that at this time all transferred cells already underwent intensive proliferation and thus the IL2/CD25 feedback-loop becomes dispensable. In line with this, the expression of IL2 by OVA-specific CD8⁺ T cells re-covered from spleens and livers remained equally low, independent of the genotype.

In case of CD44, the same frequency of CD44^{high} CD8⁺ T cells was detected in both genotypes. More than 40% OVA-specific CD8⁺ T cells from spleens were CD44^{high} and more than 80% were CD44^{high} in livers, irrespective of the IκB_{NS} genotype (see Figure 21B). Nevertheless, in comparison to OVA-specific CD8⁺ T cells re-analyzed on day 3 post infection, generally less CD44^{high} T cells were detectable in spleens on day 5 post infection. However, in contrast to day 3 post infection where no distinct CD44^{low} populations were detected in spleen samples of both genotypes, both mouse groups exhibited a distinct CD44^{low} CFSE^{low} low population by day 5 post infection. In liver samples, more than 80% of OT-I x WT and OT-I x IκB_{NS}^{-/-} CD8⁺ T cells were found to be CD44^{high} CFSE^{low}.

In case of IFN γ secretion no difference between OT-I x WT and OT-I x IκB_{NS}^{-/-} CD8⁺ T cells was observed, i.e. almost all cells re-covered from spleens expressed high amounts of IFN γ (\geq 95%)

independent of the presence or absence of $\text{I}\kappa\text{B}_{\text{NS}}$. When looking at the representative contour plots from spleens it becomes obvious that especially CD8^+ T cells that underwent extensive proliferation show the highest IFN γ expression.

The OVA-specific CD8^+ T cells from spleens were furthermore analyzed with respect to the expression of PD1 and TNF α . The frequencies of PD1 $^+$ cells were comparable between both genotypes (10-15%), but were in general lower than on day 3 post infection. In the spleen OVA-specific CD8^+ T cells from OT-I x $\text{I}\kappa\text{B}_{\text{NS}}^{-/-}$ expressed significantly more TNF α than OVA-specific CD8^+ T cells from OT-I x WT mice (OT-I x WT spleen: 25.9% \pm 2.8%, OT-I x $\text{I}\kappa\text{B}_{\text{NS}}^{-/-}$ spleen: 44.4% \pm 5.6%) This phenomenon was observed already on day 3 post infection (compare to Figure 20C).



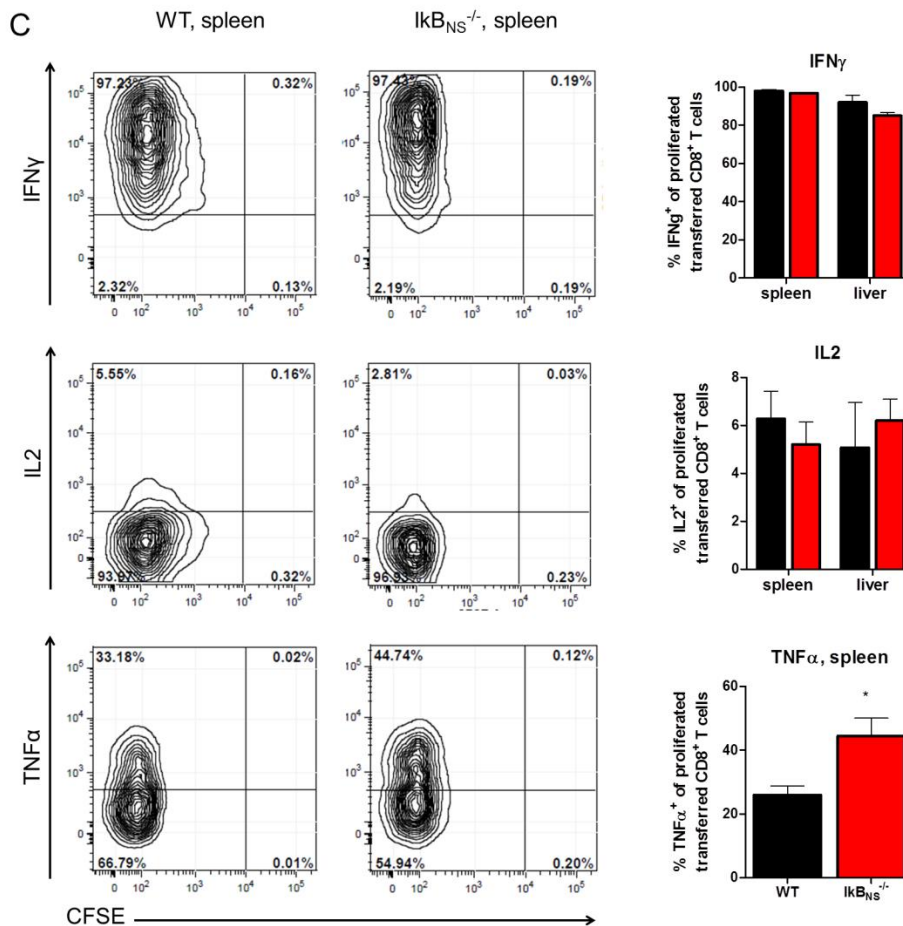


Figure 21: Phenotype of adoptively transferred OT-I x WT and OT-I x IkB_{NS}^{-/-} CD8⁺ T cells 5 days after LM-OVA infection. CD8⁺ OT-I x WT (■) and OT-I x IkB_{NS}^{-/-} CD8⁺ T cells with Thy1.1 congenic background were MACS-purified, CFSE-labeled and 3×10^6 T cells were adoptively transferred into naïve C57BL/6 recipient mice, respectively. One day post transfer recipient mice were i.v. infected with 5000 CFU LM-OVA. 5 days post infection recipient mice were sacrificed and lymphocytes from spleen and liver were stained with antibodies against CD25, CD44, PD1 or IFN γ , IL2 and TNF α and re-analyzed by FACS. Prior to intracellular staining of IFN γ , IL2 and TNF α cells were re-stimulated with 1 μ g/mL OVA₂₅₇₋₂₆₄ peptide for 5 h, with brefeldin A added for the last 4 h of incubation. FACS data (n= 5 mice/group) were constrained to alive singlet Thy1.1⁺ CD8⁺ T cells. Data are depicted as mean \pm SEM. (A) Representative CFSE histograms and summary plots indicating proliferation as percentage of CFSE^{low} T cells. (B) Representative contour plots with 5% probability without outliers for CD25, CD44 and PD1 vs. CFSE from OT-I x WT and OT-I x IkB_{NS}^{-/-} CD8⁺ T cells. Summary plots indicate percentage of CD25, CD44^{hi} and PD1⁺ T cells, respectively, within the CFSE^{low} fraction. (C) Representative contour plots with 5% probability without outliers for IFN γ , IL2 and TNF α vs. CFSE from OT-I x WT and OT-I x IkB_{NS}^{-/-} CD8⁺ T cells. Summary plots indicate percentage of IFN γ ⁺, IL2⁺ and TNF α ⁺ T cells, respectively, within the CFSE^{low} fraction. Statistics were performed using two-tailed unpaired student's *t*-test comparing WT and IkB_{NS}^{-/-} CD8⁺ T cells. * *p* < 0.05, ** *p* < 0.01, *** *p* < 0.001.

In summary, the results largely confirmed the aforementioned observations made on day 3 post infection. The *in vivo* proliferation capacity of OVA-specific CD8⁺ T cells is not affected by a loss of IkB_{NS} neither in spleens nor in liver samples. The differences observed on day 3 post infection regarding the CD25 and PD1 expression were gone, which might be due to slightly delayed expression of activation markers in IkB_{NS}-deficient CD8⁺ T cells which can be compensated by time. However, even on day 5 post infection the frequency of TNF α ⁺ CFSE^{low} OT-I x IkB_{NS}^{-/-} CD8⁺ T cells is increased compared to the WT counterparts indicating that IkB_{NS} might have a suppressive role in the regulation of TNF α . In contrast to the above mentioned results obtained following *in vitro* CD8⁺ T cell stimulation that revealed significantly impaired IFN γ secretion in absence of IkB_{NS} (refer to chapter 4.1.2), no impact on the IFN γ expression was detected in the applied *in vivo* setting. This clearly

indicates that the overall setting in which the specific T cell functions are analyzed plays an important role. Several factors such as microenvironment in which T cell priming occurs or the cytokine milieu generated by the host's immune response to infection could influence activation and proliferation of the transferred T cells so that it may happen that some specific effects of I κ B_{NS}-deficiency in CD8⁺ T cells observed in *in vitro* stimulation assays might be rescued *in vivo* and *vice versa*.

4.2.3 Impact of I κ B_{NS} in CD4⁺ and CD8⁺ T cells on pathogen clearance

Next to *in vivo* proliferation capacity and activation status of adoptively transferred OVA-specific CD4⁺ and CD8⁺ T cells (refer to Chapter 4.2.1 and 4.2.2), their ability to contribute to the clearance of the LM-OVA pathogen in the respective organs in dependency of I κ B_{NS} was elucidated.

To this end, spleens of LM-OVA infected recipient C57BL/6 mice were sampled at various times post infection (CD4⁺ T cell transfers: d3, d5, d7; CD8⁺ T cell transfers: d1, d3, d5), homogenized and serial dilutions were plated on BHI agar plates to determine the colony forming units (CFU) and thus to define the contribution of the transferred LM-OVA-specific T cells to the control of bacterial burden depending on the presence or absence of I κ B_{NS} in CD4⁺ or CD8⁺ T cells. As depicted in Figure 22A, there was a high bacterial load on day 3 post infection in spleens of mice that received OT-II x WT or OT-II x I κ B_{NS}^{-/-} CD4⁺ T cells, respectively. However, on day 5 post infection a strong decrease in the bacterial load could be observed in both mouse groups, i.e. independent of the genotype of the transferred CD4⁺ T cells, indicating onset of bacterial clearance. No bacteria were detectable on day 7 post infection, suggesting efficient elimination of the bacteria in both mouse groups. Since the adaptive immunity in LM infection typically kicks in around day 5 to day 7 post infection, the observed bacterial clearance in this time frame is likely to be dominated by the adaptive immune response of the host's immune system. Thus, if indeed there would be differences with respect to pathogen-specific effector functions between the two genotypes of transferred LM-OVA-specific CD4⁺ T cells and thus a differential contribution to the clearance of LM-OVA, this could probably only be clearly attributed to the transferred T cells during an early phase of the infection.

In case of recipient mice that received OT-I x WT or OT-I x I κ B_{NS}^{-/-} CD8⁺ T cells, an equally high bacterial load was observed in the spleen on day 1 post infection. In spleens of mice that received OT-I x WT CD8⁺ T cells, an effective clearance already was detected on day 3 post infection with far less bacteria compared to day 1 post infection. Strikingly, mice that received OT-I x I κ B_{NS}^{-/-} CD8⁺ T cells exhibited no reduction of bacterial load by day 3 post infection suggesting that the transferred LM-OVA specific I κ B_{NS}^{-/-} CD8⁺ T cells in contrast to their LM-OVA specific WT counterparts did not have any beneficial effect with respect to pathogen clearance at this time. This was unexpected, since the expression of effector molecules in response to LM-OVA by transferred OVA-specific CD8⁺ T cells such as IFN γ was previously found to be independent of I κ B_{NS} (compare to Figure 20). In any case, on day 5 post infection no bacteria were detectable at all, irrespective of the genotype of the transferred T cells. These results suggest that CD8⁺ T cells from OT-I x I κ B_{NS}^{-/-} mice might be compromised in cytotoxicity especially in the early phase of the LM infection which is likely to be compensated by the host's adaptive immune response constituting in the later infection phase.

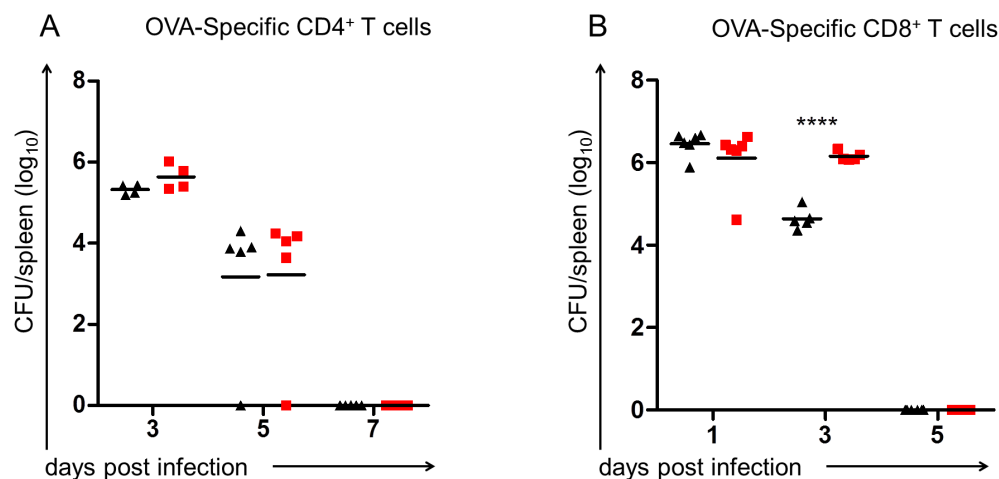


Figure 22: Clearance of LM-OVA infection in C57BL/6 mice which received transgenic OVA-specific CD4⁺ or CD8⁺ T cells from lkb_{NS} sufficient or deficient donors. (A) CD4⁺ T cells and (B) CD8⁺ T cells from OT-II x WT (▲) or OT-II x lkb_{NS}^{-/-} (■) mice were MACS purified, CFSE-labeled and 3×10^6 cells were adoptively transferred into C57BL/6 recipient mice, respectively. One day post transfer recipient mice were i.v. infected with 5000 CFU LM-OVA. At indicated days post infection, recipient mice were sacrificed and CFU in spleens was determined. The mean CFU value of each experimental group is indicated by the horizontal line. Statistical analyses were performed with two-way ANOVA and Bonferroni post-test. **** $p < 0.0001$.

Given the delayed pathogen clearance observed in OT-II x lkb_{NS}^{-/-} CD8⁺ T cell recipient mice compared to OT-II x WT CD8⁺ T cell recipients, hinting at a potentially impaired cytotoxic function of the CD8⁺ T cells lacking lkb_{NS}, *in vivo* cytotoxicity in absence of lkb_{NS} was next studied in more detail.

4.2.4 Impact of lkb_{NS} on *in vivo* cytotoxicity

In order to evaluate CD8⁺ T cell-mediated cytotoxicity in lkb_{NS}^{-/-} mice in frame of LM infection an *in vivo* cytotoxicity assay (CTL) was performed (refer to Chapter 3.9). As mentioned above, it cannot be excluded that in the chosen adoptive transfer model the host's immune system is involved in the clearance of the pathogen as well. Since in the chosen experimental setting the immune system of the recipient host is proficient for lkb_{NS}, we refrained from using the transfer model to probe for *in vivo* cytotoxicity. Instead, conventional lkb_{NS}^{-/-} mice lacking lkb_{NS} in all cells were used to analyze the cytotoxic response to LM-OVA in comparison to WT mice. WT and lkb_{NS}^{-/-} mice were infected with a sublethal dose (10^4 CFU/mouse) of LM-OVA or, as a control, were left untreated. After 9 days post infection they received a pool of CFSE-stained splenocytes (1×10^7 /mouse) from uninfected C57BL/6 mice, consisting of SIINFEKL peptide-pulsed ($1 \mu\text{g/mL}$ OVA₂₅₇₋₂₆₄, CFSE^{high}) and unpulsed (CFSE^{low}) cells in a 1:1 ratio. Here, the CFSE^{low} labeled cell fraction that was not loaded with antigenic peptide serves as background control for unspecific cell lysis. 12 h after cell injection, splenocytes were re-isolated from the infected recipient animals and the *in vivo* cytotoxicity was determined by comparing the frequency of the CFSE^{high} and CFSE^{low} fraction by flow cytometry.

As represented in Figure 23 no obvious differences regarding the specific lysis were observed between the genotypes. In the uninfected control animals, same frequencies of CFSE^{high} and CFSE^{low} cells were detected, thus indicating the absence of unspecific background cytotoxicity. Both, the infected WT and lkb_{NS}^{-/-} mice could eliminate approximately 100% of the transferred peptide-pulsed

splenocytes, indicating that independent of the genotype there was an efficient formation of LM-OVA specific cytotoxic CD8⁺ T cells.

To test whether potential differences in the cytotoxic function between I κ B_{NS}-sufficient and deficient CD8⁺ T cells would become evident with lower antigen doses, the very same experiment was repeated with 10-times lower amount of SIINFEKL-antigen (0.1 μ g/mL OVA₂₅₇₋₂₆₄) used for splenocytes loading. As depicted in Figure 23B both infected mouse groups were able to almost completely lyse the peptide-pulsed cells, indicating that even with lower amounts of antigen the cytotoxic lysis is equally efficient and neither dependent on the amount of antigen used for peptide-pulsing nor dependent on the genotype of the cytotoxic CD8⁺ T cells.

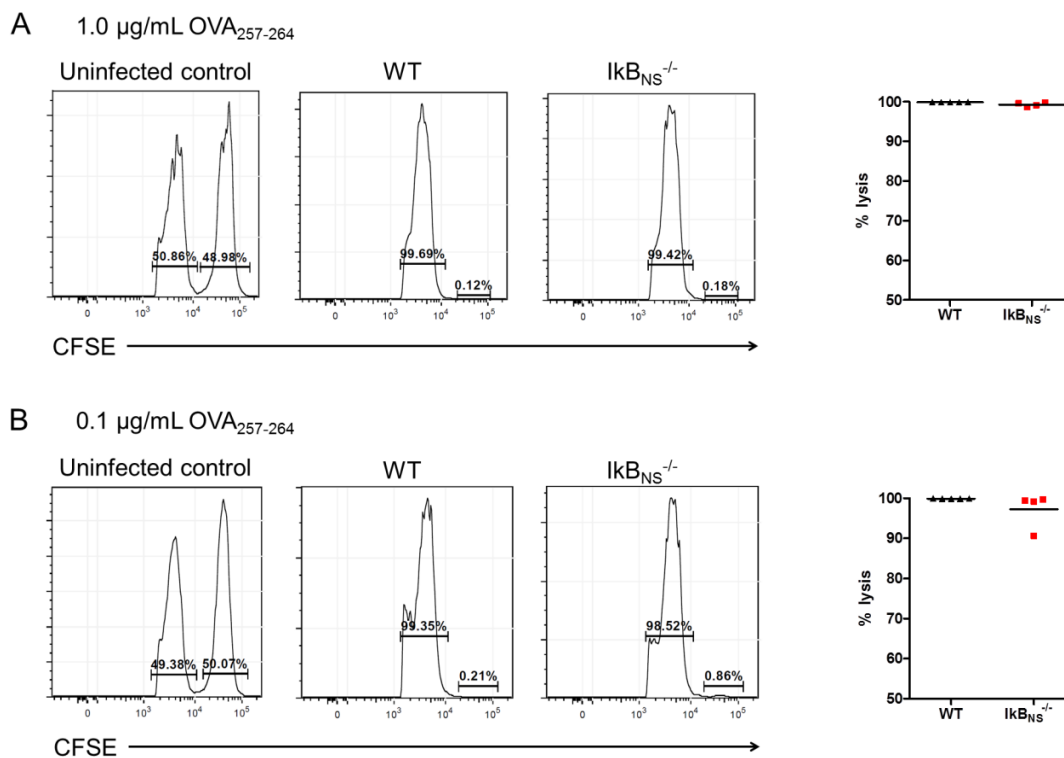


Figure 23: *In vivo* analysis of LM-OVA induced CD8⁺ T cell cytotoxicity in WT and I κ B_{NS}^{-/-} mice following LM-OVA infection. WT (\blacktriangle) and I κ B_{NS}^{-/-} (\blacksquare) mice were infected i.v. with 10.000 CFU LM-OVA or left uninfected as controls. 9 days post infection splenocytes from naïve C57BL/6 mice were isolated, CFSE labeled and pulsed with (A) 1.0 μ g/mL OVA₂₅₇₋₂₆₄ or (B) 0.1 μ g/mL OVA₂₅₇₋₂₆₄ peptide and mixed with unpulsed cells in a 1:1 ratio. The unpulsed CFSE^{low} fraction serves as negative control. 12 h after cell injection, splenocytes of the recipient mice were isolated, analyzed by flow cytometry and subsequently the specific cell lysis based on cell frequencies of peptide-pulsed CFSE^{high} and unpulsed CFSE^{low} cell fractions was calculated. WT, n=5; I κ B_{NS}^{-/-}, n=4. Data represent mean \pm SEM.

In summary, the antigen-specific activation of CD4⁺ T cells following *in vivo* pathogen encounter relies strongly on I κ B_{NS}. Especially the differentiation into Th1 effector CD4⁺ T cells seems to be affected indicated by a significantly reduced proliferation and expression of effector molecules in CD4⁺ T cells lacking I κ B_{NS}. The pathogen-specific *in vivo* activation of CD8⁺ T cells is less affected by I κ B_{NS}-deficiency, and here especially proliferation and secretion of the effector cytokine IFN γ does not depend on I κ B_{NS}. In contrast, I κ B_{NS}^{-/-} CD8⁺ T cells show higher expression of the activation marker CD25 on day 3 post infection compared to their WT counterparts, a difference which is however gone on day 5 post infection. One might speculate that this is due to a slightly delayed activation program in I κ B_{NS}^{-/-} CD8⁺ T cells. With respect to TNF α production higher frequencies of I κ B_{NS}-deficient CD8⁺ T cells were detected in the LM-OVA infected host, suggesting that I κ B_{NS} has a suppressive effect on the expression of this pro-inflammatory cytokine. However, despite significantly impaired function to control the pathogen during the early phase of the infection as observed in the adoptive transfer experiments, the aforementioned differences observed between both genotypes did not affect the capacity of I κ B_{NS}^{-/-} CD8⁺ T cells to establish cytotoxic T cell responses as shown by efficient induction of a CTL response after LM-OVA infection in I κ B_{NS}^{-/-} mice.

4.3 The role of I κ B_{NS} in immunity against *Listeria monocytogenes*

Previous studies showed that I κ B_{NS} does not only contribute to the control of T cell responses, but is also involved in the regulation of innate immune responses. For example it has been shown that I κ B_{NS} is strongly induced upon TLR ligation in macrophages (Kuwata et al., 2006). Nevertheless, so far no comprehensive study addressing the influence of I κ B_{NS} on innate immune responses during systemic bacterial infection has been published.

In order to further address the impact of I κ B_{NS} on pathogen-specific immune responses, WT and I κ B_{NS}^{-/-} mice were infected with *Listeria monocytogenes*. To combat this pathogen, in addition to adaptive immunity the innate immune response is required. Therefore, LM represents a suitable tool to study the role of I κ B_{NS} not only in adaptive immune cells, but as well in the context of innate immunity.

4.3.1 I κ B_{NS}-deficiency confers robust protection against high-dose LM infection

To get a first hint regarding the effects of a complete loss of I κ B_{NS} on the immune response towards the intracellular pathogen *Listeria monocytogenes* the weight loss as an indicator for infection-associated disease severity as well as the overall survival following LM infection were monitored. To this end, I κ B_{NS}-sufficient (WT), I κ B_{NS}-deficient (I κ B_{NS}^{-/-}) and I κ B_{NS}-heterozygous (I κ B_{NS}^{+/-}) mice were infected via the tail vein with graded doses of LM (10⁴, 5x10⁴, 10⁵ CFU/mouse). All genotypes showed no weight loss in response to the low dose LM infection (10⁴) and only a slight weight loss in response to the intermediate infection dose (5x10⁴) (data not shown). Strikingly, as represented in Figure 24A all mouse groups lost between 10-15% of their initial body weight until day 4 post infection when infected with the high-dose of LM (10⁵). Despite no significant differences in weight loss were observed during the first days post infection, still the I κ B_{NS}^{-/-} mice appeared less sick than their WT counterparts and also the heterozygous mice. Most of the WT mice had scruffy-looking fur, a crooked posture, inflamed eyes, and were apathetic whereas the I κ B_{NS}^{-/-} mice exhibited far less severe disease symptoms. In line with their aggravated disease symptoms, WT mice succumbed to the infection between day 4 and day 6 post infection. Strikingly and in direct contrast, 100% of I κ B_{NS}-deficient mice survived the high-dose LM infection. A clear indicator that this observation is directly linked to I κ B_{NS} is that about 50% of the heterozygous mice which lack only one functional allele for I κ B_{NS} survived the high-dose infection (see Figure 24).

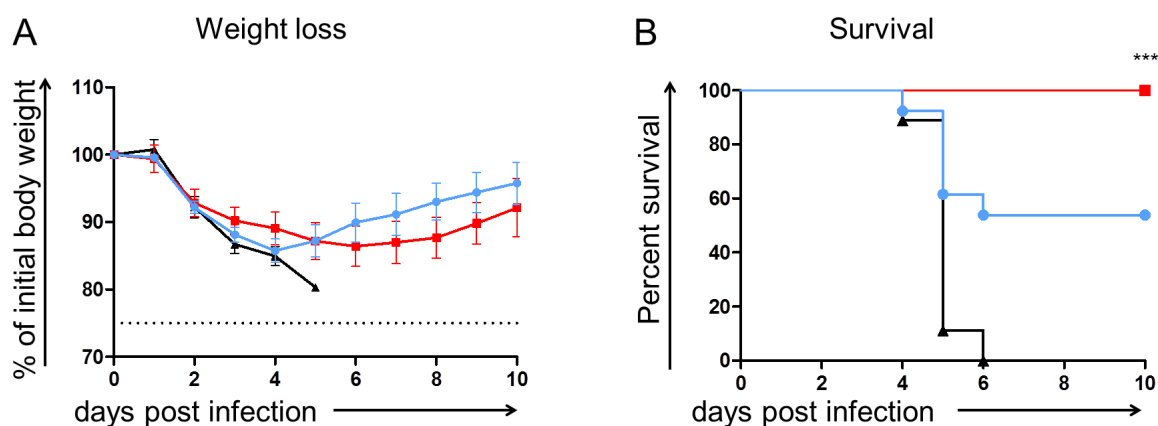


Figure 24: Weight loss and survival of $IkB_{NS}^{+/+}$, $IkB_{NS}^{+/-}$ and $IkB_{NS}^{-/-}$ mice following high-dose Listeria infection. WT (\blacktriangle), heterozygous (\bullet) and $IkB_{NS}^{-/-}$ (\blacksquare) mice were infected i.v. with a high-dose (10^5 CFU) of LM and were daily monitored. (A) Body weight loss depicted as percent of initial body weight. WT: $n=9$; $IkB_{NS}^{+/-}$: $n=13$; $IkB_{NS}^{-/-}$: $n=13$. Dashed line indicates 75% bodyweight loss (abort criterion). Data represent mean values \pm SEM. (B) Kaplan-Meier plot for survival following high-dose LM infection. Statistical analyses were performed using Log-rank (Mantel-Cox) test. *** $p=0.0003$.

Taken together, all WT mice succumbed within few days post high-dose LM infection while IkB_{NS} -deficient mice were completely protected. These data suggest that IkB_{NS} is involved in the regulation of inflammatory pathways especially within the early innate immune response.

4.3.2 Bacterial clearance in high-dose LM infection is not affected by IkB_{NS} -deficiency

Given the previous finding of complete protection of IkB_{NS} -deficient mice against high-dose LM infection it is reasonable to evaluate their capacity to control bacterial growth in spleen and liver, which are the main replication sites of LM. Due to the observation that WT mice had inflamed eyes and some of them exhibited slightly swollen heads, which might be indicative for encephalitis resulting from a fulminant dissemination of the bacteria into the brain, the bacterial burden in the brain was also determined.

For this purpose, spleen, liver and brain samples were collected from high-dose LM infected WT and $IkB_{NS}^{-/-}$ mice at different times post infection (day 2, 3, 4, 5 and 6). This particular time frame was chosen since at the latest 6 days after high-dose LM infection all WT mice would have succumbed to the infection and hence their bacterial burden could not be compared to the $IkB_{NS}^{-/-}$ group anymore. The organ homogenates were plated on BHI agar plates and the bacterial burden was determined by counting the CFU after 24 h incubation at 37°C. As depicted in Figure 25, the bacterial burden is almost identical in spleen and liver samples on day 2 and 3 post infection. Especially on day 4 post infection, there is a tendency for an improved pathogen clearance in $IkB_{NS}^{-/-}$ mice which does, however, not reach statistical significance. In both genotypes a slight decrease in bacterial burden is observed on day 5 and 6 post infection (compared to day 4), whereas this decrease is more evident in spleen samples.

The bacterial load in the brain is clearly lower than in spleen and liver samples. Strikingly, especially on day 6, when all WT mice ultimately succumbed to the infection, the highest number of bacteria was reached in their brains. In direct contrast to the WT animals, $IkB_{NS}^{-/-}$ mice were capable to completely eliminate the bacteria from the brain by day 5 post infection.

To investigate whether, $\text{IkB}_{\text{NS}}^{-/-}$ mice that survived the high-dose LM infection would be capable to completely clear the pathogen, the bacterial burden was additionally determined on day 10 post infection. Indeed, at this time no bacteria were detectable in neither spleen, liver nor brain samples (data not shown).

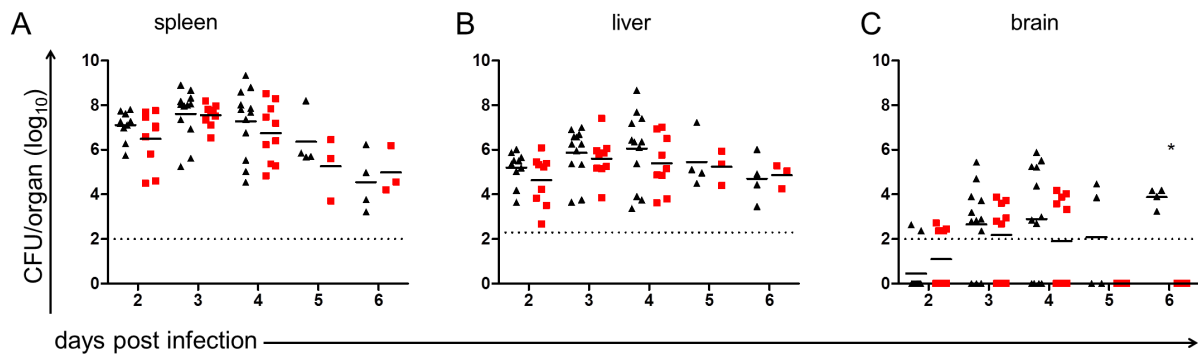


Figure 25: CFU in different organs in high-dose LM infected WT and $\text{IkB}_{\text{NS}}^{-/-}$ mice. At indicated times post high-dose (10^5 CFU/mouse) i.v. LM infection (A) spleens, (B) livers and (C) brains of WT (\blacktriangle , n= 4-12) and $\text{IkB}_{\text{NS}}^{-/-}$ (\blacksquare , n= 3-10) mice were homogenized and plated on BHI agar plates. Colonies were counted after 24 h of incubation at 37°C and total CFU/organ was determined. Data represent \log_{10} (CFU/organ) with the mean per group indicated. Dashed lines represent limit of detection for each organ. Statistical analyses were performed using two-way ANOVA with Bonferroni post-test. * $p < 0.05$.

Taken together, these results show that the pathogen clearance in spleens and livers is not affected by the loss of IkB_{NS} . Thus, the improved survival and the overall milder disease course in $\text{IkB}_{\text{NS}}^{-/-}$ mice is likely not the result of an improved pathogen clearance. To further clarify the mechanism underlying the robust protection of IkB_{NS} -deficient mice against high-dose LM infection, a histopathological examination of the infected organs was performed.

4.3.3 Reduced immunopathology in IkB_{NS} -deficient mice following LM infection

As described in the previous chapter, IkB_{NS} -deficient mice showed milder disease symptoms and in contrast to their WT counterparts survived the high-dose LM infection. However, the bacterial burden in liver and spleen did not significantly differ between both genotypes. This suggests that the improved outcome of infection is not due to a better control of bacterial growth, but rather a result of reduced immunopathology in the infected organs. In line with this, macroscopic evaluation of the mice revealed clearly visible liver pathology which was more pronounced in WT mice compared to IkB_{NS} -deficient mice. Moreover, the spleens were spotted with white lesions that macroscopically resembled granulomas, which were also more pronounced in WT mice than in $\text{IkB}_{\text{NS}}^{-/-}$ mice (data not shown). Due to these observations, spleen and liver samples were assessed histopathologically day 0 and day 4 post high-dose LM infection. Furthermore, the brains were included as well in the analyses due to the prior observed head swelling in WT mice and the documented bacterial infection of the brains in both genotypes.

Histological analyses were performed by Dr. Olivia Kershaw (Freie Universität Berlin). Prepared organ slices were stained with hematoxylin and eosin (H&E) and numerically scored in a systematic, blinded manner and summarized in a score representing the degree of inflammation. Of note, brain samples of

both genotypes did not reveal histological particularities, which is surprising in as much as high bacterial burden was found in most brains 4 days post high-dose infection (refer to Figure 25).

The histological findings of livers of uninfected mice were inconspicuous irrespective of the genotype. As expected, in both mouse groups a normal liver architecture was observed (Figure 26A, upper row). Following LM infection, generally all liver samples showed foci with leukocyte aggregates and severe acute, necrotizing inflammation-related structural changes. Strikingly and well in line with the improved disease course, the degree of inflammation was clearly less pronounced in livers of IkB_{NS} -deficient mice (Figure 26, lower row) with far lower number of foci detectable in livers of $\text{IkB}_{\text{NS}}^{-/-}$ mice compared to the WT group.

Spleen samples of both uninfected genotypes showed a normal structure as well. The white pulp (marked by the blue circles, Figure 26B, upper row) showed an intact shape. The LM infection resulted in a dramatic change of the splenic architecture which was severely aggravated in spleens of WT animals. Here, the basic structure of the organ was nearly completely destroyed, exemplified by the large white areas within the H&E stained tissue slices. Absence of H&E stainable intact cells in those regions indicates multifocal necrosis. In contrast to that, the severity of organ destruction was less pronounced in spleens of IkB_{NS} -deficient mice. Here, hardly any completely destroyed areas lacking H&E staining are present. Structural differences between both IkB_{NS} genotypes also become apparent when splenic white pulp areas are compared. The white pulp or the splenic lymphoid nodules are distinguishable in H&E staining by areas of dark blue color. Comparing the white pulp distribution throughout the spleens of WT and $\text{IkB}_{\text{NS}}^{-/-}$ mice (Figure 26B, lower row) clearly demonstrates that necrotic lesions have substantially scattered the white pulp of WT mice into a multitude of smaller patches, whereas the white pulp in $\text{IkB}_{\text{NS}}^{-/-}$ mice is structurally largely intact. However, in general in both genotypes a multifocal, acute and necrotizing splenitis was observed. In terms of scoring the degree of inflammation, higher scores were determined in the spleens of WT mice compared to $\text{IkB}_{\text{NS}}^{-/-}$ mice. Noticeable, for both genotypes the inflammation scores in the spleens were overall higher than in the according livers. Furthermore it should be noted that in spleen samples of WT mice a scoring with respect to lymphatic depletion was not possible due to the severity of necrosis.

Taken together, the histological examination confirmed a mitigated immunopathology 4 days post LM infection in liver and spleen samples of IkB_{NS} -deficient compared to WT mice. As described above the reduced immunopathology of $\text{IkB}_{\text{NS}}^{-/-}$ mice is not linked to an improved pathogen clearance, which was comparable in both genotypes. Therefore, it seems more likely that the reduced immunopathology in IkB_{NS} -deficient mice is a result of an attenuated inflammatory response to the pathogen, which ultimately would lead to reduced tissue injury.

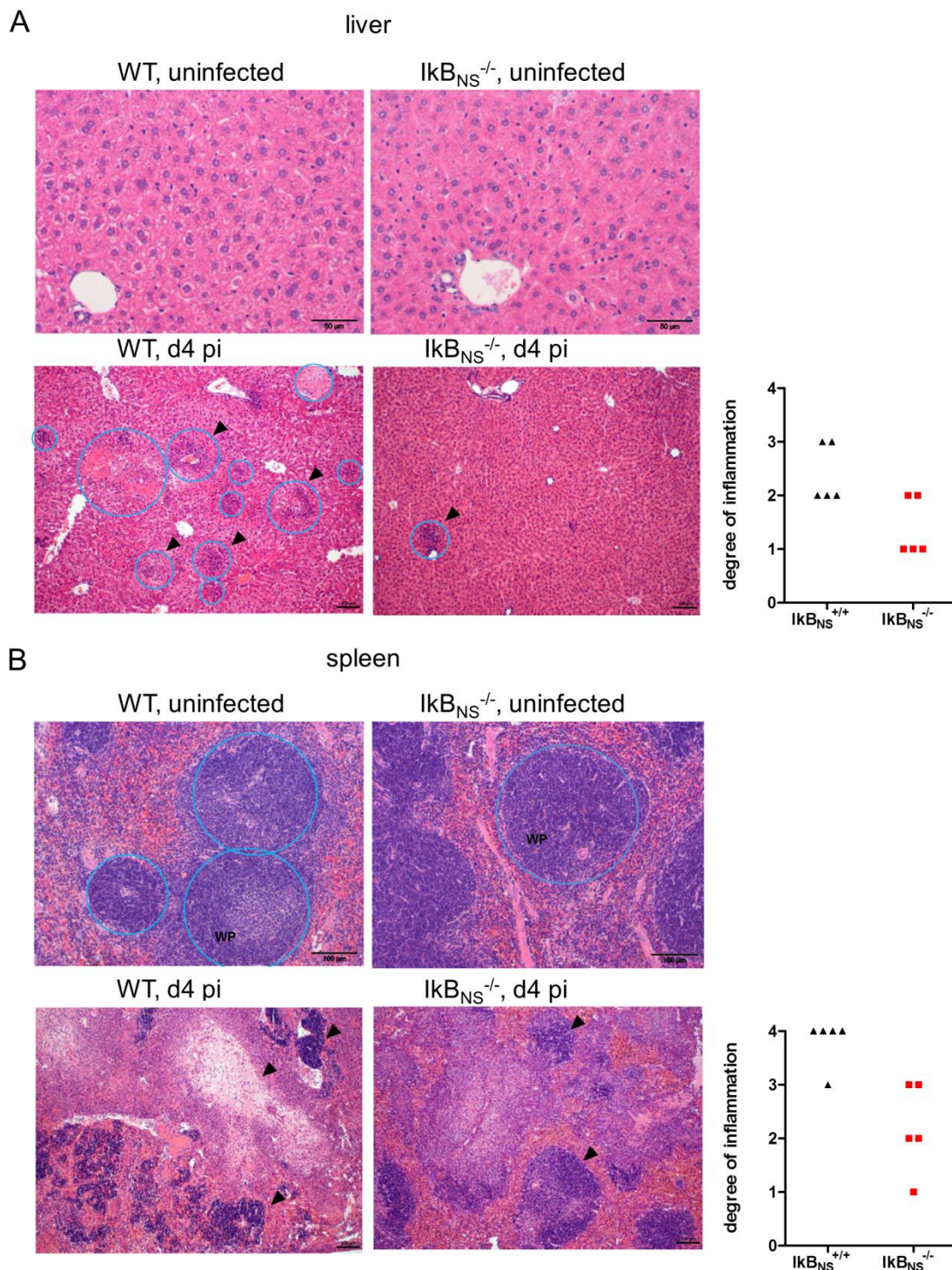


Figure 26: Histopathological examinations of uninfected and day 4 LM infected liver and spleen samples. WT (▲) and $I\kappa B_{NS}^{-/-}$ (■) mice were infected i.v. with 10^5 CFU LM or left uninfected as controls. Uninfected mice and mice 4 days post infection were sacrificed, liver and spleen excised and stored in 4% PFA. After slicing and staining with hematoxylin and eosin (H&E), organ slices were scored by a veterinarian in a blinded manner for the degree of inflammation. (A) Upper row: Liver sections show normal organ architecture. Lower row: Liver histology revealed leukocyte aggregates and necrotic foci indicated by the arrows and blue circles, while WT liver showed more foci compared to $I\kappa B_{NS}^{-/-}$ mice. Scoring revealed the degree of inflammation. (B) Upper row: Uninfected spleens show normal structure with well visible splenic lymphoid nodules (dark blue H&E staining). Lower row: White pulp (WP) is largely destroyed 4 days post LM infection, while necrotic lesions are more pronounced in WT mice compared to $I\kappa B_{NS}^{-/-}$ mice. Scoring revealed the degree of inflammation. The black bars at the bottom right corners represent a distance of 50 μ m (d0) and 100 μ m (d4) for liver sections and 100 μ m (d0, d4) for spleen sections.

4.3.4 Blunted inflammatory immune response in $\text{IkB}_{\text{NS}}^{-/-}$ mice

As described in the previous chapter, the histological examination of livers and spleens from WT and $\text{IkB}_{\text{NS}}^{-/-}$ mice revealed severe immunopathology 4 days post LM infection, which was less pronounced in the organs of $\text{IkB}_{\text{NS}}^{-/-}$ mice. To further confirm the described differences in liver damage, the serum level of the enzyme alanine aminotransferase (ALT), which is a reliable and sensitive marker for liver inflammation, was measured. In case of liver injury ALT is released from the damaged liver cells and increasing levels of ALT are detectable in the serum (Kim et al., 2008) where it is not present in healthy conditions.

For this purpose, the cardiac blood from high-dose LM infected (10^5 CFU/mouse) WT and $\text{IkB}_{\text{NS}}^{-/-}$ mice was collected day 0, 2, 3 and 4 post infection and the ALT level in sera were determined to assess the stage of liver inflammation. Since WT mice started to succumb on day 4 post infection, this day was selected as the latest time point for analysis. Livers and spleens from these mice were collected for RT-PCR analyses of selected inflammatory mediators. The reason behind this is that host resistance to LM infection is conferred by cell-mediated immunity that is mainly driven by the expression of pro-inflammatory cytokines (Mizuki et al., 2002). Especially cytokines such as $\text{TNF}\alpha$, IL6, $\text{IFN}\gamma$ and IL1 were described to play important roles in the host resistance against LM infection (Havell 1987; Hoge et al., 2013; Buchmeier and Schreiber, 1985; Petit et al., 1988). Furthermore, those cytokines were described to have also opposite effects on the host. On the one hand, they are needed to solve the infection, but on the contrary elevated levels of for example $\text{TNF}\alpha$ can cause immunopathology (Nakane et al., 1999). In addition, high levels of $\text{TNF}\alpha$ and $\text{IFN}\gamma$ were described to be crucially involved in the development of septic shock (Nakane et al., 1999).

Thus, potential differences in the gene expression level of these inflammatory mediators in LM infected liver and spleen homogenates should provide insights regarding potential alterations in the inflammatory response of infected IkB_{NS} -deficient mice, which ultimately could result in less pronounced immunopathology in the infected organs.

As depicted in Figure 27A, the levels of serum ALT are equally low (WT: 32 ± 1 mU/mL, $\text{IkB}_{\text{NS}}^{-/-}$: 31 ± 4 mU/mL) in both genotypes in the uninfected state (d0). Also on day 2 and day 3 post infection no differences regarding ALT level were observed in WT and $\text{IkB}_{\text{NS}}^{-/-}$ mice, although the ALT levels were significantly increased compared to day 0. Strikingly, on day 4 post infection significantly elevated serum ALT levels were detected in WT animals (490 ± 90 mU/mL), while at this time post infection ALT level remained almost constant in $\text{IkB}_{\text{NS}}^{-/-}$ mice compared to day 2 and 3 post infection (90 ± 59 mU/mL). These data confirm immunohistology results revealing pronounced liver damage in WT but not in IkB_{NS} -deficient animals. Livers and spleens from LM infected mice were further processed for RT-PCR assays in which the mRNA expression of the aforementioned pro-inflammatory cytokines $\text{TNF}\alpha$, IL6, $\text{IFN}\gamma$, IL1 β and IL1 α were quantified.

As depicted in Figure 27B, 2 days post infection no differences in the mRNA levels of either gene was observed comparing livers from WT and $\text{IkB}_{\text{NS}}^{-/-}$ mice. On day 3 post infection a small increase of $\text{TNF}\alpha$ mRNA level in WT livers was observed in contrast to liver samples from IkB_{NS} -deficient. This increase became statistically significant on day 4 post infection demonstrating higher levels of $\text{TNF}\alpha$ expression in WT compared to $\text{IkB}_{\text{NS}}^{-/-}$ mice. A similar principle pattern of increased mRNA levels on

day 4 post infection, and in part also on day 3 post infection, could be observed for IL6, IFN γ , IL1 β and IL1 α in livers of WT compared to I κ B_{NS}^{-/-} mice. This suggests that the inflammatory immune response to LM in livers of mice lacking I κ B_{NS} is blunted and that differences in the expression of pro-inflammatory genes in the liver become most obvious by day 3-4 post infection.

These differences in gene expression are however not as obvious in spleen samples (Figure 27C). Here, throughout the course of infection no clear differences in TNF α or IL6 expression between both genotypes were observed. In case of IFN γ a by tendency higher expression level was determined in spleens of WT mice on day 2 post infection in comparison to spleens of I κ B_{NS}^{-/-} mice. However, this difference was gone by day 3 and day 4 post infection. The splenic mRNA expression of the two inflammatory cytokines IL1 β and IL1 α was very low on day 2 post infection in both genotypes. Still on day 3 post infection in both genotypes a similar increase was detectable with overall higher levels of IL1 α than IL1 β . Finally, on day 4 post infection a pronounced increase of the mRNA levels of both IL1 β and IL1 α was observed, but only in spleen samples of WT and not I κ B_{NS}^{-/-} mice.

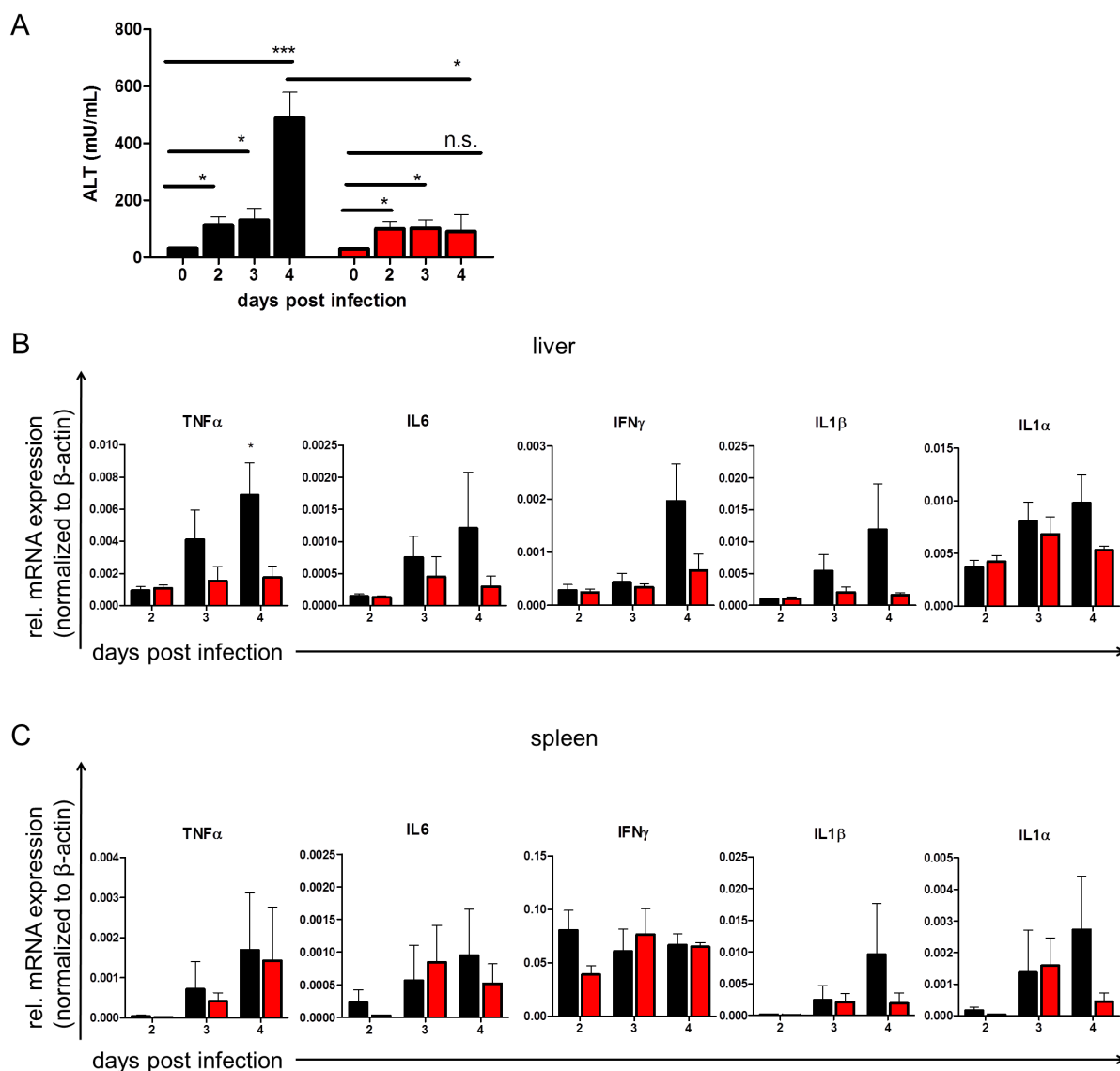


Figure 27: Serum ALT levels and expression of inflammatory cytokines in spleen and liver of WT and *IkBNS*^{-/-} mice during the course of LM infection. WT (\blacktriangle , n= 3-5) and *IkBNS*^{-/-} (\blacksquare , n= 3-4) were infected with 10^5 CFU LM and serum, spleen and liver were sampled at indicated times post infection. (A) Determination of the liver enzyme alanine transaminase (ALT) level in serum samples. Statistical analyses were performed by using two-tailed unpaired student's *t*-test (* *p* < 0.05, ** *p* < 0.01, *** *p* < 0.001). (B and C) Relative mRNA expression levels of pro-inflammatory cytokines (TNF α , IL6, IFN γ , IL1 β and IL1 α) in liver (B) and spleen (C) homogenates normalized to β -actin expression. All data are presented as mean \pm SEM. Data in B and C were confirmed with two independent experiments with similar results. Results of one experiment are shown. Statistical analyses were performed by two-way ANOVA with Bonferroni post-test. * *p* < 0.05.

Taken together, obtained results confirmed that WT mice indeed produce large amounts of inflammatory mediators in the liver especially on day 4 post infection, which is the critical time when the mice start to succumb to the high-dose LM infection. In direct contrast, livers of *IkBNS*^{-/-} mice showed markedly lower levels of TNF α , IL6, IFN γ and IL1 expression indicating that the inflammatory immune response towards LM is blunted compared to their WT counterparts. This blunted inflammatory response in *IkBNS*^{-/-} mice could be an explanation for the reduced immunopathology. An unbiased genome-wide transcriptome analysis could provide deeper insight into the mechanisms underlying the resistance of *IkBNS*^{-/-} mice to an otherwise lethal LM infection.

4.3.5 Broad alterations in the gene expression profile in the liver of I κ B_{NS}^{-/-} mice during LM infection

Given the finding, that I κ B_{NS}^{-/-} mice showed a milder immunopathology in response to LM infection and that the expression of typically pro-inflammatory mediators is reduced on day 4 post infection, it is reasonable to gain next more detailed overview regarding the gene expression profile in both mouse groups in response to LM infection.

For this, a comparative genome-wide transcriptome analysis of whole liver homogenates from WT and conventional I κ B_{NS}^{-/-} mice sampled on day 0 (uninfected) and on day 2, 3 and 4 post LM infection with 10⁵ CFU/mouse was performed. Microarray procedures are explained in detail in section 3.19. Briefly, total RNA was isolated from liver homogenates. DNA was removed by means of DNase treatment followed by molecular biological mRNA-specific sample amplification and cDNA synthesis *in vitro*. Samples were hybridized onto the GeneST 2.0 microarrays (Affymetrix Company), stained, washed and scanned according to manufacturer recommendations. Microarray data processing, normalization and filtering were performed with R Bioconductor package and Microsoft Excel. Briefly, microarray data were summarized with the RMA-algorithm, signal intensity data were log₂ transformed, quantile normalized and a signal intensity percentile filter was applied to exclude transcripts with consistently low abundance across all samples.

Given the data structure being linked to the underlying experimental design the most reasonable approach for microarray analysis is to ask which consecutive transcriptional alterations arise in livers of WT and conventional I κ B_{NS}^{-/-} mice on day 2, 3 and 4 post LM infection compared to day 0, respectively. This approach reveals the general transcriptional response of the liver tissue as well as contributions of the ongoing immune response and allows in a secondary meta-analysis to compare the resulting time-sequential alterations between the WT and I κ B_{NS}^{-/-} genotype for each considered point in time (see schema in Figure 28A). Moreover, to exclude that there are general alterations in the transcriptional expression of genes between both genotypes even in the uninfected state (d0), a direct comparison of gene expression on day 0 was performed. As shown in Figure 28B, this analysis revealed that there are no general genotype-dependent alterations in the uninfected state with the exception of one up-regulated transcript (*Serpina-ps1*) and 5 down-regulated transcripts (e.g. *Sult2a5*, *Cyb2b13*, *Cyb2b9*) in I κ B_{NS}^{-/-} mice compared to their WT counterparts. However, these results revealed that in general all alterations in gene transcription mentioned later on are due to the response to the LM infection and the influence of I κ B_{NS} on the infection-mediated immune response.

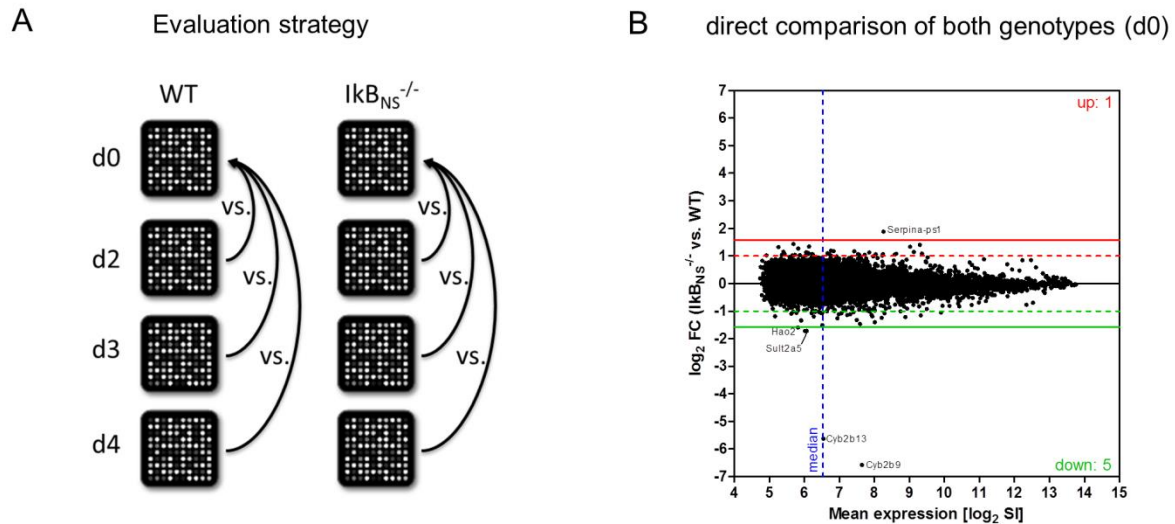


Figure 28: Schematic overview about the evaluation strategy and direct comparison of both genotypes in the uninfected state. (A) Schematic representation of the analysis and evaluation of the microarrays. Each sampling point in time (d2, d3, d4) is compared to the uninfected state (d0) for WT and $\text{IkB}_{\text{NS}}^{-/-}$ mice. (B) RA scatter plot of annotated genes assessed by microarray analysis from whole liver homogenates of uninfected (d0) WT and $\text{IkB}_{\text{NS}}^{-/-}$ mice. Equal amounts of RNA ($n=3-4$ mice per genotype) were pooled and applied to Affymetrix Gene 2.0 ST microarray analysis. Shown data represent normalized \log_2 -transformed signal intensities (SI) and \log_2 -transformed fold change of expressed genes from $\text{IkB}_{\text{NS}}^{-/-}$ compared to WT samples. As threshold fold change (FC) > 3 was applied, indicated by red and green lines. Up- or down-regulated transcripts based on FC threshold ± 3 are stated. Dashed lines indicate a FC threshold of ± 2 . The vertical blue line represents the median of all signal intensities.

Initially, to get an overview about the numbers of regulated genes alongside with the overall extend of transcriptional expression of a given gene, the processed data were plotted in RA-plots. This plot correlates the averaged signal intensity of each transcript (average over all 8 microarrays in the experiment) with the according fold change of differential regulation resulting from the comparison of its signal intensity on d2, d3, d4 vs. d0, respectively. A transcript was considered differentially expressed in a given pairwise microarray comparison if the resulting fold change in this comparison was bigger than ± 3 . Figure 29 summarizes all RA-plots resulting from this approach. As depicted in Figure 29 (left side) it became apparent that in WT mice during the course of infection plenty of genes are up-regulated compared to the uninfected state (d2: 224, d3: 388, d4: 385). Furthermore, due to the infection also a lot of genes were down-regulated compared to d0 (d2: 119, d3: 246, d4: 243). These numbers indicate that the strongest differential regulation is seen on day 3 and on day 4 post LM infection. When compared to the $\text{IkB}_{\text{NS}}^{-/-}$ mice (see Figure 29, right side), less regulated genes were detected on each point in time (up-regulated: d2:197, d3: 231, d4:253; down-regulated: d2:96, d3: 116, d4: 88). In the IkB_{NS} -deficient mice day 4 post infection is the day where most genes were up-regulated and day 3 post infection the one with most down-regulated genes. Taken together, LM infection clearly induces differential gene expression in the liver with increasing extends over time. This induction of differential gene expression appears however to be impaired in $\text{IkB}_{\text{NS}}^{-/-}$ mice.

In addition, Figure 29 shows the top 5 most up- and down-regulated genes in both genotypes on the different times post infection, respectively. In both genotypes *Saa3* (serum amyloid A) is strongly up-regulated during the course of infection. In $\text{IkB}_{\text{NS}}^{-/-}$ mice other members of this acute phase proteins are regulated too, e.g. *Saa2* on day 3 post infection and *Saa1* on day 4 post infection. All those

members of the *SAA* family are mainly produced in the liver and secreted from hepatocytes during tissue injury and inflammation (Zhang et al., 2005), which clearly is the case in acute LM infection. For further analysis the lists of differentially regulated genes were joined and filtered in a way that allows comparing the genotypes side-by-side throughout the course of infection. Thus, only transcripts having a fold change $>\pm 3$ in at least one out of 6 binary microarray comparisons ((WT d2 vs. d0), (WT d3 vs. d0), (WT d4 vs. d0), ($\text{IkB}_{\text{NS}}^{-/-}$ d2 vs. d0), ($\text{IkB}_{\text{NS}}^{-/-}$ d3 vs. d0), ($\text{IkB}_{\text{NS}}^{-/-}$ d4 vs. d0)) were retained. This resulted in a set of in total 856 transcripts.

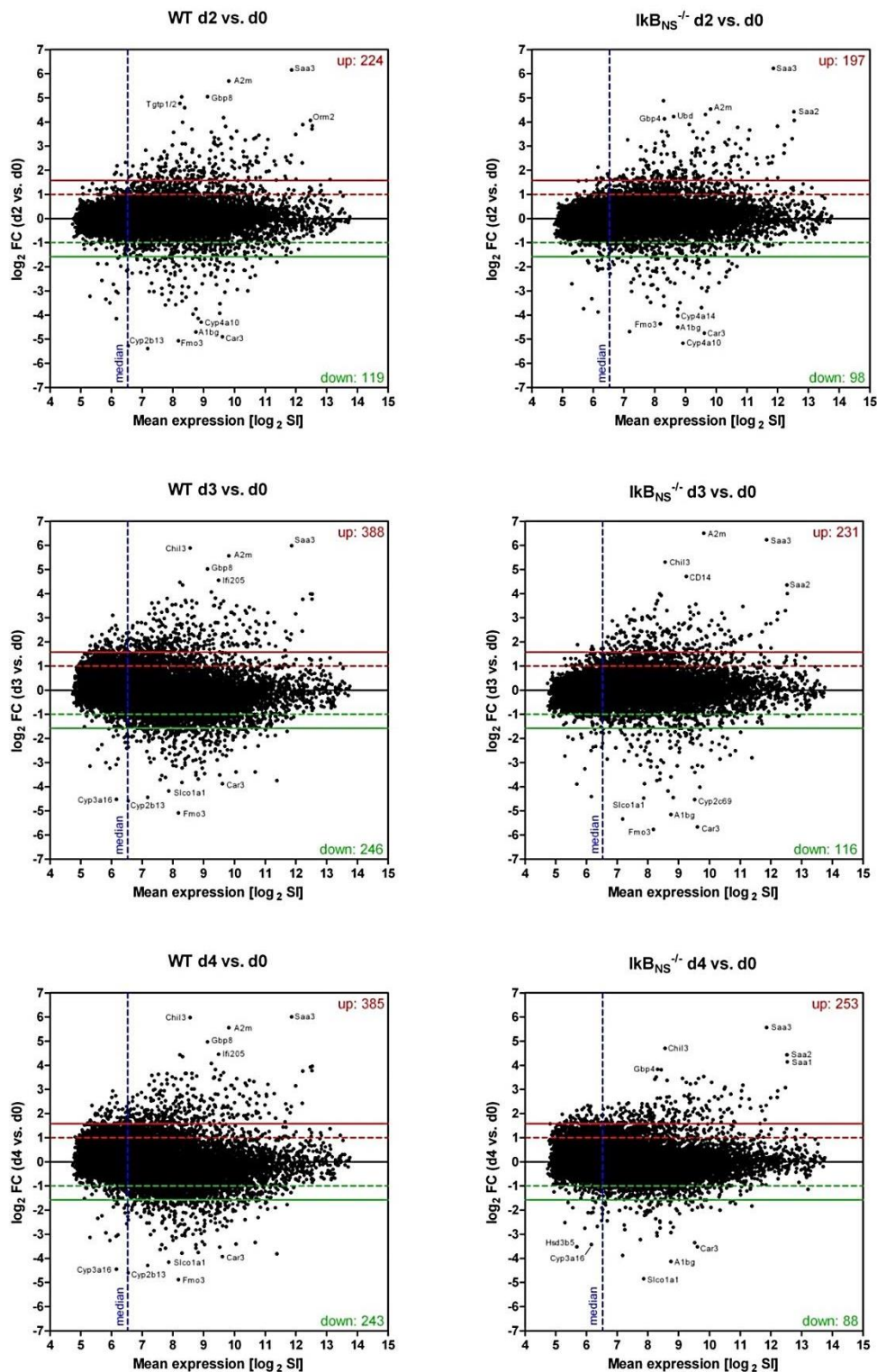


Figure 29: RA scatter plots of annotated genes assessed by microarray analysis from whole liver homogenates within the course of LM infection compared to uninfected controls. WT and $IkB_{NS}^{-/-}$ mice were infected with 10^5 CFU LM i.v. or left uninfected (d0). Mice were sacrificed on day 2, 3 and 4 post infection and liver homogenates were prepared and sampled for total RNA isolation. Equal amounts of RNA from $n=3-5$ mice per genotype and analysis point in time were pooled per experimental group and applied to Affymetrix Gene 2.0 ST microarray analysis. Shown data represent normalized \log_2 -transformed signal intensities (SI). The x-axis indicates the mean \log_2 (SI) of each annotated transcript averaged over all 8 microarrays. The y-axis represents the \log_2 -transformed fold change values from indicated comparisons (left: WT, right: $IkB_{NS}^{-/-}$). As threshold $FC > 3$ was applied, indicated by red and green lines. Numbers of up- and down-regulated transcripts based on $FC \text{ threshold} \pm 3$ are stated in each plot. Dashed red and green lines indicate a FC threshold of ± 2 . The vertical blue lines represent the median of all signal intensities. The 5 top up- and down-regulated genes in each RA-plot are labeled according to their gene symbol.

To sum up the RA-plots and the 856 transcripts, Figure 30 gives a conclusive enumeration of the regulated genes and the conditions in which they were found to have a fold change above ± 3 in Venn diagrams. This diagram gives a final overview about the amount of overlapping genes which have been regulated more than once in the course of infection. In brief, in WT mice more genes are regulated during LM infection (743 regulated genes) compared to $\text{IkB}_{\text{NS}}^{-/-}$ mice (531 regulated genes) (see Figure 30). Moreover, the decisive time where most of genes are regulated due to the infection are day 3 and day 4 post infection. In case of the WT mice, 324 genes were found to be regulated on day 3 and 4 post infection. In contrast to this only 44 regulated genes were found in $\text{IkB}_{\text{NS}}^{-/-}$ mice on day 3 and 4.

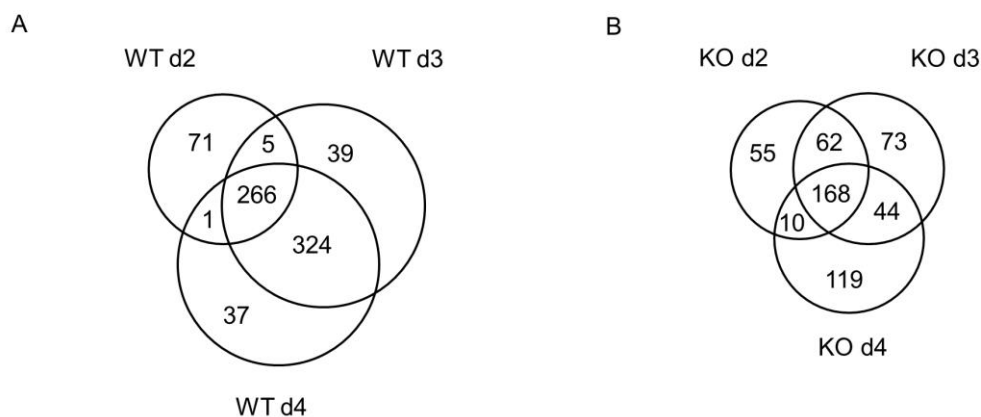


Figure 30: Venn diagrams comparing the identified regulated genes from Microarray analysis of whole liver homogenates from WT and $\text{IkB}_{\text{NS}}^{-/-}$ mice. Visualization of the number of identified genes with a $\text{FC} \geq \pm 3$ which are regulated (A) in WT and (B) in $\text{IkB}_{\text{NS}}^{-/-}$ mice on each time post infection (d2, d3, d4). In addition, the amount of overlapping genes is also indicated.

For a better overview of these 856 genes, their normalized \log_2 transformed signal intensities were z-score transformed and clustered using k-means cluster algorithm (KMC, with $k=6$). A meaningful order of the resulting KMC clusters was manually chosen such that their order reflects time-sequential expression of genes in the course of LM infection. This means e.g. cluster 1 contains genes with predominant gene expression already on day 2 (compared to the other points in time) and cluster 6 contains genes whose expression is predominantly high on day 3 or 4 post infection. This approach resulted in 6 clusters containing 171 (cluster 1), 130 (cluster 2), 75 (cluster 3), 156 (cluster 4), 161 (cluster 5) and 163 (cluster 6) genes (see Figure 31). In each cluster the left side describes the situation in WT mice at each sampling time post infection (d0, d2, d3 and d4) and the right side shows the same for the $\text{IkB}_{\text{NS}}^{-/-}$ mice. The color code for the z-score is also depicted in Figure 31 representing comparably high expression in red, whereas green represents comparably low expression of a gene and yellow is indicative for an averaged expression. Based on the expression pattern in the WT mouse group the clusters can be classified as follows: cluster 1 contains genes that are down-regulated on day 2, 3 and 4 post infection and cluster 2 summarizes genes which are down-regulated predominantly on day 3 and 4 post infection. Cluster 3 is the smallest and represents genes that are strongly up-regulated on day 2 post infection followed by a minor drop in expression on day 3 and 4. In cluster 4 genes can be found that are moderately up-regulated from day 2 on and more or less keep

their expression level throughout day 3 and 4 post infection. Cluster 5 contains genes that are moderately up-regulated on day 2, but become even stronger up-regulated on day 3 and keeping this level throughout day 4 post infection. Finally, cluster 6 shows genes which are strongly up-regulated only on day 3 and 4 after infection. Representative gene symbols of top-regulated genes in each cluster are stated in Figure 31 to give an impression on the type of genes belonging to an according KMC cluster.

Many of the identified and top-regulated genes from cluster 1 belong to the cytochrome family, actually, 19 out of 171 genes (~11%). The cytochrome superfamily belongs to the hemoproteins and is involved in a variety of enzymatic processes such as metabolism of drugs, chemicals and endogenous substrates. Hepatic cytochromes are also described as being involved in the pathogenesis of liver diseases (Villeneuve and Pichette, 2004). Anyway, this cluster does not signify systemic expressional differences between the two genotypes. Also it is known that LM infection causes a down-regulation of the hepatic cytochrome P450 (Armstrong and Renton, 1994), which was confirmed by the microarray analysis where in both genotypes after LM infection the different cytochromes become down-regulated compared to the uninfected controls.

Cluster 2 contains many genes coding for metabolic enzymes and clearly signifies differences between WT and $\text{IkB}_{\text{NS}}^{-/-}$ mice. Especially, on day 3 post infection a stronger down-regulation of identified genes could be observed in WT mice compared to their $\text{IkB}_{\text{NS}}^{-/-}$ counterparts. This is also detectable on day 4. Functionally, many genes in this cluster are related to the lipid and steroid metabolism (e.g. *Scd1*, *Sult2a1*, *Acacb*) which thus could be more active on day 3 and 4 after infection in $\text{IkB}_{\text{NS}}^{-/-}$ mice.

Cluster 3 was classified through up-regulation of 75 genes on day 2 post infection in WT mice, which is however also the case in the IkB_{NS} -deficient mice. Though most genes in this cluster slightly lose again expression on day 3 and 4 post infection, a portion remains stronger expressed after day 2, but only in $\text{IkB}_{\text{NS}}^{-/-}$ mice. Functionally, this cluster is enriched with genes involved in general cytokine responses (e.g. *Isg15*, *Il17ra*, *Socs3*, *Tnfrsf23*) and more specifically IFN β response (e.g. *Xaf1*, *Ifit1*, *Ifitm2*, *Bst2*), all of which make sense to be induced at onset of LM infection.

The top expressed candidates of cluster 4 are members of the Saa-family (e.g. *Saa1*, *Saa2* and *Saa3*) which are typical acute phase proteins with increasing levels during inflammation (Malle et al., 1993). Indeed, they were classified in cluster 4 which is defined by steady up-regulation on day 2, 3 and 4 post infection with more or less similar extend of fold-induction (compared to d0) in both genotypes. Nevertheless, plenty of immunologically important transcripts are contained in this cluster (see appendix Table 1) having a function as chemokine (e.g. *Cxcl10*, *Cxcl1*, *Cxcl9* and *Ccl24*) or cytokine/chemokine receptor (e.g. *Ccr5*, *Ccr12*, *Il22ra1*, *Il1r1*, *Osmr*, *Cd74*) or in Toll-like receptor signaling (e.g. *Tlr2*, *Tlr3*, *Tlr13*, *Rsad2*, *Irak3*, *Cd14*, *Cd180*, *Lbp*).

Furthermore, some genes of the guanylate-binding protein (Gbp)- family were identified (*Gbp2*, *Gbp4*, *Gbp5*, *Gbp8*) which belong to the family of guanosine triphosphates (GTPases) that are induced by IFN γ and exhibit key functions in protective immunity against microbial and also viral pathogens (Tripal et al., 2007).

Cluster 5 is remarkable in as much as it is one of the biggest clusters with 161 genes and importantly it shows clear differential expression patterns when comparing WT to $\text{IkB}_{\text{NS}}^{-/-}$ mice. Genes in this cluster are strongly up-regulated in WT mice only by day 3 post infection and keep this elevated level until day 4. This pattern is however clearly different in $\text{IkB}_{\text{NS}}^{-/-}$ mice, where many genes of the cluster are not as strongly induced by the LM infection as in WT mice. Larger groups of genes being enriched in cluster 5 relate to chemokines (e.g. *Ccl2*, *Ccl3*, *Ccl5*, *Ccl6*), cell adhesion (e.g. *Clec4a1*, *Clec4a3*, *Clec4d*, *Clec4e*, *Cd300e*) and immune globulin binding (*Fcgr1*, *Fcgr3*, *Fcgr4*, *Fcer1g*, *Lgals3*).

Chemoattractants such as *Ccl3*, which is important for the attraction of macrophages, monocytes and neutrophils (Weber, 2003), and *Ccl5*, which is chemotactic for T cells, eosinophils and basophils play a role in recruiting leukocytes into inflammatory sites (Soria and Ben-Baruch, 2008). In addition, strong induction of the pro-inflammatory *Il1 β* especially in WT mice (FC WT d3: 11.7, d4: 11.0; $\text{IkB}_{\text{NS}}^{-/-}$ d3: 7.8, d4: 3.6) was found, which was already confirmed in section 4.3.4 (see Figure 27B) by real-time PCR. Since many genes in this cluster show less pronounced gene expression in $\text{IkB}_{\text{NS}}^{-/-}$ mice on day 3 and 4 post infection compared to WT mice, this cluster reflects (next to cluster 2) IkB_{NS} -dependent transcriptional alterations in the LM infected liver.

Similarly, cluster 6 demonstrates clear genotype dependent expression patterns as well. Strikingly, it contains transcripts that are strongly induced in $\text{IkB}_{\text{NS}}^{-/-}$ mice only on day 4, but at the same time on day 3 and 4 in WT mice. This indicates almost complete absence of expressional induction of genes on day 3 in this cluster when IkB_{NS} is missing, when otherwise WT mice already shown clear transcriptional induction. Cluster 6 is one of the largest cluster with 163 genes and contains lot of micro RNAs, small non-coding RNAs (about 7%) that functions in RNA silencing and post-transcriptional regulation of gene expression (Ambros, 2004). Of note, the vast majority of genes in this cluster are not-annotated transcripts (about 62%). Due to the lack in canonical gene annotation it is hard to derive meaningful interpretation of the transcriptional profile in this cluster.

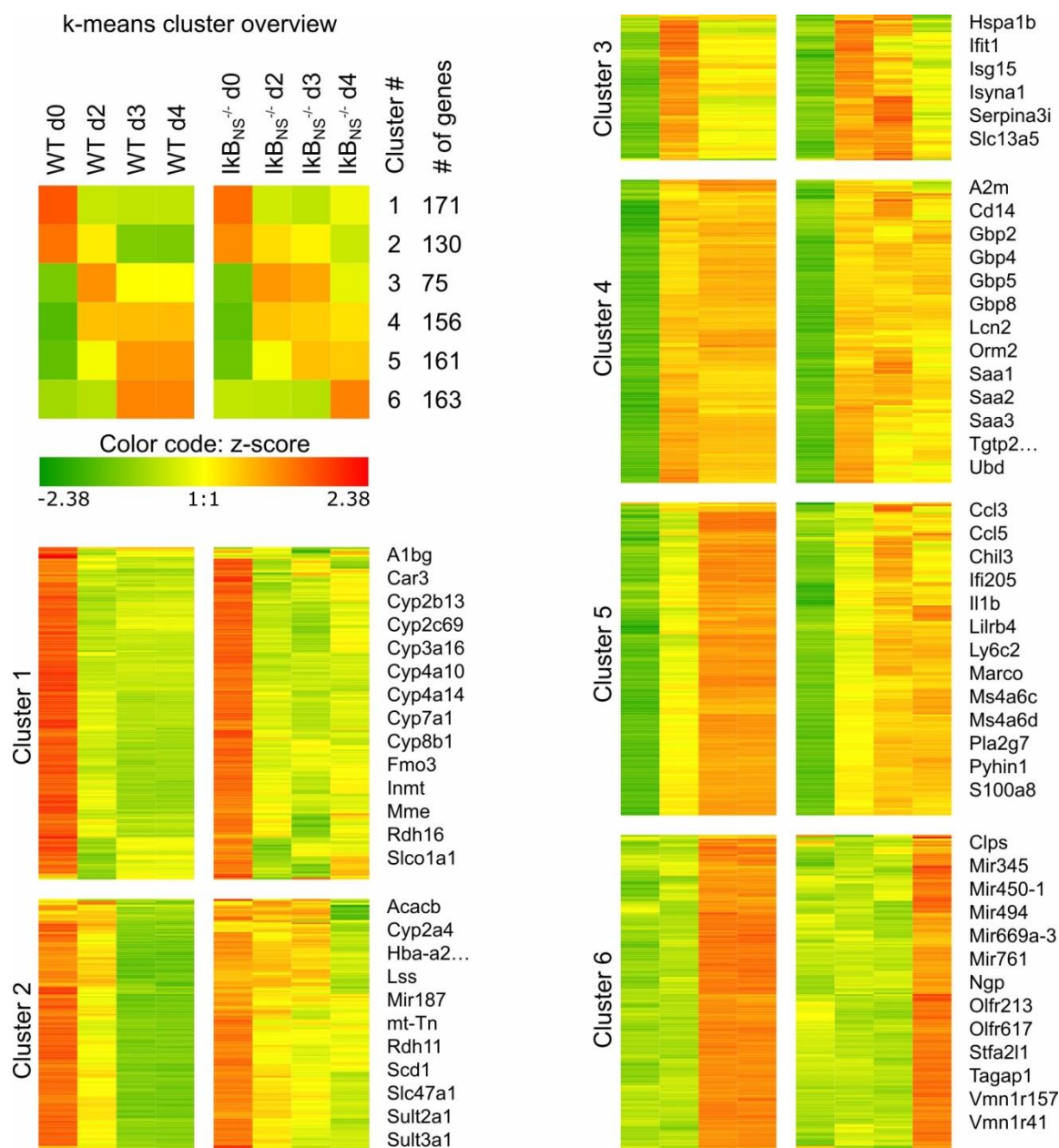


Figure 31: Transcriptional profile of whole liver tissue from WT and lkb_{NS}^{-/-} mice in the course of LM infection. WT and lkb_{NS}^{-/-} mice were infected with 10⁵ CFU LM i.v. or left untreated (d0). Mice were sacrificed on day 2, 3 and 4 post infection and liver homogenates were prepared and sampled for total RNA isolation. Equal amounts of RNA from n= 3-5 mice per genotype and sampling time were pooled per experimental group and applied to Affymetrix Gene 2.0 ST microarray analysis. Log₂(SI) data of conditionally filtered 856 regulated genes were z-score transformed and k-means clustered according to expression profile similarities. Resulting k-means clusters were additionally hierarchically clustered. For each cluster selected gene symbols with the highest FC within a given cluster are stated. Shown data represent color-coded z-scores. Top left subfigure: Summarized representation of k-means clusters in time-sequential order of overall gene induction showing z-scores averaged over all genes in a cluster. Numbers of genes per cluster are indicated.

In order to elucidate functional meaning of the observed differences in gene expression within LM infected livers of WT and lkb_{NS}^{-/-} mice in an unbiased way, Gene ontology (GO) enrichment analyses of the previously identified dataset of 856 transcripts were performed. Using GO-term-enrichment analysis over-represented GO terms were identified. In tables 18, 19 and 20 the top ten annotations for the GO categories “Biological process”, “Molecular function” and “Immune system process” are listed and ranked according to their -log₁₀ transformed Bonferroni corrected p-value of one-sided

hypergeometric enrichment statistics. Moreover, the top ten annotations were grouped according to biological similarity to get a better overview about the identified GO terms.

When considering the enriched GO terms of the meta-category “Biological Process” (see table 18) in a global way, the identified GO terms can be divided into the following 4 main categories: “leukocyte chemotaxis”, “pattern recognition receptors and signaling”, “fatty acid metabolism” and “cytokine secretion and signaling”.

As example for the defined category “leukocyte chemotaxis” the most enriched GO term was “granulocyte chemotaxis” with the lowest p-value and 23 genes prevalent in the experimentally derived dataset (e.g. *Ccl2*, *Ccl3*, *Ccl5* and *Cxcl1*). Indeed, all of these mentioned genes are important regulators for monocyte and neutrophil chemotactic processes, which are all less induced in livers of $\text{IkB}_{\text{NS}}^{-/-}$ mice during LM infection with the exception of *Cxcl1* which is up-regulated in $\text{IkB}_{\text{NS}}^{-/-}$ mice compared to WT mice.

The sub-category “pattern recognition receptors and signaling” represents the second largest enriched group of genes found in the meta-category “Biological Process”. The most enriched GO-term with the lowest p-value is “toll-like receptor signaling pathway” including genes such as *CD14*, *Irak3* and *Tlr2* which were found to be differentially regulated between both IkB_{NS} genotypes. Interestingly, *CD14* is strongly up-regulated in $\text{IkB}_{\text{NS}}^{-/-}$ mice on day 3 post infection and declines strongly on day 4 post infection, whereas it remains on a constant level in WT mice in the course of LM infection (d2, d3 and d4). Induction of *Irak3* was induced to a lesser extend in $\text{IkB}_{\text{NS}}^{-/-}$ mice in the course of LM infection compared to their WT counterparts and *Tlr2* is induced to a greater extend in $\text{IkB}_{\text{NS}}^{-/-}$ mice on day 2 and 3 post infection which is remarkable in as much as TLR2 is known to be crucial for an optimal control of *Listeria monocytogenes* infection and TLR2-deficient mice were shown being more susceptible to the systemic LM infection (Torres et al., 2004).

The most enriched GO term with the lowest p-value of the third defined sub-category “fatty acid metabolism” is “long-chain fatty acid metabolic process” with 20 genes prevalent in the obtained dataset (e.g. *Ptgs2*, *Elovl6* and *Cy2b9*). Those genes were also found differentially regulated between WT and $\text{IkB}_{\text{NS}}^{-/-}$ mice during LM infection. The prostaglandin synthetase *Ptgs2* for example was detected to be more induced in WT mice on day 3 and day 4 post infection. Regarding *Cyp2b9*, a strong down-regulation in WT mice in the course of LM infection was observed, whereas it is strongly up-regulated in $\text{IkB}_{\text{NS}}^{-/-}$ mice only on day 2 post infection. Of note, many of the enriched GO terms share similar genes which are cross-annotated in thematically different GO categories and even meta-categories. In this respect the heme containing cytochrome P450 proteins (Cyp) are causative for the significant enrichment of GO categories like the already mentioned “fatty acid metabolism” in the GO family “Biological process”, but importantly also for basically all enriched GO-categories in the GO-family “Molecular function” stated in table 20. In general, CyPs belong to the group of monooxygenases (Hannemann et al., 2007) which are found at highest concentrations in the liver (Nelson et al., 1993) and are involved in the metabolism of drugs, chemicals and endogenous substrates, but can also be involved in the pathogenesis of several liver diseases (Villeneuve and

Pichette, 2004). Most of the identified Cyps are down-regulated or even strongly down-regulated during LM infection, which was already described. In case of infections or inflammatory stimuli the expression of Cyps is normally suppressed (Morgan 1997). On the other hand, some forms can also be induced upon inflammation suggesting that those forms are involved in specific homeostatic roles and might be necessary for the catabolism of bio-reactive metabolites (Morgan 2001). Of note, most identified Cyps are enriched in nearly all GO terms of the meta-category “Molecular function”, whereas the regulation between both IkB_{NS} genotypes is nearly comparable with the exception of *Cyp2b13* and *Cyp2b9*. For both genes, a strongly down-regulation was found in WT mice during the course of LM infection compared to $IkB_{NS}^{-/-}$ mice with only marginal reduction in gene expression during the course of LM infection.

Finally, the most enriched GO term of the last main group of GO meta category “Biological process” is represented by “cytokine secretion” with genes such as *Ccl3*, *Il1a*, *Il1b*, *Nos2* and *Gbp5*. Most of the genes from this GO term can be found in the already mentioned cluster 4 and 5 (refer Figure 31). In general, most of the genes from this group are up-regulated during LM infection and with greater extend in WT mice compared to $IkB_{NS}^{-/-}$ mice, which strengthens the assumption of a blunted inflammatory immune response in IkB_{NS} -deficient mice.

Table 18: Gene ontology (GO) enrichment of regulated genes from WT and $IkB_{NS}^{-/-}$ mice during LM infection and compared to uninfected controls ($FC \geq \pm 3$). Top ten GO terms from the meta category “Biological process” according to the p-value. Annotation Database from Oct. 2017

GO Biological Process				
GO ID	GO Term (GO level > 8)	Nr. Genes	% Associated Genes	$-\log_{10}$ (Bonferroni corrected p-value)
71621	granulocyte chemotaxis	23	21,1	11,0
2687	positive regulation of leukocyte migration	21	16,4	7,7
2224	toll-like receptor signaling pathway	20	22,5	9,9
2221	pattern recognition receptor signaling pathway	22	17,3	8,6
34121	regulation of toll-like receptor signaling pathway	14	25,5	7,0
1676	long-chain fatty acid metabolic process	20	22,0	9,7
33559	unsaturated fatty acid metabolic process	20	20,2	8,9
46459	short-chain fatty acid metabolic process	7	63,6	5,7
50663	cytokine secretion	22	11,1	4,8
1961	positive regulation of cytokine-mediated signaling pathway	10	26,3	4,6

Table 19: Gene ontology (GO) enrichment of regulated genes from WT and $IkB_{NS}^{-/-}$ mice during LM infection and compared to uninfected controls ($FC \geq \pm 3$). Top ten GO terms from the meta category “Molecular Function” according to the p-value. Annotation Database from Oct. 2017

GO Molecular Function				
GO ID	GO Term (GO level > 8)	Nr. Genes	% Associated Genes	$-\log_{10}$ (Bonferroni corrected p-value)
16705	oxidoreductase activity, acting on paired donors, with incorporation or reduction of molecular oxygen	37	18,0	17,5
4497	monooxygenase activity	30	20,7	15,6
5506	iron ion binding	36	16,3	15,4
20037	heme binding	32	18,3	15,1
8395	steroid hydroxylase activity	19	32,8	13,5
43168	anion binding	137	5,0	10,1
8392	arachidonic acid epoxygenase activity	13	37,1	9,6
16712	oxidoreductase activity, acting on paired donors, with incorporation or reduction of molecular oxygen, reduced flavin or flavoprotein as one donor, and incorporation of one atom of oxygen	15	27,8	9,2
46914	transition metal ion binding	65	6,1	7,2
70330	aromatase activity	11	31,4	7,0

The third GO meta category “Immune System Process” can be classified into 3 major groups “Interferon-gamma responses and migration processes”, “pattern recognition receptors and innate immune response” and “Fc-gamma signaling and antigen processing”. The most enriched GO term out of the first major group is the term “response to interferon gamma” with 32 associated genes and the lowest p-value. Nearly 30% of the identified genes from this term are guanylate binding proteins (GBPs) belonging to a family of guanosine triphosphate (GTPase) induced by $IFN\gamma$ (Vestal and Jeyaratnam, 2011). Most of them are strongly induced in WT mice especially on day 3 post infection. For example, *Gbp8* is induced to a great extent during LM infection in WT mice (FC: WT d2: 33, d3: 32,6, d4: 31,3; $IkB_{NS}^{-/-}$ d2: 14.9, d3: 6.6, d4: 11).

In the second defined group of this meta-category the GO term “toll-like receptor signaling pathway” is most enriched with 20 prevalent genes. Certainly a lot of TLR genes were identified (e.g. *Tlr13*, *Tlr2*, *Tlr3*, *Tlr7*, *Tlr8*), which were all induced in the course of LM infection.

In addition, a lot of genes were found that were also enriched in the meta-category “Biological function” (see table 18) and were already described in detail such as the aforementioned *Irak3* or *Cd14*.

Finally, to conclude the GO enrichment analysis, the last GO term from the third group of the meta category “Immune System Process” is “Antigen processing and presentation of exogenous peptides”. In this term some Fc receptors are enriched (e.g. *Fcgr1*, *Fcgr3*, *Fcer1g*) and as the GO term already stated some histocompatibility class II molecules involved in antigen-presentation (e.g. *H2-Aa*, *H2-Ab1*, *H2-Eb1*) which are induced upon LM infection, but without appreciable differences between both IkB_{NS} genotypes.

Table 20: Gene ontology (GO) enrichment of regulated genes from WT and $\text{IkB}_{\text{NS}}^{-/-}$ mice during LM infection and compared to uninfected controls ($\text{FC} \geq \pm 3$). Top ten GO terms from the meta category “Immune system process” according to the p-value. Annotation Database from Oct. 2017

GO Immune System Process				
GO ID	GO Term (GO level > 8)	Nr. Genes	% Associated Genes	$-\log_{10}$ (Bonferroni corrected p-value)
34341	response to interferon-gamma	32	29,4	10,6
71346	cellular response to interferon-gamma	26	29,9	8,4
97530	granulocyte migration	26	21,1	4,9
71621	granulocyte chemotaxis	23	21,1	4,1
2224	toll-like receptor signaling pathway	20	22,5	3,8
34121	regulation of toll-like receptor signaling pathway	14	25,5	2,8
2221	pattern recognition receptor signaling pathway	22	17,3	2,4
45088	regulation of innate immune response	34	13,7	2,2
2478	antigen processing and presentation of exogenous peptide	8	36,4	2,1
38094	Fc-gamma receptor signaling pathway	6	54,5	2,4

In summary, the comparative genome-wide transcriptome analysis revealed altered gene regulation in both IkB_{NS} genotypes during LM infection. As reminder, the previous chapters 4.3.3 and 4.3.4 clearly indicate that IkB_{NS} -deficient mice showed a blunted immunopathology on day 4 post LM infection compared to their WT counterparts. Thus, the transcriptome analysis ultimately confirmed those observations. Plenty of genes are differentially regulated in WT mice compared to $\text{IkB}_{\text{NS}}^{-/-}$ mice. In addition, on the critical points in time (d3 and d4), where the WT mice start to die, expression of especially a lot of pro-inflammatory mediators are strongly up-regulated. Moreover, the GO enrichment showed that the LM infection leads to severe inflammation with strong enrichment in interferon-responses, chemotaxis and leukocytes migration. Since a lot of chemokines contributing to leukocyte migration were found to be differentially regulated between WT and $\text{IkB}_{\text{NS}}^{-/-}$ mice in the course of LM infection, the next step would be to have a closer look on the cellular distribution in the liver and also in the spleen, to identify possible differences in the migration behavior in the response to LM and to verify if a differentially regulated chemotaxis results in an altered cellular composition in the organs of WT and $\text{IkB}_{\text{NS}}^{-/-}$ mice.

4.3.6 IkB_{NS} expression in hematopoietic and non-hematopoietic liver cells during the course of LM infection

Since the microarray analyses were performed from whole liver homogenates composed of hematopoietic (CD45^+) and non-hematopoietic (CD45^-) cells, it is reasonable to next identify how high-dose LM infection would influence IkB_{NS} expression in these two cellular subsets ($\text{CD45}^+/\text{CD45}^-$). Since IkB_{NS} was described to be inducible in T cells and in *in vitro* stimulated macrophages (Schuster et al., 2012, Hirotani et al., 2005), it was expected that CD45^+ hematopoietic cells underlie certain variations regarding IkB_{NS} expression in response to LM infection. In case of non-hematopoietic cells in the liver, nothing is known so far regarding the IkB_{NS} expression profile.

To address this issue, enzymatically digested liver homogenates were prepared from WT mice infected with 10^5 CFU/mouse LM on day 1, 2, 3 and 4 post infection (3-4 mice per point in time) as well as from uninfected control mice. As additional negative control, infected $\text{IkB}_{\text{NS}}^{-/-}$ mice were

included and analyzed for I κ B_{NS} expression at the different points in time post LM infection. CD45⁺ and CD45⁻ cells were separated using magnetic cell isolation. Purity of isolated CD45⁺ and CD45⁻ was checked by flow cytometry and was generally > 95% for each cell fraction. Splenocytes, which are generally CD45⁺, were isolated from the same mice and used for comparison. 1 x 10⁶ cells were lysed in RLT buffer and after isolation of RNA and reverse transcription into cDNA, samples were used to determine mRNA expression of I κ B_{NS}.

Figure 32 summarizes the I κ B_{NS} gene expression profile normalized to the house-keeping gene β -*actin* during the course of LM infection. For statistics I κ B_{NS} expression following LM infection was compared to initial expression in uninfected animals.

In the hematopoietic CD45⁺ cell fraction from the liver relatively high and constant I κ B_{NS} expression could be observed in uninfected mice and on day 1 post infection (Figure 32A). Interestingly, I κ B_{NS} expression significantly drops down on day 2 post infection and only marginally recovers on day 3 and day 4. This clearly indicates that hematopoietic CD45⁺ cells from the liver exhibit a robust basal I κ B_{NS} expression which decreases upon infection.

The overall kinetic of I κ B_{NS} expression in non-hematopoietic CD45⁻ liver cells (Figure 32B) is similar to that of CD45⁺ liver cells. The initial expression on day 0 is however slightly lower than in CD45⁺ cells. In contrast, I κ B_{NS} expression in CD45⁻ liver cells already drops on day 1 post infection and decreases even further on day 2 post infection. Similar to the CD45⁺ cells I κ B_{NS} expression in CD45⁻ liver cells marginally raises again on day 3 and 4 post infection. Thus, I κ B_{NS} expression in both CD45⁺ and CD45⁻ liver cells reaches its minimum two days after LM infection.

Interestingly, during the course of LM infection no significant changes in the expression of I κ B_{NS} were observed in splenocyte samples (see Figure 32C). Here, only a slight reduction in the I κ B_{NS} mRNA level was observed on day 2 post infection compared to day 0 and day 1. After this initial drop, a slight increase in I κ B_{NS} expression occurs on day 3 and day 4. Of note, I κ B_{NS} expression in CD45⁺ liver cells from uninfected mice is about twice as high than in CD45⁺ splenocytes from the same mice, suggesting an overall higher steady state abundance of I κ B_{NS} in resident immune cells of the liver compared to spleen. Moreover, in both CD45⁺ and CD45⁻ liver cells as well as in splenocytes of I κ B_{NS}-deficient mice no I κ B_{NS} expression was detected, as expected (data not shown).

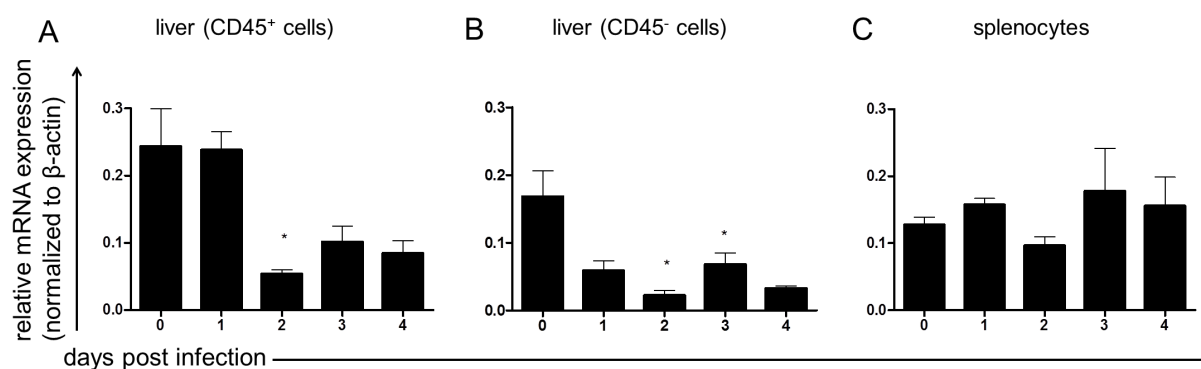


Figure 32: IκB_{NS} mRNA expression in CD45⁺ and CD45⁻ liver cells as well as in splenocytes of WT mice during LM infection. WT mice (■, n= 3-4) were infected with 10⁵ CFU LM, liver and spleen were sampled at indicated times post infection. Liver samples were further processed by MACS to obtain CD45⁺ and CD45⁻ cell fractions. RNA was isolated from CD45⁺/CD45⁻ liver cells and splenocytes, reverse transcribed into cDNA and IκB_{NS} expression was analyzed by real-time PCR normalized to β-actin. (A) IκB_{NS} expression in CD45⁺ liver cells (B) in CD45⁻ liver cells and (C) in splenocytes. Data are presented as mean ± SEM. Statistical analyses were performed by two-way ANOVA with Bonferroni post-test. * p < 0.05.

In summary, the expression of IκB_{NS} undergoes infection-associated dynamic alterations in an organ-specific manner. In both the CD45⁺ and CD45⁻ cell fractions of liver samples the highest IκB_{NS} expression was observed in the steady state (i.e. on day 0) indicating strong basal expression. Thus, it is likely that IκB_{NS} expression and its down-regulation during LM infection is mechanistically linked to the regulation of acute phase or secondary response genes as suggested by the strong differences in microarray analyses between both genotypes especially on day 3 and day 4 post infection.

4.3.7 Altered immune cell distribution in livers and spleens of IκB_{NS}-deficient mice during the course of LM infection

Due to the broad changes in gene expression in WT and IκB_{NS}^{-/-} mice especially in functional gene categories such as chemotaxis and leukocyte migration observed by microarray analysis, next an important issue was to determine potential differences in the immune cell composition in spleens and livers during LM infection. For this, detailed flow cytometric analyses were performed to characterize distribution of most of lymphocytic and myeloid cell subsets and to get an overview of how IκB_{NS} would influence the cellular distribution during high-dose LM infection in the main bacterial replication sites liver and spleen. For simultaneous identification and quantification of 13 different immune cell subsets (e.g. B cells, T cells, NK cells, neutrophils, eosinophils, monocytes, macrophages and dendritic cells) in non-infected and infected tissue a protocol developed by Yu and colleagues was used (Yu et al., 2016). Detailed information about the antibodies and gating strategy used can be found in section 3.16.

A major drawback in the understanding of the function of IκB_{NS} within individual immune cell subsets during LM infection is, that so far it is largely unknown to what extent they rely on the function of IκB_{NS}. As described above (section 4.3.6) IκB_{NS} expression is strongly down-regulated within 2 days after LM infection within the entire CD45⁺ leukocyte cell fraction in the liver suggesting that IκB_{NS} is of importance for the activation and/ or function of immune cells early on during infection. Still it is unclear if this IκB_{NS} expression pattern is valid for all immune cell subsets. Thus, to gather knowledge on cell-specific IκB_{NS} expression during LM infection and by this to more clearly correlate lack of IκB_{NS} with

the improved pathological phenotype, altered cellular composition and differential gene expression, promoter activity of the *Nfkbid* gene encoding for I κ B_{NS} was studied in all 13 immune cell subsets included in this survey. To this end, the *Nfkbid*^{LacZ} reporter mouse line derived from the EUCOMM consortium and provided by Ingo Schmitz and colleagues from Helmholtz Centre for Infection Research Braunschweig was utilized. Of note, this reporter mouse has only one functional allele of *Nfkbid*, since the second one has been substituted by lacZ-reporter cassette, leading formally to a heterozygous *Nfkbid* knockout mouse. This genotype, based on previous results (section 4.3.1), should render the mice more susceptible to the high-dose LM infection. In order to gather information on *Nfkbid* promoter activity in all cell subsets and throughout the entire time frame of 4 days of LM infection, it had to be guaranteed that all mice would survive the infection. Thus, the reporter mice were infected with a non-lethal dose of LM (3×10^4 CFU/mouse). The lacZ-reporter expression is linked to that of the *Nfkbid* gene. Thus, the *Nfkbid* expression can be indirectly quantified by assessing the lacZ enzymatic activity per cell using the conditional fluorescent surrogate substrate analogue fluorescein-di- β -D-galactopyranosid (FDG). FDG is enzymatically cleaved by the lacZ enzyme resulting in intracellular accumulation of fluorescently active fluorescein. For a better visualization and comparison the fluorescein intensities were z-score normalized over all mice and all cell populations analyzed on a given day post infection.

When applied to uninfected lacZ reporter mice, the immune cell identification panel in conjunction with the lacZ reporter assay gives conclusive impressions of the initial I κ B_{NS} promoter activity in 13 immune cell subsets based on the MFI of fluorescein per cell subset in spleen and liver (Table 21 and Table 22). Interestingly, in lymphocytes, i.e. B cells, T cells and NK cells from spleen and liver the lacZ activity was comparatively low. In contrast, the myeloid cells and here especially monocytes and macrophages showed the strongest steady state lacZ activity indicative for the highest *Nfkbid* promoter activity. Neutrophils, DCs and eosinophils showed an intermediate *Nfkbid* promoter activity. Importantly, the overall strength of *Nfkbid* promoter activity in specific cellular subsets does not much differ between spleen and liver, indicating that the *Nfkbid* promoter activity is independent of the cellular microenvironment and thus is likely to be a cell intrinsic property.

Table 21: *Nfkbid* promoter activity in different immune cell subsets in spleens of uninfected mice. Uninfected *Nfkbid*^{lacZ} reporter mice (n= 5) were sacrificed, spleens were sampled and the lacZ reporter activity was determined using an intracellular FDG assay and flow cytometry. Data represent the averaged median fluorescence intensity of fluorescein and the standard deviation.

Cell population	Averaged median fluorescence intensity (MFI) ± standard deviation
Inflammatory Monocytes	61500 ± 6950
Resident Monocytes	37740 ± 6537
Interstitial Macrophages	34571 ± 6890
CD11b ⁺ DC	34442 ± 8185
Neutrophils	29424 ± 2110
CD11b ⁻ DC	21520 ± 4312
NK cells	19385 ± 2540
Resident Macrophages	15200 ± 3132
Eosinophils	14543 ± 2200
CD4 ⁻ CD8 ⁻ lymphocytes	11510 ± 2121
B cells	7897 ± 1017
CD4 ⁺ T cells	5978 ± 1060
CD8 ⁺ T cells	5182 ± 935

Table 22: *Nfkbid* promoter activity in different immune cell subsets in livers of uninfected mice. Uninfected *Nfkbid*^{lacZ} reporter mice (n= 5) were sacrificed, livers were sampled and the lacZ reporter activity was determined using an intracellular FDG assay and flow cytometry. Data represent the averaged median fluorescence intensity of fluorescein and the standard deviation.

Cell population	Averaged median fluorescence intensity (MFI) ± standard deviation
Inflammatory Monocytes	64937 ± 4110
Resident Monocytes	54154 ± 1113
Interstitial Macrophages	43592 ± 5387
Neutrophils	30892 ± 3268
CD11b ⁻ DC	27281 ± 3810
Resident Macrophages	21705 ± 1695
NK cells	19476 ± 1504
CD11b ⁺ DC	18659 ± 5048
CD4 ⁻ CD8 ⁻ lymphocytes	17423 ± 337
CD4 ⁺ T cells	14947 ± 582
Eosinophils	13132 ± 1074
B cells	9266 ± 334
CD8 ⁺ T cells	6089 ± 942

To correlate immune cell prevalence with *Nfkbid* promoter activity in these particular cells throughout the course of LM infection, the next figures show on the one hand the cellular distribution of individual immune cell subsets in livers and spleens of high-dose infected (10^5 CFU/mouse) WT and *IkBNS*^{-/-} mice (see Figure 33, 34, 35A) and on the other hand the lacZ enzymatic activity from non-lethally infected (3×10^4 CFU/mouse) *Nfkbid*^{lacZ} reporter mice (see Figure 33, 34, 35B).

Due to an inflammation-associated damage of the organ structures, high auto-fluorescence and significant changes in the lineage marker expression especially in WT mice it was not possible to obtain reliable FACS data from all anticipated immune cell populations at the late stage of infection.

For that reason, day 4 post infection was excluded from the analyses of high-dose LM infected mice WT and $I\kappa B_{NS}^{-/-}$ mice.

The prevalence of cells is represented as absolute cell numbers. In addition, the relative percentages of all cell subsets based on alive, single cells gated on $CD45^{+}$ can be found in the appendix for comparison.

Figure 33A summarizes the identified lymphocytic cell populations. In general, in uninfected WT mice (day 0) the proportionally largest cell population in the liver is represented by $CD4^{+}$ T cells ($\sim 1.8 \times 10^6$ cells) followed by B cells with about 1.2×10^6 cells, $CD8^{+}$ T cells ($\sim 5 \times 10^5$ cells), $CD4^{-}CD8^{-}$ lymphocytes (6×10^5 cells) and NK cells ($\sim 3.2 \times 10^5$ cells). The cellular composition in the spleen of uninfected WT mice is composed of a majority of B cells ($\sim 7 \times 10^6$ cells) followed by $CD4^{+}$ T cells ($\sim 2.5 \times 10^6$ cells), $CD8^{+}$ T cells (1.5×10^6 cells), $CD4^{-}CD8^{-}$ lymphocytes ($\sim 3.5 \times 10^6$ cells) and finally NK cells ($\sim 8 \times 10^4$ cells). Taken together, the lymphocytic cell populations are the major immune cell subsets in liver (58%) and spleen (76%) during the steady state. Interestingly, when considering the lacZ enzyme activity (Figure 33B), the values of the normalized z-scores are below zero in the lymphocytic cell subsets, indicating a relatively weak *Nfkbid* promoter activity.

Surprisingly, while no differences in the percentages between both genotypes were found (refer to appendix Figure 1) significantly higher numbers of B cells, $CD4^{+}$ T cells and $CD8^{+}$ T cells were found in the livers of uninfected $I\kappa B_{NS}^{-/-}$ mice. Whereas on day 1 post infection the numbers of $CD4^{+}$ and $CD8^{+}$ T cells are still significantly higher in $I\kappa B_{NS}^{-/-}$ mice than in their WT counterparts, both genotypes show a decrease in the absolute numbers of all lymphocytic cell subsets in the liver and especially on day 2 and day 3 post infection, no significant differences between both genotypes were observed.

In contrast to the liver, the spleen of uninfected mice shows no genotype-dependent differences in regard to numbers of B cells, $CD4^{+}$ T cells, $CD8^{+}$ T cells and NK cells. However, cell numbers of all 4 lymphocytic subsets slightly increase in the spleen on day 1 post infection. At that time, spleens of WT mice even contained significantly more B cells than $I\kappa B_{NS}$ -deficient mice. By day 2 and day 3 post infection all major lymphocyte subsets show a strong drop in cell numbers below the level detected on day 0 with the exception of $I\kappa B_{NS}^{-/-}$ mice were on day 3 post infection, NK cell numbers returned to their initial cell number measured before in the uninfected state.

These results suggest that changes in the tissue distribution of the lymphocytic cells are primarily dependent on the LM infection itself and less dependent on the presence or absence of $I\kappa B_{NS}$. Interestingly, significant differences regarding lymphocyte numbers (but not relative frequencies) between WT and $I\kappa B_{NS}^{-/-}$ mice are only evident in livers of uninfected animals.

With regard to the lacZ activity, from all identified lymphocytic cell populations only NK cells showed z-scores higher than zero (above the mean of all cell subsets). In all other lymphocytic cell subsets the values of the normalized z-scores stay below zero during the course of LM infection indicating that in lymphocytic cells in general the *Nfkbid* promoter activity is not very pronounced. $CD8^{+}$ T cells show the strongest induction of lacZ activity over time amongst all lymphocyte subsets analyzed which might indicate that $I\kappa B_{NS}$ is inducible in $CD8^{+}$ T cells upon stimulation.

Another observation is the strong increase of *Nfkbid* promoter activity in NK cells on day 1 post infection in liver samples. After this strong increase on day 1 the z-score value drops down to base level and subsequently marginally rises again until day 4 post infection.

In summary, obtained results revealed that among the lymphocytic cell subsets NK cells show the highest lacZ activity in the course of LM infection. In CD8⁺ T cells an induction in lacZ activity can be observed during LM infection. Thus, NK cells and CD8⁺ T cells show dynamic alterations in *Nfkbid* promoter activity during infection. Furthermore, the lack of I κ B_{NS} in lymphocytes might not be mechanistically linked to the observed ameliorated organ-pathology in response to LM infection in I κ B_{NS}^{-/-} mice, since not only the overall number of lymphocytes in spleens and livers during LM infection decreases over time but, at the same time, all lymphocyte subsets exhibit a relatively low *Nfkbid* promoter activity throughout the course of infection.

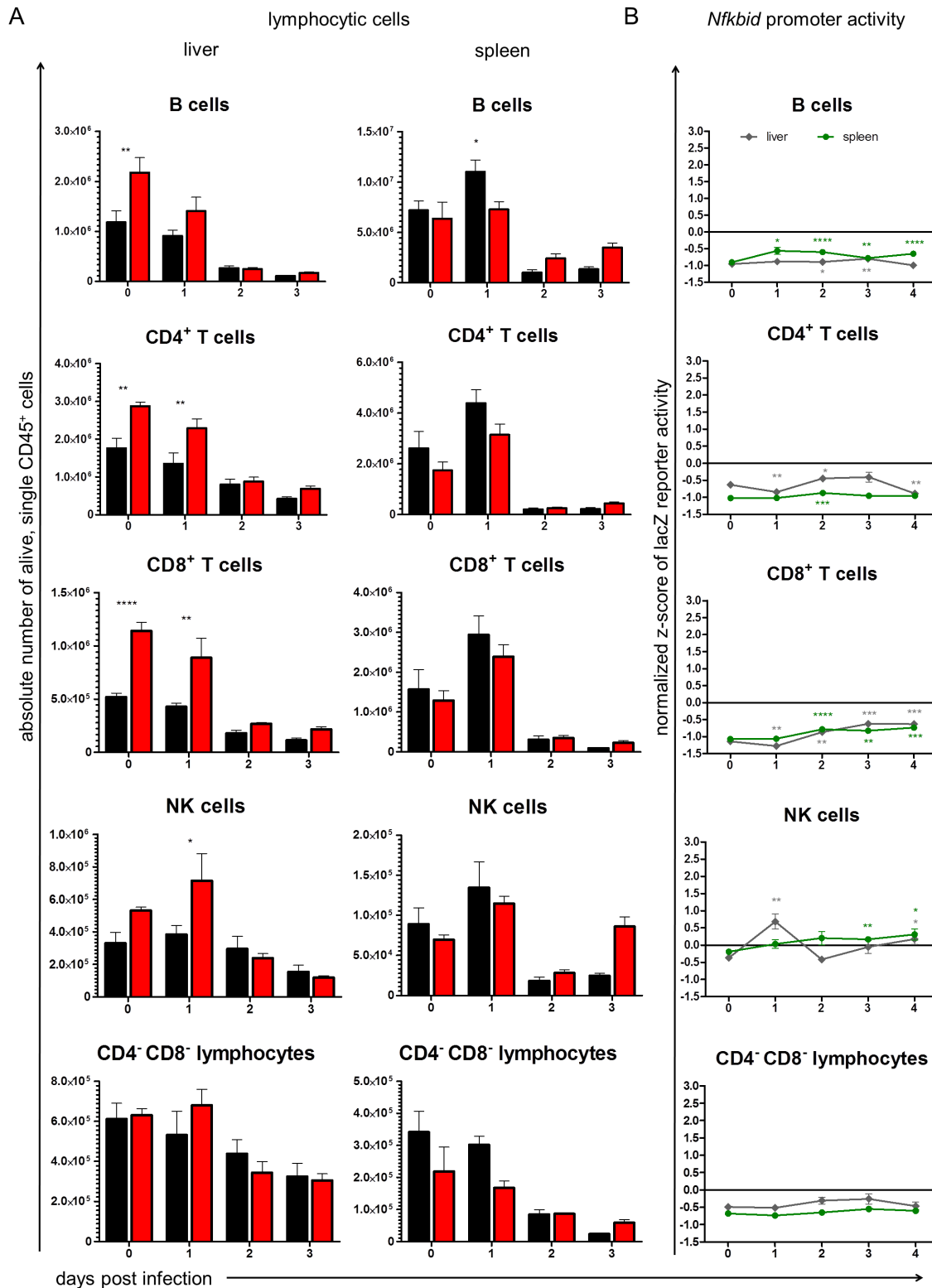


Figure 33: Lymphocyte composition of livers and spleens of WT and $lkbNS^{-/-}$ mice during the course of LM infection and correlation with *Nfkbid* promoter activity. (A) WT (■, n=3-4) and $lkbNS^{-/-}$ (■, n=3-4) mice were infected with high-dose (10^5 CFU) of *Listeria*. At indicated times post infection, mice were sacrificed and the cellular composition was determined by flow cytometry. Data are represented as mean \pm SEM of absolute cell numbers/organ. Statistical analyses were performed using two-way ANOVA with Bonferroni post-test. (B) *Nfkbid*^{lacZ} reporter mice (n=5-6/point in time) were infected with 3×10^4 CFU *Listeria*. At indicated times post infection spleens (●) and livers (●) were sampled and the lacZ reporter activity was determined using an intracellular FDG assay followed by flow cytometry. The median fluorescein intensities were z-score normalized over all mice and all cell populations on a given day post infection. Statistical analyses were performed in comparison to uninfected mice using unpaired, two-tailed student's *t*-test. **** $p < 0.0001$, *** $p < 0.001$, ** $p < 0.01$, * $p < 0.05$.

Next, the distribution of different myeloid cell subsets was analyzed in spleens and livers from WT and $\text{I}\kappa\text{B}_{\text{NS}}^{-/-}$ mice within the course of infection. In the absence of infection (day 0) only few ($< 10^5$) inflammatory monocytes, resident monocytes, interstitial macrophages and resident macrophages were detected in liver and spleen of both genotypes (Figure 34A).

On day 1 post infection the absolute number of inflammatory monocytes in both genotypes increases up to approximately 1×10^6 in the liver. The number of inflammatory monocytes subsequently decreases on day 2 to values slightly above base level and finally increases again on day 3 to values comparable to day 1 post infection. This overall dynamics of inflammatory monocytes in the liver holds true for both $\text{I}\kappa\text{B}_{\text{NS}}$ genotypes. Importantly, the secondary increase on day 3 post infection becomes even more meaningful in the light of the fact, that the leukocyte compartment in WT livers at this time constitutes about 36% inflammatory monocytes (see appendix Figure 2), making them the largest immune cell subset on day 3 post infection. Though the total number of inflammatory monocytes in WT mice on day 3 post infection is about the same as on day 1, their frequency in relation to all other immune cell subsets is drastically increased on day 3, due to decreased proportion of several previously more abundant immune cell subsets. This renders inflammatory monocytes the most abundant and thus in terms of disease course and immunopathology probably the most influential immune cell subset in livers of WT mice 3 days post infection.

In this respect it appears even more important that inflammatory monocytes in the liver of $\text{I}\kappa\text{B}_{\text{NS}}^{-/-}$ mice on day 3 post infection constitute only about 26% of all leukocytes, with their absolute number being slightly reduced compared to WT mice. Given their pro-inflammatory nature and their relative predominance on day 3 post infection, the difference in liver inflammatory monocytes frequencies between WT and $\text{I}\kappa\text{B}_{\text{NS}}$ -deficient mice may provide an important clue in understanding immune-pathological processes leading to death of WT but not $\text{I}\kappa\text{B}_{\text{NS}}$ -deficient mice between day 4-6 post infection.

Compared to the liver, numbers of inflammatory monocytes in the spleen between day 0 and day 2 are comparably low in both genotypes, but start to rise to 3×10^5 cells especially in $\text{I}\kappa\text{B}_{\text{NS}}^{-/-}$ mice on day 3 post infection. Though the overall numbers of inflammatory monocytes in spleens are generally far lower than in the liver, the numerical difference seen in WT vs. $\text{I}\kappa\text{B}_{\text{NS}}^{-/-}$ livers is apparently inverted in the spleen. Since the overall relative cellular composition of the spleen on day 3 post infection is not dominated by inflammatory monocytes (see appendix Figure 2) as it is the case for the liver, the meaning of the knock-out specific increase in inflammatory monocytes in the spleen is more difficult to interpret, but demonstrates organ-specific influx behavior of certain immune cell subsets in absence of $\text{I}\kappa\text{B}_{\text{NS}}$. In this respect, it is important to note that inflammatory monocytes show the highest *Nfkbid* promoter activity of all analyzed immune cell subsets throughout the course of LM infection, both in liver and spleen (Figure 34B). Thus, the relative cellular predominance of inflammatory monocytes observed on day 3 post infection in the liver raises the question of an altered cellular phenotype of $\text{I}\kappa\text{B}_{\text{NS}}$ -deficient inflammatory monocytes, which apparently amongst all other immune cell subsets, depend on $\text{I}\kappa\text{B}_{\text{NS}}$ expression the most or at least have the most active $\text{I}\kappa\text{B}_{\text{NS}}$ promoter region.

The absolute numbers of resident monocytes in livers of WT mice showed a constant increase until day 2 post infection where the highest number was detectable with approximately 2.4×10^5 cells. On

day 3 post infection the number of resident monocytes decreases again to about 1.2×10^5 cells. In contrast to this, the absolute numbers of resident monocytes in livers of $\text{IkB}_{\text{NS}}^{-/-}$ mice reach their peak already on day 1 post infection. In contrast to their inflammatory counterparts, resident monocytes generally account for only minor fractions (1- 5%) of all leukocytes throughout the course of infection. In the spleen the only numerical peculiarity is the significant difference of resident monocytes in WT vs. $\text{IkB}_{\text{NS}}^{-/-}$ mice on day 3 post infection. Here, IkB_{NS} -deficient mice exhibit about 5×10^4 resident monocytes, whereas WT mice only contain about 10^4 of these cells in the spleen. The most interesting feature about resident monocytes is however their dynamic change in *Nfkbid* promoter activity during the course of infection, being the only cell type in which the lacZ activity significantly declines during infection (Figure 34B), both in spleen and liver from a relatively high lacZ activity in the steady state (compare table 21 and 22) to an intermediate level by day 3 and 4 post infection.

Hardly any interstitial and resident macrophages were detected in livers of WT and $\text{IkB}_{\text{NS}}^{-/-}$ mice before day 1 post infection. On day 2 post infection an increase of both cell types in livers of both genotypes was observed. Worth to mention is that on day 2 post infection both macrophage subsets together account for about 20% of all leukocytes in both genotypes. Both absolute and relative numbers decrease by day 3 post infection where macrophages account for only 13% of all leukocytes. Though the dynamic changes of both interstitial and resident macrophages frequencies are comparable between genotypes and organs, they differ in their course of *Nfkbid* promoter activity profile. Here, interstitial macrophages clearly show higher lacZ- and thus *Nfkbid* promoter activity, which throughout the course of infection continuously increases to levels close to that of inflammatory monocytes (i.e. on day 4 post infection). During LM infection interstitial macrophages thus show the highest dynamic increase in lacZ activity of all leukocyte subsets analyzed. The fact that they account for 13% of all leukocytes in the liver on day 3 post infection showing at the same time very high lacZ activity, renders interstitial macrophages next to inflammatory monocytes a second subset of innate immune cells that may potentially contribute to the dramatic differences in immunopathology in the liver of LM infected WT vs. $\text{IkB}_{\text{NS}}^{-/-}$ mice that eventually may account at least in part for the obvious differences in terms of survival of high-dose LM infection.

In summary, all analyzed splenic monocyte and macrophage subsets demonstrate consistent differences in terms of absolute cell numbers when WT and $\text{IkB}_{\text{NS}}^{-/-}$ mice are compared. Here IkB_{NS} -deficient mice exhibit consistently higher cell numbers than their WT counterparts. Mechanistically this may suggest either a stronger recruitment of these cells or an improved survival of monocytes and macrophages in the spleens of mice lacking IkB_{NS} .

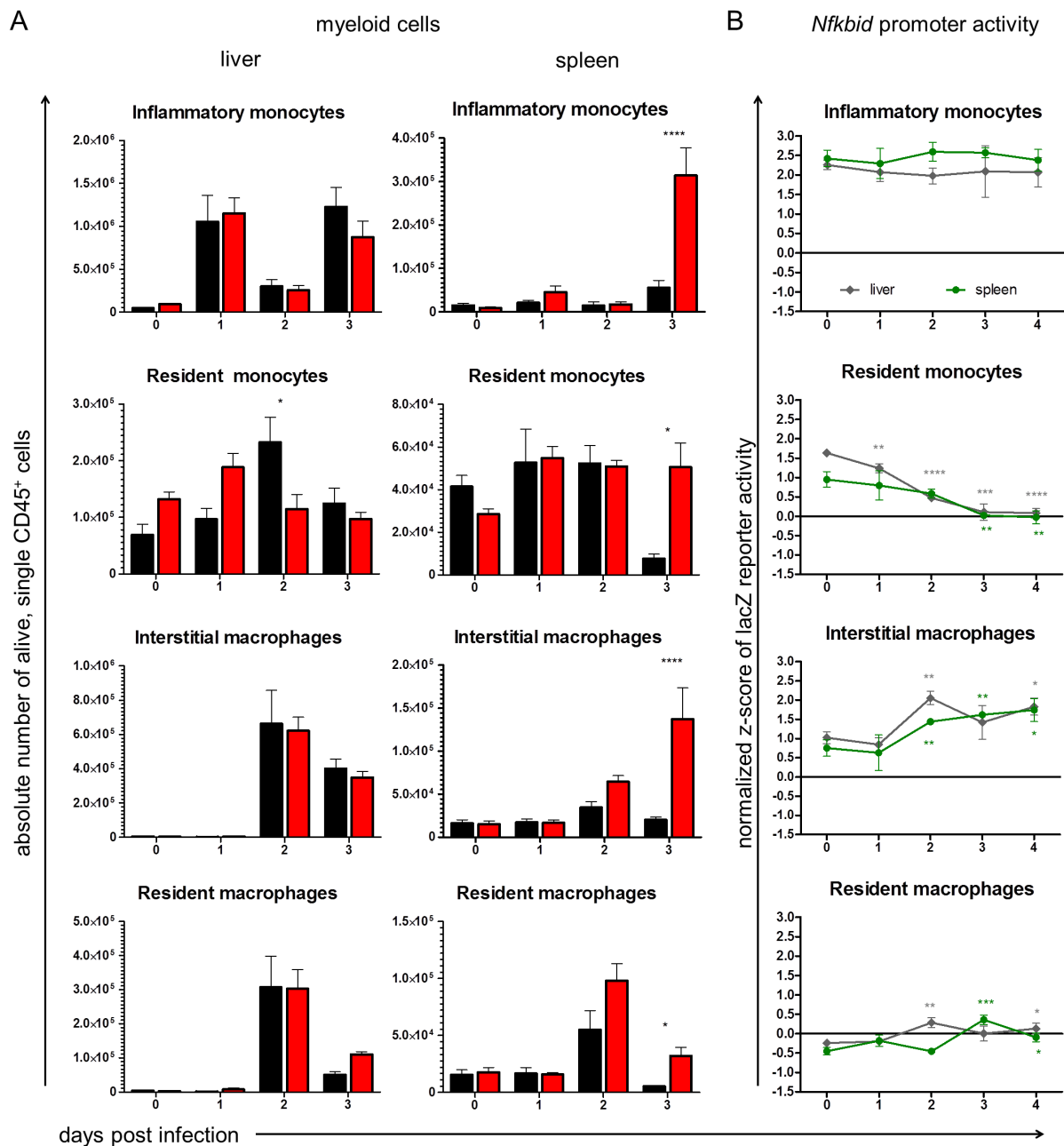


Figure 34: Cellular composition of monocytes and macrophages in livers and spleens of WT and *IkBNS*^{-/-} mice during the course of LM infection and correlation with *Nfkbid* promoter activity. (A) WT (■, n=3-4) and *IkBNS*^{-/-} (■, n=3-4) mice were infected with a high-dose (10⁵ CFU) of *Listeria*. At indicated times post infection, mice were sacrificed and the cellular composition was determined by flow cytometry. Data are represented as mean ± SEM of absolute cell numbers/organ. Statistical analyses were performed using two-way ANOVA with Bonferroni post-test. (B) *Nfkbid*^{lacZ} reporter mice (n=5-6/point in time) were infected with 3×10⁴ CFU *Listeria*. At indicated times post infection spleens (●) and livers (●) were sampled and the lacZ reporter activity was determined using an intracellular FDG assay followed by flow cytometry. The median fluorescein intensities were z-score normalized over all mice and all cell populations on a given day post infection. Statistical analyses were performed in comparison to uninfected mice (day0) using unpaired, two-tailed student's t-test. **** p < 0.0001, *** p < 0.001, ** p < 0.01, * p < 0.05.

Next, the distribution of neutrophils, eosinophils, CD11b⁺ DCs and CD11b⁻ DCs in livers and spleens of WT and I κ B_{NS}^{-/-} mice during the course of LM infection was analyzed (Figure 35A). In the absence of infection (day 0) only few ($< 10^4$) neutrophils were detected in WT livers. Within the first two days of infection the number of neutrophils increases to approximately 5.2×10^5 cells. Then on day 3 post infection, the number decreases again to values similar to day 0. In I κ B_{NS}^{-/-} mice, the highest number of neutrophils in livers was detected already on day 1 with more than 1×10^6 cells. Subsequently, the numbers decreased within the next days of infection and reached the same values as in their WT counterparts. Thus, I κ B_{NS}^{-/-} mice show significantly elevated numbers of neutrophils in the liver on day 1 post infection. Absolute numbers of neutrophils in spleens are similar between the genotypes in the absence of infection. Upon LM infection neutrophils showed the same influx behavior on day 1 and day 2 after infection in both mouse strains. Of note, neutrophils in WT spleen account for over 15% (I κ B_{NS}^{-/-}: 10%) of all leukocytes on day 2 post infection. On day 3 post infection a strong decrease in the number of neutrophils was observed in WT mice, whereas their number in I κ B_{NS}^{-/-} mice remains comparably high. Relative frequencies of neutrophils on day 3 post infection range between 2.5% (WT) and 5% (I κ B_{NS}^{-/-}). With regard to their *Nfkbid* promoter activity, neutrophils compared to other immune cells show an average activity which slightly declines over time in both organs.

Strikingly, higher numbers of eosinophils were observed in the steady state and day 1 post infection in livers of I κ B_{NS}-deficient mice compared to WT mice. Especially in uninfected mice, eosinophils account for nearly 10% of all leukocytes in I κ B_{NS}^{-/-} livers. At later times post infection numbers of eosinophils decline and no differences between both genotypes are observed anymore.

In spleens of I κ B_{NS}-deficient mice significantly more eosinophils were detected on day 1 post (I κ B_{NS}^{-/-}: 1.5×10^6 , WT: 7.5×10^4) and day 3 post infection (I κ B_{NS}^{-/-}: 1.2×10^5 , WT: 2.5×10^4). *Nfkbid* promoter activity was comparably low in eosinophils with little but significant variations throughout the course of LM infection.

The absolute numbers of CD11b⁺ and CD11b⁻ DCs in the liver decrease during the course of LM infection in both genotypes, with the exception of day 1 post infection, on which I κ B_{NS}^{-/-} mice show a significant increase of hepatic CD11b⁺ DCs compared to WT mice. Both subsets are clearly reduced in numbers by day 2 and 3 post infection in livers with no differences between the genotypes. Liver DCs from both genotypes share overall a similar dynamic as their splenic counterparts. On day 0 and 1 post infection both CD11b⁺ and CD11b⁻ DCs display stable absolute cell numbers (about 4×10^4) which then significantly drop on day 2 and day 3 post infection. The only exception here is that CD11b⁺ DCs in I κ B_{NS}^{-/-} mice on day 3 are as high in numbers as on day 1 post infection, which is significantly different compared to WT mice. In both DC subsets *Nfkbid* promoter activity in spleens slightly decreases during the infection, whereas in liver samples the infection induces a slight increase of the promoter activity.

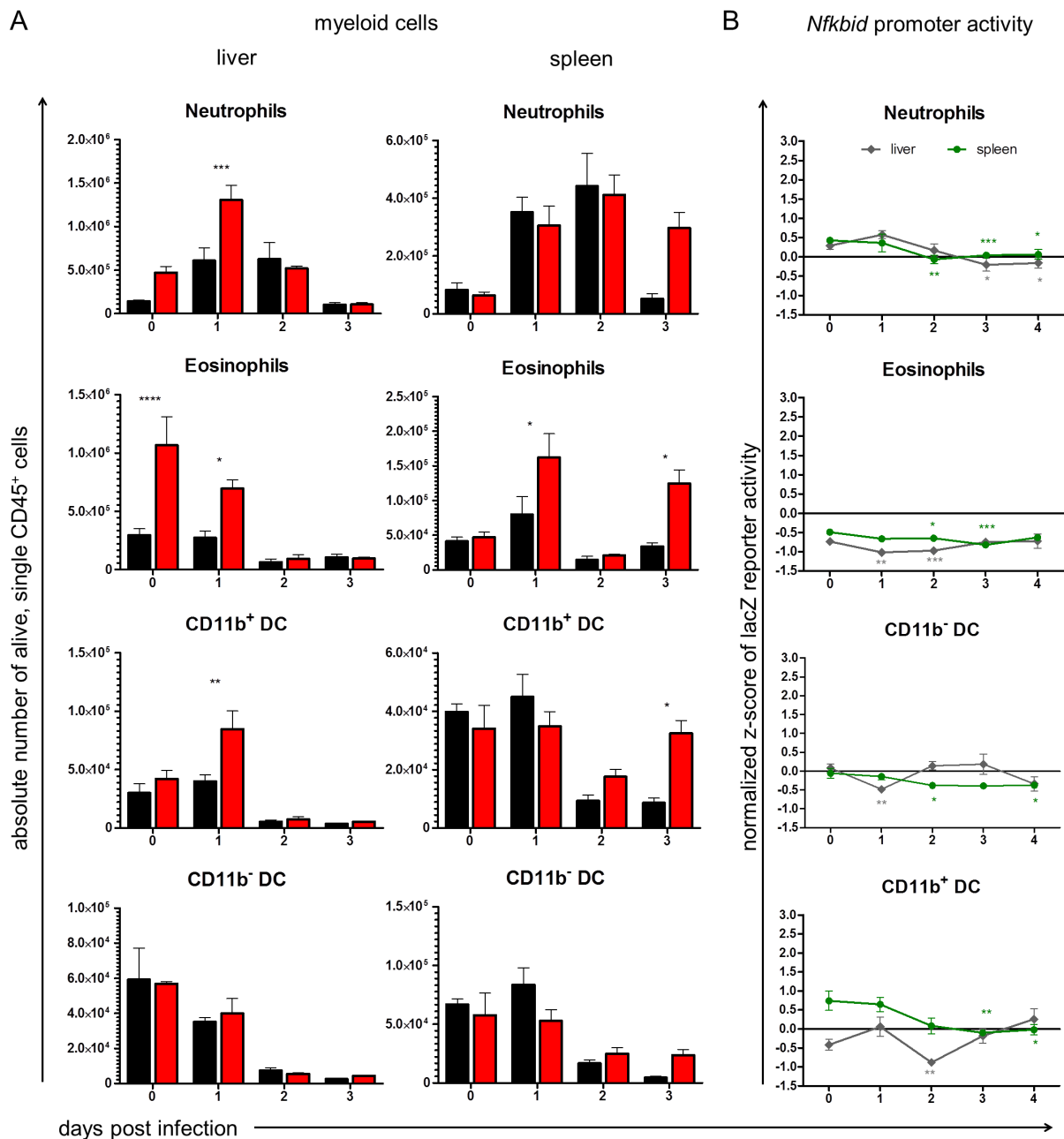


Figure 35: Cellular composition of myeloid cell subsets in livers and spleens of WT and $\text{IkB}_{\text{NS}}^{-/-}$ mice during the course of LM infection and correlation with *Nfkbid* promoter activity. (A) WT (■, n=3-4) and $\text{IkB}_{\text{NS}}^{-/-}$ (■, n=3-4) mice were infected with high-dose (10^5 CFU) of *Listeria*. At indicated times post infection, mice were sacrificed and the cellular composition was determined by flow cytometry. Data are represented as mean \pm SEM of absolute cell numbers/organ. Statistical analyses were performed using two-way ANOVA with Bonferroni post-test. (B) *Nfkbid*^{lacZ} reporter mice (n=5-6/point in time) were infected with 3×10^4 CFU *Listeria*. At indicated times post infection spleens (●) and livers (●) were sampled and the lacZ reporter activity was determined using an intracellular FDG assay followed by flow cytometry. The median fluorescein intensities were z-score normalized over all mice and all cell populations on a given day post infection. Statistical analyses were performed in comparison to uninfected mice using unpaired, two-tailed student's *t*-test. *****p* < 0.0001, ****p* < 0.001, ***p* < 0.01, **p* < 0.05.

Taken together, obtained results revealed that high-dose LM infection leads to brought alterations in the cellular composition in spleens and livers and that there are IkB_{NS} -dependent alterations in cell migration and influx patterns. Importantly, the lack of IkB_{NS} has a distinct impact on the cellular distribution and/or abundance of myeloid cells, and here especially on monocytes and macrophages in spleen and liver during LM infection. This may account for the fact that under normal conditions

monocytes and macrophages not only show the highest *Nfkbid* promoter activity among all immune cell subsets analyzed, but as well numerically dominate the leukocyte composition in livers and spleens at later stages of the infection (e.g. day 3 post infection). Thus, the lack of I κ B_{NS} protein expression is likely to affect monocytes and macrophages during LM infection the most. In order to further decipher whether I κ B_{NS} would affect the inflammatory program of monocytes during the course of LM infection and thus would contribute to the observed protection of I κ B_{NS}^{-/-} mice from an otherwise lethal infection, the inflammatory response of monocytes to LM infection was studied in more detail.

4.3.8 I κ B_{NS}-dependent activation of an inflammatory program in monocytes as potential underlying mechanism for the detrimental course of high-dose LM infection

The analysis of the *Nfkbid* promoter activity clearly indicates that especially in monocytes and macrophages I κ B_{NS} is constitutively expressed and its expression remains stable during the course of LM infection (refer to chapter 4.3.7). Together with the results obtained from the microarray analysis (refer to chapter 4.3.5) showing that a high number of pro-inflammatory mediators (e.g. *Nos2*, *Il1 β* , *Ccl2*, *Ccl5*) were differentially expressed in WT compared to I κ B_{NS}-deficient mice, this leads to the assumption that especially the inflammatory response of monocytes and macrophages is regulated by I κ B_{NS} and that I κ B_{NS}-dependent activation of certain genes encoding for pro-inflammatory mediators may be involved in the fatal outcome of the high-dose LM infection in WT mice. To prove this hypothesis more detailed analysis of inflammatory monocytes was performed. For this, WT and I κ B_{NS}^{-/-} mice were infected with 10⁵ CFU LM per mouse and on day 3 post infection, mice were sacrificed, spleen and liver were removed and single cell suspensions of both organs were prepared. In this experimental set-up day 3 post infection was chosen, because the microarray analysis (section 4.3.5) revealed that at this point in time the most pronounced differential gene expression could be observed between both genotypes. Cells from 4-5 individual mice were pooled, stained for inflammatory monocytes according the staining panel listed in table 6 and sorted using FACS. RNA was isolated from sorted cells of both genotypes, reversely transcribed into cDNA and used for RT-PCR to determine the gene expression of *Nfkbid*, *Il6*, *Nos2* and *Il1 β* . These genes were selected since they were found previously to be far less induced in livers of LM infected I κ B_{NS}-deficient compared to WT mice in the microarray analysis performed on day 3 post infection and moreover, decreased *Il6* expression in mice lacking I κ B_{NS} was confirmed in liver homogenates in real-time PCR (refer to chapter 4.3.4). Additionally, IL6 and IL1 β are inflammation-associated cytokines with macrophages and monocytes being their most important cellular sources (Gabay, 2006). Furthermore, activated macrophages do express the inducible nitric oxide (NO) synthase encoded by the *Nos2* gene (Myers et al., 2003) and are thus effective producers of NO, which promotes anti-listerial activities. For this reason, the expression of *Nos2* was also determined in sorted inflammatory monocytes by RT-PCR.

As depicted in Figure 36A and as included as internal control, inflammatory monocytes from spleens of I κ B_{NS}^{-/-} mice showed no I κ B_{NS} expression, which was expected and confirms the results from chapter 4.3.6. Remarkably, sorted inflammatory monocytes from WT spleens showed higher mRNA expression of *Il6*, *Nos2* and *Il1 β* on day 3 post infection compared to the monocytes from I κ B_{NS}-

deficient mice. Especially *Nos2* and *Il1 β* expression was extremely strong as seen by relative expression values $\gg 1$ compared to the house-keeping gene *RPS9*, which means about eight-times higher expression of *Nos2* compared to house-keeping gene in WT mice. This suggests that especially the inflammatory monocytes may contribute to severe inflammation by secreting pro-inflammatory mediators, which in turn may lead to the overwhelming immune response and thereby possibly promoting death of WT animals within few days of LM infection. This strong pro-inflammatory program is blunted in IkB_{NS} -deficient monocytes, demonstrated by moderate expression levels of all above mentioned cytokines. The same observation holds true for the inflammatory monocytes sorted from liver samples of high-dose infected WT and IkB_{NS} ^{-/-} mice. Here, strongly increased levels of *IL6*, *Nos2* and *Il1 β* were detected in monocytes from WT compared to monocytes from IkB_{NS} ^{-/-} livers.

To confirm that those mediators are secreted predominantly by hematopoietic cells of which inflammatory monocytes constitute a major subset, RT-PCR analyses of the same genes were as well performed with the aforementioned CD45⁻ liver cell fraction (refer to section 4.3.6). Indeed, no mRNA expression of *Il6*, *Nos2* and *Il1 β* could be observed in CD45⁻ liver cells (data not shown), suggesting that non-hematopoietic cells in the liver are not the main producers of the aforementioned pro-inflammatory mediators during LM infection.

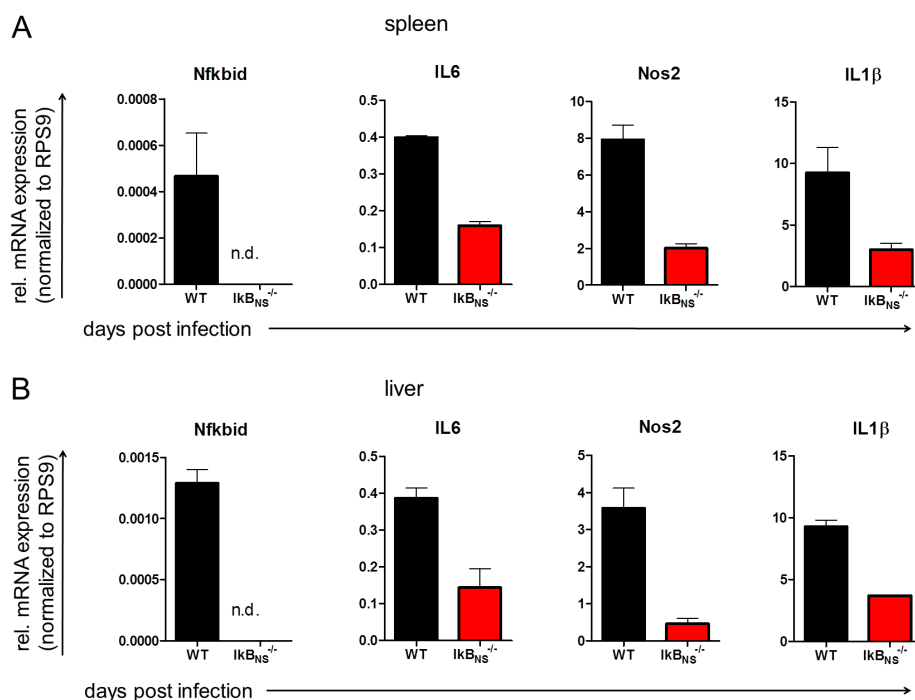


Figure 36: Expression of inflammatory mediators by inflammatory monocytes sorted from spleen and livers of WT and IkB_{NS} ^{-/-} mice on day 3 post LM infection. WT (■, n=5) and IkB_{NS} ^{-/-} (■, n=5) mice were infected with 10^5 CFU LM per mouse and were sampled on day 3 post infection. Cells from spleens and livers were isolated, pooled per mouse group to obtain two independent samples representing 2 and 3 mice, antibody stained and sorted by FACS to obtain inflammatory monocytes. RNA was isolated, reversely transcribed into cDNA and used for RT-PCR for selected transcripts. Data represent relative mRNA expression level of *Nfkbid*, *IL6*, *Nos2* and *IL1 β* normalized to *Rps9* from (A) spleen samples and (B) liver samples. Data are presented as mean \pm SEM.

In summary, these results confirm the hypothesis that especially inflammatory monocytes contribute to the excessive inflammation in response to high-dose LM infection in WT animals and that this inflammatory program is impaired in $\text{I}\kappa\text{B}_{\text{NS}}$ -deficient mice. Ultimately, protection of $\text{I}\kappa\text{B}_{\text{NS}}$ -deficient mice from overwhelming inflammation might result in protection against an otherwise lethal LM infection.

To ultimately test this hypothesis, a conditional knock-out mouse line $\text{Nfkbid}^{\text{f/f1}}\times\text{LysMCre}^{\text{tg/wt}}$ harboring a specific knock-out of $\text{I}\kappa\text{B}_{\text{NS}}$ in macrophages and granulocytes (refer to chapter 2.6) was utilized. If an $\text{I}\kappa\text{B}_{\text{NS}}$ -driven inflammatory program in monocytes would indeed make significant contributions to lethality and liver pathology in high-dose LM infection, $\text{Nfkbid}^{\text{f/f1}}\times\text{LysMCre}^{\text{tg/wt}}$ mice should be less susceptible to LM compared to WT mice.

$\text{Nfkbid}^{\text{f/f1}}\times\text{LysMCre}^{\text{tg/wt}}$ mice were infected with 10^5 CFU LM per mouse and the survival was monitored over a period of 8 days post infection (Figure 37). As a WT control for normal $\text{I}\kappa\text{B}_{\text{NS}}$ expression in macrophages and granulocytes, $\text{Nfkbid}^{\text{f/f1}}\times\text{LysMCre}^{\text{wt/wt}}$ mice with floxed *Nfkbid* but lacking Cre recombinase were used.

As expected, the majority of $\text{Nfkbid}^{\text{f/f1}}\times\text{LysMCre}^{\text{wt/wt}}$ animals succumbed to the high-dose LM infection between 3-5 days post infection as already described for the $\text{I}\kappa\text{B}_{\text{NS}}$ -sufficient wild type mice in chapter 4.3.1.

While the unequivocal resistance towards high-dose LM infection prior shown for the conventional $\text{I}\kappa\text{B}_{\text{NS}}$ -deficient mice could not be confirmed (i.e. only 18% of high-dose LM infected conditional $\text{Nfkbid}^{\text{f/f1}}\times\text{LysMCre}^{\text{tg/wt}}$ survived the infection), the onset of death is markedly delayed in animals lacking $\text{I}\kappa\text{B}_{\text{NS}}$ specifically in macrophages and granulocytes. On day 3 post LM infection, only 66% of $\text{Nfkbid}^{\text{f/f1}}\times\text{LysMCre}^{\text{wt/wt}}$ mice were still alive, compared to 91% of $\text{Nfkbid}^{\text{f/f1}}\times\text{LysMCre}^{\text{tg/wt}}$ mice that survived the infection until this point in time. The same holds true for day 4 post infection where already 50% of the $\text{Nfkbid}^{\text{f/f1}}\times\text{LysMCre}^{\text{wt/wt}}$ had succumbed from the infection whereas 82% of the $\text{Nfkbid}^{\text{f/f1}}\times\text{LysMCre}^{\text{tg/wt}}$ were still alive. Despite the obvious delay in lethality of mice lacking $\text{I}\kappa\text{B}_{\text{NS}}$ in macrophages and granulocytes, both survival curves drop dramatically on day 5 post infection ($\text{Nfkbid}^{\text{f/f1}}\times\text{LysMCre}^{\text{wt/wt}}$: 16% alive, $\text{Nfkbid}^{\text{f/f1}}\times\text{LysMCre}^{\text{tg/wt}}$: 23% alive). Of note, remaining animals survived and regained body weight independent of the genotype.

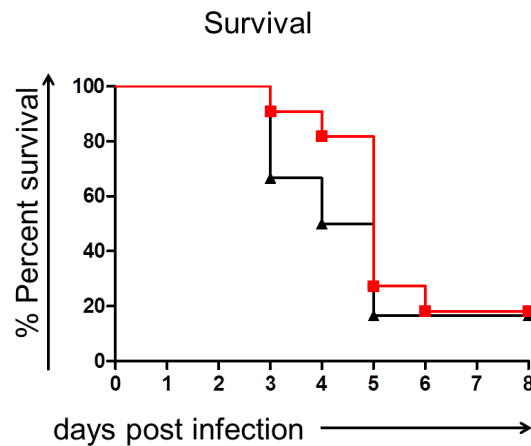


Figure 37: Survival of conditional knock-out mice harboring a specific deletion of I κ B_{NS} in macrophages and granulocytes following high-dose *Listeria* infection. Nfkbid^{fl/fl} x Cre^{wt/wt} (\blacktriangle , n= 6) and Nfkbid^{fl/fl} x Cre^{tg/wt} (\blacksquare , n= 11) mice were infected i.v. with a high-dose (10^5 CFU) of *Listeria* and daily monitored. Survival data are presented as Kaplan-Meier-Plot.

Taken together, preliminary infection studies performed in mice lacking I κ B_{NS} in a subset of myeloid cells support the hypothesis that I κ B_{NS}-dependent induction of hyperinflammation in LM infected mice can, at least in part, be attributed to inflammatory monocytes. Moreover, whole genome transcriptional profiling revealed that I κ B_{NS} is especially important in the regulation of inflammation-associated genes upon LM infection. Overall, the second part of this thesis revealed that I κ B_{NS} plays a detrimental role in high-dose LM infection by supporting the induction of pro-inflammatory genes resulting in the exaggerated release of inflammatory mediators from innate immune cells, which promote hyperinflammation, severe immunopathology and eventually death of WT mice. Lack of I κ B_{NS} obviously results in curbing of the inflammatory signaling cascade which is beneficial to the host in as much as it prevents hyperinflammation and thus protects the mice from fatal course of high-dose LM infection.

5. Discussion

The immune system is the host's defense system comprising cellular and molecular processes and a complex interplay between innate and adaptive immunity that protects against pathogens and diseases. Immune responses are subjected to strict regulation processes. The transcription factor NF- κ B is involved in a variety of cellular immune regulation processes in innate as well as adaptive immunity. Therefore, a tight regulation of NF- κ B is necessary. Regulation of NF- κ B is governed by classical and atypical inhibitory proteins. The atypical inhibitory protein I κ B_{NS} can act as activator as well as suppressor of NF- κ B mediated gene expression. In the present study the impact of I κ B_{NS} on the activation of effector CD4⁺ and CD8⁺ T cells *in vitro* and *in vivo* during systemic LM infection was addressed. Moreover, the general role of I κ B_{NS} in innate immunity during LM infection was characterized in more detail.

The present study revealed that I κ B_{NS} indeed has an impact on the antigen-specific activation of T cells in LM infection. In the chosen experimental setting antigen-specific CD8⁺ T cells exhibit only a slight delay in their activation when I κ B_{NS} is missing. In contrast to this, I κ B_{NS} is indispensable for the activation and proliferation of antigen-specific CD4⁺ T cells.

Interestingly, the analysis of the overall immune response during high-dose LM infection of WT and conventional I κ B_{NS}^{-/-} mice revealed that the presence of I κ B_{NS} is detrimental for the course of the infection. Mice lacking I κ B_{NS} showed an overall blunted inflammatory immune response, which conferred resistance to and survival of the otherwise lethal LM infection.

5.1 Impact of I κ B_{NS} on antigen-specific T cell activation

Initially, the impact of I κ B_{NS} on antigen-specific T cell activation was analyzed *in vitro* using transgenic mouse lines as donors for T cells recognizing OVA model antigens.

Though in the literature reports can be found that already described I κ B_{NS} function in T cells, attention has to be paid when these studies are compared to each other, since they differ in their experimental setups, readouts and biological background of the T cells.

Touma and colleagues analyzed the proliferative capacity of polyclonal I κ B_{NS}-deficient thymocytes and lymph node (LN)-derived CD4⁺ and CD8⁺ T cells in response to stimuli such as plate-bound α CD3 and plate-bound α CD3+ α CD28, respectively, which results in TCR crosslinking or in response to agents such as PMA/ionomycin that do not directly act through TCR ligation. In both settings I κ B_{NS}-deficient and WT T cells were stimulated in the presence of irradiated WT splenocytes and the proliferation was measured by [³H] thymidine incorporation. They observed significantly reduced proliferation of I κ B_{NS}-deficient thymocytes, as well as LN-derived CD4⁺ and CD8⁺ T cells compared to their WT counterparts. I κ B_{NS}-deficient thymocytes and LN-derived CD8⁺ T cells showed also a reduced secretion of IL2 and IFN γ in response to α CD3 and α CD3+ α CD28. Reduced proliferation was less pronounced upon PMA/ionomycin stimulation or by addition of exogenous IL2 (Touma et al., 2007). In addition to antigen-unspecific T cell stimulation, they performed studies with cognate antigen stimulation. For this I κ B_{NS}^{-/-} mice were crossed to TCR-transgenic mice expressing a TCR specific for vesicular stomatitis virus nuclear octapeptide (N52-59, VSV8) presented on MHC class I molecule

H 2k^b. Thymocytes and LN-derived CD8⁺ T cells were tested for proliferative response to peptide-loaded, irradiated splenocytes by [³H] thymidine incorporation. Again, they observed a reduced proliferation of thymocytes and LN-derived CD8⁺ T cells in the absence of I κ B_{NS} (Touma et al., 2007).

Surprisingly, the overall reduced proliferation of I κ B_{NS}-deficient T cells could not be completely confirmed in frame of this thesis. AutoMACS isolated OVA-specific CD4⁺ and CD8⁺ T cells were co-cultured with irradiated syngeneic WT splenocytes and stimulated with OT-I/OT-II peptides, or as a control, were agonistically stimulated with α CD3+ α CD28. Surprisingly, the results from the α CD3+ α CD28 stimulation differed from those stated in the publication by Touma. In the current study, no differences between both I κ B_{NS} genotypes regarding proliferation, CD44, CD25 and IFN γ expression in case of CD4⁺ T cells were detected. In contrast, I κ B_{NS}-deficient CD8⁺ T cells did show significantly reduced proliferation towards α CD3+ α CD28 treatment as well as reduced CD44 and CD25 expression compared to WT CD8⁺ T cells, whereas IFN γ secretion was not affected (refer to section 4.1). Thus, especially I κ B_{NS}^{-/-} CD4⁺ T cells clearly responded different to *in vitro* mitogenic stimulation, while mitogen stimulated I κ B_{NS}^{-/-} CD8⁺ T cells differed in IFN γ production when compared to Touma and colleagues. To better integrate *in vitro* T cell results from this study into knowledge from published data, a closer comparison of the underlying experimental conditions and readouts is needed.

One major difference to the data published by Touma et al. is the concentration of α CD3+ α CD28 used in the present thesis. In case of α CD3 a 20-fold and in case of α CD28 a 10-fold lower concentration was used compared to Touma and colleagues. The fact that the strength of TCR ligation and co-stimulation in general has major impact on the extent and quality of the subsequent proliferation of effector T cell responses is very well known. Strong stimulation prolongs the TCR signaling, whereas weak stimulation results in delayed T cell responses (Corse et al., 2011).

However, since with the relatively low α CD3+ α CD28 concentrations used in this thesis WT and I κ B_{NS}^{-/-} CD4⁺ T cells showed more than 80% proliferation, the chosen stimulus is obviously sufficient to activate them and higher concentrations are not necessarily needed. The question if and how I κ B_{NS} influences the cellular response to mitogenic TCR-ligation in CD4⁺ and CD8⁺ T cells cannot be answered in general, but rather may depend on the strength of the applied TCR trigger.

With this notion in mind, the results from the peptide-specific *in vitro* stimulations can be interpreted in a broader sense. In the present thesis, no differences between both I κ B_{NS} genotypes neither in OT-II-derived CD4⁺ T cells nor in OT-I-derived CD8⁺ T cells were observed, when stimulated with the cognate OVA peptides. This is again in direct contrast to the results from Touma and colleagues.

Since Touma and colleagues used a completely different model-antigen in conjunction with a different transgenic mouse model as source for peptide-specific T cells, it is difficult to compare their results to the ones in section 4.1. Touma's use of peptide-pulsed irradiated APCs makes it even more difficult to say how high the effective peptide dose the T cells were actually confronted with really was. At least, it makes it difficult to compare with the peptide concentrations provided to the T cells in this study. This is even more the case, as it has been already described that the capacity of APCs to induce TCR signaling can be modulated by the affinity of the peptide:MHC II/ MHC I (pMHC) complex for a specific TCR and also by the quantity of pMHC present on the surface of APCs (van Panhuys, 2016). Thus, it

is reasonable that the effective TCR signal strength in both OVA-specific and VSV8-specific transgenic T cells is causative for different downstream responses of TCR signaling leading to altered NF- κ B activation and ultimately to altered impact of I κ B_{NS} this process. Given the notion of I κ B_{NS}-dependent differences in CD4⁺/CD8⁺ T cell activation became visible only using higher α CD3+ α CD28 concentrations than necessary, as stated by Touma et al., it may be interesting to check escalating OVA-peptide concentrations in conjunction with OVA-specific OT-I/OT-II T cells, even though the actually chosen peptide concentrations in principle were clearly sufficient to induce fulminant T cell proliferation (refer to Figure 9 and Figure 11), which in fact does not necessarily imply a need for higher peptide amounts. Anyway, it might also be possible that proliferation measurement with [³H] thymidine incorporation as used in the Touma paper is more sensitive to detect differences between both genotypes, due to direct measurement of the extent of newly synthesized DNA compared to analysis of CFSE dilution. Nevertheless, the used OT-I/OT-II transgenic mouse model is a well-established antigen-specific T cell model and due to the fact, that CD4⁺ and CD8⁺ T cells derived from OT-II and OT-I transgenic mice are generally able to respond to the cognate antigen in the present thesis, understanding of the exact reasons for the conflicting observations between the work of Touma and this study require more complex but defined *in vitro* stimulation assays e.g. using a broader range of peptide-concentrations. On the other hand the relevance of observable I κ B_{NS}-dependent differences within T cells under non-physiological peptide-specific TCR-stimulation conditions *in vitro* is questionable.

To circumvent many of the known and unknown experimental factors influencing *in vitro* T cell activation and proliferation, the present thesis focused mainly on the impact of I κ B_{NS} on *in vivo* CD4⁺ and CD8⁺ T cell activation with recombinant LM-OVA as physiological stimulus. Surprisingly and in contrast to the expectations raised by the *in vitro* data, the adoptive transfer of I κ B_{NS}-deficient OT-II CD4⁺ T cells into LM-OVA infected C57BL/6 mice revealed a significantly reduced proliferation and significantly impaired expression of CD44, CD25 as well as IFN γ and IL2 on day 5 post infection compared to adoptively transferred WT OT-II CD4⁺ T cells. This is interesting in as much as *in vitro* stimulation of OT-II-derived CD4⁺ T cells revealed no genotype-dependent differences upon antigen-specific stimulation. This highlights the overall importance of the experimental setting. In general, several aspects in the adoptive transfer model may influence the experimental outcome such as adoptive transfer of donor cells into recipient mice prior or after LM-OVA infection. However, transferring the cells before LM-OVA infection of recipient mice has the advantage that the transferred cells find a natural “steady state” environment. In case of infection prior T cell transfer, it cannot be excluded that the transferred cells get already primed through an inflammatory environment of the host’s immune system before they had the chance to naturally spread throughout the entire host. Given this notion, this may otherwise mask possible effects of I κ B_{NS} on the antigen-specific T cell activation. A second important factor is the sampling time. In the present thesis, day 3, 5 and 7 were selected for re-analysis of the transferred OVA-specific WT or I κ B_{NS}^{-/-} CD4⁺ T cells to ensure antigen encountering in infected organs and draining lymph nodes and sufficient priming of the transferred T cells. Obviously, day 3 post infection was too early for the re-analysis. Here, only transferred CFSE^{high} WT and I κ B_{NS}^{-/-} OT-II CD4⁺ T cells were detected in spleen and liver which did not underwent

proliferation yet. Moreover, only very few cells were recovered from livers, whereas on day 5 post infection huge numbers of proliferated OVA-specific T cells were recovered from livers and spleens, which might also be indicative for an infection-related re-migration of the transferred cells to the main replication sites of LM. Interestingly, on day 7 post infection fewer cells than on any other day post infection were re-covered from spleens and livers of recipient mice. Thus, it might be possible that on this particular point in time the transferred cells were already in the contraction phase or migrated out from spleen and liver into the periphery.

The obvious difference between *in vitro* and *in vivo* analysis of OVA-specific CD4⁺ T cell responses in dependency of I κ B_{NS} may be explained by the fact that in an *in vivo* situation more complex variables influence the strength of TCR stimulation such as TCR-pMHC binding partners, rare encounter of T cells and antigen-bearing APCs which affects the stability of pMHC complexes, as well as antigen-persistence within lymphoid organs. All of those parameters are less decisive for optimal TCR stimulation in *in vitro* systems (Corse et al., 2011).

One of the most important observations of the present thesis is that the Th1 CD4⁺ effector T cell differentiation is significantly impaired in the absence of I κ B_{NS} as indicated by reduced proliferation and reduced expression of CD44, IL2 and IFN γ of I κ B_{NS}^{-/-} OT-II CD4⁺ T cells in response to LM-OVA.

Prior studies already described an impact of I κ B_{NS} on differentiation into certain CD4⁺ T cell subsets. For instance, Annemann and colleagues performed adoptive transfers in a DSS-induced colitis model with injection of CD4⁺CD25⁻ T cells from WT and I κ B_{NS}^{-/-} mice i.p. into RAG1^{-/-} recipient mice. They observed significantly increased colon damage in RAG1^{-/-} mice that received I κ B_{NS}^{-/-} CD4⁺CD25⁻ T cells compared to mice that received WT cells. Moreover, they demonstrated a blunted formation of Th17 differentiation indicated by a significantly reduced induction of IL17A⁺IFN γ ⁻ and IL17A⁻IFN γ ⁺ T cells resulting in enhanced susceptibility to colitis. To further confirm these observations, they analyzed T cell proliferation under specific Th-polarizing conditions *in vitro*. Indeed, I κ B_{NS}^{-/-} Th17 cells showed reduced proliferation compared to their WT counterparts leading to the conclusion that I κ B_{NS} appears to be involved in the regulation of Th17 differentiation (Annemann et al., 2015).

Moreover, Schuster and colleagues described I κ B_{NS} as a regulator of Treg cell development by regulation of Foxp3, the master transcription factor for Treg development. By performing native chromatin immunoprecipitation (ChIP) of stimulated WT and I κ B_{NS}^{-/-} CD4⁺CD25⁻ T cells, they observed binding of I κ B_{NS} to the Foxp3 promoter and more specifically to the conserved non-coding sequence 3 (CNS3). Additional pull-down experiments revealed binding of I κ B_{NS}, cRel and p50 to the single kB site of CNS3. Moreover, they showed that I κ B_{NS}-deficient mice exhibit a 50% reduction of mature Tregs, thus, they concluded from their results that binding of I κ B_{NS} to the Foxp3 promoter is necessary for full transcriptional activation of the *Foxp3* locus (Schuster et al., 2012).

A similar set-up would also be useful, to identify the possible mechanism resulting in the impaired Th1 CD4⁺ effector T cell differentiation observed in the present thesis. One option would be to directly analyze the induction of Tbet, the master transcription factor for Th1 cell differentiation, in stimulated OT-II-derived WT and I κ B_{NS}^{-/-} CD4⁺ T cells. One could perform ChIP analyzes to evaluate if I κ B_{NS} together with NF- κ B subunits binds to kB sites in the promoter of the *Tbet* gene locus. This would provide insights into how I κ B_{NS} is involved in Th1 CD4⁺ T effector cell differentiation, which was clearly

shown to be impaired in adoptively transferred OT-II-derived $\text{I}\kappa\text{B}_{\text{NS}}^{-/-}$ CD4^{+} T cells in LM-OVA infected C57BL/6 mice.

In case of *in vivo* stimulation of OT-I-derived WT and $\text{I}\kappa\text{B}_{\text{NS}}^{-/-}$ CD8^{+} T cells a different outcome than with OT-II-derived CD4^{+} T cells was observed. Surprisingly, the results suggest that $\text{I}\kappa\text{B}_{\text{NS}}$ is dispensable for the proliferation of adoptively transferred CD8^{+} T cells in LM-OVA infected recipients. No genotype-dependent differences were detected regarding proliferation on day 3 and day 5 post infection in spleens and livers (see Figure 19). Moreover, the expression of CD44, $\text{IFN}\gamma$ and IL2 in OVA-specific CD8^{+} T cells was not affected by the absence of $\text{I}\kappa\text{B}_{\text{NS}}$. This was quite unexpected, since Touma and colleagues described reduced proliferation, IL2 and $\text{IFN}\gamma$ expression of $\text{I}\kappa\text{B}_{\text{NS}}^{-/-}$ CD8^{+} T cells upon *in vitro* stimulation (Touma et al., 2007). Additionally, the results from the present thesis revealed that the antigen-specific *in vitro* stimulation of OT-I $\text{I}\kappa\text{B}_{\text{NS}}^{-/-}$ CD8^{+} T cells led to reduced $\text{IFN}\gamma$ secretion compared to OT-I WT CD8^{+} T cells, leading to the expectation that this would also hold true for the *in vivo* setting. However, it is important to note that even in OT-I WT CD8^{+} T cells the frequencies of $\text{IFN}\gamma^{+}$ cells were rather low *in vitro* (~20%) compared to the frequencies obtained in the *in vivo* setting (>90%). It has been already described that naïve CD8^{+} T cells failed to synthesize sufficient amounts of $\text{IFN}\gamma$ *in vitro* upon exposure to the cognate antigen, but when challenged *in vivo* in a natural microenvironment with physiological costimulatory signals, $\text{IFN}\gamma$ can be rapidly induced (Hosking et al., 2014). Thus, it might be possible that $\text{I}\kappa\text{B}_{\text{NS}}$ has a minor impact on the $\text{IFN}\gamma$ production of CD8^{+} T cells, which becomes only detectable under certain conditions such as weak TCR signaling strength, but upon *in vivo* antigen encounter with costimulatory signals and strong TCR signaling strength this impact becomes negligible and can be rescued.

Another surprising aspect of the present work was the rather low expression of IL2 on day 3 and day 5 post infection of both OT-I WT and $\text{I}\kappa\text{B}_{\text{NS}}^{-/-}$ CD8^{+} T cells recovered from spleens and livers of LM-OVA infected recipients. Normally, IL2 is synthesized by T cells and promotes further T cell expansion and effector T cell differentiation after initial activation through TCR signaling (Cho et al., 2013). Due to high genotype-independent frequencies of both $\text{CD44}^{\text{high}}$ and $\text{IFN}\gamma^{+}$ CD8^{+} T cells on day 3 and day 5 post infection, it can be assumed that CD8^{+} T cells were, despite the reduced IL2 secretion, able to develop effector functions. It might be possible that *in vivo* endogenous IL2 produced by other immune cell types of the infected host is consumed out of the cellular microenvironment by the CD8^{+} T cells resulting in their effector differentiation without further need to synthesize it on their own.

However, the most obvious *in vivo* differences between both genotypes of OVA-specific CD8^{+} T cells were observed regarding the expression of CD25, PD1 and $\text{TNF}\alpha$. On day 3 post infection significantly more CD25^{+} and $\text{TNF}\alpha^{+}$ as well as significantly fewer PD1^{+} OVA-specific $\text{I}\kappa\text{B}_{\text{NS}}^{-/-}$ CD8^{+} T cells were detected compared to WT CD8^{+} T cells. On day 5 post infection the frequencies of CD25^{+} and PD1^{+} OVA-specific CD8^{+} T cells were comparable between both genotypes and were in general rather low, whereas $\text{TNF}\alpha$ was still more prominent on OVA-specific $\text{I}\kappa\text{B}_{\text{NS}}^{-/-}$ CD8^{+} T cells compared to WT counterparts. When considering the CD25 activation marker, Mannering and colleagues showed that upon polyclonal T cell activation during LM infection increased numbers of CD25^{+} CD4^{+} and CD8^{+} T

cells are detectable, which peak on day 4 post infection and returned to normal levels by day 7 post infection. Though early expression of CD25 was matched with strong proliferation of T cells, the proliferation also continued after the loss of CD25 expression (Mannering et al., 2002).

Due to the fact that in this study OVA-specific CD8⁺ T cells of both genotypes showed extensive proliferation on day 3 and day 5 post infection and alongside reduced frequencies of CD25⁺ cells on day 5 post infection, it might be reasonable that OT-I-derived WT CD8⁺ T cells are activated faster and already reach their peak in CD25 expression earlier. Thus on day 3 post infection, they might have already down-regulated CD25 expression to normal levels, whereas in OT-I-derived $\text{I}\kappa\text{B}_{\text{NS}}^{-/-}$ CD8⁺ T cells CD25 is still highly expressed. Another result which is well in line with this notion is the transient expression of PD1 on OT-I WT CD8⁺ T cells. A transient expression of PD1 was shown to be initiated upon T cell activation, whereas sustained expression is a classical marker of T cell exhaustion (Catakovic et al., 2017). The transient PD1 expression on WT CD8⁺ T cells compared to only marginal frequencies of PD1⁺ $\text{I}\kappa\text{B}_{\text{NS}}^{-/-}$ CD8⁺ T cells on both days (3 and 5) post infection might indicate that the activation is not as efficient as in WT CD8⁺ T cells.

The hypothesis of a marginally delayed activation program of CD8⁺ T cells in absence of $\text{I}\kappa\text{B}_{\text{NS}}$ is also supported by the result that in spleens of LM-OVA infected recipients that received OVA-specific $\text{I}\kappa\text{B}_{\text{NS}}^{-/-}$ CD8⁺ T cells significantly more bacteria were found on day 3 post infection compared to mice having received OVA-specific WT CD8⁺ T cells. However, this difference in pathogen control was gone on day 5 post infection as the main differences regarding the expression of activation markers were gone as well at this point in time.

In case of the elevated frequencies of TNF α ⁺ OT-I $\text{I}\kappa\text{B}_{\text{NS}}^{-/-}$ CD8⁺ T cells on day 3 and 5 post infection compared to OT-I WT CD8⁺ T cells (see Figure 20C and Figure 21C) one might speculate that $\text{I}\kappa\text{B}_{\text{NS}}$ acts as suppressor of this pro-inflammatory cytokine. Sierra-Mondragón and colleagues analyzed the dynamic regulation of NF- κ B in the uterus of mice throughout the estrous cycle and found TNF α expression to be regulated by $\text{I}\kappa\text{B}_{\text{NS}}$. More specifically, they found an inverse relationship between TNF α expression and presence of $\text{I}\kappa\text{B}_{\text{NS}}$ and Bcl-3 (Sierra-Mondragón et al., 2015).

In summary, the obtained results revealed that $\text{I}\kappa\text{B}_{\text{NS}}$ has a differential impact on antigen-specific activation and proliferation of CD4⁺ and CD8⁺ T cells, which is highly dependent on the experimental set-up (*in vitro* vs. *in vivo* stimulation). Whereas $\text{I}\kappa\text{B}_{\text{NS}}$ is dispensable for activation and proliferation of *in vitro* stimulated CD4⁺ T cells, it is strongly involved in the CD4⁺ Th1 effector cell differentiation in an *in vivo* infection setting. As future prospects one could choose different *in vivo* infection models, which mainly triggers Th2-mediated CD4⁺ T cell responses (e.g. *Toxoplasma gondii*, *Leishmania*) to elucidate if $\text{I}\kappa\text{B}_{\text{NS}}$ -deficiency as well affects Th2 differentiation. Moreover, one could address the impact of $\text{I}\kappa\text{B}_{\text{NS}}$ on pathogen-specific T cell responses to a pathogen that induces organ-specific local infections and does not cause systemic infections.

5.2 The role of I κ B_{NS} in the immune response against *Listeria monocytogenes*

The second part of the present thesis describes the impact of I κ B_{NS} on innate immune responses towards systemic bacterial LM infection. WT and conventional I κ B_{NS}^{-/-} mice were infected with LM (10⁵ CFU/mouse) and detailed analyses regarding the early immune response were performed and compared between both genotypes.

Strikingly, a strong resistance of I κ B_{NS}-deficient mice against the otherwise lethal LM infection was observed while the WT animals succumbed to the infection within 4- 6 days post infection, indicating that especially an altered innate immune response contributes to the observed phenotype.

In a first step, the bacterial burden was determined in the main replication sites, liver and spleen to evaluate if I κ B_{NS} in immune cells has an impact on pathogen clearance. Interestingly, excessive bacterial load is not the decisive factor for the early death of WT mice. Both genotypes showed equally high bacterial burden in the respective organs, indicating that the improved survival is not due to a better pathogen control early on during infection (Figure 25).

This suggests that the resistance of I κ B_{NS}^{-/-} mice is dependent on major differences in the nature of immune cell responses and/or immunopathology caused by them. Genotype-dependent histopathological differences in the liver 4 days post LM infection (section 4.3.3) even more underline this notion. Histological examination revealed significant lymphocyte depletion in both genotypes, which matched with the FACS-based analysis of the cellular composition in the infected tissues (section 4.3.7). Here, a clear reduction of T cells, B cells and NK cells became obvious during the course of infection in both livers and spleens. This observation is confirmed by Merrick and colleagues who also found massive lymphocyte apoptosis at sites where macrophages and neutrophils infiltrate and coincide with the presence of LM. Alongside, they also histologically described necrotic foci and a massive infection of lymphoid organs that is accompanied by a massive apoptosis-induced death of lymphocytes (Merrick et al., 1997).

A definite hint towards an altered cellular immune response between WT and I κ B_{NS}^{-/-} mice in this study, is the huge number of cellular infiltrates histopathologically observed in liver samples of WT mice on day 4 post infection, which was far less pronounced in I κ B_{NS}^{-/-} mice. These results are indicative for pronounced immune-cell-mediated immunopathology in WT mice in response to LM infection which is blunted when I κ B_{NS} is missing. As the FACS-based cell influx analysis clearly shows that by day 3 post infection the myeloid compartment dominates the immune cell composition and I κ B_{NS} is relatively high expressed in myeloid cells, it is tempting to attribute an altered cellular immune response in I κ B_{NS}^{-/-} mice to myeloid cells and to speculate that presence of I κ B_{NS} in WT myeloid cells has a detrimental impact on their capacity to promote immunopathology in liver and spleen.

Secretion of pro-inflammatory mediators by immune cell subsets can significantly contribute to the development of severe immunopathology. To gain deeper insights in the gene regulation of response genes to the LM infection and to identify these mediators, which are regulated most prominently during infection, microarray analyses are useful.

To address, which host immune factors are mainly contributing to the severe outcome of LM infection, Ng and colleagues in 2005 performed gene expression profiles from liver and blood samples of BALB/c mice infected with graded doses of LM to evaluate genes that are contributing to the severity

of infection and thereby to provide information regarding the molecular mechanisms and to identify early biomarker (Ng et al., 2005). For example, they described 4 regulated genes, which were found in a class prediction model (*Saa3*, *Tgtp*, *Ifi47* and *Cxcl9*). Indeed, those mentioned genes were also found to be regulated in the present thesis, whereas especially *Saa3* is highly up-regulated in WT mice on day 4 post infection compared to $\text{I}\kappa\text{B}_{\text{NS}}^{-/-}$ mice (FC WT: 64, FC $\text{I}\kappa\text{B}_{\text{NS}}^{-/-}$: 47). *Saa3* belongs to the family of acute phase proteins that are released during liver injury and inflammation (Zhang et al., 2005). Moreover, Hatanaka and colleagues described that serum amyloid A (SAA) stimulates the expression and release of TNF α from cultured human blood neutrophils and monocytes (Hatanaka et al., 2004). This also matches the elevated levels of TNF α mRNA expression found in livers of WT mice on day 4 post infection (ref. Figure 27B) compared to $\text{I}\kappa\text{B}_{\text{NS}}^{-/-}$ mice. This might be a direct consequence of the elevated levels of serum amyloid A in WT mice which in turn triggers the expression of TNF α from recruited immune cell subsets.

Especially TNF α is known to be a major mediator of acute inflammatory responses and is induced by inflammatory cytokines and bacterial products (Streetz et al., 2001). It is also known that an uncontrolled release of TNF α is associated with severity of infections and inflammatory processes and with systemic septic complications (Hatanaka et al., 2004). Indeed, the high expression levels of TNF α in liver samples of WT mice could be a hint that WT mice succumb from septic shock due to the hyper-inflammation in response to high-dose LM infection.

Another candidate, which was found to be differentially regulated in the microarray analysis of both $\text{I}\kappa\text{B}_{\text{NS}}$ genotypes is *Irak3* (also known as *Irak-M*) belonging to the interleukin-1 receptor-associated kinases (IRAK). This specific class of kinases is involved in the negative regulation of TLR signaling that occupies a crucial role in the activation of macrophages upon first encounter of the immune system with pathogens (Kobayashi et al., 2002).

Hoogerwerf and colleagues described that IRAK-M-deficient mice demonstrate an improved host defense during pneumonia caused by the gram-negative bacterium *Klebsiella pneumonia* that commonly causes sepsis (Hoogerwerf et al., 2012). They showed an up-regulation of IRAK-M mRNA in lungs of WT mice and that the absence of IRAK-M resulted in a strongly improved host defense reflected by a reduced bacterial growth in lungs, diminished dissemination to distant body sites and with less peripheral tissue injury and better survival rates in response to *Klebsiella pneumonia* infection (Hoogerwerf et al., 2012).

The array analysis of the present thesis revealed that *Irak3* is induced to a lesser extent on day 4 post infection in livers of $\text{I}\kappa\text{B}_{\text{NS}}^{-/-}$ mice compared to WT mice (FC WT: 6.4, FC $\text{I}\kappa\text{B}_{\text{NS}}^{-/-}$: 3.0). Since it has been described that *Irak3* expression is regulated by NF- κ B (Janssens et al., 2003), it might be possible that the NF- κ B-induced expression of *Irak3* additionally relies on $\text{I}\kappa\text{B}_{\text{NS}}$ as a co-factor. In the liver of $\text{I}\kappa\text{B}_{\text{NS}}$ -deficient mice it is expressed to a lesser extent in all analyzed points in time compared to WT mice. In conjunction with the study of Hoogerwerf and colleagues, where the absence of IRAK-M leads to an improved host defense and less peripheral tissue injury in response to *Klebsiella pneumonia* infection, one can speculate that dampened levels of *Irak3* in $\text{I}\kappa\text{B}_{\text{NS}}$ -deficient mice contributes to a blunted inflammatory response and also to less severe immunopathology in liver and spleen (refer to Figure 26).

Moreover, the transcriptome analyses revealed that most of the known guanylate binding proteins (Gbp) were induced in response to LM infection in both $I\kappa B_{NS}$ genotypes, though nearly all identified members of this protein family (*Gbp2*, *Gbp4*, *Gbp5*, *Gbp8*, *Gbp9* and *Gbp11*) were up-regulated to a greater extent in WT mice. In general, the IFN γ -inducible Gbps are beneficial for the host's defense against invading pathogens by orchestrating oxidative and vesicular trafficking processes and by delivering antimicrobial peptides to autophagolysosomes (Kim et al., 2011). *Gbp1*, *Gbp6*, *Gbp7* and *Gbp10* were shown to confer cell-autonomous immunity to listerial or mycobacterial infection within macrophages (Kim et al., 2011). Since Gbps are inducible by IFN γ -signaling, it is important to note that WT mice indeed exhibited elevated levels of IFN γ in the liver on day 4 post infection (refer to Figure 27B). Since IFN γ levels in the liver were reduced in $I\kappa B_{NS}^{-/-}$ animals at the same time, this might explain the overall reduced expression of Gbp proteins in these mice.

In summary, the comparative genome-wide transcriptome analysis indicates that in livers of the LM infected WT mice a hyperinflammation occurs, which is likely to be the principle reason for the severe outcome of LM infection. Interestingly, $I\kappa B_{NS}$ -deficient mice show a dampened form of the inflammation, which is in turn beneficial for infection outcome.

Important to note, all identified differentially regulated genes in both genotypes are not necessarily a direct consequence of $I\kappa B_{NS}$ interaction with NF- κ B complexes on κ B sites in the promoter regions of the found genes. This is because gene regulation observed by microarray analysis may be also the result of secondary or tertiary signaling circuits in which NF- κ B might not necessarily be involved.

Instead it is more likely that observed transcriptional alterations are the result of a mixture of direct $I\kappa B_{NS}$ -influences in conjunction with NF- κ B complexes and more indirect influences in which lack of $I\kappa B_{NS}$ leads to altered transcription of for example signaling components. In consequence, certain signaling cascades may work less efficient than they should, though the target genes of such a signaling cascade might not be influenced by $I\kappa B_{NS}$ interference with their promoter regions at all. On the other hand, if a target gene has dedicated κ B-sites, responsible for its regulation by NF- κ B transcription factors, does not automatically mean that indeed $I\kappa B_{NS}$ is involved in modification of this gene regulatory feature. Thus, the exact mechanistical contributions of $I\kappa B_{NS}$ to the observed genotype-dependent transcriptional alterations in the liver remain difficult to dissect.

To overall conclude the impact of $I\kappa B_{NS}$ on the observed phenotype the mRNA expression of $I\kappa B_{NS}$ itself was determined in hematopoietic (CD45⁺) and non-hematopoietic (CD45⁻) liver cell fractions of LM infected WT mice (refer to section 4.3.6). Of note, it has been described in a comprehensive RNA-seq of mouse tissues that $I\kappa B_{NS}$ is comparatively low expressed in liver compared to spleen or thymus (Yue et al., 2014). Despite this fact, it is even more interesting, that in both liver cell fractions a robust $I\kappa B_{NS}$ expression was detected in the steady state and still on day 1 post infection. Strikingly, $I\kappa B_{NS}$ expression significantly drops down on day 2 post infection. This observation has a special meaning in the context of the observed transcriptional differences seen in the microarray analysis and shows in the course of LM infection a time-sequential expression of $I\kappa B_{NS}$ in liver and spleen. As already described, most differences between WT and $I\kappa B_{NS}^{-/-}$ mice were observed on day 3 and day 4 post infection, suggesting that especially the drop-down of $I\kappa B_{NS}$ on day 2 post infection in WT mice may

lay the ground for the subsequent transcriptional alterations on the consecutive days. Since it can be excluded that transcriptional alterations between both genotypes are present in the steady state (see Figure 28B), all observed alterations result from the LM infection. Thus, transcriptional differences between both genotypes throughout the infection are not the result of divergent initial configurations. This highlights the idea that I κ B_{NS} only takes effect after signaling cascades and NF- κ B activation in response to the LM infection have been triggered. This mechanism might be dysregulated resulting to the observed milder hyperinflammation in I κ B_{NS}^{-/-} mice, and the other way round, leading to death of WT mice if I κ B_{NS} is present.

Regarding I κ B_{NS} expression, Schuster and colleagues showed the induction of I κ B_{NS} in the nucleus of T cells within 4 h after *in vitro* PMA/ionomycin stimulation and its disappearance after 16 h (Schuster et al., 2012).

The same was observed in *in vitro* LPS stimulated macrophages, in which I κ B_{NS} mRNA expression was strongly induced 1 h post stimulation with declining expression to low levels 5 h post stimulation (Kuwata et al., 2006). Those studies showed induction of I κ B_{NS} within short periods of time in dedicated and isolated immune cell subsets. In contrast to that, the present study shows for the first time I κ B_{NS} expression in an organ-wide manner and that it is important to follow I κ B_{NS} expression during a longer period of time especially in the context of infections to gather detailed insights about the functionality of I κ B_{NS}.

Since I κ B_{NS} expression was determined in whole organs or the entire hematopoietic cell lineage, it was reasonable to determine its expression in defined lymphoid and myeloid immune subsets in liver and spleen. For this purpose, *Nfkbid*^{lacZ} reporter mice were used (refer to section 4.3.7). Of note, it is important to know that promoter activity of the *Nfkbid* gene cannot automatically be linked to either high protein expression of I κ B_{NS} nor to actual I κ B_{NS} functionality, but gives an overall impression which cells rely on I κ B_{NS} gene expression in general. Thus, the promoter activity of the reporter construct is not directly comparable with I κ B_{NS} gene transcript expression of whole organ from WT mice (refer to section 4.3.6). The significant drop-down in I κ B_{NS} mRNA expression seen on day 2 post infection in WT mice was not observed in the reporter assay. But the most obvious results were that lymphocytes (e.g. CD4⁺ T cells, CD8⁺ T cells, B cells) showed a comparably low *Nfkbid* promoter activity. However, a slight increase of the *Nfkbid* promoter activity was detectable in CD8⁺ T cells during the course of LM infection, which matches the observation from Schuster and colleagues that especially in T cells I κ B_{NS} is inducible upon stimulation.

The most interesting finding is that especially cells of the myeloid cell lineage such as inflammatory and resident monocytes and also interstitial macrophages have the highest basal *Nfkbid* promoter activity in spleen and liver (d0). During LM infection the *Nfkbid* promoter activity of inflammatory monocytes remained at constantly high levels suggesting that I κ B_{NS} plays important roles in the biology of this subset.

Indeed, transcriptome analyses confirmed that in WT mice typical inflammatory mediators (e.g. *IL6*, *Nos2*, *Tnfrsf23* and *IL1 β*) are produced by inflammatory monocytes, but are down-regulated in the same subset from I κ B_{NS}^{-/-} mice, both in liver and spleen. Especially in inflammatory monocytes from WT mice enormous expression levels were detected for *Nos2* and *IL1 β* by real-time PCR on day 3 post

infection. On the one hand, inflammatory monocytes are necessary for the resolution of bacterial infection, but on the other hand inflammatory monocytes can be detrimental in the course of LM infection by inducing hyperinflammation (Shi and Pamer, 2011). Moreover, it has been described that during systemic LM infection Ly6C⁺ monocytes can be parasitized by LM leading to bacterial invasion into the brain. Additionally, the monocyte influx was shown to coincide with upregulation of *Ccl2* gene expression (Drevets et al., 2004). This would fit to the results of the present thesis, where especially on day 3 and day 4 bacteria were found in the brains of LM infected WT and $\text{IkB}_{\text{NS}}^{-/-}$ mice. $\text{IkB}_{\text{NS}}^{-/-}$ mice were however able to control the pathogen load in brains compared to the WT animals. Furthermore, microarray analyses of liver samples showed that *Ccl2* was highly upregulated in WT mice compared to $\text{IkB}_{\text{NS}}^{-/-}$ mice (FC WT d3 vs. d0: 8.6, WT d4 vs. d0: 8.9; FC $\text{IkB}_{\text{NS}}^{-/-}$ d3 vs. d0: 5.2, $\text{IkB}_{\text{NS}}^{-/-}$ d4 vs. d0: 2.1). Moreover, Ly6C⁺ monocytes represented the dominant cellular immune subset in livers of WT mice on day 3 post infection, whereas some seems to act as Trojan horse leading to the brain invasion of LM.

Data obtained within this present thesis clearly demonstrate the IkB_{NS} -dependent induction of an inflammatory program in inflammatory monocytes that most probably make a major contribution to the observed fatal outcome to high-dose LM infection in WT but not $\text{IkB}_{\text{NS}}^{-/-}$ mice. To further verify this hypothesis conditional KO mice ($\text{Nfkbid}^{\text{f/f1}} \times \text{LysMCre}^{\text{tg/wt}}$) harboring a specific deletion of IkB_{NS} in myeloid cells (i.e. monocytes, macrophages and neutrophils) were infected with a high-dose of LM. Though lethality was markedly delayed in $\text{Nfkbid}^{\text{f/f1}} \times \text{LysMCre}^{\text{tg/wt}}$ pointing at a partial protection from fatal hyperinflammation in these mice, the complete protection from LM infection as seen in $\text{IkB}_{\text{NS}}^{-/-}$ mice could not be confirmed and in the end only 23% of the infected $\text{Nfkbid}^{\text{f/f1}} \times \text{LysMCre}^{\text{tg/wt}}$ animals survived the infection. It is important to note that these infection studies are considered as preliminary data as only a limited number of experimental animals were included in the survey, which moreover were neither age- nor sex-matched. It has already been described that sex-dependent factors influence the susceptibility to LM infection (Pasche et al., 2005), a fact that was taken into account for all other experiments performed in frame of this thesis where otherwise only female mice were used for the *in vivo* infections. Therefore, it might be possible that the inclusion of male mice masks the effects of IkB_{NS} deletion specifically in monocytes, macrophages and neutrophils. Moreover, it has been shown that in case of monocytes, macrophages and neutrophils the *Nfkbid* promoter activity differs during the course of LM infection (refer to Figure 34 and 35) suggesting that a direct impact of IkB_{NS} on inflammatory monocyte function might be hidden by the concomitant deletion of IkB_{NS} in macrophages and neutrophils. One major drawback of the used conditional knockout mouse line is that IkB_{NS} is not only deleted in monocytes and macrophages, but as well in neutrophils. Thus, it would be more appropriate to combine the results with a conditional KO mouse strain with a specific deletion of IkB_{NS} exclusively in neutrophils and exclusively in monocytes and macrophages to verify that there is no overlay of the impact of IkB_{NS} on these different myeloid cell subsets. However, the next step in this experimental setup would be the increase of the numbers of infected $\text{Nfkbid}^{\text{f/f1}} \times \text{LysMCre}^{\text{tg/wt}}$ animals and to use age- and sex-matched animals to obtain a final conclusion about the impact of a specific deletion of IkB_{NS} in monocytes, macrophages and neutrophils.

Taken together, the results clearly indicate that I κ B_{NS} seems to be responsible for dysregulated and unbalanced immune responses especially in inflammatory monocytes leading to the observed hyperinflammation. This hyperinflammation caused by dysregulated signaling cascades and target gene regulation might be the principal reason for why WT mice succumb to the infection, whereas mice lacking I κ B_{NS} show blunted inflammatory signature leading to survival of the otherwise lethal LM infection.

As future prospects the exact molecular mechanism has to be elucidated to identify at which certain stage I κ B_{NS} leads to the dysregulation of proper signaling cascades and to identify molecular targets that are specifically influenced by I κ B_{NS} and decisive for the severe outcome of inflammation. This would render I κ B_{NS} as a potential therapeutic target for the treatment of diseases driven by hyperinflammation to prevent fatal outcomes including septic shock.

References

- Actor, Jeffrey K. (2014): T Lymphocytes. In: Jeffrey K. Actor (Hg.): *Introductory Immunology*: Elsevier, S. 42–58.
- Agace, William W. (2006): Tissue-tropic effector T cells. Generation and targeting opportunities. In: *Nature reviews. Immunology* 6 (9), S. 682–692. DOI: 10.1038/nri1869.
- Ambros, Victor (2004): The functions of animal microRNAs. In: *Nature* 431 (7006), S. 350–355. DOI: 10.1038/nature02871.
- Annemann, Michaela; Wang, Zuobai; Plaza-Sirvent, Carlos; Glauben, Rainer; Schuster, Marc; Ewald Sander, Frida et al. (2015): IkbNS regulates murine Th17 differentiation during gut inflammation and infection. In: *Journal of immunology (Baltimore, Md. : 1950)* 194 (6), S. 2888–2898. DOI: 10.4049/jimmunol.1401964.
- Arase, H.; Saito, T.; Phillips, J. H.; Lanier, L. L. (2001): Cutting Edge. The Mouse NK Cell-Associated Antigen Recognized by DX5 Monoclonal Antibody is CD49b (2 Integrin, Very Late Antigen-2). In: *The Journal of Immunology* 167 (3), S. 1141–1144. DOI: 10.4049/jimmunol.167.3.1141.
- Armstrong, S. G.; Renton, K. W. (1994): Factors involved in the down-regulation of cytochrome P450 during *Listeria monocytogenes* infection. In: *International journal of immunopharmacology* 16 (9), S. 747–754.
- Auffray, Cedric; Sieweke, Michael H.; Geissmann, Frederic (2009): Blood monocytes. Development, heterogeneity, and relationship with dendritic cells. In: *Annual review of immunology* 27, S. 669–692. DOI: 10.1146/annurev.immunol.021908.132557.
- Austyn, J. M.; Gordon, S. (1981): F4/80, a monoclonal antibody directed specifically against the mouse macrophage. In: *European journal of immunology* 11 (10), S. 805–815. DOI: 10.1002/eji.1830111013.
- Au-Yeung, Byron B.; Smith, Geoffrey Alexander; Mueller, James L.; Heyn, Cheryl S.; Jaszczak, Rebecca Garrett; Weiss, Arthur; Zikherman, Julie (2017): IL-2 Modulates the TCR Signaling Threshold for CD8 but Not CD4 T Cell Proliferation on a Single-Cell Level. In: *Journal of immunology (Baltimore, Md. : 1950)* 198 (6), S. 2445–2456. DOI: 10.4049/jimmunol.1601453.
- Baaten, Bas Jg; Li, Cheng-Rui; Bradley, Linda M. (2010): Multifaceted regulation of T cells by CD44. In: *Communicative & integrative biology* 3 (6), S. 508–512. DOI: 10.4161/cib.3.6.13495.
- Bajnok, Anna; Ivanova, Maria; Rigó, János; Toldi, Gergely (2017): The Distribution of Activation Markers and Selectins on Peripheral T Lymphocytes in Preeclampsia. In: *Mediators of inflammation* 2017, S. 8045161. DOI: 10.1155/2017/8045161.
- Bamburg, James R. (2011): *Listeria monocytogenes* cell invasion. A new role for cofilin in co-ordinating actin dynamics and membrane lipids. In: *Molecular microbiology* 81 (4), S. 851–854. DOI: 10.1111/j.1365-2958.2011.07759.x.
- Becher, Burkhard; Schlitzer, Andreas; Chen, Jinmiao; Mair, Florian; Sumatoh, Hermi R.; Teng, Karen Wei Weng et al. (2014): High-dimensional analysis of the murine myeloid cell system. In: *Nature immunology* 15 (12), S. 1181–1189. DOI: 10.1038/ni.3006.
- Bhatt, Dev; Ghosh, Sankar (2014): Regulation of the NF- κ B-Mediated Transcription of Inflammatory Genes. In: *Frontiers in immunology* 5, S. 71. DOI: 10.3389/fimmu.2014.00071.
- Bindea, Gabriela; Mlecnik, Bernhard; Hackl, Hubert; Charoentong, Pornpimol; Tosolini, Marie; Kirilovsky, Amos et al. (2009): ClueGO. A Cytoscape plug-in to decipher functionally grouped gene ontology and pathway annotation networks. In: *Bioinformatics (Oxford, England)* 25 (8), S. 1091–1093. DOI: 10.1093/bioinformatics/btp101.
- Bleesing, Jack J. H.; Fleisher, Thomas A. (2003): Human B cells express a CD45 isoform that is similar to murine B220 and is downregulated with acquisition of the memory B-cell marker CD27. In: *Cytometry. Part B, Clinical cytometry* 51 (1), S. 1–8. DOI: 10.1002/cyto.b.10007.
- Bonazzi, Matteo; Lecuit, Marc; Cossart, Pascale (2009): *Listeria monocytogenes* internalin and E-cadherin. From structure to pathogenesis. In: *Cellular microbiology* 11 (5), S. 693–702. DOI: 10.1111/j.1462-5822.2009.01293.x.
- Bours, V.; Franzoso, G.; Azarenko, V.; Park, S.; Kanno, T.; Brown, K.; Siebenlist, U. (1993): The oncoprotein Bcl-3 directly transactivates through kappa B motifs via association with DNA-binding p50B homodimers. In: *Cell* 72 (5), S. 729–739.
- Boyman, Onur; Sprent, Jonathan (2012): The role of interleukin-2 during homeostasis and activation of the immune system. In: *Nature reviews. Immunology* 12 (3), S. 180–190. DOI: 10.1038/nri3156.
- Bradley, L. M.; Watson, S. R.; Swain, S. L. (1994): Entry of naive CD4 T cells into peripheral lymph nodes requires L-selectin. In: *The Journal of experimental medicine* 180 (6), S. 2401–2406.
- Brehm, Michael A.; Daniels, Keith A.; Welsh, Raymond M. (2005): Rapid production of TNF-alpha following TCR engagement of naive CD8 T cells. In: *The Journal of Immunology* 175 (8), S. 5043–5049.

- Buchmeier, N. A.; Schreiber, R. D. (1985): Requirement of endogenous interferon-gamma production for resolution of *Listeria monocytogenes* infection. In: *Proceedings of the National Academy of Sciences* 82 (21), S. 7404–7408.
- Caamaño, J. H.; Perez, P.; Lira, S. A.; Bravo, R. (1996): Constitutive expression of Bcl-3 in thymocytes increases the DNA binding of NF-kappaB1 (p50) homodimers in vivo. In: *Molecular and cellular biology* 16 (4), S. 1342–1348.
- Cai, Yanhui; Sugimoto, Chie; Arainga, Mariluz; Alvarez, Xavier; Didier, Elizabeth S.; Kuroda, Marcelo J. (2014): In vivo characterization of alveolar and interstitial lung macrophages in rhesus macaques. Implications for understanding lung disease in humans. In: *Journal of immunology (Baltimore, Md. : 1950)* 192 (6), S. 2821–2829. DOI: 10.4049/jimmunol.1302269.
- Campbell, D. J.; Shastri, N. (1998): Bacterial surface proteins recognized by CD4+ T cells during murine infection with *Listeria monocytogenes*. In: *Journal of immunology (Baltimore, Md. : 1950)* 161 (5), S. 2339–2347.
- Catakovic, Kemal; Klieser, Eckhard; Neureiter, Daniel; Geisberger, Roland (2017): T cell exhaustion. From pathophysiological basics to tumor immunotherapy. In: *Cell communication and signaling : CCS* 15 (1), S. 1. DOI: 10.1186/s12964-016-0160-z
- Chen, Lieping; Flies, Dallas B. (2013): Erratum. Molecular mechanisms of T cell co-stimulation and co-inhibition. In: *Nature reviews. Immunology* 13 (7), S. 542. DOI: 10.1038/nri3484.
- Chen, Lin-Feng; Greene, Warner C. (2004): Shaping the nuclear action of NF-kappaB. In: *Nature reviews. Molecular cell biology* 5 (5), S. 392–401. DOI: 10.1038/nrm1368.
- Cho, Jae-Ho; Kim, Hee-Ok; Kim, Kyu-Sik; Yang, Deok-Hwan; Surh, Charles D.; Sprent, Jonathan (2013): Unique features of naive CD8+ T cell activation by IL-2. In: *Journal of immunology (Baltimore, Md. : 1950)* 191 (11), S. 5559–5573. DOI: 10.4049/jimmunol.1302293.
- Clarke, S. R.; Barnden, M.; Kurts, C.; Carbone, F. R.; Miller, J. F.; Heath, W. R. (2000): Characterization of the ovalbumin-specific TCR transgenic line OT-I. MHC elements for positive and negative selection. In: *Immunology and cell biology* 78 (2), S. 110–117. DOI: 10.1046/j.1440-1711.2000.00889.x
- Córbí, A. L.; Lopéz-Rodríguez, C. (1997): CD11c integrin gene promoter activity during myeloid differentiation. In: *Leukemia & lymphoma* 25 (5-6), S. 415–425. DOI: 10.3109/10428199709039028.
- Corr, Sinead C.; O'Neill, Luke A. J. (2009): *Listeria monocytogenes* infection in the face of innate immunity. In: *Cellular microbiology* 11 (5), S. 703–709. DOI: 10.1111/j.1462-5822.2009.01294.x
- Corse, Emily; Gottschalk, Rachel A.; Allison, James P. (2011): Strength of TCR-peptide/MHC interactions and in vivo T cell responses. In: *Journal of immunology (Baltimore, Md. : 1950)* 186 (9), S. 5039–5045. DOI: 10.4049/jimmunol.1003650.
- Curtsinger, Julie M.; Mescher, Matthew F. (2010): Inflammatory cytokines as a third signal for T cell activation. In: *Current opinion in immunology* 22 (3), S. 333–340. DOI: 10.1016/j.coi.2010.02.013.
- Dagvadorj, Jargalsaikhan; Naiki, Yoshikazu; Tumurkhuu, Gantsetseg; Noman, Abu Shadat Mohammod; Iftekar-E-Khuda, Imtiaz; Koide, Naoki et al. (2009): Interleukin (IL)-10 attenuates lipopolysaccharide-induced IL-6 production via inhibition of I kappa B-zeta activity by Bcl-3. In: *Innate immunity* 15 (4), S. 217–224. DOI: 10.1177/1753425909103738.
- Davies, Luke C.; Jenkins, Stephen J.; Allen, Judith E.; Taylor, Philip R. (2013): Tissue-resident macrophages. In: *Nature immunology* 14 (10), S. 986–995. DOI: 10.1038/ni.2705.
- Dobrzanski, P.; Ryseck, R. P.; Bravo, R. (1993): Both N- and C-terminal domains of RelB are required for full transactivation. Role of the N-terminal leucine zipper-like motif. In: *Molecular and cellular biology* 13 (3), S. 1572–1582.
- Drevets, D. A.; Dillon, M. J.; Schawang, J. S.; van Rooijen, N.; Ehrchen, J.; Sunderkotter, C.; Leenen, P. J. M. (2004): The Ly-6Chigh Monocyte Subpopulation Transports *Listeria monocytogenes* into the Brain during Systemic Infection of Mice. In: *The Journal of Immunology* 172 (7), S. 4418–4424. DOI: 10.4049/jimmunol.172.7.4418.
- Ertelt, James M.; Rowe, Jared H.; Johanns, Tanner M.; Lai, Joseph C.; McLachlan, James B.; Way, Sing Sing (2009): Selective priming and expansion of antigen-specific Foxp3- CD4+ T cells during *Listeria monocytogenes* infection. In: *Journal of immunology (Baltimore, Md. : 1950)* 182 (5), S. 3032–3038. DOI: 10.4049/jimmunol.0803402.
- Fagerlund, Riku; Behar, Marcelo; Fortmann, Karen T.; Lin, Y. Eason; Vargas, Jesse D.; Hoffmann, Alexander (2015): Anatomy of a negative feedback loop. The case of Ikbα. In: *Journal of the Royal Society, Interface* 12 (110), S. 262. DOI: 10.1098/rsif.2015.0262.
- Fazekas de St Groth, Barbara; Smith, Adrian L.; Higgins, Caroline A. (2004): T cell activation. In vivo veritas. In: *Immunology and cell biology* 82 (3), S. 260–268. DOI: 10.1111/j.0818-9641.2004.01243.x

- Finelli, A.; Kerksiek, K. M.; Allen, S. E.; Marshall, N.; Mercado, R.; Pilip, I. et al. (1999): MHC class I restricted T cell responses to *Listeria monocytogenes*, an intracellular bacterial pathogen. In: *Immunologic research* 19 (2-3), S. 211–223. DOI: 10.1007/BF02786489.
- Fiorini, Emma; Schmitz, Ingo; Marissen, Wilfred E.; Osborn, Stephanie L.; Touma, Maki; Sasada, Tetsuro et al. (2002): Peptide-Induced Negative Selection of Thymocytes Activates Transcription of an NF- κ B Inhibitor. In: *Molecular Cell* 9 (3), S. 637–648. DOI: 10.1016/S1097-2765(02)00469-0.
- Fornas, Oscar; Domingo, Joan Carles; Marin, Pedro; Petriz, Jordi (2002): Flow cytometric-based isolation of nucleated erythroid cells during maturation. An approach to cell surface antigen studies. In: *Cytometry* 50 (6), S. 305–312. DOI: 10.1002/cyto.10158.
- Francisco, Loise M.; Sage, Peter T.; Sharpe, Arlene H. (2010): The PD-1 pathway in tolerance and autoimmunity. In: *Immunological reviews* 236, S. 219–242. DOI: 10.1111/j.1600-065X.2010.00923.x.
- Gabay, Cem (2006): Interleukin-6 and chronic inflammation. In: *Arthritis research & therapy* 8 Suppl 2, S3. DOI: 10.1186/ar1917.
- Gerberick, G. F.; Cruse, L. W.; Miller, C. M.; Sikorski, E. E.; Ridder, G. M. (1997): Selective modulation of T cell memory markers CD62L and CD44 on murine draining lymph node cells following allergen and irritant treatment. In: *Toxicology and applied pharmacology* 146 (1), S. 1–10. DOI: 10.1006/taap.1997.8218.
- Ghosh, S.; May, M. J.; Kopp, E. B. (1998): NF- κ B and Rel proteins. Evolutionarily conserved mediators of immune responses. In: *Annual review of immunology* 16, S. 225–260. DOI: 10.1146/annurev.immunol.16.1.225.
- Ghosh, Sankar; Hayden, Matthew S. (2008): New regulators of NF- κ B in inflammation. In: *Nature reviews. Immunology* 8 (11), S. 837–848. DOI: 10.1038/nri2423.
- Gilmore, T. D. (2006): Introduction to NF- κ B. Players, pathways, perspectives. In: *Oncogene* 25 (51), S. 6680–6684. DOI: 10.1038/sj.onc.1209954.
- Goldrath, A. W.; Bevan, M. J. (1999): Selecting and maintaining a diverse T-cell repertoire. In: *Nature* 402 (6759), S. 255–262. DOI: 10.1038/46218.
- Guermonprez, Pierre; Valladeau, Jenny; Zitvogel, Laurence; Théry, Clotilde; Amigorena, Sebastian (2002): Antigen presentation and T cell stimulation by dendritic cells. In: *Annual review of immunology* 20, S. 621–667. DOI: 10.1146/annurev.immunol.20.100301.064828.
- Guleria, I.; Pollard, J. W. (2001): Aberrant macrophage and neutrophil population dynamics and impaired Th1 response to *Listeria monocytogenes* in colony-stimulating factor 1-deficient mice. In: *Infection and Immunity* 69 (3), S. 1795–1807. DOI: 10.1128/IAI.69.3.1795-1807.2001.
- Haeryfar, S. M. Mansour; Hoskin, David W. (2004): Thy-1. More than a mouse pan-T cell marker. In: *The Journal of Immunology* 173 (6), S. 3581–3588.
- Hamon, Mélanie; Bierne, Hélène; Cossart, Pascale (2006): *Listeria monocytogenes*. A multifaceted model. In: *Nature reviews. Microbiology* 4 (6), S. 423–434. DOI: 10.1038/nrmicro1413.
- Hannemann, Frank; Bichet, Andreas; Ewen, Kerstin M.; Bernhardt, Rita (2007): Cytochrome P450 systems -- biological variations of electron transport chains. In: *Biochimica et biophysica acta* 1770 (3), S. 330–344. DOI: 10.1016/j.bbagen.2006.07.017.
- Harty, J. T.; Tinnereim, A. R.; White, D. W. (2000): CD8+ T cell effector mechanisms in resistance to infection. In: *Annual review of immunology* 18, S. 275–308. DOI: 10.1146/annurev.immunol.18.1.275.
- Hatanaka, Elaine; Furlaneto, Cristiane J.; Ribeiro, Fernanda P.; Souza, Glaucia Mendes; Campa, Ana (2004): Serum amyloid A-induced mRNA expression and release of tumor necrosis factor- α (TNF- α) in human neutrophils. In: *Immunology letters* 91 (1), S. 33–37.
- Havell, E. A. (1987): Production of tumor necrosis factor during murine listeriosis. In: *The Journal of Immunology* 139 (12), S. 4225–4231.
- Hayden, Matthew S.; Ghosh, Sankar (2004): Signaling to NF- κ B. In: *Genes & development* 18 (18), S. 2195–2224. DOI: 10.1101/gad.1228704.
- Hinz, Michael; Arslan, Seda Çöl; Scheidereit, Claus (2012): It takes two to tango. I κ Bs, the multifunctional partners of NF- κ B. In: *Immunological reviews* 246 (1), S. 59–76. DOI: 10.1111/j.1600-065X.2012.01102.x.
- Hirotsu, T.; Lee, P. Y.; Kuwata, H.; Yamamoto, M.; Matsumoto, M.; Kawase, I. et al. (2005): The Nuclear I κ B Protein I κ BNS Selectively Inhibits Lipopolysaccharide-Induced IL-6 Production in Macrophages of the Colonic Lamina Propria. In: *The Journal of Immunology* 174 (6), S. 3650–3657. DOI: 10.4049/jimmunol.174.6.3650.
- Hoffmann, Alexander; Levchenko, Andre; Scott, Martin L.; Baltimore, David (2002): The I κ B-NF- κ B signaling module. Temporal control and selective gene activation. In: *Science* 298 (5596), S. 1241–1245. DOI: 10.1126/science.1071914.

- Hoge, Judith; Yan, Isabell; Jänner, Nathalie; Schumacher, Valéa; Chalaris, Athena; Steinmetz, Oliver M. et al. (2013): IL-6 controls the innate immune response against *Listeria monocytogenes* via classical IL-6 signaling. In: *Journal of immunology (Baltimore, Md. : 1950)* 190 (2), S. 703–711. DOI: 10.4049/jimmunol.1201044.
- Hogquist, K. A.; Jameson, S. C.; Heath, W. R.; Howard, J. L.; Bevan, M. J.; Carbone, F. R. (1994): T cell receptor antagonist peptides induce positive selection. In: *Cell* 76 (1), S. 17–27.
- Hoogerwerf, Jacobien J.; van der Windt, Gerritje J. W.; Blok, Dana C.; Hoogendijk, Arie J.; Vos, Alex F. de; van 't Veer, Cornelis et al. (2012): Interleukin-1 receptor-associated kinase M-deficient mice demonstrate an improved host defense during Gram-negative pneumonia. In: *Molecular medicine (Cambridge, Mass.)* 18, S. 1067–1075. DOI: 10.2119/molmed.2011.00450.
- Hosking, Martin P.; Flynn, Claudia T.; Whitton, J. Lindsay (2014): Antigen-specific naive CD8+ T cells produce a single pulse of IFN- γ in vivo within hours of infection, but without antiviral effect. In: *Journal of immunology (Baltimore, Md. : 1950)* 193 (4), S. 1873–1885. DOI: 10.4049/jimmunol.1400348.
- Hsieh, C.; Macatonia, S.; Tripp, C.; Wolf, S.; O'Garra, A.; Murphy, K. (1993): Development of TH1 CD4+ T cells through IL-12 produced by *Listeria*-induced macrophages. In: *Science* 260 (5107), S. 547–549. DOI: 10.1126/science.8097338.
- Itano, Andrea A.; Jenkins, Marc K. (2003): Antigen presentation to naive CD4 T cells in the lymph node. In: *Nature immunology* 4 (8), S. 733–739. DOI: 10.1038/ni957.
- Janeway CA Jr, Travers P, Walport M, et al. (2008): *Janeway's Immunobiology*. 7. Edition. New York: Garland Science, Taylor and Francis Group, LLC
- Janssens, Sophie; Beyaert, Rudi (2003): Functional diversity and regulation of different interleukin-1 receptor-associated kinase (IRAK) family members. In: *Molecular Cell* 11 (2), S. 293–302.
- Jeffrey K. Actor (Hg.) (2014): *Introductory Immunology*: Elsevier.
- Kanarek, Naama; Ben-Neriah, Yinon (2012): Regulation of NF- κ B by ubiquitination and degradation of the I κ Bs. In: *Immunological reviews* 246 (1), S. 77–94. DOI: 10.1111/j.1600-065X.2012.01098.x.
- Karin, M.; Ben-Neriah, Y. (2000): Phosphorylation meets ubiquitination. The control of NF- κ B activity. In: *Annual review of immunology* 18, S. 621–663. DOI: 10.1146/annurev.immunol.18.1.621.
- Kaufmann, S. H. (1993): Immunity to intracellular bacteria. In: *Annual review of immunology* 11, S. 129–163. DOI: 10.1146/annurev.iy.11.040193.001021.
- Keir, Mary E.; Butte, Manish J.; Freeman, Gordon J.; Sharpe, Arlene H. (2008): PD-1 and its ligands in tolerance and immunity. In: *Annual review of immunology* 26, S. 677–704. DOI: 10.1146/annurev.immunol.26.021607.090331.
- Kim, Bae-Hoon; Shenoy, Avinash R.; Kumar, Pradeep; Das, Rituparna; Tiwari, Sangeeta; MacMicking, John D. (2011): A family of IFN- γ -inducible 65-kD GTPases protects against bacterial infection. In: *Science* 332 (6030), S. 717–721. DOI: 10.1126/science.1201711.
- Kim, H. P.; Kelly, J.; Leonard, W. J. (2001): The basis for IL-2-induced IL-2 receptor alpha chain gene regulation. Importance of two widely separated IL-2 response elements. In: *Immunity* 15 (1), S. 159–172.
- Kim, W. Ray; Flamm, Steven L.; Di Bisceglie, Adrian M.; Bodenheimer, Henry C. (2008): Serum activity of alanine aminotransferase (ALT) as an indicator of health and disease. In: *Hepatology (Baltimore, Md.)* 47 (4), S. 1363–1370. DOI: 10.1002/hep.22109.
- Kitamura, Hiroshi; Kanehira, Katsushi; Okita, Keisuke; Morimatsu, Masami; Saito, Masayuki (2000): MAIL, a novel nuclear I κ B protein that potentiates LPS-induced IL-6 production. In: *FEBS Letters* 485 (1), S. 53–56. DOI: 10.1016/S0014-5793(00)02185-2.
- Kobayashi, Koichi; Hernandez, Lorraine D.; Galán, Jorge E.; Janeway, Charles A.; Medzhitov, Ruslan; Flavell, Richard A. (2002): IRAK-M is a negative regulator of Toll-like receptor signaling. In: *Cell* 110 (2), S. 191–202.
- Kobayashi, Shuhei; Hara, Akira; Isagawa, Takayuki; Manabe, Ichiro; Takeda, Kiyoshi; Maruyama, Takashi (2014): The nuclear I κ B family protein I κ BNS influences the susceptibility to experimental autoimmune encephalomyelitis in a murine model. In: *PLoS one* 9 (10), e110838. DOI: 10.1371/journal.pone.0110838.
- Korwek, Zbigniew; Tudelska, Karolina; Nałęcz-Jawecki, Paweł; Czerkies, Maciej; Prus, Wiktor; Markiewicz, Joanna et al. (2016): Importins promote high-frequency NF- κ B oscillations increasing information channel capacity. In: *Biology direct* 11 (1), S. 61. DOI: 10.1186/s13062-016-0164-z.
- Kursar, M.; Bonhagen, K.; Kohler, A.; Kamradt, T.; Kaufmann, S. H. E.; Mittrucker, H.-W. (2002): Organ-Specific CD4+ T Cell Response During *Listeria monocytogenes* Infection. In: *The Journal of Immunology* 168 (12), S. 6382–6387. DOI: 10.4049/jimmunol.168.12.6382.
- Kuwata, Hirotaka; Matsumoto, Makoto; Atarashi, Koji; Morishita, Hideaki; Hirotani, Tomohiro; Koga, Ritsuko; Takeda, Kiyoshi (2006): I κ BNS inhibits induction of a subset of Toll-like receptor-dependent genes and limits inflammation. In: *Immunity* 24 (1), S. 41–51. DOI: 10.1016/j.immuni.2005.11.004.

- Lara-Tejero, María; Pamer, Eric G. (2004): T cell responses to *Listeria monocytogenes*. In: *Current opinion in microbiology* 7 (1), S. 45–50. DOI: 10.1016/j.mib.2003.12.002.
- Lazarski, Christopher A.; Chaves, Francisco A.; Sant, Andrea J. (2006): The impact of DM on MHC class II-restricted antigen presentation can be altered by manipulation of MHC-peptide kinetic stability. In: *The Journal of experimental medicine* 203 (5), S. 1319–1328. DOI: 10.1084/jem.20060058.
- LeBien, Tucker W.; Tedder, Thomas F. (2008): B lymphocytes. How they develop and function. In: *Blood* 112 (5), S. 1570–1580. DOI: 10.1182/blood-2008-02-078071.
- Levidiotou, S.; Charalabopoulos, K.; Vrioni, G.; Chaidos, A.; Polysoidis, K.; Bourantas, K.; Stefanou, D. (2004): Fatal meningitis due to *Listeria monocytogenes* in elderly patients with underlying malignancy. In: *International Journal of Clinical Practice* 58 (3), S. 292–296. DOI: 10.1111/j.1368-5031.2004.00076.x.
- Liu, Mingyong; Chen, Keqiang; Yoshimura, Teizo; Liu, Ying; Gong, Wanghua; Wang, Aimin et al. (2012): Formylpeptide receptors are critical for rapid neutrophil mobilization in host defense against *Listeria monocytogenes*. In: *Scientific reports* 2, S. 786. DOI: 10.1038/srep00786.
- Malek, Thomas R.; Castro, Iris (2010): Interleukin-2 receptor signaling. At the interface between tolerance and immunity. In: *Immunity* 33 (2), S. 153–165. DOI: 10.1016/j.immuni.2010.08.004.
- Malle, E.; Steinmetz, A.; Raynes, J. G. (1993): Serum amyloid A (SAA). An acute phase protein and apolipoprotein. In: *Atherosclerosis* 102 (2), S. 131–146.
- Manavalan, Balachandran; Basith, Shaheer; Choi, Yong-Min; Lee, Gwang; Choi, Sangdun (2010): Structure-function relationship of cytoplasmic and nuclear I κ B proteins. An in silico analysis. In: *PLoS one* 5 (12), e15782. DOI: 10.1371/journal.pone.0015782.
- Mannering, Stuart I.; Zhong, Jie; Cheers, Christina (2002): T-cell activation, proliferation and apoptosis in primary *Listeria monocytogenes* infection. In: *Immunology* 106 (1), S. 87–95. DOI: 10.1046/j.1365-2567.2002.01408.x.
- Mateus, Teresa; Silva, Joana; Maia, Rui L.; Teixeira, Paula (2013): Listeriosis during Pregnancy. A Public Health Concern. In: *ISRN obstetrics and gynecology* 2013, S. 851712. DOI: 10.1155/2013/851712.
- Medzhitov, R. (2001): Toll-like receptors and innate immunity. In: *Nature reviews. Immunology* 1 (2), S. 135–145. DOI: 10.1038/35100529.
- Merad, Miriam; Sathé, Priyanka; Helft, Julie; Miller, Jennifer; Mortha, Arthur (2013): The dendritic cell lineage. Ontogeny and function of dendritic cells and their subsets in the steady state and the inflamed setting. In: *Annual review of immunology* 31, S. 563–604. DOI: 10.1146/annurev-immunol-020711-074950.
- Merrick, J. C.; Edelson, B. T.; Bhardwaj, V.; Swanson, P. E.; Unanue, E. R. (1997): Lymphocyte apoptosis during early phase of *Listeria* infection in mice. In: *The American journal of pathology* 151 (3), S. 785–792.
- Misharin, Alexander V.; Morales-Nebreda, Luisa; Mutlu, Gökhan M.; Budinger, G. R. Scott; Perlman, Harris (2013): Flow cytometric analysis of macrophages and dendritic cell subsets in the mouse lung. In: *American journal of respiratory cell and molecular biology* 49 (4), S. 503–510. DOI: 10.1165/rcmb.2013-0086MA.
- Mizuki, Mayuko; Nakane, Akio; Sekikawa, Kenji; Tagawa, Yoh-ich; Iwakura, Yoichiro (2002): Comparison of host resistance to primary and secondary *Listeria monocytogenes* infections in mice by intranasal and intravenous routes. In: *Infection and Immunity* 70 (9), S. 4805–4811.
- Morgan, E. T. (1997): Regulation of cytochromes P450 during inflammation and infection. In: *Drug metabolism reviews* 29 (4), S. 1129–1188. DOI: 10.3109/03602539709002246.
- Morgan, E. T. (2001): Regulation of cytochrome p450 by inflammatory mediators. Why and how? In: *Drug metabolism and disposition: the biological fate of chemicals* 29 (3), S. 207–212.
- Mosavi, Leila K.; Cammett, Tobin J.; Desrosiers, Daniel C.; Peng, Zheng-Yu (2004): The ankyrin repeat as molecular architecture for protein recognition. In: *Protein science: a publication of the Protein Society* 13 (6), S. 1435–1448. DOI: 10.1110/ps.03554604.
- Müller, Christoph W.; Harrison, Stephen C. (1995): The structure of the NF- κ B p50. DNA-complex a starting point for analyzing the Rel family. In: *FEBS Letters* 369 (1), S. 113–117. DOI: 10.1016/0014-5793(95)00541-G.
- Murray, E. G. D.; Webb, R. A.; Swann, M. B. R. (1926): A disease of rabbits characterised by a large mononuclear leucocytosis, caused by a hitherto undescribed bacillus *Bacterium monocytogenes* (n.sp.). In: *J. Pathol.* 29 (4), S. 407–439. DOI: 10.1002/path.1700290409.
- Myers, J. T.; Tsang, A. W.; Swanson, J. A. (2003): Localized Reactive Oxygen and Nitrogen Intermediates Inhibit Escape of *Listeria monocytogenes* from Vacuoles in Activated Macrophages. In: *The Journal of Immunology* 171 (10), S. 5447–5453. DOI: 10.4049/jimmunol.171.10.5447.
- Nakane, Akio; Yamada, Kyogo; Hasegawa, Suguru; Mizuki, Daisuke; Mizuki, Mayuko; Sasaki, Sanae; Miura, Tomisato (1999): Endogenous cytokines during a lethal infection with *Listeria monocytogenes* in mice. In: *FEMS Microbiology Letters* 175 (1), S. 133–142. DOI: 10.1111/j.1574-6968.1999.tb13612.x.

- Nakano, A.; Harada, T.; Morikawa, S.; Kato, Y. (1990): Expression of leukocyte common antigen (CD45) on various human leukemia/lymphoma cell lines. In: *Acta pathologica japonica* 40 (2), S. 107–115.
- Newell, Evan W.; Davis, Mark M. (2014): Beyond model antigens: high-dimensional methods for the analysis of antigen-specific T cells. In: *Nature biotechnology* 32 (2), S. 149–157. DOI: 10.1038/nbt.2783.
- Ng, Hanna H.; Frantz, Christopher E.; Rausch, Linda; Fairchild, David C.; Shimon, Julie; Riccio, Edward et al. (2005): Gene expression profiling of mouse host response to *Listeria monocytogenes* infection. In: *Genomics* 86 (6), S. 657–667. DOI: 10.1016/j.ygeno.2005.07.005.
- NISBET, Andrew D.; SAUNDRY, Richard H.; MOIR, Arthur J. G.; FOTHERGILL, Linda A.; FOTHERGILL, John E. (1981): The Complete Amino-Acid Sequence of Hen Ovalbumin. In: *Eur J Biochem* 115 (2), S. 335–345. DOI: 10.1111/j.1432-1033.1981.tb05243.x.
- Nolan, G. P.; Fujita, T.; Bhatia, K.; Huppi, C.; Liou, H. C.; Scott, M. L.; Baltimore, D. (1993): The bcl-3 proto-oncogene encodes a nuclear I kappa B-like molecule that preferentially interacts with NF-kappa B p50 and p52 in a phosphorylation-dependent manner. In: *Molecular and cellular biology* 13 (6), S. 3557–3566.
- Oeckinghaus, Andrea; Ghosh, Sankar (2009): The NF-kappaB family of transcription factors and its regulation. In: *Cold Spring Harbor perspectives in biology* 1 (4), a000034. DOI: 10.1101/cshperspect.a000034.
- Ohno, H. (1990): The candidate proto-oncogene bcl-3 is related to genes implicated in cell lineage determination and cell cycle control. In: *Cell* 60 (6), S. 991–997. DOI: 10.1016/0092-8674(90)90347-H.
- Ooi, Say Tat; Lorber, Bennett (2005): Gastroenteritis due to *Listeria monocytogenes*. In: *Clinical infectious diseases : an official publication of the Infectious Diseases Society of America* 40 (9), S. 1327–1332. DOI: 10.1086/429324.
- Park, Koog Chan; Jeong, Jiyeong; Kim, Keun Il (2014): Regulation of mlkBNS stability through PEST-mediated degradation by proteasome. In: *Biochemical and biophysical research communications* 443 (4), S. 1291–1295. DOI: 10.1016/j.bbrc.2013.12.140.
- Pasche, Bastian; Kalaydjiev, Svetoslav; Franz, Tobias J.; Kremmer, Elisabeth; Gailus-Durner, Valérie; Fuchs, Helmut et al. (2005): Sex-dependent susceptibility to *Listeria monocytogenes* infection is mediated by differential interleukin-10 production. In: *Infection and Immunity* 73 (9), S. 5952–5960. DOI: 10.1128/IAI.73.9.5952-5960.2005.
- Petit, J.-C.; Burghoffer, B.; Richard, G.; Daguët, G.-L. (1988): Kinetics of interleukin-1 production by macrophages during infection with *Listeria monocytogenes*. In: *International journal of immunopharmacology* 10 (7), S. 875–878. DOI: 10.1016/0192-0561(88)90012-4.
- Pieper, Kathrin; Grimbacher, Bodo; Eibel, Hermann (2013): B-cell biology and development. In: *The Journal of allergy and clinical immunology* 131 (4), S. 959–971. DOI: 10.1016/j.jaci.2013.01.046.
- Pipkin, Matthew E.; Sacks, Jilian A.; Cruz-Guilloty, Fernando; Lichtenheld, Mathias G.; Bevan, Michael J.; Rao, Anjana (2010): Interleukin-2 and inflammation induce distinct transcriptional programs that promote the differentiation of effector cytolytic T cells. In: *Immunity* 32 (1), S. 79–90. DOI: 10.1016/j.immuni.2009.11.012.
- Prlic, Martin; Bevan, Michael J. (2008): Exploring regulatory mechanisms of CD8+ T cell contraction. In: *Proceedings of the National Academy of Sciences of the United States of America* 105 (43), S. 16689–16694. DOI: 10.1073/pnas.0808997105.
- Rao, Xiyu; Huang, Xuelin; Zhou, Zhicheng; Lin, Xin (2013): An improvement of the 2^{-ΔΔCT} method for quantitative real-time polymerase chain reaction data analysis. In: *Biostatistics, bioinformatics and biomathematics* 3 (3), S. 71–85.
- Reiser, John; Banerjee, Arnob (2016): Effector, Memory, and Dysfunctional CD8(+) T Cell Fates in the Antitumor Immune Response. In: *Journal of immunology research* 2016, S. 8941260. DOI: 10.1155/2016/8941260.
- Ren, Ke; Torres, Richard (2009): Role of interleukin-1beta during pain and inflammation. In: *Brain research reviews* 60 (1), S. 57–64. DOI: 10.1016/j.brainresrev.2008.12.020.
- Richard, M.; Louahed, J.; Demoulin, J. B.; Renaud, J. C. (1999): Interleukin-9 regulates NF-kappaB activity through BCL3 gene induction. In: *Blood* 93 (12), S. 4318–4327.
- Robertson, J. M.; Jensen, P. E.; Evavold, B. D. (2000): DO11.10 and OT-II T Cells Recognize a C-Terminal Ovalbumin 323-339 Epitope. In: *The Journal of Immunology* 164 (9), S. 4706–4712. DOI: 10.4049/jimmunol.164.9.4706.
- Rogers, S.; Wells, R.; Rechsteiner, M. (1986): Amino acid sequences common to rapidly degraded proteins. The PEST hypothesis. In: *Science* 234 (4774), S. 364–368. DOI: 10.1126/science.2876518.
- Romero, Ana I.; Thorén, Fredrik B.; Brune, Mats; Hellstrand, Kristoffer (2006): NKp46 and NKG2D receptor expression in NK cells with CD56dim and CD56bright phenotype. Regulation by histamine and reactive oxygen species. In: *British journal of haematology* 132 (1), S. 91–98. DOI: 10.1111/j.1365-2141.2005.05842.x.

- Rose, Shawn; Misharin, Alexander; Perlman, Harris (2012): A novel Ly6C/Ly6G-based strategy to analyze the mouse splenic myeloid compartment. In: *Cytometry. Part A : the journal of the International Society for Analytical Cytology* 81 (4), S. 343–350. DOI: 10.1002/cyto.a.22012.
- Rushlow, C.; Warrior, R. (1992): The rel family of proteins. In: *BioEssays : news and reviews in molecular, cellular and developmental biology* 14 (2), S. 89–95. DOI: 10.1002/bies.950140204.
- Saccani, Simona; Pantano, Serafino; Natoli, Gioacchino (2003): Modulation of NF- κ B Activity by Exchange of Dimers. In: *Molecular Cell* 11 (6), S. 1563–1574. DOI: 10.1016/S1097-2765(03)00227-2.
- Sancho, David; Gómez, Manuel; Sánchez-Madrid, Francisco (2005): CD69 is an immunoregulatory molecule induced following activation. In: *Trends in immunology* 26 (3), S. 136–140. DOI: 10.1016/j.it.2004.12.006.
- Schlech, W. F. (2000): Foodborne listeriosis. In: *Clinical infectious diseases : an official publication of the Infectious Diseases Society of America* 31 (3), S. 770–775. DOI: 10.1086/314008.
- Schoenborn, Jamie R.; Wilson, Christopher B. (2007): Regulation of Interferon- γ During Innate and Adaptive Immune Responses. In: Bd. 96: Elsevier (Advances in Immunology), S. 41–101.
- Schuchat, A.; Deaver, K. A.; Wenger, J. D.; Plikaytis, B. D.; Mascola, L.; Pinner, R. W. et al. (1992): Role of foods in sporadic listeriosis. I. Case-control study of dietary risk factors. The Listeria Study Group. In: *JAMA* 267 (15), S. 2041–2045.
- Schuster, Marc; Glaubien, Rainer; Plaza-Sirvent, Carlos; Schreiber, Lisa; Annemann, Michaela; Floess, Stefan et al. (2012): I κ B(NS) protein mediates regulatory T cell development via induction of the Foxp3 transcription factor. In: *Immunity* 37 (6), S. 998–1008. DOI: 10.1016/j.immuni.2012.08.023.
- Seaman, M. S.; Wang, C. R.; Forman, J. (2000): MHC class Ib-restricted CTL provide protection against primary and secondary Listeria monocytogenes infection. In: *The Journal of Immunology* 165 (9), S. 5192–5201.
- Sen, R.; Baltimore, D. (1986): Inducibility of kappa immunoglobulin enhancer-binding protein Nf-kappa B by a posttranslational mechanism. In: *Cell* 47 (6), S. 921–928.
- Serbina, Natalya V.; Jia, Ting; Hohl, Tobias M.; Pamer, Eric G. (2008): Monocyte-mediated defense against microbial pathogens. In: *Annual review of immunology* 26, S. 421–452. DOI: 10.1146/annurev.immunol.26.021607.090326.
- Serbina, Natalya V.; Salazar-Mather, Thais P.; Biron, Christine A.; Kuziel, William A.; Pamer, Eric G. (2003): TNF/ iNOS -Producing Dendritic Cells Mediate Innate Immune Defense against Bacterial Infection. In: *Immunity* 19 (1), S. 59–70. DOI: 10.1016/S1074-7613(03)00171-7.
- Serbina, Natalya V.; Shi, Chao; Pamer, Eric G. (2012): Monocyte-mediated immune defense against murine Listeria monocytogenes infection. In: *Advances in immunology* 113, S. 119–134. DOI: 10.1016/B978-0-12-394590-7.00003-8.
- Sharma, K.; Wang, R. X.; Zhang, L. Y.; Yin, D. L.; Luo, X. Y.; Solomon, J. C. et al. (2000): Death the Fas way. Regulation and pathophysiology of CD95 and its ligand. In: *Pharmacology & therapeutics* 88 (3), S. 333–347.
- Shaughnessy, Lee M.; Swanson, Joel A. (2007): The role of the activated macrophage in clearing Listeria monocytogenes infection. In: *Frontiers in bioscience : a journal and virtual library* 12, S. 2683–2692.
- Shedlock, D. J.; Whitmire, J. K.; Tan, J.; MacDonald, A. S.; Ahmed, R.; Shen, H. (2003): Role of CD4 T Cell Help and Costimulation in CD8 T Cell Responses During Listeria monocytogenes Infection. In: *The Journal of Immunology* 170 (4), S. 2053–2063. DOI: 10.4049/jimmunol.170.4.2053.
- Shen, H.; Slifka, M. K.; Matloubian, M.; Jensen, E. R.; Ahmed, R.; Miller, J. F. (1995): Recombinant Listeria monocytogenes as a live vaccine vehicle for the induction of protective anti-viral cell-mediated immunity. In: *Proceedings of the National Academy of Sciences* 92 (9), S. 3987–3991. DOI: 10.1073/pnas.92.9.3987.
- Shi, Chao; Pamer, Eric G. (2011): Monocyte recruitment during infection and inflammation. In: *Nature reviews. Immunology* 11 (11), S. 762–774. DOI: 10.1038/nri3070.
- Siebenlist, Ulrich; Brown, Keith; Claudio, Estefania (2005): Control of lymphocyte development by nuclear factor-kappaB. In: *Nature reviews. Immunology* 5 (6), S. 435–445. DOI: 10.1038/nri1629.
- Solovjov, Dmitry A.; Pluskota, Elzbieta; Plow, Edward F. (2005): Distinct roles for the alpha and beta subunits in the functions of integrin alphaMbeta2. In: *The Journal of biological chemistry* 280 (2), S. 1336–1345. DOI: 10.1074/jbc.M406968200.
- Soria, Gali; Ben-Baruch, Adit (2008): The inflammatory chemokines CCL2 and CCL5 in breast cancer. In: *Cancer letters* 267 (2), S. 271–285. DOI: 10.1016/j.canlet.2008.03.018.
- Stavru, Fabrizia; Archambaud, Cristel; Cossart, Pascale (2011): Cell biology and immunology of Listeria monocytogenes infections. Novel insights. In: *Immunological reviews* 240 (1), S. 160–184. DOI: 10.1111/j.1600-065X.2010.00993.x.

- Stoiber, D.; Stockinger, S.; Steinlein, P.; Kovarik, J.; Decker, T. (2001): *Listeria monocytogenes* Modulates Macrophage Cytokine Responses Through STAT Serine Phosphorylation and the Induction of Suppressor of Cytokine Signaling 3. In: *The Journal of Immunology* 166 (1), S. 466–472. DOI: 10.4049/jimmunol.166.1.466.
- Streetz, K. L.; Wüstefeld, T.; Klein, C.; Manns, M. P.; Trautwein, C. (2001): Mediators of inflammation and acute phase response in the liver. In: *Cellular and molecular biology (Noisy-le-Grand, France)* 47 (4), S. 661–673.
- Sturn, Alexander; Quackenbush, John; Trajanoski, Zlatko (2002): Genesis. Cluster analysis of microarray data. In: *Bioinformatics (Oxford, England)* 18 (1), S. 207–208.
- Sun, Shao-Cong (2011): Non-canonical NF- κ B signaling pathway. In: *Cell research* 21 (1), S. 71–85. DOI: 10.1038/cr.2010.177.
- Swain, Susan L. (1994): Generation and in vivo persistence of polarized Th1 and Th2 memory cells. In: *Immunity* 1 (7), S. 543–552. DOI: 10.1016/1074-7613(94)90044-2.
- Takaba, Hiroyuki; Takayanagi, Hiroshi (2017): The Mechanisms of T Cell Selection in the Thymus. In: *Trends in immunology* 38 (11), S. 805–816. DOI: 10.1016/j.it.2017.07.010.
- Tamoutounour, Samira; Henri, Sandrine; Lelouard, Hugues; Bovis, Béatrice de; Haar, Colin de; van der Woude, C. Janneke et al. (2012): CD64 distinguishes macrophages from dendritic cells in the gut and reveals the Th1-inducing role of mesenteric lymph node macrophages during colitis. In: *European journal of immunology* 42 (12), S. 3150–3166. DOI: 10.1002/eji.201242847.
- Tecchio, Cristina; Micheletti, Alessandra; Cassatella, Marco A. (2014): Neutrophil-derived cytokines. Facts beyond expression. In: *Frontiers in immunology* 5, S. 508. DOI: 10.3389/fimmu.2014.00508.
- Torres, D.; Barrier, M.; Bihl, F.; Quesniaux, V. J. F.; Mailliet, I.; Akira, S. et al. (2004): Toll-Like Receptor 2 Is Required for Optimal Control of *Listeria monocytogenes* Infection. In: *Infection and Immunity* 72 (4), S. 2131–2139. DOI: 10.1128/IAI.72.4.2131-2139.2004.
- Touma, M.; Antonini, V.; Kumar, M.; Osborn, S. L.; Bobenchik, A. M.; Keskin, D. B. et al. (2007): Functional Role for I BNS in T Cell Cytokine Regulation As Revealed by Targeted Gene Disruption. In: *The Journal of Immunology* 179 (3), S. 1681–1692. DOI: 10.4049/jimmunol.179.3.1681.
- Touma, Maki; Keskin, Derin B.; Shiroki, Fumiko; Saito, Ibuki; Koyasu, Shigeo; Reinherz, Ellis L.; Clayton, Linda K. (2011): Impaired B cell development and function in the absence of I κ BNS. In: *Journal of immunology (Baltimore, Md. : 1950)* 187 (8), S. 3942–3952. DOI: 10.4049/jimmunol.1002109.
- Tripal, Philipp; Bauer, Michael; Naschberger, Elisabeth; Mörtinger, Thomas; Hohenadl, Christine; Cornali, Emmanuelle et al. (2007): Unique features of different members of the human guanylate-binding protein family. In: *Journal of interferon & cytokine research : the official journal of the International Society for Interferon and Cytokine Research* 27 (1), S. 44–52. DOI: 10.1089/jir.2007.0086.
- Tripp, C. S.; Wolf, S. F.; Unanue, E. R. (1993): Interleukin 12 and tumor necrosis factor alpha are costimulators of interferon gamma production by natural killer cells in severe combined immunodeficiency mice with listeriosis, and interleukin 10 is a physiologic antagonist. In: *Proceedings of the National Academy of Sciences of the United States of America* 90 (8), S. 3725–3729.
- van Lochem, E. G.; van der Velden, V. H. J.; Wind, H. K.; te Marvelde, J. G.; Westerdal, N. A. C.; van Dongen, J. J. M. (2004): Immunophenotypic differentiation patterns of normal hematopoiesis in human bone marrow. Reference patterns for age-related changes and disease-induced shifts. In: *Cytometry. Part B, Clinical cytometry* 60 (1), S. 1–13. DOI: 10.1002/cyto.b.20008.
- van Panhuys, Nicholas (2016): TCR Signal Strength Alters T-DC Activation and Interaction Times and Directs the Outcome of Differentiation. In: *Frontiers in immunology* 7, S. 6. DOI: 10.3389/fimmu.2016.00006.
- Vázquez-Boland, J. A.; Kuhn, M.; Berche, P.; Chakraborty, T.; Domínguez-Bernal, G.; Goebel, W. et al. (2001): *Listeria* pathogenesis and molecular virulence determinants. In: *Clinical microbiology reviews* 14 (3), S. 584–640. DOI: 10.1128/CMR.14.3.584-640.2001.
- Vestal, Deborah J.; Jeyaratnam, Jonathan A. (2011): The guanylate-binding proteins. Emerging insights into the biochemical properties and functions of this family of large interferon-induced guanosine triphosphatase. In: *Journal of interferon & cytokine research : the official journal of the International Society for Interferon and Cytokine Research* 31 (1), S. 89–97. DOI: 10.1089/jir.2010.0102.
- Villeneuve, J.-P.; Pichette, V. (2004): Cytochrome P450 and Liver Diseases. In: *CDM5* (3), S. 273–282. DOI: 10.2174/1389200043335531.
- Wan, Fengyi; Lenardo, Michael J. (2009): Specification of DNA binding activity of NF- κ B proteins. In: *Cold Spring Harbor perspectives in biology* 1 (4), a000067. DOI: 10.1101/cshperspect.a000067.
- Wan, Fengyi; Lenardo, Michael J. (2010): The nuclear signaling of NF- κ B. Current knowledge, new insights, and future perspectives. In: *Cell research* 20 (1), S. 24–33. DOI: 10.1038/cr.2009.137.
- Wang, Zhuangzhi; Zhao, Chunfang; Moya, Rosa; Davies, Joanna D. (2008): A novel role for CD4⁺ T cells in the control of cachexia. In: *Journal of immunology (Baltimore, Md. : 1950)* 181 (7), S. 4676–4684.

- Weber, Christian (2003): Novel mechanistic concepts for the control of leukocyte transmigration. Specialization of integrins, chemokines, and junctional molecules. In: *Journal of molecular medicine (Berlin, Germany)* 81 (1), S. 4–19. DOI: 10.1007/s00109-002-0391-x.
- Welch, M. D.; Iwamatsu, A.; Mitchison, T. J. (1997): Actin polymerization is induced by Arp2/3 protein complex at the surface of *Listeria monocytogenes*. In: *Nature* 385 (6613), S. 265–269. DOI: 10.1038/385265a0.
- Wessells, Jennifer; Baer, Mark; Young, Howard A.; Claudio, Estefania; Brown, Keith; Siebenlist, Ulrich; Johnson, Peter F. (2004): BCL-3 and NF-kappaB p50 attenuate lipopolysaccharide-induced inflammatory responses in macrophages. In: *The Journal of biological chemistry* 279 (48), S. 49995–50003. DOI: 10.1074/jbc.M404246200.
- Wing, Edward J.; Gregory, Stephen H. (2002): *Listeria monocytogenes*. Clinical and experimental update. In: *The Journal of infectious diseases* 185 Suppl 1, S18-24. DOI: 10.1086/338465.
- Witko-Sarsat, Véronique; Rieu, Philippe; Descamps-Latscha, Béatrice; Lesavre, Philippe; Halbwachs-Mecarelli, Lise (2000): Neutrophils. Molecules, Functions and Pathophysiological Aspects. In: *Lab Invest* 80 (5), S. 617–653. DOI: 10.1038/labinvest.3780067.
- Witter, Alexandra R.; Okunnu, Busola M.; Berg, Rance E. (2016): The Essential Role of Neutrophils during Infection with the Intracellular Bacterial Pathogen *Listeria monocytogenes*. In: *Journal of immunology (Baltimore, Md. : 1950)* 197 (5), S. 1557–1565. DOI: 10.4049/jimmunol.1600599.
- Yamamoto, Masahiro; Takeda, Kiyoshi (2008): Role of nuclear IkappaB proteins in the regulation of host immune responses. In: *Journal of infection and chemotherapy : official journal of the Japan Society of Chemotherapy* 14 (4), S. 265–269. DOI: 10.1007/s10156-008-0619-y.
- Yamamoto, Masahiro; Yamazaki, Soh; Uematsu, Satoshi; Sato, Shintaro; Hemmi, Hiroaki; Hoshino, Katsuaki et al. (2004): Regulation of Toll/IL-1-receptor-mediated gene expression by the inducible nuclear protein IkappaBzeta. In: *Nature* 430 (6996), S. 218–222. DOI: 10.1038/nature02738.
- Yamauchi, Shumpei; Ito, Hiroaki; Miyajima, Atsushi (2010): IkappaBeta, a nuclear IkappaB protein, positively regulates the NF-kappaB-mediated expression of proinflammatory cytokines. In: *Proceedings of the National Academy of Sciences of the United States of America* 107 (26), S. 11924–11929. DOI: 10.1073/pnas.0913179107.
- Yamazaki, S.; Muta, T.; Takeshige, K. (2001): A novel IkappaB protein, IkappaB-zeta, induced by proinflammatory stimuli, negatively regulates nuclear factor-kappaB in the nuclei. In: *The Journal of biological chemistry* 276 (29), S. 27657–27662. DOI: 10.1074/jbc.M103426200.
- Yang, Jiyeon; Zhang, Lixiao; Yu, Caijia; Yang, Xiao-Feng; Wang, Hong (2014): Monocyte and macrophage differentiation. Circulation inflammatory monocyte as biomarker for inflammatory diseases. In: *Biomarker research* 2 (1), S. 1. DOI: 10.1186/2050-7771-2-1.
- Yin, Jiyi; Ferguson, Thomas A. (2009): Identification of an IFN-gamma-producing neutrophil early in the response to *Listeria monocytogenes*. In: *Journal of immunology (Baltimore, Md. : 1950)* 182 (11), S. 7069–7073. DOI: 10.4049/jimmunol.0802410.
- Yokota, M.; Tamachi, T.; Yokoyama, Y.; Maezawa, Y.; Takatori, H.; Suto, A. et al. (2017): IkBNS induces Muc5ac expression in epithelial cells and causes airway hyper-responsiveness in murine asthma models. In: *Allergy* 72 (7), S. 1043–1053. DOI: 10.1111/all.13079.
- Yu, Yen-Rei A.; O'Koren, Emily G.; Hotten, Danielle F.; Kan, Matthew J.; Kopin, David; Nelson, Erik R. et al. (2016): A Protocol for the Comprehensive Flow Cytometric Analysis of Immune Cells in Normal and Inflamed Murine Non-Lymphoid Tissues. In: *PLoS one* 11 (3), e0150606. DOI: 10.1371/journal.pone.0150606.
- Yu, Yonghui; Wan, Yu; Huang, Chuanshu (2009): The biological functions of NF-kappaB1 (p50) and its potential as an anti-cancer target. In: *Current cancer drug targets* 9 (4), S. 566–571.
- Yue, Feng; Cheng, Yong; Breschi, Alessandra; Vierstra, Jeff; Wu, Weisheng; Ryba, Tyrone et al. (2014): A comparative encyclopedia of DNA elements in the mouse genome. In: *Nature* 515 (7527), S. 355–364. DOI: 10.1038/nature13992.
- Zenewicz, Lauren A.; Shen, Hao (2007): Innate and adaptive immune responses to *Listeria monocytogenes*. A short overview. In: *Microbes and infection* 9 (10), S. 1208–1215. DOI: 10.1016/j.micinf.2007.05.008.
- Zhang, N.; Ahsan, M. H.; Purchio, A. F.; West, D. B. (2005): Serum Amyloid A-Luciferase Transgenic Mice. Response to Sepsis, Acute Arthritis, and Contact Hypersensitivity and the Effects of Proteasome Inhibition. In: *The Journal of Immunology* 174 (12), S. 8125–8134. DOI: 10.4049/jimmunol.174.12.8125.
- Zhao, Chunfang; Davies, Joanna D. (2010): A peripheral CD4+ T cell precursor for naive, memory, and regulatory T cells. In: *The Journal of experimental medicine* 207 (13), S. 2883–2894. DOI: 10.1084/jem.20100598.
- Zhu, Jinfang; Yamane, Hidehiro; Paul, William E. (2010): Differentiation of effector CD4 T cell populations (*). In: *Annual review of immunology* 28, S. 445–489. DOI: 10.1146/annurev-immunol-030409-101212.

Appendix

Appendix Table 1: List of regulated genes in course of LM infection identified by microarray analyses of livers from $\text{IkB}_{\text{NS}}^{-/-}$ vs. WT mice. Differentially regulated genes were identified as follows. Per genotype the comparisons: d2 vs. d0, d3 vs. d0 and d4 vs. d0 were considered, resulting in together 6 different conditions. Next, a list of genes was compiled only containing entries with a fold change of differential gene expression of $> \pm 3$ in at least one out of the 6 previous conditions. Stated for each gene are the \log_2 normalized signal intensity, the fold change of the according microarray condition and the k-means cluster correlation according to Figure 31. Gene identifier together with the microarray transcript ID is indicated as well. Genes are sorted according to their k-means cluster number and within the clusters decendingly sorted by the average \log_2 signal intensity. Genes above the applied fold change threshold ($> \pm 3$) are color-coded (green: down-regulated, red: up-regulated).

See table on the next page.

Annotation		log ₂ normalized signal intensity (SI)									Fold changes					Cluster #	
Transcripts Cluster ID	Gene Symbol	WT	WT	WT	WT	lkb _{NS} ^{-/-}	lkb _{NS} ^{-/-}	lkb _{NS} ^{-/-}	lkb _{NS} ^{-/-}	average	[WT d2]	[WT d3]	[WT d4]	[lkb _{NS} ^{-/-} d2]	[lkb _{NS} ^{-/-} d3]	[lkb _{NS} ^{-/-} d4]	k-means cluster assignment
		d0	d2	d3	d4	d0	d2	d3	d4	log ₂ SI	vs. [WT d0]	vs. [WT d0]	vs. [WT d0]	vs. [lkb _{NS} ^{-/-} d0]	vs. [lkb _{NS} ^{-/-} d0]	vs. [lkb _{NS} ^{-/-} d0]	
17233769	Gm5424	12.8	11.6	11.1	11.0	12.7	11.5	11.3	11.8	11.7	-2.4	-3.3	-3.4	-2.2	-2.6	-1.9	1
17358690	Paps2	12.2	10.8	10.5	10.5	12.2	10.7	10.4	10.8	11.0	-2.7	-3.1	-3.1	-2.8	-3.3	-2.6	1
17283573	Serpina6	12.3	10.6	10.4	10.4	12.2	10.9	9.7	10.4	10.9	-3.1	-3.6	-3.7	-2.5	-5.7	-3.3	1
17359287	Cyp2c29	12.7	10.3	9.3	9.4	12.5	10.5	9.8	10.8	10.7	-5.1	-10.5	-10.2	-4.0	-6.4	-3.2	1
17511748	Ces1g	11.7	9.8	10.5	10.5	11.4	10.2	9.4	11.1	10.6	-4.0	-2.4	-2.4	-2.3	-4.0	-1.3	1
17527581	Cyp1a2	11.8	9.4	10.3	10.4	11.8	9.9	9.4	11.2	10.5	-5.5	-2.8	-2.7	-3.7	-5.2	-1.5	1
17455175	Cyp3a11	12.1	9.1	10.4	10.4	11.5	9.4	9.6	11.1	10.4	-8.0	-3.4	-3.4	-4.4	-3.8	-1.4	1
17213021	Aox3	11.2	9.5	10.1	10.2	11.5	9.7	10.0	10.9	10.4	-3.2	-2.1	-2.0	-3.4	-2.9	-1.6	1
17449322	Ugt2b1	12.0	9.8	9.6	9.6	12.2	10.0	9.4	10.2	10.3	-4.4	-5.2	-5.3	-4.6	-7.3	-4.0	1
17529398	Me1	11.6	10.0	10.0	9.9	11.2	10.3	9.9	9.9	10.3	-3.0	-3.1	-3.2	-1.9	-2.5	-2.6	1
17304794	Had1	11.5	10.0	9.6	9.6	11.4	9.9	10.5	10.3	10.3	-2.8	-3.7	-3.8	-2.8	-1.8	-2.1	1
17365001	Cyp2c44	11.8	9.6	9.8	9.9	11.9	9.5	9.6	10.4	10.3	-4.4	-3.8	-3.7	-5.3	-4.7	-2.7	1
17396479	Slc2a2	11.6	8.7	10.0	10.0	11.5	8.8	9.3	10.7	10.1	-7.6	-2.9	-2.9	-6.3	-4.5	-1.7	1
17449332		10.9	9.7	9.8	9.8	10.8	10.1	9.1	10.2	10.0	-2.3	-2.2	-2.2	-1.6	-3.1	-1.5	1
17269521	Acly	11.3	9.9	9.4	9.3	10.8	9.9	9.8	9.8	10.0	-2.8	-3.8	-4.1	-1.9	-2.0	-2.1	1
17256707	G6pc	11.4	9.5	9.5	9.5	11.0	9.4	9.6	9.7	10.0	-3.7	-3.9	-3.9	-2.9	-2.6	-2.4	1
17457330	Akr1d1	11.3	9.1	9.4	9.5	10.9	9.5	9.7	10.2	10.0	-4.6	-3.7	-3.4	-2.7	-2.4	-1.6	1
17399266	Plkr	11.1	9.3	9.4	9.3	11.0	9.5	9.5	9.4	9.8	-3.6	-3.3	-3.5	-2.9	-2.8	-3.0	1
17359316	Cyp2c37	11.8	9.2	9.3	9.3	11.5	9.2	8.3	9.6	9.8	-5.9	-5.5	-5.5	-4.8	-9.0	-3.6	1
17548153		10.7	9.2	8.9	9.0	10.7	9.7	9.8	10.1	9.8	-2.7	-3.3	-3.1	-2.0	-1.8	-1.4	1
17339574	Ehd3	10.3	9.4	9.3	9.3	10.7	8.9	10.2	9.9	9.7	-1.8	-1.9	-2.0	-3.5	-1.4	-1.7	1
17280062	Lpin1	11.2	9.3	8.5	8.5	11.8	9.0	9.6	10.0	9.7	-3.7	-6.6	-6.4	-7.2	-4.8	-3.4	1
17284919	Akr1c14	10.8	9.5	9.1	9.2	10.5	9.8	8.9	9.7	9.7	-2.3	-3.1	-3.0	-1.6	-3.1	-1.7	1
17329220	Ehhadh	11.2	9.1	9.4	9.4	10.8	9.1	9.4	9.3	9.7	-4.4	-3.6	-3.5	-3.3	-2.7	-2.8	1
17359327		11.8	8.8	9.5	9.5	11.6	8.5	7.5	10.3	9.7	-8.3	-5.0	-5.1	-8.0	-16.2	-2.3	1
17288876	Arrdc3	10.5	9.4	9.2	9.3	11.0	9.2	9.2	9.7	9.7	-2.1	-2.3	-2.3	-3.5	-3.7	-2.5	1
17472497	Gys2	10.7	9.4	9.1	9.1	10.5	9.5	9.6	9.3	9.7	-2.4	-3.0	-2.9	-2.0	-1.8	-2.4	1
17362369	Slc22a26	11.3	9.8	8.6	8.6	11.3	9.8	8.2	9.4	9.6	-2.9	-6.4	-6.3	-2.7	-8.6	-3.7	1
17396152	Car3	13.1	8.2	9.2	9.2	12.8	8.1	7.1	9.3	9.6	-29.8	-14.7	-15.2	-26.8	-50.7	-11.4	1
17409130	Gstm3	10.5	9.1	9.6	9.5	10.2	9.6	8.2	10.1	9.6	-2.5	-1.9	-1.9	-1.5	-4.0	-1.0	1
17394297	Pltp	10.8	9.5	9.1	9.1	10.2	9.3	9.2	9.2	9.5	-2.5	-3.4	-3.3	-1.9	-2.0	-1.9	1
17402558	Elov6	10.9	9.1	8.8	8.8	10.7	9.3	9.4	9.3	9.5	-3.5	-4.4	-4.2	-2.6	-2.4	-2.6	1
17364452	Cyp2c54	11.8	8.2	9.2	9.3	11.3	8.4	7.9	10.1	9.5	-11.5	-5.8	-5.7	-7.4	-10.6	-2.3	1
17364440	Cyp2c69	12.4	8.5	8.9	8.9	12.3	8.6	7.7	8.9	9.5	-15.2	-11.4	-11.6	-12.9	-23.1	-10.2	1
17449363	Ugt2a3	10.9	8.9	9.1	9.0	10.9	9.0	8.7	9.2	9.5	-4.0	-3.6	-3.7	-3.8	-4.6	-3.2	1
17211405	Gsta3	10.6	9.1	8.9	8.9	10.4	9.5	8.4	9.8	9.5	-2.9	-3.2	-3.1	-1.9	-4.0	-1.6	1
17511731	Ces1f	11.4	9.3	8.5	8.6	11.2	9.5	8.0	9.2	9.4	-4.3	-7.4	-7.1	-3.2	-9.2	-4.0	1
17425954		10.5	8.7	9.2	9.1	10.5	9.2	8.8	9.5	9.4	-3.4	-2.3	-2.6	-2.3	-3.2	-2.0	1
17241934	Gstt1	10.8	9.2	8.7	8.8	10.8	9.1	8.8	9.2	9.4	-3.2	-4.3	-4.0	-3.2	-4.1	-3.1	1
17242842	Gamt	11.2	8.4	8.9	9.0	10.8	8.7	8.8	9.5	9.4	-6.7	-4.7	-4.4	-4.2	-3.9	-2.5	1
17343488	Cyp4f14	11.0	8.6	8.5	8.5	10.9	9.0	9.1	9.5	9.4	-5.4	-5.4	-5.8	-3.6	-3.5	-2.6	1
17504477	Ces2a	10.9	8.9	8.4	8.5	10.9	9.1	8.7	9.6	9.4	-3.8	-5.7	-5.1	-3.4	-4.4	-2.4	1
17492478	ldh2	10.4	8.9	8.8	8.8	10.1	9.1	9.0	9.3	9.3	-2.8	-3.2	-3.2	-2.0	-2.2	-1.8	1
17504616	Ces3b	10.6	8.3	8.7	8.7	10.9	8.5	9.0	9.3	9.3	-4.8	-3.8	-3.8	-5.5	-3.7	-3.0	1
17258851	Afmid	10.6	8.9	8.4	8.3	10.5	9.1	8.7	9.4	9.3	-3.2	-4.4	-4.7	-2.6	-3.5	-2.2	1
17252912	Tlcd2	10.9	8.6	8.4	8.5	10.7	8.9	8.8	9.0	9.2	-5.1	-5.9	-5.5	-3.4	-3.7	-3.3	1
17513655	Car5a	10.3	9.0	8.5	8.5	10.2	9.1	8.8	9.3	9.2	-2.5	-3.4	-3.5	-2.2	-2.7	-1.9	1
17230408	Adck3	10.8	8.9	8.5	8.6	10.3	8.9	8.5	9.2	9.2	-3.7	-4.8	-4.7	-2.6	-3.4	-2.1	1
17340099	Abcg8	10.1	8.9	8.4	8.4	10.0	9.2	8.5	9.2	9.1	-2.2	-3.1	-3.2	-1.8	-3.0	-1.7	1
17475026	Ethe1	10.2	8.9	8.4	8.4	10.0	8.9	8.9	8.9	9.1	-2.4	-3.4	-3.4	-2.0	-2.1	-2.1	1
17482230	Acsm5	10.3	8.9	8.4	8.4	10.1	9.1	8.2	9.1	9.1	-2.6	-3.7	-3.6	-2.0	-3.8	-2.1	1
17378359	Acss2	11.1	8.8	7.7	7.7	10.8	9.1	8.4	8.7	9.0	-5.1	-11.0	-10.8	-3.3	-5.3	-4.4	1
17219231	Nr1i3	10.1	8.4	8.5	8.6	10.2	8.6	8.6	9.3	9.0	-3.2	-3.1	-2.9	-3.0	-3.0	-1.8	1
17310259	Prir	10.5	8.5	8.4	8.4	10.2	8.6	8.4	9.1	9.0	-3.9	-4.2	-4.2	-3.0	-3.6	-2.1	1
17528629	Lipc	10.4	8.5	8.4	8.4	10.3	8.6	8.2	9.1	9.0	-3.8	-4.2	-4.0	-3.3	-4.4	-2.4	1
17493432	Thrsp	11.1	8.3	7.8	7.7	11.0	8.8	7.9	9.0	9.0	-6.5	-9.4	-9.9	-4.7	-8.8	-4.1	1
17417223	Cyp4a10	11.7	7.4	8.7	8.7	11.1	5.9	8.8	9.1	8.9	-19.7	-8.0	-7.8	-35.9	-4.9	-3.9	1
17455554	N4bp211	9.5	8.6	8.4	8.5	10.1	8.8	8.4	8.9	8.9	-1.9	-2.1	-1.9	-2.5	-3.3	-2.3	1
17476424	Prodh2	10.2	8.6	8.2	8.2	9.9	8.6	8.7	8.8	8.9	-3.0	-4.0	-3.9	-2.5	-2.3	-2.2	1
17473941	Sult2a2	10.7	9.0	7.9	7.9	9.5	9.2	7.8	9.1	8.9	-3.3	-7.1	-7.0	-1.2	-3.3	-1.3	1
17547877	Deptor	9.9	8.6	8.1	8.2	10.0	8.6	8.8	8.6	8.8	-2.5	-3.4	-3.1	-2.7	-2.3	-2.5	1
17467062	Inmt	11.6	7.5	8.0	7.9	11.6	8.1	7.1	8.8	8.8	-17.7	-12.8	-13.5	-11.2	-21.8	-6.6	1
17437765	Klb	9.8	8.4	8.0	8.1	9.8	8.7	8.7	8.8	8.8	-2.6	-3.3	-3.2	-2.1	-2.0	-2.0	1
17486707	2810007J24Rik	11.3	7.5	8.4	8.4	11.2	7.4	7.6	8.3	8.8	-13.4	-7.4	-7.1	-13.4	-12.1	-7.6	1
17428457	Cyp4a14	11.3	8.2	7.9	7.8	10.7	6.7	8.3	9.1	8.7	-8.5	-10.6	-10.9	-16.4	-5.2	-3.1	1
17317398	A1bg	12.1	7.4	8.6	8.6	11.7	7.2	6.6	7.6	8.7	-26.1	-11.5	-11.9	-22.7	-35.4	-17.5	1
17519649	Gsta4	10.3	8.2	8.6	8.6	10.0	8.2	7.6	8.4	8.7	-4.4	-3.2	-3.3	-3.4	-5.3	-3.0	1
17334819	O610011F06Rik	9.7	8.6	8.0	8.2	9.6	8.5	8.7	8.6	8.7	-2.2	-3.1	-2.7	-2.1	-1.9	-2.0	1
17267685	Pcpt	10.0	8.4	8.1	8.1	9.7	8.4	8.7	8.3	8.7	-3.0	-3.8	-3.8	-2.4	-2.0	-2.7	1
17400124	Selenbp2	9.8	8.4	8.0	8.0	10.3	8.5	8.2	8.5	8.7	-2.5	-3.4	-3.4	-3.4	-4.3	-3.5	1
17417738	Hyi	9.8	8.5	8.2	8.2	9.8	8.5	8.3	8.4	8.7	-2.4	-3.0	-2.9	-2.4	-2.8	-2.5	1
17423051	Cyp7a1	11.0	7.1	8.1	8.0	10.8	8.1	6.6	9.5	8.7	-15.6	-7.6	-8.0	-6.5	-18.1	-2.4	1
17214106	Igfbp2	10.1	8.1	7.9	7.9	10.1	8.2	8.4	8.5	8.7	-3.9	-4.5	-4.4	-3.7	-3.3	-3.0	1
17225320	Gm20528	9.9	8.2	7.9	8.0	9.6	8.6	8.2	8.6	8.6	-3.2	-3.9	-3.8	-2.0	-2.6	-2.1	1
17472364	Scol1a4	10.6	7.7	7.8	7.8	10.3	7.7	7.3	8.8	8.5	-7.1	-6.7	-6.8	-6.2	-8.0	-2.9	1
17455193		9.5	8.3	7.9	8.1	9.4	7.8	8.2	8.6	8.5							

Annotation		log ₂ normalized signal intensity (SI)								Fold changes						Cluster #	
Transcripts Cluster ID	Gene Symbol	WT	WT	WT	WT	lkb _{NS} ^{-/-}	lkb _{NS} ^{-/-}	lkb _{NS} ^{-/-}	lkb _{NS} ^{-/-}	average	[WT d2]	[WT d3]	[WT d4]	[lkb _{NS} ^{-/-} d2]	[lkb _{NS} ^{-/-} d3]	[lkb _{NS} ^{-/-} d4]	k-means cluster assignment
		d0	d2	d3	d4	d0	d2	d3	d4	log ₂ SI	vs. [WT d0]	vs. [WT d0]	vs. [WT d0]	vs. [lkb _{NS} ^{-/-} d0]	vs. [lkb _{NS} ^{-/-} d0]	vs. [lkb _{NS} ^{-/-} d0]	
17408336	Hsd3b3	10.0	8.1	6.8	6.8	9.8	8.2	6.9	8.2	8.1	-3.7	-8.8	-8.9	-3.2	-7.6	-3.1	1
17511693	Ces1d	10.5	6.9	7.6	7.6	10.1	7.2	6.9	8.0	8.1	-11.9	-7.4	-7.4	-7.6	-9.0	-4.1	1
17425926		9.3	7.9	7.4	7.1	9.2	8.0	7.6	8.1	8.1	-2.6	-3.7	-4.4	-2.2	-3.0	-2.2	1
17357861	Keg1	9.8	7.4	7.4	7.3	9.8	7.6	7.2	8.1	8.1	-5.1	-5.3	-5.4	-4.6	-6.3	-3.3	1
17271350	Abca8a	9.6	7.4	7.2	7.3	9.7	7.6	8.0	7.7	8.1	-4.7	-5.2	-4.9	-4.2	-3.3	-4.1	1
17520073	Nt5e	9.7	7.7	7.4	7.3	9.4	7.8	7.3	7.7	8.0	-4.1	-5.1	-5.3	-3.2	-4.4	-3.4	1
17519673	Gm3776...	9.3	7.5	8.3	8.3	8.3	7.8	6.8	7.8	8.0	-3.5	-2.0	-2.1	-1.5	-2.8	-1.5	1
17294135	Srd5a1...	9.1	7.6	7.5	7.4	9.3	7.8	7.6	7.8	8.0	-2.7	-3.1	-3.3	-2.7	-3.3	-2.8	1
17511714	Ces1e	10.2	7.4	7.1	7.0	9.9	7.7	7.0	7.8	8.0	-7.2	-8.7	-9.5	-4.6	-7.4	-4.3	1
17410672	0610031O16Rik	9.1	7.3	7.4	7.3	8.9	7.4	8.4	8.0	8.0	-3.5	-3.4	-3.5	-2.9	-1.4	-1.9	1
17445922	Reln	9.1	7.5	7.7	7.7	8.8	7.3	7.9	7.8	8.0	-3.2	-2.8	-2.7	-2.8	-1.8	-1.9	1
17248263	Hba-a2...	9.3	7.8	7.6	7.6	8.1	8.1	7.6	7.6	7.9	-2.7	-3.2	-3.2	1.0	-1.4	-1.4	1
17532063	Acaa1b	9.9	6.8	8.0	7.8	9.6	6.8	7.2	7.4	7.9	-8.4	-3.7	-4.1	-6.7	-5.1	-4.6	1
17407956	Car14	9.2	6.9	7.4	7.6	9.2	7.1	7.4	8.6	7.9	-4.9	-3.5	-3.1	-4.5	-3.5	-1.6	1
17241921	Gstt3...	9.4	7.8	7.0	7.2	9.5	7.9	7.0	7.4	7.9	-3.1	-5.1	-4.6	-3.0	-5.7	-4.2	1
17318118	9030619P08Rik	9.8	7.0	7.1	7.5	10.1	7.4	6.2	7.9	7.9	-6.8	-6.2	-4.8	-6.8	-14.7	-4.7	1
17472385	Slc1a1	10.6	7.2	6.4	6.4	11.3	7.8	6.8	6.4	7.9	-10.4	-18.0	-17.8	-11.1	-22.1	-28.8	1
17311504	Colec10	9.3	6.8	7.4	7.4	9.2	6.8	7.9	8.1	7.9	-5.7	-3.8	-3.8	-5.3	-2.4	-2.1	1
17334468	Igfals	8.9	7.3	7.2	7.2	9.1	7.3	7.5	7.8	7.8	-3.1	-3.3	-3.4	-3.5	-2.9	-2.5	1
17244705	Acsc3	9.7	7.5	6.9	6.9	9.4	7.3	7.0	7.5	7.8	-4.5	-7.1	-6.8	-4.2	-5.1	-3.7	1
17397990	Mme	10.6	7.0	6.9	7.0	10.0	6.8	6.9	6.8	7.8	-12.0	-12.2	-11.9	-9.6	-8.6	-9.3	1
17371847	Pdk1	8.9	7.3	7.4	7.4	8.6	7.5	7.5	7.3	7.7	-3.0	-2.8	-2.8	-2.2	-2.2	-2.6	1
17405746	Rarres1	8.9	7.2	7.3	7.3	8.5	7.3	7.6	7.7	7.7	-3.2	-2.9	-2.9	-2.4	-2.0	-1.8	1
17215539	Spp2	9.4	7.4	6.9	7.0	9.1	7.6	7.2	7.2	7.7	-4.0	-5.5	-5.1	-2.9	-3.6	-3.6	1
17467209	Fam13a	8.7	7.7	7.2	7.3	8.6	7.8	6.6	7.6	7.7	-2.0	-2.7	-2.6	-1.7	-4.1	-2.0	1
17290781	Sugct	9.2	7.6	6.8	6.8	8.7	7.5	7.3	7.4	7.7	-3.1	-5.4	-5.5	-2.3	-2.7	-2.5	1
17475385	Cyp2b9	11.7	8.6	9.1	9.2	5.1	7.6	4.8	5.0	7.6	-8.8	-6.0	-5.8	5.4	-1.2	-1.1	1
17238172	Rdh16	10.0	7.1	6.5	6.6	9.6	6.9	6.9	7.5	7.6	-7.4	-11.6	-10.8	-6.5	-6.5	-4.3	1
17324416	C730014E05Rik	8.9	7.1	6.9	6.9	8.4	7.2	7.4	7.6	7.5	-3.4	-3.9	-4.0	-2.3	-1.9	-1.7	1
17274184	Socs2...	8.7	6.8	7.2	7.3	8.9	6.5	7.1	7.6	7.5	-3.7	-2.8	-2.7	-5.2	-3.6	-2.5	1
17444697	Cyp3a59	8.8	6.7	7.2	7.3	8.9	6.9	6.5	7.5	7.5	-4.4	-3.0	-2.8	-3.8	-5.1	-2.7	1
17355443	Lipg	8.7	6.7	7.1	7.1	9.0	6.9	6.8	7.1	7.4	-3.9	-3.0	-3.0	-4.5	-4.7	-3.8	1
17281312	Slc25a21	8.4	7.2	6.7	6.8	8.4	7.2	7.2	7.4	7.4	-2.3	-3.3	-3.1	-2.4	-2.5	-2.1	1
17300544	Fitm1	8.8	7.1	7.1	7.1	8.2	7.1	7.1	6.9	7.4	-3.2	-3.3	-3.3	-2.2	-2.2	-2.5	1
17423577	Atp6v0d2	9.7	6.6	6.8	6.8	8.8	6.7	6.3	7.4	7.4	-8.1	-7.2	-7.2	-4.1	-5.8	-2.7	1
17345391	Slc22a7	8.9	6.2	7.3	7.2	8.7	6.2	6.7	7.3	7.3	-6.4	-3.1	-3.3	-5.7	-4.1	-2.7	1
17359918	Elov3	8.4	7.2	6.5	6.3	9.3	6.3	7.5	6.5	7.2	-2.3	-3.7	-4.3	-8.1	-3.6	-7.0	1
17455159	Cyp3a44	9.4	6.4	6.6	6.9	9.2	6.5	6.3	6.6	7.2	-8.1	-7.0	-5.8	-6.3	-7.6	-6.2	1
17337750	Gpr110	8.5	6.7	6.6	6.4	8.5	6.9	7.2	7.0	7.2	-3.4	-3.8	-4.2	-3.0	-2.6	-3.0	1
17548219		8.6	6.6	6.5	6.5	8.3	6.9	7.1	7.2	7.2	-4.1	-4.2	-4.4	-2.5	-2.4	-2.1	1
17277152	Acot3	8.5	6.8	6.7	6.7	8.2	6.8	6.8	6.8	7.2	-3.3	-3.5	-3.6	-2.6	-2.5	-2.6	1
17404191		10.8	5.4	6.3	6.5	10.6	5.9	5.2	6.7	7.2	-41.8	-21.8	-19.6	-25.8	-40.4	-14.7	1
17397932	Sucnr1	9.1	6.8	6.5	6.5	8.2	6.9	6.4	6.8	7.2	-4.9	-5.8	-5.8	-2.5	-3.4	-2.7	1
17248127		7.5	6.3	7.0	7.0	8.3	6.5	6.6	7.7	7.1	-2.3	-1.4	-1.5	-3.5	-3.1	-1.5	1
17277146	Acot4	8.4	6.7	6.6	6.4	8.0	6.7	7.2	6.6	7.1	-3.2	-3.3	-3.9	-2.5	-1.8	-2.8	1
17250582		8.1	6.6	6.5	6.5	7.6	7.0	6.5	6.9	7.0	-2.9	-3.0	-3.0	-1.6	-2.1	-1.7	1
17364426		8.6	6.4	6.5	6.3	8.4	6.6	6.0	6.8	7.0	-4.7	-4.3	-4.8	-3.4	-5.2	-2.9	1
17498663	C330021F23Rik	8.1	6.4	6.5	6.5	7.8	6.2	6.4	6.6	6.8	-3.3	-3.0	-3.0	-3.1	-2.7	-2.4	1
17381717	Itpa8	7.9	6.2	6.8	6.8	7.3	6.2	6.7	6.7	6.8	-3.1	-2.0	-2.2	-2.1	-1.5	-1.5	1
17449394	Sult1b1	8.2	6.7	6.1	6.1	7.7	6.9	6.4	6.6	6.8	-2.9	-4.3	-4.4	-1.7	-2.5	-2.1	1
17469656	Srgap3	7.7	6.8	6.3	6.3	7.9	6.3	6.4	6.5	6.8	-2.0	-2.8	-2.7	-3.1	-2.8	-2.7	1
17298126	Lrtm1	7.9	6.7	6.2	6.2	7.4	6.6	6.4	6.6	6.8	-2.4	-3.3	-3.2	-1.8	-2.0	-1.8	1
17397575	Postn	7.8	6.7	6.4	6.0	7.5	6.4	6.3	7.0	6.8	-2.2	-2.7	-3.4	-2.2	-2.3	-1.5	1
17392022	LOC102633833...	7.9	6.5	6.0	6.2	7.7	6.5	6.4	6.4	6.7	-2.6	-3.8	-3.4	-2.4	-2.5	-2.5	1
17504512	Ces2c	8.2	6.0	6.3	6.4	8.4	6.5	5.6	6.0	6.7	-4.8	-3.7	-3.7	-3.7	-7.2	-5.5	1
17277140	Acot1	7.3	6.3	6.4	6.4	7.8	6.0	6.7	6.0	6.6	-2.0	-1.9	-1.9	-3.4	-2.1	-3.5	1
17418757	170080G11Rik	8.3	5.4	6.4	6.5	7.8	5.6	6.2	6.1	6.5	-7.4	-3.8	-3.5	-4.9	-3.0	-3.3	1
17475373	Cyp2b13	11.1	5.8	6.5	6.5	5.5	5.4	5.1	6.4	6.5	-38.7	-24.1	-24.2	-1.0	-1.3	2.0	1
17414507	Gm13773	8.1	6.0	5.9	5.8	8.1	6.1	5.9	6.2	6.5	-4.3	-4.5	-4.8	-4.2	-4.6	-3.9	1
17339460	Lpin2	7.6	6.5	6.0	6.2	7.8	5.8	6.6	5.6	6.5	-2.1	-2.9	-2.6	-3.8	-2.2	-4.5	1
17291821	Eci3	7.7	6.4	5.9	5.9	7.2	6.6	6.1	6.3	6.5	-2.4	-3.5	-3.4	-1.5	-2.3	-1.9	1
17417255	Cyp4a32	7.5	6.2	6.1	6.1	7.7	5.8	6.9	5.8	6.5	-2.4	-2.7	-2.6	-3.7	-1.7	-3.7	1
17408323	Hsd3b2	8.0	5.8	5.6	5.4	8.5	6.4	6.1	6.1	6.5	-4.5	-5.3	-5.9	-4.2	-5.1	-5.4	1
17345989	Sult1c2	7.8	6.3	5.9	6.0	7.4	6.3	5.9	6.2	6.5	-2.8	-3.7	-3.4	-2.1	-2.9	-2.4	1
17510484	Cib3	6.6	5.7	6.4	6.3	7.5	5.9	5.7	6.4	6.3	-2.0	-1.2	-1.3	-3.0	-3.5	-2.1	1
17463443	Clec2h	7.6	5.6	6.1	6.1	7.8	5.7	5.4	6.1	6.3	-3.9	-2.8	-2.8	-4.2	-5.0	-3.2	1
17223946	Erbp4	7.4	5.8	5.9	5.9	7.5	5.8	5.9	5.9	6.3	-3.0	-2.8	-2.8	-3.3	-3.1	-3.1	1
17359239	Cyp2c55	8.5	5.4	5.7	5.5	7.8	5.7	5.4	5.7	6.2	-8.5	-7.2	-8.1	-4.2	-5.1	-4.3	1
17330463	Gm19522	7.5	5.9	5.7	5.8	7.3	5.8	5.8	5.8	6.2	-3.1	-3.6	-3.4	-2.7	-2.7	-2.8	1
17455111	Cyp3a16	9.4	5.2	4.9	4.9	9.1	5.3	4.7	5.7	6.2	-17.8	-23.0	-21.9	-14.6	-21.2	-10.8	1
17362383	Slc22a27	8.6	5.5	5.5	5.5	7.7	5.6	5.2	5.6	6.2	-8.1	-8.5	-8.5	-4.4	-5.6	-4.3	1
17220249	9130409I23Rik	7.4	6.0	5.7	5.6	7.0	6.3	5.2	5.9	6.1	-2.6	-3.2	-3.4	-1.6	-3.4	-2.1	1
17291323	Gm23340	5.9	5.1	6.1	6.0	7.0	5.0	7.4	6.4	6.1	-1.7	1.2	1.1	-4.0	1.3	-1.5	1
17473932	Sult2a5	7.8	5.1	5.9	5.9	6.1	5.8	5.2	6.7	6.1	-6.6	-3.8	-3.7	-1.3	-1.9	1.5	1
17414520	Gm13775	8.5	5.0	5.3	5.3	8.2	4.9	5.0	5.5	5.9	-11.3	-9.4	-9.6	-10.0	-9.6	-6.7	1
17404180	Car1	7.0	5.1	5.7	5.6	7.2	5.3	5.2	5.8	5.8	-3.7	-2.5	-2.5	-3.6	-3.9	-2.6	1
17408360	Hao2	8.4	5.1	5.4	5.5	6.8	5.1	5.0	5.3								

Annotation		log ₂ normalized signal intensity (SI)								Fold changes					Cluster #		
Transcripts Cluster ID	Gene Symbol	WT	WT	WT	WT	lkb _{NS} ^{-/-}	lkb _{NS} ^{-/-}	lkb _{NS} ^{-/-}	lkb _{NS} ^{-/-}	average	[WT d2]	[WT d3]	[WT d4]	[lkb _{NS} ^{-/-} d2]	[lkb _{NS} ^{-/-} d3]	[lkb _{NS} ^{-/-} d4]	k-means cluster assignment
		d0	d2	d3	d4	d0	d2	d3	d4	log ₂ SI	vs. [WT d0]	vs. [WT d0]	vs. [WT d0]	vs. [lkb _{NS} ^{-/-} d0]	vs. [lkb _{NS} ^{-/-} d0]	vs. [lkb _{NS} ^{-/-} d0]	
17286487	Bphl	11.1	10.1	9.5	9.5	10.8	10.1	10.0	10.1	10.1	-2.1	-3.1	-3.1	-1.6	-1.7	-1.6	2
17429632	Mfsd2a	11.0	10.0	9.2	9.2	10.7	10.0	10.0	10.3	10.1	-2.0	-3.4	-3.5	-1.5	-1.2	-1.3	2
17475399	Cyp2a4	11.7	10.2	8.3	8.3	11.7	11.1	9.2	9.8	10.0	-2.8	-10.4	-10.6	-1.6	-5.6	-3.7	2
17244350	Amdhd1	11.0	10.2	8.9	8.9	10.8	10.3	9.8	9.7	10.0	-1.7	-4.2	-4.1	-1.4	-1.9	-2.0	2
17535434	Nsdhl	11.1	10.1	8.6	8.6	11.0	10.3	10.3	9.4	9.9	-2.0	-5.6	-5.4	-1.6	-1.6	-3.0	2
17445308	Cyp51	10.6	10.1	8.7	8.7	10.4	10.3	9.9	9.4	9.8	-1.4	-3.7	-3.7	-1.1	-1.4	-2.0	2
17331102	Nit2	10.7	9.7	8.9	9.0	10.4	9.8	9.5	9.7	9.7	-2.0	-3.4	-3.3	-1.5	-1.8	-1.6	2
17409575	Amy1	10.8	9.9	8.7	8.8	10.5	9.6	9.7	9.6	9.7	-1.8	-4.2	-3.9	-1.8	-1.8	-1.9	2
17521211	Abhd14b	10.5	9.6	8.7	8.6	10.3	9.7	9.4	9.5	9.5	-1.8	-3.4	-3.6	-1.5	-1.8	-1.8	2
17420777	Aldh4a1...	10.5	9.5	8.7	8.8	10.2	9.6	9.4	9.5	9.5	-2.1	-3.4	-3.4	-1.5	-1.8	-1.6	2
17246284	Suox	10.3	9.6	8.7	8.8	10.2	9.5	9.4	9.4	9.5	-1.7	-3.0	-2.9	-1.6	-1.8	-1.7	2
17509629	Msmo1	10.3	9.8	8.3	8.4	10.2	10.0	9.8	9.0	9.5	-1.4	-3.9	-3.6	-1.1	-1.3	-2.2	2
17406908	Fdps	10.6	9.7	8.3	8.5	10.3	9.9	9.6	9.0	9.5	-1.9	-4.8	-4.3	-1.3	-1.6	-2.4	2
17532605	mt-Tm	10.3	9.6	8.4	8.3	10.3	9.9	9.7	9.3	9.5	-1.6	-3.7	-4.0	-1.3	-1.5	-2.0	2
17233873	Pbid1	10.4	9.3	8.5	8.6	10.1	9.3	9.6	9.5	9.4	-2.1	-3.5	-3.3	-1.7	-1.4	-1.5	2
17295233	Hmgcr	10.5	9.4	8.3	8.3	10.5	9.6	9.5	8.9	9.4	-2.1	-4.6	-4.5	-1.8	-2.0	-3.1	2
17268884	Nr1d1	10.1	9.6	8.7	8.6	10.6	9.5	8.9	8.8	9.3	-1.4	-2.7	-2.8	-2.2	-3.1	-3.5	2
17460826	Klf15	10.1	9.5	8.2	8.2	10.1	9.5	9.2	9.1	9.2	-1.5	-3.6	-3.6	-1.5	-1.9	-1.9	2
17217083	Pm20d1	10.1	9.4	8.0	8.1	10.1	9.5	9.3	8.7	9.2	-1.6	-4.2	-4.2	-1.6	-1.7	-2.6	2
17462145	8430408G22Rik	10.0	9.2	8.5	8.3	9.8	9.1	9.4	8.8	9.1	-1.7	-2.9	-3.2	-1.6	-1.3	-2.0	2
17232426	Echdc1	10.1	9.2	8.4	8.4	9.9	9.3	9.0	8.7	9.1	-1.8	-3.2	-3.3	-1.5	-1.8	-2.3	2
17263673	Shmt1	10.3	9.1	8.2	8.2	10.0	9.3	8.6	9.0	9.1	-2.3	-4.3	-4.3	-1.6	-2.7	-2.0	2
17232489	Sult3a1	10.2	9.6	7.7	7.7	10.0	9.6	8.5	9.1	9.0	-1.5	-5.9	-5.9	-1.3	-2.9	-1.8	2
17518310	Gm23344	9.5	9.4	8.2	8.2	7.9	9.6	9.5	9.6	8.5	-1.1	-2.4	-3.0	-1.1	-1.0	-2.2	2
17312567	Gpt	10.3	9.1	8.0	7.9	10.0	9.1	8.6	9.1	9.0	-2.4	-4.9	-5.4	-1.9	-2.6	-1.9	2
17532641	mt-Tn	10.2	9.7	7.3	7.4	9.9	9.8	9.5	8.5	9.0	-1.5	-7.7	-7.3	-1.0	-1.3	-2.6	2
17282158	Rdh11	10.5	9.1	7.9	7.8	10.2	9.3	8.8	8.6	9.0	-2.6	-6.3	-6.4	-1.8	-2.6	-3.0	2
17285056	Idi1...	10.1	9.0	7.9	7.9	9.9	9.4	9.1	8.5	9.0	-2.2	-4.5	-4.5	-1.5	-1.7	-2.7	2
17224133	Pecr	10.1	8.7	8.2	8.2	9.9	8.9	8.9	8.9	9.0	-2.6	-3.9	-4.0	-1.9	-1.9	-2.0	2
17295503	Mccc2	9.8	9.1	8.2	8.2	9.6	9.2	8.8	8.6	8.9	-1.7	-3.2	-3.2	-1.3	-1.7	-2.0	2
17541917	Snord61	9.7	9.3	7.6	7.6	9.5	9.5	9.5	8.5	8.9	-1.3	-4.1	-4.1	-1.0	-1.0	-2.0	2
17263765	Slc47a1	10.3	8.7	7.7	7.7	10.0	8.7	8.5	8.8	8.8	-3.1	-5.8	-5.8	-2.5	-2.9	-2.4	2
17229466	Hsd17b7	9.7	8.9	7.9	7.9	9.6	9.1	9.1	8.2	8.8	-1.7	-3.5	-3.5	-1.4	-1.4	-2.6	2
17314074	Selo	9.7	8.7	8.1	8.0	9.7	8.8	8.7	8.2	8.7	-2.0	-3.1	-3.3	-1.8	-1.9	-2.7	2
17364392	Cyp2c38	10.2	8.8	7.7	7.9	10.4	8.4	8.6	7.9	8.7	-2.6	-5.3	-5.0	-4.2	-3.6	-5.7	2
17441490	Fbxo21	9.6	8.6	7.9	8.0	9.5	8.7	8.6	8.5	8.7	-1.9	-3.1	-3.0	-1.7	-1.8	-1.9	2
17441949		9.5	8.5	7.9	7.9	9.4	8.8	8.7	8.6	8.7	-2.0	-3.0	-3.1	-1.5	-1.7	-1.7	2
17491035	Abcc6	9.5	8.8	7.7	7.8	9.6	8.8	8.6	8.3	8.7	-1.6	-3.3	-3.3	-1.6	-1.9	-2.3	2
17460342	Tprkb	9.6	8.7	7.9	8.0	9.4	8.6	8.5	8.5	8.6	-2.0	-3.3	-3.2	-1.8	-2.0	-2.0	2
17224125	Mreg	9.5	8.6	7.9	8.1	9.2	8.7	8.8	8.2	8.6	-1.9	-3.0	-2.6	-1.5	-1.4	-2.0	2
17337816	Cyp39a1	9.3	8.7	7.7	7.6	9.6	8.8	8.6	8.5	8.6	-1.6	-3.1	-3.3	-1.8	-2.0	-2.1	2
17361921	Tm7sf2	9.9	8.6	7.6	7.6	9.7	8.7	8.3	8.2	8.6	-2.4	-4.9	-4.8	-2.0	-2.7	-2.8	2
17329494	Gm20319	9.5	8.4	7.9	7.8	9.5	8.4	8.7	8.5	8.6	-2.1	-2.9	-3.1	-2.1	-1.7	-2.0	2
17468926		9.3	8.3	7.5	7.5	9.2	8.7	8.8	8.9	8.5	-2.0	-3.7	-3.5	-1.5	-1.3	-1.3	2
17312396	Cycl1	9.3	8.4	7.7	7.6	9.2	8.6	8.5	8.2	8.4	-1.9	-3.2	-3.4	-1.5	-1.6	-1.9	2
17263535	Sreb1	9.4	8.2	7.7	7.7	9.1	8.6	8.2	8.5	8.4	-2.3	-3.2	-3.2	-1.4	-1.8	-1.5	2
17248276	Hba-a2...	10.2	8.6	7.4	7.3	9.5	8.9	8.2	7.1	8.4	-3.0	-7.2	-7.7	-1.5	-2.5	-5.5	2
17234552	Lss	9.7	8.7	7.2	7.1	9.2	8.8	8.6	7.8	8.4	-2.0	-5.4	-6.0	-1.3	-1.5	-2.5	2
17241789	Cisd1	9.4	8.2	7.7	7.7	9.2	8.4	8.2	8.1	8.4	-2.3	-3.3	-3.1	-1.7	-2.0	-2.2	2
17383588	Ccbl1	9.4	8.7	7.0	6.8	9.5	8.8	8.7	7.9	8.3	-1.6	-5.3	-6.1	-1.6	-1.7	-3.1	2
17399474	Pmvk	9.7	8.3	7.5	7.6	9.4	8.5	8.2	7.6	8.3	-2.7	-4.5	-4.3	-1.9	-2.2	-3.3	2
17467575	Thns12	9.2	8.4	7.5	7.5	8.8	8.4	8.1	8.2	8.3	-1.8	-3.3	-3.4	-1.2	-1.5	-1.5	2
17278239	Serpina4-ps1	8.2	7.5	7.6	7.7	10.1	8.0	9.3	7.7	8.3	-1.6	-1.6	-1.4	-4.2	-1.8	-5.1	2
17279167	Snora28...	8.9	8.4	7.3	7.3	9.0	8.6	8.7	7.8	8.2	-1.4	-3.1	-3.2	-1.3	-1.2	-2.2	2
17239616	Pex7	9.1	8.4	7.4	7.5	8.7	8.5	8.3	8.0	8.2	-1.7	-3.3	-3.2	-1.2	-1.4	-1.7	2
17517605	Imp3	8.9	8.4	7.2	7.2	8.9	8.6	8.4	8.0	8.2	-1.5	-3.2	-3.2	-1.2	-1.4	-1.8	2
17440826	Acacb	9.7	8.3	7.0	7.0	9.5	8.3	7.9	7.5	8.2	-2.6	-6.3	-6.3	-2.3	-2.9	-3.8	2
17291361	Aldh5a1	9.1	8.0	7.4	7.4	9.1	8.1	8.0	7.9	8.1	-2.1	-3.4	-3.4	-2.0	-2.0	-2.2	2
17463169	Scnn1a	9.1	8.0	7.4	7.4	9.0	7.9	8.3	7.9	8.1	-2.3	-3.2	-3.4	-2.0	-1.5	-2.1	2
17451536	Mmab	8.9	8.3	7.2	7.1	9.0	8.4	8.2	7.7	8.1	-1.5	-3.2	-3.4	-1.4	-1.7	-2.4	2
17353358	Stard4	9.2	8.0	7.2	7.1	9.1	8.3	8.1	7.8	8.1	-2.4	-4.2	-4.4	-1.7	-2.0	-2.4	2
17303722	Kcnk5	9.0	8.1	6.9	6.9	8.8	8.3	8.3	8.2	8.1	-1.9	-4.1	-4.1	-1.5	-1.5	-1.6	2
17438940	5830473C10Rik	9.5	8.1	6.8	7.0	9.3	8.1	8.2	7.5	8.1	-2.7	-6.4	-5.8	-2.2	-2.1	-3.5	2
17312511	Adck5	9.0	7.8	7.2	7.1	9.3	7.8	8.2	7.9	8.1	-2.2	-3.4	-3.6	-2.8	-2.1	-2.6	2
17438062	Nipa1	9.3	8.1	7.1	7.1	9.3	8.2	7.8	7.5	8.0	-2.3	-4.6	-4.6	-2.1	-2.9	-3.4	2
17374738	Gchfr	9.2	7.9	7.1	7.2	9.0	7.9	8.1	8.0	8.0	-2.6	-4.4	-4.2	-2.2	-1.9	-2.0	2
17232082	Raet1e...	9.0	8.6	7.3	7.3	8.2	8.1	8.1	7.4	8.0	-1.4	-3.5	-3.3	-1.1	-1.1	-1.6	2
17211526	Gm5524	9.7	8.2	6.8	6.6	9.5	8.3	7.3	7.5	8.0	-2.9	-7.8	-8.5	-2.3	-4.5	-4.0	2
17532593	mt-Tf	8.8	7.7	7.2	7.1	8.6	8.1	8.5	7.6	7.9	-2.1	-3.1	-3.3	-1.4	-1.0	-2.0	2
17386479		8.8	8.1	7.1	7.3	8.4	8.3	8.6	6.9	7.9	-1.6	-3.1	-2.8	-1.1	1.1	-2.9	2
17513681	Mvd	8.8	8.1	7.1	7.0	8.5	8.4	8.1	7.4	7.9	-1.5	-3.3	-3.3	-1.1	-1.3	-2.2	2
17309397	Tgds	8.6	8.1	7.0	7.1	8.2	8.2	8.2	7.5	7.8	-1.4	-3.0	-2.8	1.0	1.0	-1.6	2
17504293	Mmp15	8.5	8.0	7.1	7.3	8.4	8.1	8.1	6.8	7.8	-1.5	-2.6	-2.2	-1.2	-1.3	-3.1	2
17290288	Akr1c20	8.8	8.0	6.8	6.8	8.6	8.4	7.4	7.5	7.8	-1.7	-4.0	-3.9	-1.2	-2.3	-2.2	2
17517112		8.7	7.7	6.9	7.0	8.4	7.9	8.2	7.4	7.8	-2.0	-3.4	-3.2	-1.4	-1.2	-2.0	2
17548238	Fabp5...	8.5	7.8	6.7	6.7	8.7	8.1	8.2	7.3	7.8	-1.7	-3.5	-3.6	-1.5	-1.4	-2.6	2
17381424	Dhtkd1	8.7	7.7	6.9	6.9	8.8	7.7	7.5	7.7	7.7	-2.1	-3					

Annotation		log ₂ normalized signal intensity (SI)								Fold changes					Cluster #		
Transcripts Cluster ID	Gene Symbol	WT	WT	WT	WT	lkb _{NS} ^{-/-}	lkb _{NS} ^{-/-}	lkb _{NS} ^{-/-}	lkb _{NS} ^{-/-}	average	[WT d2]	[WT d3]	[WT d4]	[lkb _{NS} ^{-/-} d2]	[lkb _{NS} ^{-/-} d3]	[lkb _{NS} ^{-/-} d4]	k-means cluster assignment
		d0	d2	d3	d4	d0	d2	d3	d4	log ₂ SI	vs. [WT d0]	vs. [WT d0]	vs. [WT d0]	vs. [lkb _{NS} ^{-/-} d0]	vs. [lkb _{NS} ^{-/-} d0]	vs. [lkb _{NS} ^{-/-} d0]	
17353141	Mir187	8.4	8.2	5.5	5.4	8.4	7.9	7.8	6.5	7.3	-1.2	-7.9	-8.1	-1.4	-1.5	-3.7	2
17262644	Leap2	8.1	7.7	6.0	6.2	7.7	7.6	7.7	6.7	7.2	-1.3	-4.4	-3.7	-1.0	1.0	-2.0	2
17498370	Nadsyn1	7.9	7.4	6.3	6.3	7.8	7.6	7.5	6.9	7.2	-1.3	-3.0	-3.0	-1.2	-1.2	-1.8	2
17406745	Pmf1	8.2	7.2	6.6	6.5	7.6	7.2	7.3	6.9	7.2	-2.0	-3.0	-3.3	-1.4	-1.2	-1.7	2
17349774	Hars2	8.0	7.7	6.3	6.3	7.7	7.7	7.3	6.6	7.2	-1.2	-3.1	-3.3	1.0	-1.3	-2.1	2
17513878	Spata2l	8.2	7.1	6.4	6.3	8.2	7.2	7.2	6.9	7.2	-2.1	-3.4	-3.8	-1.9	-2.0	-2.3	2
17442185	Gm6444	8.2	7.4	6.5	6.5	7.2	7.5	7.5	6.6	7.2	-1.8	-3.3	-3.3	1.2	1.2	-1.6	2
17411955	LOC102640902...	7.9	7.6	6.2	6.2	7.5	7.7	7.4	6.4	7.1	-1.2	-3.2	-3.2	1.1	-1.1	-2.3	2
17306696	Emc9	8.0	7.3	6.4	6.4	7.7	7.3	7.0	6.6	7.1	-1.5	-2.9	-3.0	-1.3	-1.7	-2.2	2
17241954	Gstt2	8.2	7.3	6.3	6.2	8.3	7.0	7.0	6.2	7.1	-1.9	-3.8	-4.1	-2.4	-2.4	-4.0	2
17359088	Cyp26a1	8.2	7.0	6.3	6.1	8.1	7.4	6.7	6.6	7.1	-2.3	-3.9	-4.2	-1.6	-2.6	-2.8	2
17283770		7.9	7.0	6.3	6.4	7.5	7.1	7.3	7.0	7.1	-1.9	-3.0	-2.8	-1.3	-1.1	-1.4	2
17488117	LOC102632321...	7.9	6.7	6.3	6.1	7.9	7.2	6.8	7.2	7.0	-2.3	-3.1	-3.4	-1.6	-2.1	-1.6	2
17426108	Mup21	7.2	7.9	6.1	5.6	7.0	7.8	7.1	5.8	6.8	1.6	-2.1	-3.0	1.7	1.1	-2.2	2
17256321		7.3	7.2	6.2	5.9	7.4	7.2	7.4	5.3	6.7	-1.1	-2.2	-2.6	-1.1	1.0	-4.3	2
17414529	Gm12909	7.7	6.8	5.8	5.7	7.6	6.9	6.6	6.2	6.7	-1.9	-3.8	-4.0	-1.6	-1.9	-2.5	2
17399402	Gm22642	6.8	6.9	6.0	6.0	7.2	7.2	7.2	5.5	6.6	1.1	-1.7	-1.7	-1.0	-1.0	-3.2	2
17475469	Cyp2a5	7.6	7.2	5.3	5.2	7.3	7.8	5.5	6.5	6.6	-1.3	-5.1	-5.3	1.4	-3.5	-1.8	2
17406921	Gm22935	7.4	6.9	5.4	5.3	7.6	6.4	7.3	6.2	6.5	-1.4	-3.8	-4.3	-2.3	-1.3	-2.7	2
17277267		7.7	6.4	5.5	5.5	7.2	6.7	6.2	6.3	6.4	-2.3	-4.5	-4.3	-1.4	-2.0	-2.0	2
17548398		7.7	6.3	5.8	5.8	7.0	6.6	6.2	6.0	6.4	-2.8	-3.9	-3.8	-1.4	-1.7	-2.0	2
17261333		6.7	6.7	5.6	5.5	7.6	6.7	7.1	4.9	6.4	1.0	-2.1	-2.2	-1.8	-1.4	-6.4	2
17547016		6.6	6.6	5.7	5.7	7.1	6.5	6.5	5.2	6.2	-1.0	-1.9	-1.8	-1.6	-1.6	-3.8	2
17531981	n-R592	7.1	6.5	5.5	5.5	6.3	6.4	6.6	5.6	6.2	-1.5	-3.0	-3.0	1.1	1.2	-1.7	2
17465210		6.2	6.5	4.9	5.0	6.9	7.0	7.1	4.8	6.1	1.2	-2.4	-2.3	1.1	1.1	-4.3	2
17459332	Igkv2-112	6.8	6.3	5.2	5.4	6.1	6.0	6.2	5.3	5.9	-1.5	-3.0	-2.7	-1.1	1.0	-1.8	2
17433942	Gm25982	5.7	5.5	4.8	4.7	6.9	5.5	4.9	5.2	5.4	-1.2	-1.9	-2.0	-2.6	-3.8	-3.2	2
17510345	Bst2	10.6	12.2	11.5	11.5	10.8	12.2	11.2	11.0	11.4	3.0	1.9	1.9	2.7	1.3	1.1	3
17313998	Crel2	9.1	11.3	10.4	10.3	9.4	11.1	10.7	10.3	10.3	4.6	2.4	2.3	3.2	2.4	1.9	3
17371310	B3galt1	9.0	10.7	9.7	9.7	9.3	10.4	11.2	10.1	10.0	3.2	1.6	1.6	2.1	3.7	1.7	3
17350921	F830016B08Rik	8.7	11.1	10.1	10.1	9.1	11.0	9.5	9.7	9.9	5.3	2.5	2.5	3.7	1.3	1.5	3
17434023	Isg15	8.3	11.2	10.5	10.5	8.3	11.1	10.2	9.2	9.9	7.5	4.5	4.6	6.8	3.6	1.9	3
17278200	Ifi27	9.2	10.5	9.6	9.6	9.1	10.7	10.1	9.2	9.8	2.5	1.4	1.3	3.0	2.0	1.1	3
17497713	Ifitm2	8.5	10.3	9.5	9.5	8.6	10.4	10.3	9.6	9.6	3.4	2.1	1.9	3.4	3.2	1.9	3
17455507	Hsph1	8.6	10.7	9.5	9.5	8.7	10.4	9.1	9.4	9.5	4.2	1.8	1.8	3.3	1.3	1.7	3
17404432	Fndc3b	8.5	10.0	9.5	9.4	8.7	9.8	10.4	9.4	9.5	2.7	1.9	1.9	2.3	3.3	1.7	3
17336446	Psmb8	8.6	10.3	9.6	9.6	8.4	10.2	9.3	9.4	9.4	3.2	2.1	2.0	3.4	1.8	2.0	3
17328625	Sdf2l1	8.4	10.4	9.0	9.0	8.6	10.2	9.8	9.3	9.4	3.8	1.5	1.5	3.0	2.3	1.6	3
17501976	Isyna1	7.0	10.2	9.3	9.4	7.4	10.2	10.9	10.2	9.3	9.1	5.0	5.1	7.0	11.0	6.9	3
17326801	Jam2	8.3	10.0	9.3	9.3	8.4	10.1	9.9	9.5	9.3	3.4	2.0	2.0	3.1	2.7	2.1	3
17462437	Usp18	8.0	10.1	9.7	9.7	8.2	10.2	9.7	9.1	9.3	4.5	3.3	3.2	3.9	2.7	1.8	3
17496514	Mvp	8.5	9.9	9.3	9.5	8.3	10.0	9.7	9.2	9.3	2.8	1.9	2.0	3.2	2.7	1.9	3
17243525	Slc41a2	8.2	10.1	8.9	8.9	8.2	10.1	10.1	9.6	9.3	3.7	1.7	1.7	3.6	3.7	2.5	3
17358832	Ifi1	8.0	10.3	9.7	9.6	7.9	10.2	9.5	8.4	9.2	4.9	3.2	3.1	4.8	3.0	1.4	3
17327465	Ets2	8.3	9.5	9.3	9.3	8.4	9.6	10.1	8.8	9.2	2.3	1.9	2.0	2.2	3.3	1.3	3
17499394		8.4	9.4	9.3	9.4	8.0	9.3	9.9	8.5	9.0	2.0	1.9	2.1	2.5	3.8	1.5	3
17521541	Uba7	7.9	9.9	9.1	9.1	8.0	9.9	9.2	9.0	9.0	4.0	2.3	2.4	3.8	2.2	2.0	3
17482095	Nucb2	7.9	9.8	9.2	9.2	7.8	9.8	9.4	8.9	9.0	3.7	2.5	2.5	3.8	2.9	2.1	3
17441051	Oasl1	7.7	9.7	9.2	9.2	7.8	9.8	9.3	8.6	8.9	3.9	2.7	2.7	4.0	2.9	1.7	3
17252341	Xaf1	7.8	9.4	9.0	9.1	7.8	9.5	9.2	8.8	8.8	3.1	2.4	2.4	3.2	2.6	1.9	3
17462351	Ii17ra	8.0	9.4	8.6	8.7	7.9	9.2	9.5	8.6	8.7	2.6	1.6	1.6	2.4	3.1	1.6	3
17236182	Timp3	7.8	9.5	8.6	8.6	7.8	9.5	9.0	8.7	8.7	3.1	1.7	1.7	3.2	2.3	1.8	3
17404091	Fabp4	7.8	9.4	8.8	8.8	7.6	9.5	9.3	8.3	8.7	3.0	2.1	2.0	3.7	3.3	1.7	3
17287361	Gadd45g	7.6	9.6	8.4	8.4	7.5	9.4	9.9	8.5	8.7	4.0	1.7	1.7	3.8	5.1	2.0	3
17344126	Hspa1b	7.3	10.1	8.9	8.9	7.1	9.7	8.4	8.7	8.6	7.3	3.1	3.1	6.0	2.4	3.0	3
17494353		7.9	9.3	8.6	8.6	7.5	9.2	8.7	8.4	8.5	2.7	1.6	1.6	3.2	2.3	1.8	3
17483842	Tacc2	7.6	9.3	8.5	8.4	7.7	9.0	9.5	8.1	8.5	3.1	1.8	1.7	2.4	3.4	1.3	3
17233920	Dnajc12	7.5	9.1	8.5	8.5	7.2	9.1	9.0	8.9	8.5	3.0	1.9	2.0	3.7	3.6	3.3	3
17272619	Socs3	7.0	9.1	8.6	8.5	7.2	9.2	9.5	8.7	8.5	4.3	3.1	2.9	3.8	4.9	2.7	3
17378799	Gm20412	7.5	8.6	8.5	8.6	7.5	8.9	9.4	8.6	8.4	2.1	2.0	2.0	2.6	3.7	2.2	3
17347877	Gm10309	6.0	10.6	8.0	8.1	6.6	10.2	10.6	7.0	8.4	24.0	4.1	4.4	12.0	15.9	1.3	3
17354589	Gm4841	5.9	10.9	8.5	8.3	6.2	11.0	7.9	7.6	8.3	32.9	6.0	5.5	29.5	3.3	2.7	3
17281922		8.5	8.2	8.4	8.5	7.3	8.6	8.9	7.4	8.2	-1.3	-1.1	-1.0	2.4	3.1	1.1	3
17270703	Cyb561	7.1	8.8	8.2	8.2	7.2	8.9	8.9	8.4	8.2	3.1	2.1	2.1	3.2	3.3	2.2	3
17410204	Alpk1	6.8	9.0	8.4	8.4	6.4	9.0	9.4	8.3	8.2	4.5	3.0	3.1	6.4	8.2	3.8	3
17335818	Slc37a1	6.9	8.9	7.8	7.9	7.0	8.9	9.2	8.0	8.1	4.2	1.9	2.0	3.7	4.5	1.9	3
17269595	Dhx58	7.3	8.9	8.1	8.1	7.3	8.8	8.3	7.6	8.0	3.1	1.8	1.8	2.8	2.0	1.2	3
17246963	LOC102639290...	7.2	8.6	7.7	7.6	7.5	8.8	9.2	7.8	8.0	2.6	1.4	1.3	2.4	3.4	1.2	3
17494408	Trim30d	7.3	9.2	8.4	8.3	5.9	8.8	8.2	8.0	8.0	3.7	2.1	2.1	7.5	4.8	4.3	3
17265631	Slc13a5	6.2	9.2	7.8	7.7	6.3	9.1	9.4	8.2	8.0	8.2	3.1	2.8	6.8	8.4	3.7	3
17266851	Sifn9	7.0	8.7	8.3	8.2	6.9	8.8	8.1	7.7	8.0	3.3	2.5	2.4	3.7	2.4	1.8	3
17515478	Bmper	6.7	8.6	8.1	8.1	6.9	8.7	8.5	7.9	7.9	3.8	2.6	2.8	3.3	2.9	1.9	3
17402519	Tifa	7.1	8.5	7.8	7.8	7.0	8.6	8.5	7.9	7.9	2.6	1.7	1.7	3.1	2.9	1.9	3
17452054	Oas2	6.5	8.5	7.9	7.9	7.0	8.3	8.5	7.4	7.8	4.0	2.6	2.5	2.5	2.8	1.3	3
17283556	Ifi2712b	7.0	8.9	7.6	7.7	6.0	8.8	8.3	7.5	7.7	3.8	1.6	1.6	7.0	4.8	2.9	3
17344558	H2-T24	6.6	8.6	7.5	7.6	6.6	8.4	8.0	7.5	7.6	3.9	1.9	2.0	3.3	2.6	1.9	3
17217825	Gm19705	6.5	8.5	7.7	7.7	6.9	8.5	7.6	7.4	7.6	4.0</						

Annotation		log ₂ normalized signal intensity (SI)								Fold changes								Cluster #
Transcripts Cluster ID	Gene Symbol	WT	WT	WT	WT	lkb _{NS} ^{-/-}	lkb _{NS} ^{-/-}	lkb _{NS} ^{-/-}	lkb _{NS} ^{-/-}	average	[WT d2]	[WT d3]	[WT d4]	[lkb _{NS} ^{-/-} d2]	[lkb _{NS} ^{-/-} d3]	[lkb _{NS} ^{-/-} d4]	k-means cluster assignment	
		d0	d2	d3	d4	d0	d2	d3	d4	log ₂ SI	vs. [WT d0]	vs. [WT d0]	vs. [WT d0]	vs. [lkb _{NS} ^{-/-} d0]	vs. [lkb _{NS} ^{-/-} d0]	vs. [lkb _{NS} ^{-/-} d0]		
17399404	Gm15998	6.7	7.4	5.7	5.6	6.5	7.6	8.4	5.9	6.7	1.6	-2.0	-2.2	2.2	3.7	-1.4	3	
17507515	Gm15348	5.5	7.7	6.4	6.3	5.9	7.6	7.4	6.6	6.7	4.5	1.8	1.7	3.1	2.8	1.6	3	
17520903	Gm25842	5.6	7.3	6.8	6.9	5.9	7.1	7.1	6.6	6.7	3.4	2.4	2.5	2.3	2.3	1.6	3	
17546215	Gm15726	5.5	7.2	6.6	6.5	5.9	7.0	7.3	6.6	6.6	3.3	2.2	2.1	2.2	2.7	1.6	3	
17547600		5.9	6.8	6.4	6.6	5.5	7.2	7.3	6.8	6.5	1.8	1.4	1.6	3.1	3.3	2.4	3	
17364111	Ch25h	5.8	6.8	6.6	6.7	5.5	7.2	7.2	6.2	6.5	2.0	1.8	1.8	3.3	3.3	1.7	3	
17494394	Trim30a	5.3	7.2	6.6	6.7	5.4	7.0	6.4	5.9	6.3	3.5	2.4	2.6	3.1	2.0	1.5	3	
17344688		5.9	6.8	6.2	6.2	5.3	7.0	6.2	6.3	6.3	2.0	1.3	1.3	3.2	1.8	2.0	3	
17465942	Atp6v0a4	5.5	7.4	5.5	5.3	5.4	7.5	7.0	5.6	6.2	3.8	-1.0	-1.1	4.4	3.2	1.2	3	
17223637		5.5	7.3	5.7	5.5	5.5	7.2	6.8	5.3	6.1	3.6	1.1	-1.0	3.2	2.5	-1.2	3	
17219629	Olfri16	4.8	6.0	5.8	5.8	4.9	6.0	6.8	5.6	5.7	2.3	1.9	2.0	2.2	3.7	1.6	3	
17278328	Serpina3n	12.0	13.6	13.3	13.4	12.2	13.5	13.6	13.3	13.1	3.1	2.5	2.6	2.4	2.5	2.2	4	
17491205	Saa1	9.6	13.5	13.6	13.6	9.5	13.5	13.5	13.6	12.5	14.3	15.8	15.6	16.7	16.1	17.6	4	
17478195	Saa2	9.8	13.5	13.6	13.6	9.1	13.5	13.5	13.6	12.5	13.1	13.7	13.7	21.5	20.6	21.6	4	
17414747	Orm2	9.3	13.4	13.3	13.3	10.2	13.5	13.5	13.3	12.5	16.7	15.9	15.2	9.9	9.8	8.4	4	
17383892	Lcn2	9.2	13.1	13.0	13.0	10.1	13.1	13.3	13.0	12.2	14.8	13.6	13.5	8.3	9.2	7.7	4	
17434490	Steap4	10.4	12.7	12.9	12.8	10.1	12.8	13.1	12.8	12.2	4.9	5.5	5.4	6.5	7.6	6.4	4	
17283565	Serpina10	11.0	12.6	12.2	12.2	10.8	12.5	12.6	12.2	12.0	3.1	2.4	2.4	3.2	3.3	2.6	4	
17449710	Cxcl9	9.8	13.3	12.9	12.9	9.5	13.3	12.2	12.1	12.0	11.2	9.0	8.9	14.2	6.8	6.3	4	
17491193	Saa3	7.4	13.5	13.4	13.4	7.3	13.5	13.5	12.9	11.9	71.3	63.4	64.4	74.4	75.1	47.5	4	
17229960	Apcs	10.0	12.6	12.3	12.2	10.0	12.6	12.8	12.4	11.9	6.2	5.0	4.9	6.0	6.7	5.1	4	
17450501	Gbp10	10.4	12.7	12.5	12.4	10.3	12.7	11.4	12.1	11.8	5.0	4.2	4.1	5.0	2.1	3.3	4	
17227892	Prg4	10.0	12.4	12.1	12.1	10.1	12.4	12.5	12.2	11.7	5.3	4.5	4.5	4.9	5.3	4.3	4	
17378827	Lbp	10.5	12.1	11.9	11.9	10.7	12.1	12.2	12.0	11.7	3.1	2.7	2.7	2.6	2.8	2.4	4	
17212750	Stat1	9.9	12.5	12.4	12.3	9.9	12.4	11.7	12.2	11.7	5.9	5.4	5.3	5.8	3.4	4.9	4	
17346150	Lrg1	10.4	12.1	12.0	12.0	10.4	12.1	12.3	12.0	11.7	3.4	3.1	3.2	3.1	3.6	3.0	4	
17340135	Slc3a1	9.8	12.0	11.6	11.6	9.7	12.0	12.0	11.9	11.3	4.7	3.5	3.5	4.8	4.9	4.7	4	
17350982	Cd74	9.4	11.8	12.2	12.2	9.4	11.9	11.6	12.0	11.3	5.2	7.0	7.1	5.6	4.8	6.1	4	
17548644	Edv...	9.5	11.5	11.5	11.6	10.4	11.3	11.9	11.2	11.1	3.9	3.8	4.0	1.9	2.8	1.7	4	
17548313	Edv...	9.5	11.5	11.5	11.6	10.4	11.3	11.9	11.2	11.1	3.9	3.8	4.0	1.9	2.8	1.7	4	
17548642	Edv...	9.5	11.5	11.5	11.6	10.4	11.3	11.9	11.2	11.1	3.9	3.8	4.0	1.9	2.8	1.7	4	
17548311	Edv...	9.5	11.5	11.5	11.6	10.4	11.3	11.9	11.2	11.1	3.9	3.8	4.0	1.9	2.8	1.7	4	
17318083	Ly6a	8.8	12.1	12.0	12.0	8.4	12.0	11.8	11.6	11.1	9.7	9.3	9.3	12.7	11.1	9.0	4	
17249980	lgtp	9.1	12.1	11.8	11.9	8.8	12.0	11.0	11.7	11.1	7.6	6.5	6.6	9.8	4.7	7.7	4	
17357810	Mpeg1	9.2	11.8	11.5	11.5	9.2	11.9	11.3	11.5	11.0	6.4	5.2	5.1	6.4	4.4	4.9	4	
17393789	Tgm2	9.5	11.2	11.3	11.4	9.5	11.2	11.5	11.1	10.8	3.3	3.5	3.5	3.3	3.9	3.1	4	
17411147	Ifi44	8.7	12.1	11.4	11.4	9.0	11.9	11.1	10.7	10.8	10.9	6.7	6.7	7.5	4.2	3.2	4	
17259078	Rnf213	9.3	11.6	11.3	11.3	9.6	11.6	11.1	10.5	10.8	5.0	4.2	4.1	4.1	2.9	1.9	4	
17403224	Gbp7	9.1	11.6	11.5	11.5	9.0	11.6	10.5	11.1	10.7	5.9	5.3	5.3	5.9	2.7	4.1	4	
17212185	Il1r1	9.0	11.3	10.9	11.0	9.7	11.1	11.7	11.1	10.7	5.1	3.8	4.0	2.6	4.0	2.5	4	
17497813	Irf7	9.1	11.5	11.2	11.2	9.3	11.5	11.1	10.8	10.7	5.3	4.3	4.3	4.6	3.7	2.9	4	
17272785	Lgals3bp	9.6	11.2	10.9	10.9	9.8	11.2	11.3	10.8	10.7	3.2	2.5	2.6	2.6	2.9	2.1	4	
17548055	LOC630751...	8.7	12.1	11.6	11.6	8.2	12.0	10.4	11.0	10.7	10.2	7.2	7.3	13.7	4.6	7.0	4	
17494651	Gm8979...	8.3	11.6	11.7	11.7	8.5	11.6	11.0	10.7	10.6	9.9	10.1	10.0	8.5	5.5	4.6	4	
17249990	Irgm2	9.2	11.4	11.1	11.1	8.8	11.4	10.8	11.0	10.6	4.6	3.8	3.8	6.0	3.8	4.5	4	
17336494	H2-Ab1	8.7	11.0	11.3	11.3	8.5	11.0	10.8	11.6	10.5	5.2	6.1	6.1	5.8	5.0	8.5	4	
17344593	H2-T22...	9.5	11.2	10.7	10.7	9.3	11.2	10.4	10.5	10.5	3.3	2.3	2.3	3.7	2.1	2.3	4	
17324446	Rtp4	9.0	11.1	10.9	11.0	9.0	11.2	11.0	10.4	10.4	4.2	3.7	3.9	4.4	3.8	2.7	4	
17330099	Parp14	9.1	11.1	10.9	10.9	9.2	11.1	10.7	10.4	10.4	3.9	3.5	3.4	3.7	2.8	2.4	4	
17544837	Serpina7	8.8	11.3	11.2	11.2	8.1	11.4	11.3	10.0	10.4	5.8	5.5	5.5	9.7	9.2	3.7	4	
17283445	Lgmn	9.1	10.6	10.9	10.9	9.2	10.6	11.0	10.8	10.4	2.9	3.5	3.5	2.7	3.4	3.1	4	
17494664	Gm8979...	8.1	11.3	11.4	11.3	8.2	11.3	10.8	10.4	10.4	9.5	9.8	9.5	8.3	5.7	4.5	4	
17458962	Herc6	8.8	11.4	10.7	10.7	9.1	11.3	10.2	10.2	10.3	5.9	3.8	3.8	4.6	2.2	2.3	4	
17395079	Zbp1	8.3	11.1	11.1	11.1	8.1	11.2	10.8	10.7	10.3	6.9	6.6	6.6	8.9	6.5	6.1	4	
17324420	St6gal1	9.4	10.5	10.4	10.4	9.3	10.5	11.0	10.3	10.2	2.1	2.0	2.1	2.4	3.3	2.1	4	
17403268	Gbp2	7.7	11.3	11.2	11.1	7.3	11.3	10.2	10.6	10.1	12.3	11.3	10.9	15.8	7.4	9.8	4	
17393658	Samhd1	8.4	10.4	10.8	10.8	8.4	10.4	10.2	10.6	10.0	4.2	5.5	5.5	3.9	3.5	4.4	4	
17417699	Gm12840	9.1	10.4	10.9	10.9	8.9	10.1	10.1	9.5	10.0	2.5	3.6	3.5	2.3	2.2	1.5	4	
17336432	Tap1	8.5	10.6	10.4	10.4	8.4	10.7	10.0	10.3	9.9	4.5	3.9	3.9	4.6	3.0	3.6	4	
17494643	Gm4070...	7.6	11.0	10.9	10.8	7.9	10.9	10.1	10.2	9.9	10.1	9.3	9.0	7.6	4.6	4.7	4	
17494656	Gm4070...	7.6	11.0	10.8	10.8	7.9	10.8	10.1	10.2	9.9	10.4	9.3	9.0	7.7	4.8	5.1	4	
17337122	H2-Q6...	9.0	10.2	10.4	10.4	8.6	10.2	9.9	9.9	9.8	2.3	2.8	2.7	3.1	2.5	2.5	4	
17462492	A2m	5.6	11.3	11.2	11.2	6.1	10.7	12.6	9.7	9.8	51.7	47.2	47.1	23.2	90.5	11.5	4	
17518007	Pkm	8.2	10.0	10.5	10.5	8.5	10.1	10.2	10.3	9.8	3.6	5.0	5.0	3.1	3.4	3.5	4	
17441037	Oasl2	7.4	11.2	10.4	10.4	7.6	11.1	10.0	9.5	9.7	14.1	8.1	8.1	11.8	5.4	3.8	4	
17249977	Gm12250	6.9	11.0	10.6	10.6	6.8	11.1	10.0	10.3	9.7	18.1	12.9	13.0	19.7	9.1	11.0	4	
17510136	Ifi30	8.1	10.0	10.4	10.4	7.7	10.0	10.2	10.3	9.6	3.6	5.1	5.0	5.0	5.8	6.1	4	
17262202	Irgm1	8.1	10.5	10.1	10.1	8.1	10.4	9.7	10.1	9.6	5.4	3.9	3.9	5.0	3.0	4.0	4	
17350932	BC023105	8.0	10.7	10.2	10.2	7.8	10.6	9.4	9.8	9.6	6.4	4.7	4.7	7.1	3.2	4.0	4	
17548023	LOC102633627...	8.5	9.8	10.3	10.4	8.4	9.9	9.8	9.8	9.6	2.5	3.7	3.8	2.8	2.6	2.6	4	
17278268	Serpina3f	7.1	10.2	10.7	10.7	6.9	10.2	10.5	10.2	9.6	8.5	11.9	12.0	9.8	11.8	9.6	4	
17458573	Snx10	8.4	9.9	10.0	10.0	8.4	9.9	9.8	9.8	9.5	2.9	3.0	3.0	2.8	2.7	2.5	4	
17450448	Gbp9	7.4	10.4	10.2	10.2	7.7	10.4	9.6	9.7	9.5	8.1	6.9	6.9	6.5	3.9	4.2	4	
17283930	Wars	8.2	10.1	9.6	9.6	8.4	10.0	9.6	9.7	9.4	3.7	2.6	2.6	3.1	2.4	2.5	4	
17438987	Cxcl1	7.5	1															

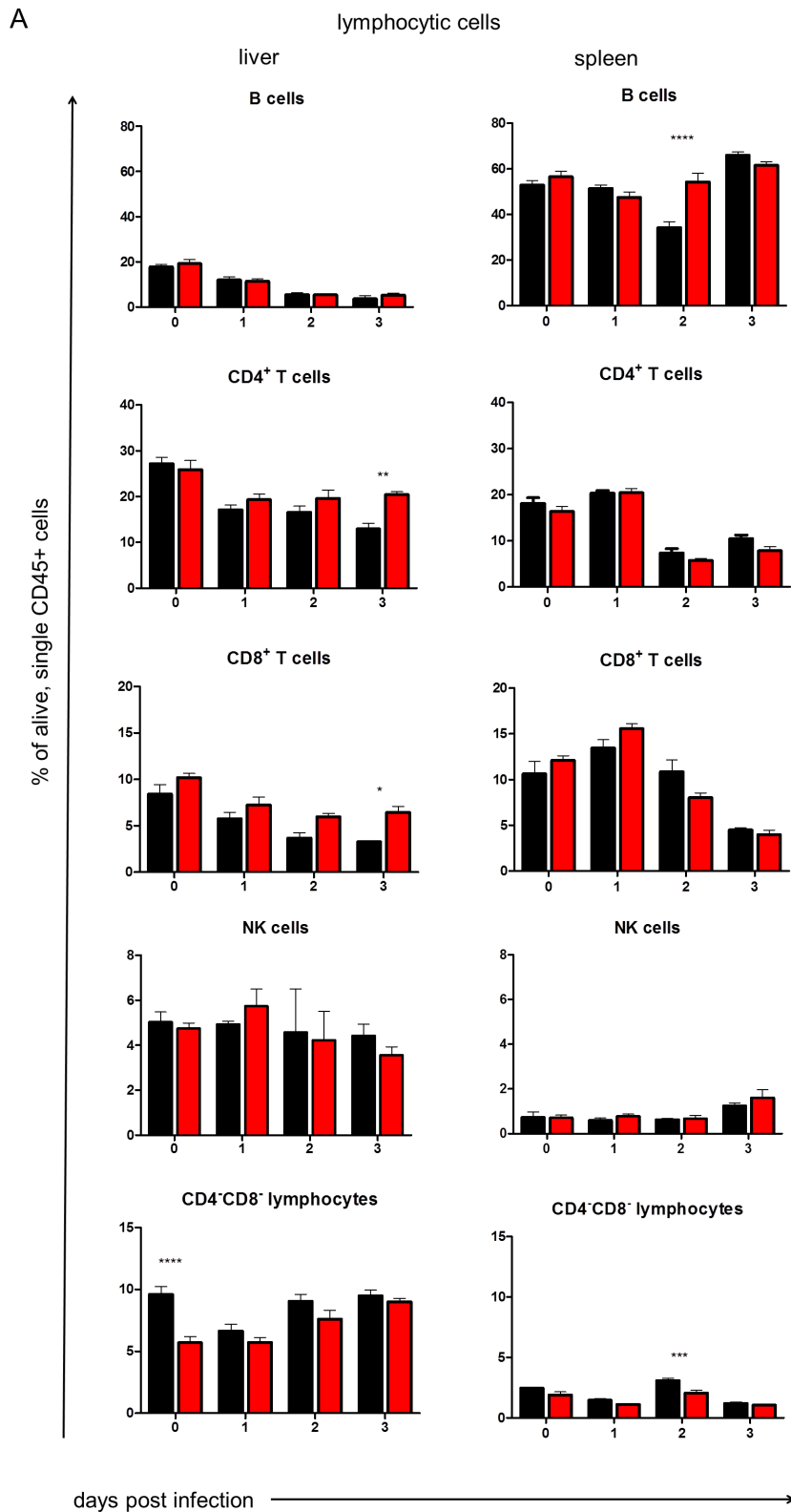
Annotation		log ₂ normalized signal intensity (SI)								Fold changes					Cluster #		
Transcripts Cluster ID	Gene Symbol	WT	WT	WT	WT	IkB _{NS} ^{-/-}	IkB _{NS} ^{-/-}	IkB _{NS} ^{-/-}	IkB _{NS} ^{-/-}	average	[WT d2]	[WT d3]	[WT d4]	[IkB _{NS} ^{-/-} d2]	[IkB _{NS} ^{-/-} d3]	[IkB _{NS} ^{-/-} d4]	k-means cluster assignment
		d0	d2	d3	d4	d0	d2	d3	d4	log ₂ SI	vs. [WT d0]	vs. [WT d0]	vs. [WT d0]	vs. [IkB _{NS} ^{-/-} d0]	vs. [IkB _{NS} ^{-/-} d0]	vs. [IkB _{NS} ^{-/-} d0]	
17315743	Osmr	7.1	9.7	9.2	9.3	7.3	9.5	9.9	8.9	8.9	6.0	4.4	4.4	4.6	6.0	3.2	4
17513076	Mkl1	7.6	9.6	9.4	9.4	7.2	9.5	9.0	9.0	8.8	3.9	3.5	3.5	5.2	3.6	3.6	4
17515074	Icam1	7.5	9.1	9.4	9.4	7.2	9.2	9.5	8.9	8.8	3.1	3.8	3.7	4.1	4.9	3.4	4
17543572	Il2rg...	7.0	9.1	9.6	9.6	7.0	9.1	9.2	9.4	8.8	4.4	6.2	6.4	4.3	4.6	5.3	4
17343789	Psmb9	7.6	9.5	8.9	8.9	7.5	9.4	8.6	8.9	8.7	3.5	2.5	2.4	3.8	2.2	2.6	4
17423490	Ripk2	7.7	8.9	9.3	9.3	7.6	9.2	9.1	8.1	8.6	2.3	3.1	3.1	2.9	2.7	1.4	4
17509101	Tlr3	7.4	9.2	9.2	9.2	7.5	9.1	9.0	8.6	8.6	3.3	3.5	3.4	3.2	2.8	2.1	4
17403255	Gbp2b	6.3	9.1	9.7	9.8	6.4	9.1	8.9	9.7	8.6	6.7	10.7	11.1	6.6	5.7	10.4	4
17419890	Il22ra1	7.7	8.9	8.9	8.9	7.5	9.1	9.2	8.7	8.6	2.4	2.4	2.4	3.2	3.5	2.4	4
17280327	Rsad2	7.7	9.2	9.3	9.3	7.8	9.0	8.7	8.0	8.6	2.9	3.0	3.1	2.2	1.8	1.1	4
17337545	Ubd	6.2	9.9	9.9	9.8	5.7	10.0	9.0	8.4	8.6	13.0	13.0	12.6	18.7	9.8	6.4	4
17377870	Hck	7.0	8.9	9.4	9.4	7.0	8.9	9.4	8.9	8.6	3.5	5.0	5.0	3.8	5.3	3.8	4
17233536	P4ha1	7.5	9.2	8.9	8.9	7.9	9.1	8.7	8.5	8.6	3.2	2.6	2.6	2.4	1.8	1.6	4
17307280	Phf11b	7.0	9.0	9.4	9.3	7.1	9.0	8.9	8.5	8.5	3.9	4.9	4.8	3.6	3.4	2.6	4
17254153	Sfn5	7.3	8.9	8.9	8.9	7.3	9.0	8.9	8.1	8.4	3.2	3.1	3.1	3.2	3.1	1.8	4
17403205	Gbp5	5.9	9.0	9.6	9.6	6.3	9.0	8.9	8.9	8.4	8.5	13.2	12.7	6.4	6.0	6.2	4
17229931	Slamf8	6.8	8.8	9.0	9.0	7.4	8.9	8.2	8.9	8.4	4.0	4.8	4.7	2.8	1.8	3.0	4
17450461	Gbp4	5.3	9.3	9.6	9.6	5.3	9.4	9.0	9.1	8.3	15.9	20.4	20.4	17.5	13.1	14.2	4
17358544	Cd274	6.2	9.3	9.0	8.9	6.1	9.2	8.9	8.8	8.3	8.5	6.6	6.6	8.1	6.6	6.2	4
17367686	Il1rn	6.2	8.8	8.9	8.9	7.2	8.7	9.4	7.9	8.2	6.3	6.7	6.5	2.7	4.5	1.6	4
17453611	Ccl24	7.0	8.7	8.6	8.5	6.6	8.9	8.6	9.0	8.2	3.2	3.1	2.8	5.0	4.2	5.2	4
17262250	Tgtp2...	4.8	9.6	9.3	9.3	5.6	9.2	9.0	9.0	8.2	27.3	22.1	21.6	12.2	10.2	10.7	4
17262241	9930111J21Rik2	6.8	8.8	8.9	9.0	7.1	8.6	8.2	8.4	8.2	3.9	4.4	4.7	2.9	2.2	2.4	4
17506279	Irf8	7.1	8.6	8.6	8.6	6.9	8.7	8.6	8.5	8.2	3.0	2.8	2.9	3.4	3.2	3.0	4
17548315		7.2	8.2	8.4	8.3	7.3	8.4	8.7	8.9	8.2	1.9	2.3	2.1	2.2	2.7	3.1	4
17290324	Pfkfb	6.8	8.6	8.9	8.9	7.0	8.4	8.5	8.3	8.2	3.3	4.1	4.3	2.8	2.8	2.5	4
17229782	Slamf7	6.2	8.5	9.2	9.2	6.6	8.4	8.4	8.6	8.1	5.0	7.7	8.0	3.6	3.4	4.1	4
17245399	Irak3	6.2	8.6	8.9	8.9	6.6	8.5	9.0	8.2	8.1	5.2	6.5	6.4	3.5	5.2	3.0	4
17372307	Itga4	6.7	8.3	8.9	8.8	6.6	8.3	8.5	8.5	8.1	3.1	4.5	4.2	3.3	3.8	3.7	4
17514424	Casp1	6.4	8.4	9.0	8.9	6.4	8.4	8.6	8.6	8.1	4.0	5.8	5.7	3.9	4.5	4.5	4
17366271	LOC101056250...	6.9	8.3	8.5	8.6	6.7	8.3	8.5	8.4	8.0	2.6	3.0	3.2	3.1	3.5	3.3	4
17452115	Oas1g	5.5	9.0	8.6	8.6	6.1	9.2	9.1	8.1	8.0	11.9	8.7	9.0	8.7	8.1	3.9	4
17289527	Cd180	6.3	8.3	8.7	8.7	6.5	8.4	8.5	8.8	8.0	4.1	5.3	5.3	3.8	4.0	4.8	4
17469488	Pdzrn3	7.0	8.3	8.2	8.2	7.4	8.0	9.0	7.9	8.0	2.3	2.3	2.3	1.5	3.1	1.4	4
17353663	Tmem173	6.6	8.5	8.5	8.5	6.5	8.3	8.5	8.4	8.0	3.6	3.6	3.5	3.5	4.1	3.6	4
17240186	Fam26f	6.6	8.5	8.5	8.6	6.3	8.6	8.1	8.6	8.0	3.9	3.9	4.0	4.9	3.7	5.0	4
17527332	Nrg4	7.0	8.3	8.2	8.2	7.0	8.2	8.7	7.7	7.9	2.4	2.2	2.2	2.2	3.1	1.6	4
17366352	LOC101056250...	6.7	8.2	8.5	8.5	6.4	8.2	8.4	8.3	7.9	2.8	3.5	3.6	3.4	4.0	3.7	4
17431174	Cd52	6.7	8.1	8.3	8.4	6.8	8.1	8.2	8.4	7.9	2.5	3.0	3.2	2.5	2.7	3.0	4
17396383	Tnfrsf10	6.4	8.5	8.3	8.3	6.5	8.6	7.9	7.7	7.8	4.5	3.8	3.9	4.3	2.5	2.3	4
17514435	Casp4	5.9	8.2	8.6	8.5	6.0	8.2	8.5	8.1	7.8	4.9	6.2	5.8	4.5	5.5	4.3	4
17512666	Smpd3	7.1	7.8	8.0	8.1	6.6	8.0	8.3	8.0	7.7	1.6	1.8	2.0	2.6	3.3	2.8	4
17265386	Scimp	6.6	7.9	8.3	8.3	6.8	8.0	7.6	8.1	7.7	2.5	3.2	3.3	2.3	1.7	2.5	4
17262209	Gm5431	5.6	8.4	8.6	8.6	6.2	8.4	7.8	8.2	7.7	6.9	7.8	7.7	4.6	2.9	3.8	4
17248911	Ifi47...	6.3	8.5	8.3	8.3	6.1	8.5	7.8	8.0	7.7	4.4	3.9	3.9	5.1	3.2	3.7	4
17227828	Pla2g4a	6.4	7.9	8.3	8.3	6.5	8.0	7.9	8.1	7.7	2.8	3.7	3.7	2.7	2.6	3.0	4
17217399	Chil1	6.3	8.0	8.1	8.1	6.6	8.2	8.3	8.0	7.7	3.2	3.5	3.5	3.1	3.3	2.7	4
17239597	Tnfrsf3	6.3	8.0	8.4	8.3	6.3	8.0	8.5	7.5	7.7	3.3	4.3	4.1	3.2	4.6	2.3	4
17262234		6.4	8.8	8.0	8.1	6.4	8.3	7.5	7.7	7.6	5.6	3.1	3.2	3.7	2.2	2.5	4
17494677	Gm1966	5.9	8.0	8.3	8.3	6.1	8.1	8.3	8.1	7.6	4.4	5.3	5.5	4.0	4.6	3.9	4
17514592	Mmp7	6.7	8.1	8.1	8.2	6.3	7.9	7.9	7.8	7.6	2.7	2.7	2.9	3.1	3.0	2.8	4
17494674	Gm8995	5.5	8.1	8.4	8.5	6.5	8.0	8.0	7.8	7.6	5.9	7.0	7.7	2.9	2.9	2.6	4
17537081	Tlr13	6.2	7.9	8.0	8.1	6.6	7.6	8.4	7.7	7.6	3.4	3.6	3.7	2.1	3.6	2.3	4
17406279	Tlr2	6.1	7.9	8.3	8.3	5.7	8.1	8.2	7.6	7.5	3.5	4.4	4.4	5.4	5.8	3.8	4
17463530	Clec9a	6.1	8.3	7.6	7.6	6.6	8.2	7.8	8.0	7.5	4.4	2.7	2.8	3.2	2.3	2.8	4
17230067	Mndal	6.3	7.9	8.0	8.2	6.5	7.9	7.8	7.7	7.5	3.0	3.3	3.7	2.6	2.5	2.3	4
17230087	Ifi203...	6.2	7.9	7.8	7.8	6.8	7.8	8.1	7.6	7.5	3.2	2.9	2.9	2.1	2.6	1.8	4
17357815	Fam111a	5.9	7.8	8.1	8.2	6.6	7.8	7.8	7.8	7.5	3.6	4.6	4.9	2.3	2.3	2.4	4
17283549	Ifi2712a	6.9	7.6	7.9	7.8	6.3	7.9	8.1	7.3	7.5	1.6	2.0	2.0	3.0	3.5	2.0	4
17292775	Hk3	6.4	7.7	8.0	8.0	6.2	7.6	7.8	7.9	7.5	2.3	3.0	3.0	2.6	3.0	3.2	4
17464530	Gm20559	5.7	8.2	7.7	7.7	6.5	7.8	7.9	7.1	7.3	5.6	3.9	4.0	2.5	2.6	1.5	4
17531705	Ccrl2	6.0	7.6	8.3	8.2	6.1	7.7	7.8	6.9	7.3	3.0	4.6	4.4	3.0	3.3	1.8	4
17293362	Ctla2a	6.0	7.7	7.7	7.8	6.7	7.8	7.3	7.3	7.3	3.3	3.2	3.4	2.2	1.6	1.6	4
17230034	Al607873	5.7	7.4	7.5	7.6	6.5	7.5	7.9	7.1	7.2	3.2	3.4	3.7	2.0	2.6	1.5	4
17318076	Ly6i	6.0	7.3	8.1	8.0	6.0	7.5	7.0	7.3	7.1	2.6	4.4	4.0	2.9	2.1	2.5	4
17405463	P2ry14	6.5	7.2	7.4	7.5	5.9	7.4	7.4	7.6	7.1	1.6	1.9	2.0	2.7	2.8	3.1	4
17357688	Ms4a6b	5.7	7.4	7.9	7.8	5.6	7.2	7.6	7.5	7.1	3.3	4.5	4.4	3.1	4.0	3.7	4
17457143	Akr1b10	5.8	7.3	7.4	7.4	6.3	7.3	7.3	7.6	7.0	2.8	3.0	3.1	1.9	1.9	2.4	4
17452126	Oas1a	6.0	7.3	7.5	7.5	5.9	7.5	7.3	7.4	7.0	2.6	2.8	2.8	3.0	2.7	2.9	4
17307033	Gzmb	5.8	7.4	7.5	7.4	6.2	7.5	7.5	6.9	7.0	3.1	3.1	3.0	2.4	2.4	1.6	4
17344132	Hspa1a	5.9	7.5	7.8	7.7	6.4	7.2	6.9	6.9	7.0	3.0	3.8	3.5	1.7	1.4	1.4	4
17366314		6.4	7.2	7.7	7.7	5.7	7.4	7.0	6.8	7.0	1.8	2.6	2.5	3.2	2.5	2.2	4
17523659	Ccr5	5.5	7.2	7.5	7.5	5.5	7.2	7.4	7.5	6.9	3.3	4.1	4.0	3.2	3.5	3.9	4
17307290	Phf11d	5.7	7.6	7.3	7.3	5.8	7.6	7.0	6.5	6.9	3.6	3.0	3.1	3.3	2.3	1.6	4
17262218	Gm12185	4.9	7.2	6.8	6.9	5.7	7.5	6.1	6.5	6.5	5.0	3.8	4.1	3.6	1.3	1.8	4
17404217	LOC100038947	4.6	6.8	7.1	7.1	4.7	6.2	6.5	6.3	6.2	4.5	5.7	5.4	2.8	3.5	3.0	4
17400375	Ctss	9.2	11.2	12.0	12.0	9.3	11.2	11.4	11.9	11.0	3.8	6.7	6.9	3.7			

Annotation		log ₂ normalized signal intensity (SI)								Fold changes					Cluster #		
Transcripts Cluster ID	Gene Symbol	WT	WT	WT	WT	IkB _{NS} ^{-/-}	IkB _{NS} ^{-/-}	IkB _{NS} ^{-/-}	IkB _{NS} ^{-/-}	average	[WT d2]	[WT d3]	[WT d4]	[[IkB _{NS} ^{-/-}	[[IkB _{NS} ^{-/-}	[[IkB _{NS} ^{-/-}	k-means cluster assignment
		d0	d2	d3	d4	d0	d2	d3	d4	log ₂ SI	vs. [WT d0]	vs. [WT d0]	vs. [WT d0]	vs. [IkB _{NS} ^{-/-} d0]	vs. [IkB _{NS} ^{-/-} d0]	vs. [IkB _{NS} ^{-/-} d0]	
17399995	S100a11...	8.7	9.7	10.3	10.2	8.2	9.8	10.3	9.6	9.6	2.0	2.9	2.8	3.0	4.1	2.6	5
17495839	Igsf6	7.5	9.3	10.9	10.9	8.0	9.3	9.9	10.2	9.5	3.4	10.7	10.5	2.5	3.7	4.6	5
17230111	Ifi205	6.5	9.8	11.1	11.0	7.3	9.9	10.4	9.9	9.5	9.8	23.5	21.9	6.1	8.7	6.3	5
17502573	Hmox1	7.7	9.1	10.5	10.5	7.6	9.4	10.3	10.1	9.4	2.8	7.0	7.0	3.3	6.3	5.6	5
17226327	Marco	7.0	9.3	10.8	10.8	7.3	9.1	10.3	10.5	9.4	4.8	14.1	14.1	3.5	7.7	9.3	5
17241409	Srgn	7.9	9.5	10.2	10.2	8.3	9.6	9.6	9.7	9.4	3.1	5.0	5.1	2.4	2.5	2.6	5
17264835	Cd68	8.0	9.3	9.9	10.0	8.0	9.4	9.9	9.9	9.3	2.5	3.8	4.0	2.7	3.7	3.7	5
17491318	Mrgpra1	8.4	9.3	10.0	10.0	7.8	9.2	9.3	9.8	9.2	1.9	2.9	2.9	2.7	2.8	4.0	5
17222149	Neur3	8.0	9.0	10.0	10.2	8.1	9.0	9.3	9.5	9.1	2.0	4.2	4.6	1.9	2.3	2.6	5
17306477	Slc7a8	7.8	9.2	9.7	9.7	8.2	9.1	9.5	9.5	9.1	2.5	3.7	3.6	1.9	2.5	2.5	5
17214197	Slc11a1	7.3	9.2	9.8	9.8	7.5	9.3	9.5	9.6	9.0	3.7	5.6	5.7	3.3	3.9	4.2	5
17376167	Sirpa	7.9	8.6	9.7	9.7	8.1	8.7	9.5	9.7	9.0	1.6	3.5	3.4	1.5	2.6	3.1	5
17227536	Ptprc	7.3	9.0	10.0	10.0	7.3	9.0	9.4	9.4	8.9	3.2	6.6	6.7	3.1	4.3	4.3	5
17234647	Itgb2	7.2	9.1	9.7	9.8	7.4	9.1	9.5	9.5	8.9	3.7	5.7	6.0	3.3	4.3	4.4	5
17408960	Cd53	7.3	9.0	9.9	9.8	7.1	9.0	9.4	9.6	8.9	3.3	6.3	5.8	3.6	4.9	5.6	5
17435089	Fgl2	7.6	9.1	9.4	9.4	7.8	9.0	9.2	9.7	8.9	2.9	3.5	3.5	2.4	2.6	3.8	5
17430906	Themis2	7.4	8.9	9.7	9.7	7.4	9.1	9.4	9.5	8.9	2.9	5.1	4.9	3.1	3.9	4.1	5
17366201	Sp140...	7.6	9.0	9.8	9.8	7.6	8.9	9.0	9.1	8.9	2.8	4.8	4.8	2.5	2.8	2.9	5
17439830	Spp1	8.3	8.9	9.2	9.3	8.0	8.5	9.8	8.8	8.9	1.5	1.9	1.9	1.4	3.4	1.7	5
17267418	A130040M12Rik	7.9	8.9	9.7	9.6	7.4	9.0	9.1	9.0	8.8	2.0	3.3	3.3	2.9	3.1	2.9	5
17279404	Plid4	7.2	8.9	9.4	9.4	7.5	9.0	9.4	9.7	8.8	3.4	4.7	4.6	2.7	3.6	4.6	5
17248860	Timd4	7.7	8.7	9.4	9.4	7.9	8.7	9.0	9.7	8.8	2.0	3.2	3.2	1.7	2.1	3.5	5
17508850	Msr1	7.7	8.7	9.4	9.4	7.9	8.8	9.3	9.3	8.8	2.1	3.3	3.2	1.9	2.7	2.6	5
17266946	Ccl5	7.1	7.9	10.7	10.7	7.5	8.1	9.1	9.1	8.8	1.8	12.2	11.7	1.6	3.0	3.1	5
17279131	Trfajp2	7.6	8.8	9.5	9.5	7.7	8.8	9.0	9.0	8.7	2.2	3.7	3.5	2.3	2.5	2.6	5
17483264	Iltgal	7.4	8.8	9.4	9.3	7.4	8.7	9.1	9.5	8.7	2.5	3.8	3.7	2.3	3.2	4.1	5
17219199	Fcgr4	6.7	9.0	9.7	9.7	6.8	8.9	9.2	9.5	8.7	4.9	8.4	8.1	4.3	5.4	6.5	5
17431612	C1qc	7.5	8.8	9.3	9.3	7.7	8.8	9.1	9.0	8.7	2.4	3.3	3.3	2.3	2.7	2.5	5
17408024	Fcgr1	7.3	8.9	9.5	9.5	7.1	8.9	9.0	9.2	8.7	3.1	4.7	4.6	3.6	3.8	4.5	5
17492661	Iqgap1	7.7	8.8	9.3	9.3	7.5	8.7	9.1	9.0	8.7	2.2	3.2	3.2	2.2	2.9	2.8	5
17260761	Plek	7.0	8.7	9.8	9.8	7.2	8.6	9.1	9.2	8.7	3.1	6.7	6.6	2.7	3.9	4.0	5
17218835	Sell	6.7	8.7	9.7	9.7	6.9	8.6	9.4	9.3	8.6	4.0	8.0	8.1	3.5	5.7	5.6	5
17325438	Hcls1	7.6	8.6	9.4	9.4	7.5	8.7	8.9	8.8	8.6	2.0	3.6	3.4	2.2	2.6	2.3	5
17491699	Mir344d-2	7.6	8.5	9.0	9.3	7.8	8.7	8.7	9.3	8.6	1.9	2.7	3.1	1.8	1.8	2.8	5
17408897	Chil3	5.3	7.4	11.2	11.3	5.4	7.1	10.7	10.1	8.6	4.5	59.2	63.1	3.3	39.6	26.1	5
17394993	Gm26489	7.1	8.8	9.3	9.2	7.8	8.6	8.4	9.0	8.5	3.1	4.4	4.3	1.8	1.5	2.3	5
17463509	Clec12a	7.1	8.4	9.7	9.5	6.9	8.6	8.8	9.1	8.5	2.4	5.9	5.3	3.3	3.7	4.5	5
17318020	Ly6d	7.0	8.6	9.4	9.6	6.7	8.5	9.2	9.0	8.5	3.1	5.4	5.9	3.3	5.4	4.9	5
17321768	Bin2	7.2	8.5	9.2	9.3	7.2	8.5	9.2	9.0	8.5	2.5	3.9	4.2	2.4	3.9	3.4	5
17254041	Ccl2	6.9	8.7	10.0	10.0	6.8	8.6	9.2	7.8	8.5	3.5	8.6	8.9	3.4	5.2	2.1	5
17431181	Sh3bgrl3	7.2	8.5	9.0	9.0	7.8	8.7	8.8	8.7	8.5	2.5	3.4	3.3	1.8	2.0	1.9	5
17230045	Ifi204	6.7	8.8	9.5	9.5	6.7	8.6	8.9	9.0	8.5	4.4	7.0	7.2	3.9	4.9	5.0	5
17449673	Naaa	7.5	8.4	9.1	9.1	7.3	8.5	8.8	8.8	8.4	1.8	3.0	3.0	2.2	2.8	2.9	5
17318100	Ly6c2	6.3	8.6	9.9	9.9	5.4	8.8	9.3	9.2	8.4	5.1	12.4	12.7	10.9	15.2	14.1	5
17338378	Trem4	7.3	8.1	9.0	8.9	7.5	8.2	8.8	9.1	8.4	1.8	3.1	2.9	1.7	2.5	3.1	5
17453288	Ncf1	7.4	8.2	9.0	8.8	7.6	8.2	8.9	8.4	8.3	1.8	3.1	2.8	1.5	2.4	1.7	5
17362973	Ms4a6d	6.2	8.7	9.7	9.6	5.4	8.6	9.0	8.9	8.3	5.6	11.2	10.7	9.0	11.9	11.4	5
17391554	Il1a	7.0	8.2	9.0	9.0	7.1	8.4	8.8	8.6	8.3	2.4	4.1	4.1	2.5	3.3	2.7	5
17450121	Plac8	6.5	8.4	9.2	9.2	6.6	8.4	8.8	8.8	8.2	3.9	6.7	6.9	3.5	4.5	4.8	5
17453819	Serpine1	6.5	8.2	9.2	9.2	7.0	8.4	9.4	7.8	8.2	3.0	6.5	6.4	2.7	5.1	1.7	5
17315570	Nckap1l	6.9	8.4	8.7	8.7	7.2	8.3	8.7	8.7	8.2	2.8	3.5	3.5	2.1	2.8	2.9	5
17254166	Sifn2	6.7	8.3	9.0	9.1	6.7	8.2	8.9	8.5	8.2	3.1	5.0	5.3	2.9	4.8	3.5	5
17243943	Spic	7.1	7.9	9.0	9.0	7.0	7.9	8.7	8.7	8.2	1.8	3.7	3.6	1.9	3.4	3.2	5
17444961	Alox5ap	6.7	7.5	9.2	9.2	6.9	7.8	8.9	8.7	8.1	1.8	5.7	5.8	1.8	3.9	3.4	5
17497334	Mki67	7.1	7.9	8.8	8.7	7.7	8.0	8.2	8.4	8.1	1.8	3.2	3.1	1.2	1.4	1.6	5
17277794	Gpr65	6.7	8.0	9.1	9.0	6.8	8.1	8.5	8.6	8.1	2.4	5.1	4.9	2.5	3.3	3.7	5
17228544	Soat1	6.8	8.1	8.8	8.7	6.8	8.1	8.6	8.8	8.1	2.5	4.0	4.0	2.5	3.5	4.1	5
17391565	Il1b	6.3	7.7	9.9	9.8	6.1	7.8	9.1	8.0	8.1	2.6	11.7	11.0	3.1	7.8	3.6	5
17515238	AB124611	6.6	8.1	8.8	8.7	7.0	8.0	8.6	8.8	8.1	2.9	4.5	4.3	2.0	3.1	3.4	5
17271769	Cd300e	6.7	8.1	8.7	8.7	6.8	8.1	8.7	8.7	8.1	2.8	4.2	4.1	2.5	3.6	3.8	5
17224813	Dock10	6.9	8.0	8.7	8.7	7.2	8.0	8.2	8.6	8.0	2.2	3.3	3.3	1.7	2.0	2.6	5
17359344	Entpd1	6.9	8.1	8.5	8.6	6.9	8.2	8.3	8.5	8.0	2.3	3.0	3.2	2.5	2.6	3.0	5
17337796	Pla2g7	5.8	7.7	9.4	9.3	6.3	7.8	8.7	8.7	8.0	3.8	11.6	11.4	2.8	5.4	5.2	5
17451437	Selplg	6.8	7.7	8.7	8.7	6.9	7.9	8.5	8.5	8.0	1.8	3.8	3.8	1.9	3.0	2.9	5
17254194	Al662270	6.9	8.2	8.7	8.6	6.8	8.0	8.1	8.3	7.9	2.4	3.4	3.3	2.4	2.5	3.0	5
17231033	Atf3	6.9	8.0	8.7	8.6	6.7	8.0	8.2	8.3	7.9	2.2	3.4	3.3	2.3	2.8	2.9	5
17489399	Fxyd5	6.6	8.1	8.8	8.8	6.6	8.0	8.5	8.1	7.9	2.9	4.5	4.5	2.7	3.7	2.8	5
17313050	Apobec3	6.3	8.2	8.6	8.6	6.8	8.1	8.5	8.3	7.9	3.5	4.9	4.8	2.4	3.1	2.8	5
17391834	Siglec1	6.9	7.7	8.5	8.6	7.2	7.7	8.5	8.4	7.9	1.8	2.9	3.2	1.4	2.5	2.4	5
17546093	Tmsb4x	6.9	7.8	8.5	8.6	7.0	7.9	8.2	8.3	7.9	1.9	3.0	3.2	1.9	2.3	2.5	5
17296558	Gm21188...	6.9	7.4	8.8	8.7	7.0	7.5	8.2	8.4	7.9	1.4	3.9	3.6	1.5	2.4	2.6	5
17341276	Fpr1	6.5	7.7	8.7	8.7	6.7	7.7	8.5	8.2	7.8	2.3	4.5	4.5	1.9	3.4	2.8	5
17483577	Iltgam	6.0	7.7	9.3	9.3	5.9	7.4	8.9	7.9	7.8	3.2	9.6	9.4	2.9	8.1	4.1	5
17229620	Fcgr3	6.8	7.7	8.2	8.5	7.1	7.7	8.1	8.5	7.8	1.8	2.6	3.2	1.6	2.0	2.8	5
17219662	Pyhin1	5.5	8.1	9.3	9.1	5.8	7.8	8.7	8.2	7.8	6.2	13.9	12.6	4.1	7.6	5.3	5
17218261	Ncf2	6.8	7.8	8.4	8.3	7.0	7.7	8.2	8.3	7.8	2.0	3.0	2.9	1.6	2.2	2.4	5
17357671	Ms4a6c	5.6	8.1	8.9	9.0	6.0	8.2	8.4	8.3	7.8	5.6	10.1					

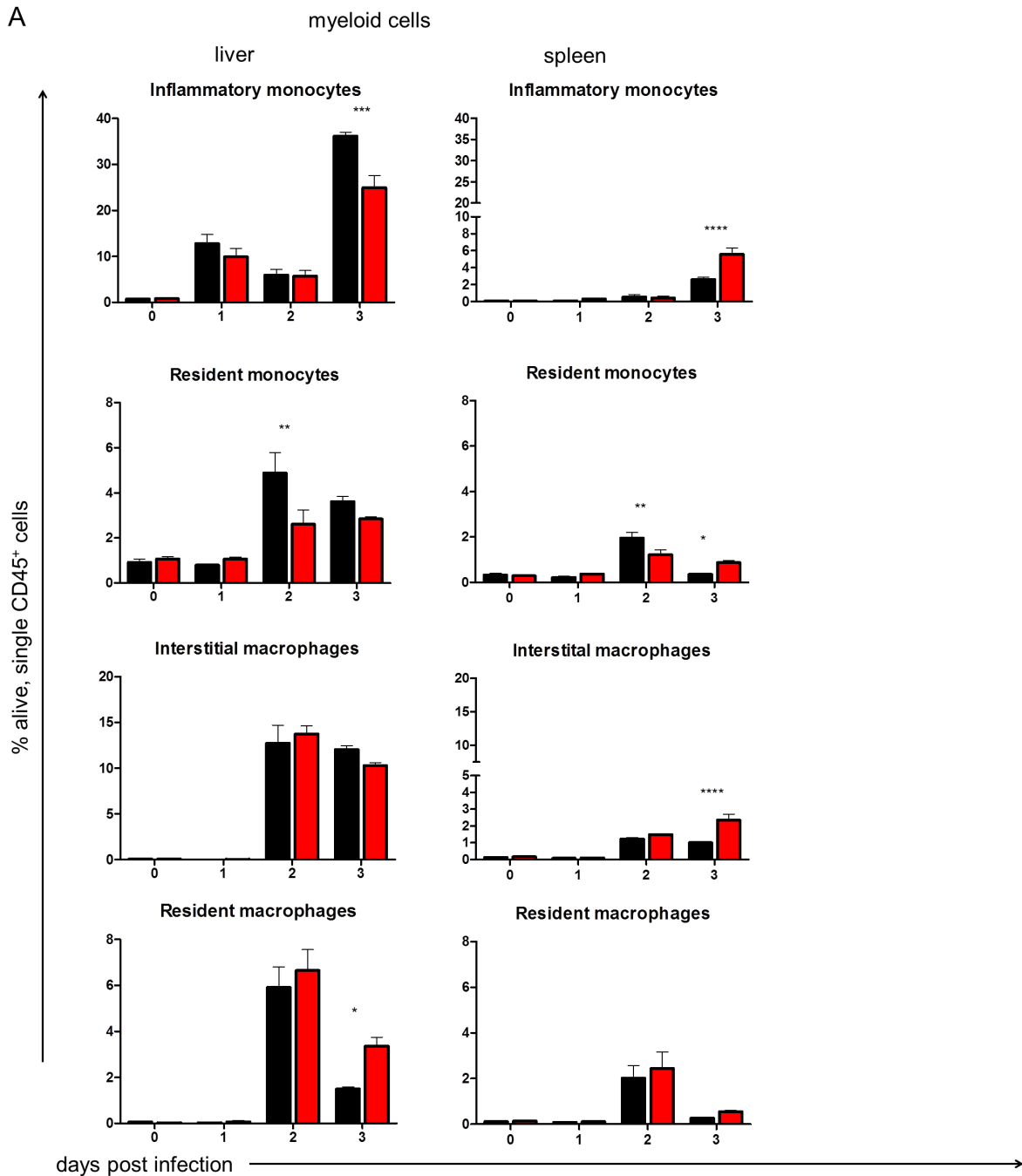
Annotation		log ₂ normalized signal intensity (SI)								Fold changes					Cluster #		
Transcripts Cluster ID	Gene Symbol	WT d0	WT d2	WT d3	WT d4	IkB _{NS} ^{-/-} d0	IkB _{NS} ^{-/-} d2	IkB _{NS} ^{-/-} d3	IkB _{NS} ^{-/-} d4	average log ₂ SI	[WT d2] vs. [WT d0]	[WT d3] vs. [WT d0]	[WT d4] vs. [WT d0]	[IkB _{NS} ^{-/-} d2] vs. [IkB _{NS} ^{-/-} d0]	[IkB _{NS} ^{-/-} d3] vs. [IkB _{NS} ^{-/-} d0]	[IkB _{NS} ^{-/-} d4] vs. [IkB _{NS} ^{-/-} d0]	k-means cluster assignment
17253707	Nos2	6.3	7.1	9.0	9.1	6.0	7.1	8.9	7.1	7.6	1.7	6.3	7.0	2.1	7.4	2.2	5
17338982	Vav1	6.4	7.7	8.1	8.0	6.9	7.7	8.0	7.9	7.6	2.5	3.2	3.0	1.7	2.2	2.0	5
17419437	Ptafr	6.9	7.3	8.2	8.3	6.6	7.4	8.2	7.6	7.6	1.4	2.6	2.7	1.7	3.0	2.1	5
17233210	Gp49a	5.9	7.6	8.8	8.8	6.2	7.4	8.2	7.6	7.6	3.4	7.5	7.4	2.3	4.1	2.7	5
17299329	Lgals3	7.1	7.5	8.0	8.0	6.4	7.7	8.0	7.7	7.6	1.3	1.9	1.9	2.4	3.1	2.5	5
17357597	Slc15a3	6.4	7.5	8.2	8.2	6.6	7.6	8.0	8.0	7.5	2.1	3.5	3.5	2.0	2.6	2.6	5
17404200	Sirpb1a	5.9	7.6	8.5	8.5	6.1	7.6	7.9	8.2	7.5	3.3	6.2	6.1	2.7	3.4	4.3	5
17266967	Ccl3	5.7	7.5	9.3	9.3	5.8	6.9	8.7	7.1	7.5	3.5	12.3	12.3	2.2	7.5	2.6	5
17433169	Pik3cd	6.7	7.3	8.1	8.2	6.2	7.6	7.8	8.1	7.5	1.6	2.8	2.9	2.6	2.9	3.7	5
17254176	Sfnf4	5.8	7.3	8.7	8.6	5.7	7.4	8.6	7.7	7.5	2.8	7.3	6.9	3.2	7.6	4.0	5
17318105	I830127L07Rik	6.3	6.9	8.0	8.2	6.6	7.7	8.0	8.0	7.5	1.4	3.1	3.6	2.0	2.5	2.5	5
17309981	Fyb	6.4	7.5	8.1	8.1	6.8	7.3	7.8	7.6	7.5	2.2	3.4	3.3	1.4	1.9	1.7	5
17505995	Ptgc2	6.8	7.6	8.0	7.9	6.2	7.4	7.8	7.6	7.4	1.7	2.2	2.0	2.3	3.1	2.7	5
17302475	Irg1	5.8	7.2	9.0	8.8	5.5	7.2	8.4	7.4	7.4	2.6	9.0	8.0	3.2	7.6	3.7	5
17266590	Evi2a...	6.3	7.3	8.0	7.9	6.7	7.4	7.6	7.9	7.4	2.0	3.1	3.0	1.7	1.9	2.4	5
17514553	Mmp8	5.5	6.9	8.8	8.8	5.8	7.0	8.6	7.8	7.4	2.8	10.5	10.2	2.3	6.9	4.2	5
17437198	Bst1	5.9	7.3	8.3	8.4	5.9	7.3	7.9	7.7	7.4	2.7	5.5	5.9	2.6	4.0	3.5	5
17399823	S100a8	5.4	6.7	9.0	9.0	5.4	6.6	8.5	7.8	7.3	2.4	12.2	11.9	2.3	8.3	5.2	5
17388733	Cd44	6.3	7.3	8.0	7.9	6.4	7.2	7.8	7.5	7.3	2.0	3.2	3.1	1.7	2.6	2.1	5
17471828	Klra2	5.7	7.5	8.2	8.2	5.9	7.3	7.9	7.6	7.3	3.4	5.8	5.7	2.6	3.8	3.1	5
17291881	F13a1	6.4	6.7	8.2	8.2	6.1	6.7	8.3	7.7	7.3	1.2	3.6	3.7	1.5	4.7	3.0	5
17404209	Sirpb1b	5.7	7.4	8.2	8.3	5.6	7.5	7.8	7.7	7.3	3.4	5.8	6.2	3.6	4.6	4.3	5
17498730	Mcomp1	6.3	7.0	8.2	8.3	6.4	6.9	7.7	7.4	7.3	1.7	3.9	4.0	1.4	2.5	2.1	5
17419483	Fgr	6.3	7.5	7.6	7.6	6.4	7.2	8.0	7.3	7.2	2.3	2.5	2.6	1.7	3.1	1.9	5
17326075	Retnlg	5.3	7.1	8.5	8.5	5.7	6.9	8.1	7.9	7.2	3.4	9.0	9.2	2.3	5.3	4.7	5
17336114	Myo1f	6.2	7.2	7.8	7.7	6.1	7.2	7.7	7.8	7.2	2.0	3.1	2.8	2.1	3.0	3.2	5
17454166	Pilra	6.1	6.8	7.9	8.0	6.4	7.0	7.7	7.7	7.2	1.6	3.5	3.5	1.5	2.4	2.5	5
17408856	I830077J02Rik	6.4	7.1	7.8	7.7	6.0	7.2	7.9	7.5	7.2	1.7	2.7	2.5	2.3	3.7	2.8	5
17333731	Fpr2	5.7	7.0	8.4	8.3	5.4	6.9	7.8	7.4	7.1	2.6	6.7	6.3	2.8	5.2	3.9	5
17290083	Emb	6.2	6.7	7.8	7.7	6.3	6.9	7.7	7.4	7.1	1.5	3.0	2.9	1.5	2.6	2.2	5
17296436	Parp8	6.0	7.1	7.8	7.7	6.0	7.1	7.6	7.5	7.1	2.2	3.6	3.3	2.2	3.0	2.8	5
17493912	Art2b	5.8	7.3	7.7	7.6	5.8	7.1	6.9	8.2	7.1	2.8	3.7	3.4	2.4	2.1	5.3	5
17401269	Ptprn2	5.9	7.1	7.6	7.5	6.2	6.9	7.2	7.6	7.0	2.3	3.2	3.0	1.6	2.0	2.8	5
17407363	S100a9	5.6	6.0	8.4	8.5	5.5	6.5	7.8	7.6	7.0	1.3	7.0	7.3	2.0	5.0	4.2	5
17316197	Fam105a	5.9	6.8	7.6	7.5	6.1	6.9	7.3	7.5	6.9	1.9	3.2	3.1	1.8	2.2	2.6	5
17268909	Top2a	5.9	6.9	7.5	7.6	6.4	7.0	7.1	7.1	6.9	2.0	3.1	3.2	1.5	1.7	1.7	5
17459744	Reg3b	6.0	7.3	7.3	7.3	5.9	6.7	8.1	6.7	6.9	2.4	2.4	2.5	1.7	4.5	1.8	5
17546101	Tlr8	5.7	6.8	7.5	7.6	6.0	6.6	7.4	7.5	6.9	2.2	3.7	3.9	1.5	2.7	2.8	5
17514482	Mmp13	6.0	6.6	7.3	7.4	6.0	7.1	7.6	6.8	6.8	1.5	2.4	2.6	2.3	3.1	1.7	5
17212174	Il1r2	5.6	6.7	8.0	7.9	5.6	6.3	7.8	7.0	6.8	2.1	5.2	5.0	1.6	4.5	2.6	5
17470627	Clec4e	5.6	6.2	8.4	8.4	5.1	6.2	8.0	6.8	6.8	1.5	7.0	6.8	2.2	7.3	3.2	5
17292569	Sema4d	5.9	6.8	7.5	7.6	6.1	6.8	7.2	6.8	6.8	1.9	3.0	3.3	1.6	2.2	1.7	5
17404230	Gm5150	5.4	6.4	7.4	7.4	6.6	6.7	7.5	7.3	6.8	2.0	4.1	4.0	1.1	1.9	1.7	5
17449417	Sult1e1	5.8	7.1	6.8	7.0	5.7	6.6	7.8	7.9	6.8	2.4	2.0	2.4	1.9	4.4	4.7	5
17527934	Kif23	6.0	6.4	7.6	7.5	5.8	6.7	6.9	7.6	6.8	1.4	3.1	3.0	1.8	2.1	3.3	5
17462796	Clec4d	5.6	6.3	7.7	7.8	6.4	6.2	6.9	6.8	6.7	1.6	4.2	4.6	-1.2	1.4	1.3	5
17357640	Ms4a4a	5.1	6.4	7.8	7.8	5.5	6.3	7.7	6.8	6.7	2.4	6.4	6.4	1.7	4.6	2.5	5
17357648	Ms4a4c	5.3	6.5	7.9	7.8	5.4	6.4	7.0	7.1	6.7	2.4	6.0	5.7	2.0	2.9	3.2	5
17485609		6.1	6.5	7.4	7.5	5.1	6.6	7.1	6.8	6.6	1.4	2.6	2.7	3.0	4.0	3.4	5
17375503	AA467197...	5.4	5.9	7.8	7.9	5.7	6.1	7.2	6.6	6.6	1.4	5.2	5.5	1.3	2.8	1.8	5
17546109	Tlr7	5.3	6.5	7.0	7.0	6.0	6.5	6.8	6.9	6.5	2.3	3.3	3.2	1.4	1.7	1.8	5
17218060	Ptgs2	5.6	6.1	7.7	7.7	5.8	6.2	7.0	5.9	6.5	1.4	4.2	4.2	1.3	2.3	1.1	5
17460465	Asprv1	5.4	5.9	7.2	7.2	5.7	6.0	6.5	6.5	6.3	1.5	3.5	3.5	1.2	1.7	1.7	5
17290894	Gpr141	5.1	6.0	7.2	7.2	5.0	6.0	6.7	6.7	6.2	1.9	4.4	4.5	2.1	3.2	3.2	5
17443801	Gm22956	6.4	6.1	6.3	6.5	4.7	5.8	5.9	6.4	6.0	-1.3	-1.1	1.0	2.1	2.3	3.2	5
17463579	Gm17631	9.5	9.9	11.4	11.4	9.7	9.8	9.7	11.6	10.4	1.4	3.9	3.8	1.0	-1.0	3.6	6
17231611	Gm25682	8.7	8.6	9.5	9.5	10.1	8.5	7.5	9.8	9.0	-1.1	1.7	1.7	-2.9	-5.9	-1.3	6
17416811	Mir761	7.7	7.7	10.0	9.9	8.1	8.0	7.8	10.1	8.7	1.0	4.8	4.6	-1.0	-1.2	4.2	6
17535471	Mir2137	8.0	8.2	9.2	9.3	7.7	8.2	8.2	9.4	8.5	1.2	2.3	2.4	1.4	1.4	3.1	6
17344686	Gm10499...	7.4	8.2	9.2	9.4	7.6	8.2	8.1	9.3	8.4	1.7	3.4	3.9	1.5	1.4	3.2	6
17379887		7.8	7.6	9.5	9.6	8.4	7.2	7.2	9.9	8.4	-1.2	3.1	3.3	-2.3	2.9	6	
17504370		7.5	7.6	9.2	9.3	7.7	8.0	9.1	8.3	8.1	-1.1	3.2	3.4	1.0	1.2	2.6	6
17248470	Gm26070	7.2	7.8	9.4	9.3	7.4	7.7	7.8	8.8	8.2	1.6	4.5	4.3	1.3	1.3	2.8	6
17229257	Gm23208	7.1	7.2	9.1	9.1	7.8	7.3	7.4	9.2	8.0	1.0	4.0	3.9	-1.4	-1.3	2.5	6
17544623	Gm25936	7.2	6.7	9.1	9.1	7.7	7.0	7.1	9.4	7.9	-1.4	3.8	3.7	-1.6	-1.5	3.2	6
17415432	Gm22804	7.3	7.3	8.9	9.0	7.1	7.4	7.4	8.8	7.9	-1.0	3.0	3.2	1.2	1.2	3.2	6
17499753	Gm15292	6.9	7.3	8.7	8.9	7.3	7.4	7.2	8.6	7.8	1.4	3.7	4.3	1.1	-1.0	2.6	6
17302356	Gm24770	7.2	7.1	8.6	8.9	7.3	7.1	6.7	8.9	7.7	-1.1	2.7	3.1	-1.2	-1.5	3.1	6
17496547	Prrt2	7.4	7.2	8.4	8.3	7.0	7.0	6.8	8.6	7.6	-1.2	2.0	1.9	1.0	-1.1	3.1	6
17241598	Gm7075	6.8	7.1	8.5	8.4	7.6	7.0	6.7	8.6	7.6	1.3	3.3	3.1	-1.5	-1.9	2.1	6
17491695	Gm23962	7.0	6.9	8.2	8.1	7.2	6.8	7.3	8.9	7.5	-1.1	2.2	2.1	-1.3	1.1	3.3	6
17278626	Mir345	6.4	7.4	8.3	8.2	7.2	7.0	7.3	8.4	7.5	2.0	3.7	3.5	-1.1	1.1	2.4	6
17328935	Gm26219	6.6	7.0	8.6	8.5	6.7	7.1	7.3	8.5	7.5	1.3	4.1	3.8	1.3			

Annotation		log ₂ normalized signal intensity (SI)								Fold changes					Cluster #		
Transcripts Cluster ID	Gene Symbol	WT	WT	WT	WT	lkb _{NS} ^{-/-}	lkb _{NS} ^{-/-}	lkb _{NS} ^{-/-}	lkb _{NS} ^{-/-}	average	[WT d2]	[WT d3]	[WT d4]	[lkb _{NS} ^{-/-} d2]	[lkb _{NS} ^{-/-} d3]	[lkb _{NS} ^{-/-} d4]	k-means cluster assignment
		d0	d2	d3	d4	d0	d2	d3	d4	log ₂ SI	vs. [WT d0]	vs. [WT d0]	vs. [WT d0]	vs. [lkb _{NS} ^{-/-} d0]	vs. [lkb _{NS} ^{-/-} d0]	vs. [lkb _{NS} ^{-/-} d0]	
17364167	Gm25611	6.2	6.6	8.2	8.1	6.8	6.5	6.7	7.8	7.1	1.3	3.9	3.8	-1.2	-1.1	2.1	6
17507788	Gm25665	6.3	6.4	8.1	8.2	7.0	6.5	6.4	7.8	7.1	1.1	3.6	3.7	-1.4	-1.5	1.8	6
17498067	Gm10153	6.0	6.6	8.0	8.0	6.6	6.5	6.8	8.1	7.1	1.5	4.3	4.1	-1.1	1.2	2.7	6
17448170	Gm22273	6.6	6.6	8.1	8.0	6.4	6.3	6.7	8.0	7.1	-1.0	2.8	2.6	-1.1	1.2	3.1	6
17399864	Sprr2b	6.7	6.9	7.4	7.3	6.5	6.7	6.6	8.2	7.0	1.2	1.7	1.5	1.2	1.1	3.1	6
17375927	Gm22889	5.9	6.2	8.2	8.2	6.8	6.9	6.1	7.7	7.0	1.2	4.9	4.7	1.1	-1.6	1.9	6
17354793	Mir143	6.2	6.5	7.9	7.9	6.6	6.5	6.4	7.7	7.0	1.2	3.4	3.3	-1.1	-1.1	2.1	6
17423207	Mir3471-1	6.3	6.0	7.9	7.8	6.9	6.3	6.1	8.3	7.0	-1.3	3.1	2.8	-1.5	-1.8	2.7	6
17368760	Mir3088	6.2	6.7	7.9	8.0	6.1	6.8	6.5	7.3	6.9	1.4	3.3	3.4	1.6	1.3	2.2	6
17281400		6.2	6.1	8.1	7.8	6.5	6.4	6.3	8.0	6.9	-1.1	3.7	3.2	-1.1	-1.2	2.8	6
17269903	Aarsd1	5.9	6.0	7.7	7.6	6.8	6.5	6.5	8.2	6.9	1.1	3.5	3.4	-1.2	-1.2	2.6	6
17516298	Olf978	6.0	6.5	7.7	7.7	6.5	6.7	6.7	7.3	6.9	1.5	3.4	3.3	1.1	1.1	1.8	6
17540136	Gm5634	5.8	5.9	7.8	7.8	6.6	6.5	6.5	7.6	6.8	1.1	3.9	4.0	-1.1	-1.1	1.9	6
17233792		6.1	6.1	7.9	7.8	6.7	5.9	5.7	8.0	6.8	-1.0	3.6	3.3	-1.7	-1.9	2.6	6
17300145	Traj54	5.9	6.6	7.7	7.5	6.2	6.3	6.1	8.1	6.8	1.6	3.5	3.0	1.0	-1.1	3.7	6
17254616		6.6	6.3	7.7	7.9	5.7	6.3	6.1	7.6	6.8	-1.2	2.2	2.6	1.6	1.3	3.8	6
17495214	Gm24154	6.7	6.1	7.5	7.5	6.0	6.5	6.1	7.7	6.8	-1.5	1.8	1.8	1.3	1.0	3.0	6
17231114	Mir3473c	6.2	6.1	7.5	7.4	7.1	6.2	5.4	8.1	6.7	-1.1	2.6	2.3	-1.9	-3.3	1.9	6
17476938		6.0	6.2	7.9	7.8	6.0	6.4	6.1	7.5	6.7	1.1	3.7	3.6	1.3	1.0	2.8	6
17462139	Olf9213	5.9	5.9	8.0	7.9	5.9	5.8	6.0	8.2	6.7	1.0	4.3	3.9	-1.0	1.1	4.8	6
17535096	Gm26487	5.8	6.1	7.7	7.6	6.2	6.3	5.6	7.8	6.6	1.3	3.7	3.7	1.1	-1.5	3.1	6
17293813		5.6	6.1	7.1	7.2	6.5	6.6	6.5	7.4	6.6	1.4	2.9	3.0	1.1	1.0	1.9	6
17467407	LOC434035...	5.5	5.8	7.7	7.7	6.3	6.0	6.2	7.7	6.6	1.2	4.5	4.5	-1.3	-1.1	2.6	6
17493308	Gm23928	5.7	5.8	7.8	7.8	6.5	5.5	5.9	8.0	6.6	1.1	4.5	4.4	-2.0	-1.5	2.7	6
17434508	Gm23993	5.9	5.7	7.8	7.9	6.1	6.3	5.9	7.4	6.6	-1.2	3.6	3.8	1.2	-1.1	2.5	6
17309022		5.9	6.1	7.3	7.5	6.4	6.4	6.0	7.2	6.6	1.2	2.8	3.2	1.0	-1.3	1.8	6
17522555	Ltf	5.9	6.0	7.5	7.8	5.6	6.1	6.6	7.3	6.6	1.1	3.0	3.6	1.4	2.0	3.2	6
17404462	Mir3092	5.7	6.3	7.2	7.4	6.0	6.1	6.5	7.4	6.6	1.5	2.7	3.2	1.1	1.4	2.8	6
17287294		5.4	6.0	7.5	7.4	6.3	6.2	5.9	7.7	6.6	1.5	4.3	4.1	-1.0	-1.3	2.8	6
17246449	Olf91818	6.2	5.7	7.6	7.7	5.7	5.8	5.9	7.9	6.5	-1.4	2.6	2.9	1.0	1.1	4.5	6
17275752	Gm22673	6.0	5.7	7.5	7.5	6.0	6.1	5.5	7.9	6.5	-1.3	2.9	2.8	1.1	-1.4	3.8	6
17498075	Gm2431	5.4	6.0	7.4	7.5	6.2	6.1	5.7	7.7	6.5	1.6	4.1	4.4	-1.0	-1.4	2.9	6
17265524	Gm23266	5.7	5.8	7.4	7.5	5.8	6.1	6.2	7.7	6.5	1.1	3.1	3.5	1.2	1.3	3.7	6
17366744	Mir669a-3	5.7	5.8	7.7	7.6	6.3	5.5	5.4	8.0	6.5	1.1	3.9	3.7	-1.8	-1.9	3.1	6
17507790	Gm24469	6.0	5.7	7.6	7.5	6.0	5.7	5.9	7.6	6.5	-1.2	2.9	2.7	-1.2	-1.0	3.0	6
17278820	Mir494	5.4	5.8	7.8	7.7	5.9	5.9	5.9	7.5	6.5	1.3	5.1	4.9	1.0	1.0	3.1	6
17547980	Olf9177...	6.2	6.0	7.3	7.4	5.5	5.9	6.0	7.5	6.5	-1.2	2.1	2.2	1.3	1.4	3.8	6
17527164		6.1	5.6	7.6	7.6	7.0	5.4	5.2	7.2	6.5	-1.5	2.8	2.8	-3.0	-3.3	1.2	6
17299830	Trav13d-1	5.8	5.8	7.3	7.5	5.8	6.0	6.3	7.1	6.4	1.0	2.9	3.2	1.2	1.4	2.5	6
17389285	Olf91303...	5.6	6.2	7.2	7.2	6.2	5.8	6.1	7.4	6.4	1.6	3.1	3.1	-1.3	-1.1	2.4	6
17246388	Olf9765	5.8	5.8	7.5	7.3	5.9	6.0	6.3	6.6	6.4	-1.0	3.1	2.8	1.1	1.3	1.7	6
17342890	Clps	5.6	5.9	7.4	7.4	5.6	6.2	6.2	7.0	6.4	1.2	3.4	3.6	1.5	1.5	2.6	6
17396401	Gm26040	5.5	5.9	7.2	7.2	6.0	5.9	6.3	7.2	6.4	1.3	3.3	3.2	-1.1	1.3	2.4	6
17367738		5.8	5.6	7.4	7.1	6.1	6.1	5.4	7.7	6.4	-1.2	3.0	2.4	-1.1	-1.6	3.0	6
17357930	Olf91487	5.5	6.5	7.0	7.1	5.7	6.1	5.7	7.5	6.4	2.1	2.9	3.1	1.3	1.0	3.4	6
17221932	Gm23785	5.4	5.4	7.6	7.6	6.0	5.6	5.6	7.7	6.4	1.0	4.7	4.5	-1.3	-1.3	3.2	6
17469444	Gm22328	5.7	5.7	7.3	7.3	6.0	6.0	5.5	7.4	6.4	-1.1	3.0	3.0	-1.0	-1.4	2.6	6
17481215	Olf9617	5.6	5.7	7.6	7.7	6.1	5.7	5.2	7.3	6.4	1.1	4.2	4.5	-1.3	-1.9	2.3	6
17223344	Gm24548	5.5	5.2	7.3	7.3	5.6	6.1	6.1	7.5	6.3	-1.2	3.6	3.6	1.4	1.5	3.7	6
17525704	Olf935	5.4	5.8	7.2	7.2	5.6	6.1	6.0	7.1	6.3	1.3	3.4	3.3	1.4	1.3	2.8	6
17311310	Gm24751	5.6	5.5	7.3	7.2	6.3	5.5	5.2	7.7	6.3	-1.0	3.3	3.0	-1.7	-2.1	2.7	6
17541769	4933416i08Rik	5.4	6.1	7.1	7.1	5.8	5.9	5.3	7.6	6.3	1.7	3.3	3.3	1.0	-1.5	3.4	6
17213570	Gm24942	5.4	5.6	7.1	7.0	5.9	5.8	5.8	7.3	6.2	1.1	3.2	3.0	-1.0	-1.1	2.7	6
17509962	Gm25906	5.3	5.5	7.0	6.9	5.8	5.8	5.8	7.3	6.2	1.1	3.3	3.1	-1.0	-1.0	2.8	6
17343525	Gm25667	5.4	5.6	7.2	7.3	5.7	5.8	5.6	6.9	6.2	1.1	3.4	3.6	1.1	-1.0	2.3	6
17326638	Gm26307	5.5	5.8	7.0	7.1	5.1	6.0	5.7	7.0	6.2	1.2	2.8	2.9	1.9	1.6	3.9	6
17311443	Gm24768	5.9	5.4	7.0	6.9	5.7	5.8	5.2	7.3	6.1	-1.4	2.1	2.1	1.1	-1.4	3.2	6
17257960	Gm26052	5.0	5.0	7.6	7.7	5.5	5.3	5.1	7.8	6.1	1.1	6.4	6.7	-1.1	-1.2	4.9	6
17442126	Gm22965	5.5	5.7	6.4	6.5	6.9	5.1	6.1	6.9	6.1	1.1	1.8	2.0	-3.4	-1.7	1.0	6
17533934	Spin2f	6.1	5.5	6.8	6.8	5.5	5.9	5.3	7.1	6.1	-1.5	1.7	1.7	1.3	-1.1	3.2	6
17302343	Gm25495	5.1	4.8	7.5	7.4	5.4	5.8	5.4	7.5	6.1	-1.3	5.0	4.8	1.3	-1.0	4.2	6
17508848	Gm23128	5.7	5.7	7.2	7.1	5.2	5.4	5.3	7.4	6.1	1.0	2.9	2.8	1.1	1.1	4.8	6
17225110	LOC102634459...	5.6	5.2	7.2	7.2	5.1	5.4	5.6	7.3	6.1	-1.3	3.0	3.1	1.2	1.4	4.5	6
17325347	Stfa1	5.6	5.6	7.2	7.2	5.7	5.4	5.4	6.7	6.1	1.0	3.0	3.0	-1.3	-1.3	1.9	6
17363158	Gm22323...	5.7	6.0	6.8	7.1	4.8	5.6	5.7	7.0	6.1	1.2	2.1	2.5	1.7	1.9	4.5	6
17363156	Gm22323...	5.7	6.0	6.8	7.0	4.8	5.6	5.7	7.0	6.1	1.2	2.0	2.5	1.7	1.9	4.5	6
17417238		5.2	5.6	6.9	6.7	6.3	5.4	5.7	6.5	6.1	1.3	3.2	2.9	-1.9	-1.5	1.1	6
17298923	Gm22469	4.7	4.9	7.8	7.6	5.2	5.4	5.1	7.5	6.0	1.2	8.6	7.7	1.2	-1.1	5.0	6
17325324	Stfa21l	4.9	5.0	7.5	7.6	4.9	5.1	6.3	6.8	6.0	1.1	5.9	6.4	1.2	2.7	3.8	6
17299473	Olf9727	5.3	5.3	6.8	6.8	5.7	5.5	5.4	7.3	6.0	-1.0	2.8	2.7	-1.2	-1.2	3.1	6
17474797	Vmn1r157	5.0	5.5	7.0	7.1	5.5	5.4	5.6	6.9	6.0	1.4	3.9	4.3	-1.1	1.0	2.7	6
17357928	Olf91484	5.2	5.1	7.0	7.2	5.7	5.4	5.3	7.0	6.0	-1.1	3.4	4.1	-1.2	-1.3	2.4	6
17242320	Gm3250	5.0	5.7	6.8	6.9	5.8	5.7	5.6	6.5	6.0	1.6	3.5	3.7	-1.1	-1.1	1.6	6

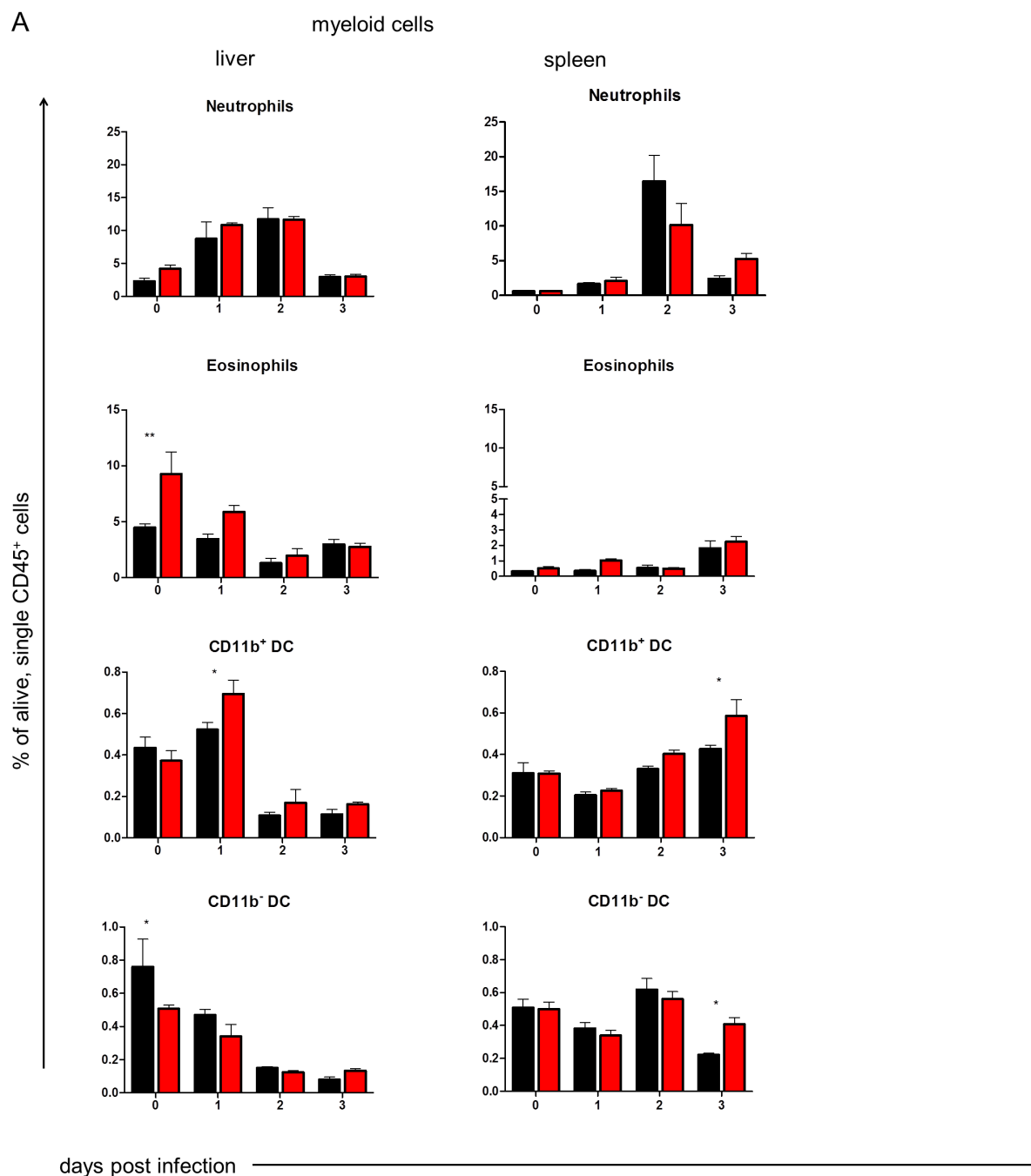
Annotation		log ₂ normalized signal intensity (SI)									Fold changes						Cluster #
Transcripts Cluster ID	Gene Symbol	WT	WT	WT	WT	IkB _{NS} ^{-/-}	IkB _{NS} ^{-/-}	IkB _{NS} ^{-/-}	IkB _{NS} ^{-/-}	average	[WT d2]	[WT d3]	[WT d4]	[IkB _{NS} ^{-/-} d2]	[IkB _{NS} ^{-/-} d3]	[IkB _{NS} ^{-/-} d4]	k-means cluster assignment
		d0	d2	d3	d4	d0	d2	d3	d4	log ₂ SI	vs. [WT d0]	vs. [WT d0]	vs. [WT d0]	vs. [IkB _{NS} ^{-/-} d0]	vs. [IkB _{NS} ^{-/-} d0]	vs. [IkB _{NS} ^{-/-} d0]	
17521068	Gm23391	5.0	5.2	7.1	7.0	5.3	5.2	5.1	6.5	5.8	1.2	4.3	4.0	-1.1	-1.1	2.3	6
17287790	H2afy	5.0	5.3	6.7	6.7	5.1	5.2	5.2	6.9	5.8	1.2	3.1	3.2	1.0	1.1	3.5	6
17516028	n-R5s82	5.3	5.4	6.5	6.5	4.8	5.6	5.1	6.7	5.7	1.1	2.3	2.4	1.7	1.3	3.8	6
17389269	Olfr1282	4.8	5.5	6.6	6.2	5.9	5.0	5.2	6.7	5.7	1.6	3.3	2.6	-1.8	-1.6	1.8	6
17417658	Gm23287	5.5	5.0	7.1	7.2	5.0	5.2	5.1	5.7	5.7	-1.3	3.1	3.3	1.1	1.1	1.6	6
17316278	Gm26416	5.3	5.0	6.6	6.3	5.3	5.1	5.2	6.9	5.7	-1.3	2.4	2.0	-1.2	-1.1	3.1	6
17370337	Olfr344	5.0	5.2	6.8	6.7	5.3	5.1	4.9	6.7	5.7	1.1	3.4	3.1	-1.1	-1.3	2.7	6
17398018	Gm23500	5.0	5.2	6.4	6.5	4.9	5.3	5.2	6.8	5.7	1.1	2.6	2.7	1.3	1.3	3.8	6
17396095		4.8	5.0	7.1	7.1	4.9	4.9	4.7	7.0	5.7	1.1	4.9	4.8	-1.0	-1.2	4.4	6
17541717	Mir450-1	4.8	5.2	6.6	6.7	5.1	5.3	4.8	6.7	5.7	1.2	3.3	3.7	1.2	-1.2	3.1	6
17529645	Mir184	5.1	5.0	6.7	6.6	5.4	4.9	4.9	6.7	5.7	-1.1	3.1	2.8	-1.4	-1.4	2.5	6
17311457	Gm23530	5.0	5.1	6.4	6.2	5.2	5.1	5.1	7.0	5.6	1.0	2.5	2.3	-1.1	-1.0	3.4	6
17298654	Gm25498	5.1	5.2	6.7	6.6	4.9	5.2	5.2	6.2	5.6	1.1	3.0	2.9	1.2	1.2	2.5	6
17361006		4.6	5.0	6.6	6.7	5.5	5.1	4.9	6.8	5.6	1.3	4.0	4.4	-1.3	-1.5	2.5	6
17459377	LOC672450	5.2	4.9	6.3	6.3	4.9	5.6	5.1	6.5	5.6	-1.2	2.2	2.1	1.7	1.2	3.1	6
17470829	Rnu7...	5.0	5.3	6.6	6.5	4.9	4.9	4.6	6.8	5.6	1.2	3.0	3.0	-1.0	-1.3	3.5	6
17480237		4.9	5.2	6.7	6.9	4.7	4.9	4.7	6.3	5.6	1.3	3.5	3.9	1.2	1.0	3.0	6
17309372	Gm22764	4.7	5.0	6.5	6.7	5.1	5.4	5.0	6.0	5.5	1.2	3.4	4.0	1.3	-1.0	1.9	6
17421469	Rex2	4.7	5.1	6.4	6.3	4.9	5.0	4.8	6.6	5.5	1.3	3.3	3.0	1.0	-1.1	3.3	6
17330093	Gm25967	4.8	4.8	6.5	6.4	5.1	4.9	4.9	6.4	5.5	-1.0	3.2	2.9	-1.2	-1.2	2.4	6
17398285	Gm25621	4.7	4.9	6.5	6.6	5.2	5.0	4.8	6.1	5.5	1.1	3.5	3.8	-1.2	-1.4	1.9	6
17481598	Olfr476	4.8	4.8	6.3	6.4	5.2	4.9	4.8	6.6	5.5	1.0	2.9	3.0	-1.2	-1.2	2.8	6
17317799	Gm24390	4.8	4.7	6.7	6.8	4.6	4.9	4.7	6.5	5.5	-1.1	3.7	4.0	1.2	1.1	3.7	6
17311189	Gm24789	4.5	4.6	6.4	6.5	4.9	5.4	4.7	6.7	5.5	1.1	3.6	3.9	1.5	-1.1	3.6	6
17222623	Gm23126	4.8	5.0	6.1	6.4	4.9	5.0	4.9	6.3	5.4	1.1	2.5	3.1	1.1	1.0	2.6	6
17429290	Olfr1328	5.0	4.7	6.7	6.3	4.9	5.0	4.8	6.0	5.4	-1.3	3.1	2.3	1.1	-1.1	2.1	6
17266617		4.5	4.5	6.7	6.8	4.8	4.7	4.7	6.3	5.4	1.0	4.7	5.0	-1.1	-1.1	2.8	6
17387624	Olfr1019	4.7	4.9	6.0	6.1	4.6	5.1	5.1	6.3	5.4	1.1	2.5	2.6	1.4	1.4	3.1	6
17248424	Gm25799	5.2	4.6	6.1	6.3	4.8	4.7	4.6	6.5	5.4	-1.5	1.8	2.1	-1.1	-1.1	3.3	6
17544269	Gm23985	4.5	4.9	6.0	6.2	4.9	4.9	4.9	6.2	5.3	1.4	2.9	3.2	-1.0	1.0	2.5	6
17351706		4.6	4.6	6.2	6.3	5.0	4.7	4.7	6.3	5.3	1.0	3.0	3.3	-1.2	-1.2	2.6	6
17238648	Olfr775	4.8	4.6	6.6	6.5	4.7	4.5	4.6	6.1	5.3	-1.1	3.6	3.3	-1.1	-1.1	2.8	6
17301534	Gm24258	4.7	4.6	6.3	6.2	4.7	4.7	4.7	6.3	5.3	-1.0	3.1	2.9	1.0	-1.0	3.2	6
17530105	Gm23949	4.6	4.9	6.1	6.2	4.7	4.6	4.7	6.1	5.2	1.2	2.7	3.1	-1.1	-1.0	2.6	6
17387712	Olfr1095	4.6	4.7	6.1	6.2	4.5	4.6	4.6	6.5	5.2	1.1	2.7	2.9	1.0	1.0	3.9	6
17269220	Gm11595	5.1	5.0	5.2	5.3	4.6	4.8	5.0	6.2	5.1	-1.1	1.1	1.2	1.2	1.3	3.0	6



Appendix Figure 1: Lymphocyte composition of livers and spleens of WT and lkbNS^{-/-} mice during the course of LM infection. WT (■, n=3-4) and lkbNS^{-/-} (■, n=3-4) mice were infected with high-dose (10⁵ CFU) of *Listeria*. At indicated times post infection, mice were sacrificed and the cellular composition was determined by flow cytometry. Data are represented as mean ± SEM of % alive, single and CD45⁺ cells. Statistical analyses were performed using two-way ANOVA with Bonferroni post-test. **** p < 0.0001, *** p < 0.001, ** p < 0.01, * p < 0.05.



Appendix Figure 2: Cellular composition of monocytes and macrophages in livers and spleens of WT and *IkBNS*^{-/-} mice during the course of LM infection. WT (■, n=3-4) and *IkBNS*^{-/-} (■, n=3-4) mice were infected with high-dose (10^5 CFU) of *Listeria*. At indicated times post infection, mice were sacrificed and the cellular composition was determined by flow cytometry. Data are represented as mean \pm SEM of % alive, single and CD45⁺ cells. Statistical analyses were performed using two-way ANOVA with Bonferroni post-test. **** $p < 0.0001$, *** $p < 0.001$, ** $p < 0.01$, * $p < 0.05$.



Appendix Figure 3: Cellular composition of myeloid cell subsets in livers and spleens of WT and IkBNS^{-/-} mice during the course of LM infection. WT (■, n=3-4) and IkBNS^{-/-} (■, n=3-4) mice were infected with high-dose (10⁵ CFU) of *Listeria*. At indicated times post infection, mice were sacrificed and the cellular composition was determined by flow cytometry. Data are represented as mean ± SEM of % alive, single and CD45⁺ cells. Statistical analyses were performed using two-way ANOVA with Bonferroni post-test. **** p < 0.0001, *** p < 0.001, ** p < 0.01, * p < 0.05.

Acknowledgements

Zuallererst möchte ich mich bei Prof. Dr. Dunja Bruder bedanken, für die Möglichkeit dieses spannende Thema unter hervorragenden Bedingungen zu bearbeiten. Danke für dein Vertrauen, deine aufbauenden und motivierenden Worte und deine Unterstützung. Du hattest immer ein offenes Ohr, egal mit welchem Anliegen ich vor deiner Tür stand und wusstest immer einen guten Rat. Ich danke dir für die großartige Betreuung!

Ein ebenso großes Dankeschön gebührt Dr. Andreas Jeron. Danke für deine Bereitschaft, mich jederzeit tatkräftig im Labor zu unterstützen, die vielen Diskussionen und Anregungen und Ideen, die einen großen Beitrag zum Gelingen dieser Arbeit geleistet haben! Danke, dass du mich immer ermutigt hast, Dinge zu hinterfragen und neue Ansätze auszuprobieren und einfach zu forschen. Die Arbeit mit dir zusammen hat mich viel gelehrt und in gewisser Weise auch geprägt- natürlich im Positiven ☺

Weiterhin möchte ich mich bei Isabel Bernal, Alexander Pausder, Martha Böning und Marat Gajsin bedanken, die im Rahmen ihrer Masterarbeiten wichtige „Puzzleteile“ zu dieser Arbeit beigetragen haben.

Ein großer Dank geht an alle, die mich immer tatkräftig im Labor unterstützt haben und jeden noch so langen Labortag durch ihre Anwesenheit und Hilfe viel erträglicher gemacht haben, danke Franzi! ☺
Weiterhin danke ich allen IREGlern aus Braunschweig, sowie den „Blutsbrüdern“ aus MD! Danke für viele interessante Diskussionen und schöne Erlebnisse und Unternehmungen, welche die gesamte Doktorandenzeit zu einem tollen Erlebnis gemacht haben!

Danken möchte ich auch all meinen Freunden, die immer dafür sorgen, dass das Leben lebenswert ist und „das Glas halb voll, statt halb leer“! ☺

Ich danke dir, Max, dass du für mich da bist und mir zur Seite stehst. Danke, dass du grad in der „Endphase“ so manch Stimmungsschwankung geduldig ertragen hast und immer weißt, wie du mich wieder zum Lachen bringst.

Zu guter Letzt, geht mein größtes Dankeschön an meine Eltern Rainer und Doreen, sowie an meine Großeltern, die mich immer unterstützen und hinter mir stehen, mir neue Kraft und Energie geben und immer dafür sorgen, dass nach jeder dunklen Wolke die Sonne wieder scheint! Danke, dass ihr mir das alles ermöglicht habt und immer für mich da seid!

Selbstständigkeitserklärung

Sarah Frentzel
Schilfbreite 22
39120 Magdeburg

Hiermit erkläre ich, dass ich die von mir eingereichte Dissertation mit dem Thema

„IkB_{NS} differentially affects *in vivo* CD4⁺ and CD8⁺ T cell activation and plays a detrimental role in innate immunity to *Listeria monocytogenes* infection in mice“

selbstständig verfasst, nicht schon als Dissertation verwendet habe und die benutzten Hilfsmittel und Quellen vollständig angegeben wurden.

Weiterhin erkläre ich, dass ich weder diese noch eine andere Arbeit zur Erlangung des akademischen Grades doktor rerum naturalium (Dr. rer. nat.) an anderen Einrichtungen eingereicht habe.

Magdeburg, den 16.04.2018

Sarah Frentzel

Curriculum vitae

Persönliche Daten

Name: Sarah Frentzel
Geburtsdatum: 02.04.1989
Geburtsort: Haldensleben
Familienstand: ledig
Nationalität: deutsch

Bildungsweg

2007 **Abitur**, Friedrich-Ludwig-Jahn Gymnasium Haldensleben

2007 - 2008 Diplomstudiengang Physik, Otto-von-Guericke Universität Magdeburg

2008 - 2012 **Bachelor of Science (B.Sc.) Biosystemtechnik**
Otto-von-Guericke Universität Magdeburg
Thema Bachelorarbeit: Durchflusszytometrische Untersuchung und Bestimmung der extrazellulären Trypsinaktivität in Influenza infizierten MDCK.SUS2 Kulturen
Durchgeführt am: Max-Planck-Institut für Dynamik komplexer technischer Systeme Magdeburg in der Arbeitsgruppe Bioprozesstechnik

2012 - 2014 **Master of Science (M.Sc.) Biosystemtechnik**
Otto-von-Guericke Universität Magdeburg
Thema Masterarbeit: Untersuchungen zu Langzeiteffekten von Influenza A Infektionen auf sekundäre adaptive Immunantworten *in vivo*
Durchgeführt am: Helmholtz-Zentrum für Infektionsforschung Braunschweig in der Arbeitsgruppe Immunregulation

2014 - 2018 **Promotion**
Thema: IkB_{NS} differentially affects *in vivo* CD4^+ and CD8^+ T cell activation and plays a detrimental role in innate immunity to *Listeria monocytogenes* infection in mice
Betreuer: Prof. Dr. Dunja Bruder
Durchgeführt: Otto-von-Guericke Universität Magdeburg, Medizinische Fakultät, Institut für Medizinische Mikrobiologie und Krankenhaushygiene in der Arbeitsgruppe Infektionsimmunologie

Sonstiges

2010 - 2013 Wissenschaftliche Hilfskraft (40 h/Monat) am Max-Planck-Institut für Dynamik komplexer technischer Systeme Magdeburg in der Arbeitsgruppe Bioprozesstechnik / Upstream Processing

Seit 2014 Mitglied der Deutschen Gesellschaft für Immunologie (DGfI)

2016 Reisestipendium, 46. Jahrestagung der Deutschen Gesellschaft für Immunologie Hamburg, Kommission zur Förderung des wissenschaftlichen Nachwuchses, Otto-von-Guericke Universität Magdeburg